ROLE OF MATRIX METALLOPROTEINASES IN UVEOSCLERAL OUTFLOW

BABLIN MOLIK (BSc)

Thesis submitted to Cardiff University in accordance with the requirements for the degree of Doctor of Philosophy in School of Optometry & Institute of Vision.

October 2007

UMI Number: U585002

All rights reserved

INFORMATION TO ALL USERS
The quality of this reproduction is dependent upon the quality of the copy submitted.

In the unlikely event that the author did not send a complete manuscript
and there are missing pages, these will be noted. Also, if material had to be removed,
a note will indicate the deletion.

UMI U585002
Published by ProQuest LLC 2013. Copyright in the Dissertation held by the Author.
Microform Edition © ProQuest LLC.
All rights reserved. This work is protected against
unauthorized copying under Title 17, United States Code.

ProQuest LLC
789 East Eisenhower Parkway
P.O. Box 1346
Ann Arbor, MI 48106-1346

DECLARATION

This work has not previously been accepted in substance for any degree and is not concurrently submitted in candidature for any degree.

Signed ... Date ...1/10/07...

STATEMENT 1

This thesis is being submitted in partial fulfilment of the requirements for the degree of PhD.

Signed ... Date ...1/10/07

STATEMENT 2

This thesis is the result of my own independent work/investigation, except where otherwise stated. Other sources are acknowledged by explicit references.

Signed ... Date ...1/10/07

STATEMENT 3

I hereby give consent for my thesis, if accepted, to be available for photocopying and for inter-library loan, and for the title and summery to be made available to outside organisations.

Signed ... Date ...1/10/07

"Everything comes to us that belongs to us if we create the capacity to receive it".
Rabindranath Tagore

"I have become my own version of an optimist. If I can't make it through one door, I'll go through another door - or I'll make a door. Something terrific will come no matter how dark the present".
Rabindranath Tagore

ABSTRACT

Prostaglandin derivatives form the most widely used medicinal treatments given to glaucoma patients to lower intraocular pressure. Prostaglandins are believed to increase matrix metalloproteinase (MMP) and tissue inhibitor of matrix metalloproteinase (TIMP) activity, leading to increased in aqueous outflow, via uveoscleral outflow pathway. However, the direct impact of MMPs on the tissues within uveoscleral pathway has not been determined. The aim of this project was to compare the direct effect of prostaglandins and MMPs on the tissues within the uveoscleral outflow pathway.

To determine the effect of known inducers of MMP activity, scleral fibroblasts and ciliary muscle cells were cultured in the presence of interleukin-1α, tumour necrosis factor, transforming growth factor β and prostaglandin F2α (PGF2α). The effect of prostaglandin F2α and MMPs on the uveoscleral pathway tissue i.e. sclera, was assessed as a measure of permeability, molecular and supramolecular scleral collagen integrity and proteoglycan composition.

A significant induction of MMP 1, 2, 3 and 9 secretion and activity with cytokines and PGF2α, within human scleral fibroblast and ciliary muscle cell cultures ($p<0.05$). A 3-fold increase in scleral permeability was observed within 24 hour of incubation in PGF2α, whereas upto 10-fold increase was observed in MMP treated. The helical rise per residue (at ~1.5nm), lateral packing (at ~0.29nm) and D-spacing (at ~66nm) of scleral collagen was unaffected by MMP and PGF2α incubation. Significant change in aggrecan degradation was observed within scleral tissue incubated in MMP and PGF2α ($p<0.05$). However, no significant change in small leucine rich proteoglycans i.e. biglycan, decorin and lumican, within sclera occurred within sclera incubated in MMP or PGF2α.

The findings of this study will help to understand how aqueous drainage can be enhanced and also provide a mechanism to improve delivery of substances to the back of the eye, without adverse effect.

Acknowledgements

There were many ups and downs throughout my PhD study and the only reason it all came together was because of my supervisors' faith in me, help and guidance throughout the years. I want to give my greatest token of appreciation to all three of my supervisors Dr. Julie Albon, Mr. James Morgan and Prof. Mike Boulton without these people it would not have been possible.

I am also very grateful to Prof. V. Duance and Dr. Emma Blain for helping me start of my work with zymography. I want to give a big thank-you to Prof. T. Wess and Clark Maxwell for their co-operation in conducting the x-diffraction work. Thank you to Prof. B. Caterson, Dr. Debbie Tudor and Dr. Alison Rees for providing me with proteoglycan antibodies and helping me with the western blotting analysis. I would also like to acknowledge the people in CTS Eye Bank, Bristol for providing the tissue required throughout the study. Thanks to Pfizer for partly sponsoring my work.

I want to thank Mrs Susan Hobbs, Leanne, Stacey and Rosie for being very helpful and friendly whenever required. Also thank-you to Steve, John, Rob and Phil for all their help with any technical or paperwork related problems. I would like to thank some friends past and present within the school: Stuart, Sarah, Jun, Vanessa, Andrew, Gill, Linda, Jen, Debbie, Llinos, Miguel, Yaden, Tina and Mat for their help, support and for making my PhD years a pleasant time to remember.

Finally I would like to thank my family. Thank you to my husband, mother, father, sisters, brother, sister-in-law and brother-in-laws for their help, support and believe in me. Thanks to all my nieces and nephews for enabling me to forget my PhD when under too much stress. My biggest thanks goes to my daughter, Mahek, she has always made me realise how important it is for me to become successful. I must also add my youngest daughter, Midhaa, who gave me just enough time to submit my thesis and do my viva before being born.

CONTENTS

1.0 INTRODUCTION	1-30
1.1 Glaucoma	2-10
1.1.1 Abnormalities leading to glaucoma	3-5
1.1.2 Methods used to treat glaucoma	5-9
1.1.2.1 Medicinal treatment	6
1.1.2.2 Laser/ surgery treatment	7
1.1.2.3 Current research, Prostaglandin analogues	8-9
1.1.3 Intraocular pressure	9-10
1.2 Aqueous Humor & the drainage pathways in the eye	10-18
1.2.1 Aqueous humor	11
1.2.2 Aqueous humor composition	11-12
1.2.3 Aqueous production	12-13
1.2.4 Aqueous drainage	14-18
1.2.4.1 Canal of Schlemm	14-16
1.2.4.2 Uveoscleral outflow pathway	16-18
1.3 Extracellular matrix in the aqueous drainage pathway	18-22
1.3.1 ECM in the ciliary muscle	19-20
1.3.2 ECM in the sclera	20-21
1.3.3 Age related changes in ECM of uveoscleral outflow pathway	21-22
1.4 ECM degradation	22-25
1.4.1 Matrix metalloproteinase in the uveoscleral outflow pathway	23
1.4.2 MMP homology	24
1.4.3 MMP synthesis and activation	24
1.4.4 Regulation of MMP action	25
1.4.5 Distribution of MMPs and TIMPs in uveoscleral outflow pathway	25

1.5 The role of MMPs & TIMPs in IOP reduction in uveoscleral outflow 25-27

1.6 Drug Delivery in the Eye 27-29
1.6.1 Posterior Drug Delivery 28-29
1.6.2 Implication of study in drug delivery 29

1.7 Aims of the project 30

2.0 METHODS 31-54
2.1 Materials 32
2.2 Characterisation of the uveoscleral outflow pathway 32-43
2.2.1 Source of tissue 32-33
2.2.2 Wax sections of human anterior chamber 33
2.2.3 Morphological staining of anterior chamber 33-34
2.2.4 Human scleral fibroblast cell culture 34-35
2.2.5 Human ciliary muscle cell culture 35-36
2.2.6 Sub-culture of confluent cells 36
2.2.7 Freezing cells 37
2.2.8 Thawing cells 37
2.2.9 Confirmation of ciliary muscle cell phenotype 37-38
2.2.10 Detection of PGF2α receptor and MMP 2 in HSFs and HCM cell cultures 38-39
2.2.11 Cell counting 39
2.2.12 Serum-free cell culture 39
2.2.12.1 Preparation of MMP-enriched medium, HSF and HCM cell conditioned medium 40

2.2.13 Zymography to detect gelatinases, stromelysins and TIMP activity on cell cultures 40-43
2.2.13.1 Preparation of samples for zymography 40
2.2.13.2 Detection of MMPs by zymography 41-42
2.2.13.3 Detection of TIMP by reverse zymography 42-43
2.2.13.4 Sensitivity of band intensity to sample concentration 43
2.2.14 Detection of MMP 1 using Enzyme-Linked ImmunoSorbent Assay (ELISA) 43
2.3 The effect of different MMP inducers on cells involved in uveoscleral outflow MMP secretion 44
2.3.1 Cell Culture 44
2.3.2 Zymography 44
2.4 The effect of MMP and PGF2α on scleral permeability 45-48
2.4.1 Scleral tissue culture 45
2.4.2 Determination of scleral permeability using Ussing chamber 45
2.4.2.1 Use of Spectrophotometer & Spectrofluorometer 45-46
2.4.2.2 Standard Absorbance-Concentration for Spectrofluorometry 47
2.4.2.3 Calculating Permeability coefficient 48
2.5 Effect of PGF2α and MMP on scleral collagen architecture 48-50
2.5.1 Scleral tissue culture 48-49
2.5.2 X-ray diffraction 49-50

2.6 Effect of PGF2α and MMP on proteoglycans in human sclera 50-54

2.6.1 Proteoglycan extraction 50-51

2.6.2 Dialysis of proteoglycan extraction fluid 51

2.6.3 Papain Digestion 51

2.6.4 Dimethylene Blue (DMMB) assay 51

2.6.5 Protein assay 52

2.6.6 Deglycosylation 52

2.6.7 Western Blotting 52-54

3.0 CHARACTERISTAION OF THE UVEOSCLERAL OUTFLOW PATHWAY 55-100

3.1 Introduction 56-58

3.1.2 Aims 58

3.2 Experimental design 59-61

3.2.1 Morphology of the anterior chamber 59

3.2.2 Identification of the presence of PGF2α and MMP 2 in HSFs and HCM cells 59

3.2.3 The MMP and TIMP profile in MMP-enriched medium (MMP-EM) 59

3.2.4 Sensitivity of Quantification 60

3.2.5 MMP and TIMP profile of HSFs and HCM cells in culture 60

3.2.6 The effect of known MMP inducers and PGF2α on MMP activation in HSF and HCM cell cultures 60-61

3.3 Results 62-95

3.3.1 Morphology of the human anterior chamber 62-63

3.3.2 Presence of PGF2α receptor and MMP 2 in HSFs and HCM cell culture 63-65

3.3.3 MMPs and TIMPs Profile in MMP-EM, HSF and HCM cells conditioned medium 66-70

3.3.3.1 Sensitivity of laser scanning densitometry of zymograms and reverse zymograms 67-68

3.3.3.2 Quantification of MMPs in serum free media MMP-EM, HSF-CM and HCM-CM 68-70

3.3.4 Effect pf growth factors on MMP secretion by human scleral fibroblast (HSFs) 70-75

3.3.5 Effect of growth factors on MMP secretion by human ciliary muscle cells 76-81

3.3.6 Effect of growth factor on MMP-1 secretion 81-83

3.3.7 Effect of prostaglandin on MMP secretion by human scleral fibroblasts 83-88

3.3.8 Effect of prostaglandin on MMP secretion by human ciliary muscle cells 89-93

3.3.9 Effect of prostaglandin on MMP-1 secretion 94-95

3.4 Discussion 96-100

4.0 EFFECT OF PGF2A AND MMP ACTIVITY ON SCLERAL CONDUCTIVITY 101-136

4.1 Introduction 102-103

4.1.2 Aims 103

4.2 Experimental design 104-107
4.2.1 Source of sclera 104
4.2.2 Effect of MMP-EM and PGF2α on scleral permeability 104-107
4.2.2.1 Scleral explants culture 104
4.2.2.2 Production of matrix metalloproteinase enriched medium 104
4.2.2.3 Setting up the Ussing Chamber 105-106
4.2.2.4 Determination of permeability coefficient 107
4.2.25 Calculation of permeability coefficient 107
4.2.2.6 Statistical analysis 107

4.3 Results 108-111
4.3.1 Quantification of scleral permeability 108
4.3.2 The effect of PGF2α and MMP-EM on transcleral permeability 108-111

4.4 Discussion 112-115

5.0 X RAY DIFFRACTION: ANALYSIS OF SCLERAL COLLAGEN ARCHITECTURE 116-136
5.1 Introduction 117-120
5.1.2 Aim 120

5.2 Experimental design 121-124
5.2.1 Source of tissue 121
5.2.2 Production of matrix metalloproteinase enriched medium 121
5.2.3 Production of conditioned media from human scleral fibroblast (HSF-CM) and human ciliary muscle cells (HCM-CM) 121

5.2.4 Scleral tissue culture 121-122
5.2.5 X-ray diffraction analysis 122-124
5.2.5.1 Wide angle x-ray diffraction images obtained at station 14.1 SRS Daresbury technical details 122-123
5.2.5.2 Small angle x-ray diffraction images station 2.1 SRS Daresbury technical details 123-124
5.2.5.3 Analysis 124

5.3 Results 125-133
5.3.1 WAXD results 125-127
5.3.2 SAXD results 128-133

5.4 Discussion 134-136

6.0 THE EFFECT OF PGF2A AND MMP ON PROTEOGLYCANS IN HUMAN SCLERA 137-152
6.1 Introduction 138-140
6.1.2Aims 140

6.2 Experimental Design 141-143
6.2.1 Tissue culture 141
6.2.2 Sulphated GAG content released into media, solubilised by Guanidine hydrochloride extraction and remaining in sclera. 141-142
6.2.2.1 GAG released into media 141
6.2.2.2 GAG solubilised 141
6.2.2.3 Determination of total GAG 142
6.2.3 Analysis of proteoglycan in sclera 142-143
6.2.3.1 Identification of proteoglycans in sclera 142
6.2.3.2 Quantification of proteoglycans 142

6.2.3.3 Deglycosylation 142
6.2.3.4 Western Blotting 142-143
6.2.4 Data analysis 143

6.3 Results 144-149
6.3.1 Effect of PGF2α and MMPs on GAG composition 144-145
6.3.2 Analysis of proteoglycans within sclera 145-149
6.3.2.1 Effect of PGF2α and MMP-EM on scleral aggrecan 145-146
6.3.2.2 Effect of PGF2α and MMP-EM on scleral biglycan 147
6.3.2.3 Effect of PGF2α and MMP-EM on scleral decorin 148
6.3.2.4 Effect of PGF2α and MMP-EM on scleral lumican 149

6.4 Discussion 150-152

7.0 DISCUSSION 153-165
7.1 Introduction 154

7.2 Induction of MMP secretion and activity in the uveoscleral outflow pathway 154-156

7.3 The effect of PGF2α and MMPs on scleral integrity 157-158

7.4 Scleral retained its collagen architecture at molecular and supramolcular levels following MMP treatment 158-159

7.5 Changes in scleral proteoglycans following MMP action 159-160

7.6 Conclusion 161-162

7.7 Future prospects 163-165

References 166-185

Appendix 184-200

8.1 Chemical & Manufacturers 185-188

8.2 Solution 189-191

8.3 Human tissue 192-195

8.4 Raw data 195-200

8.5 List of Publications 200

FIGURES

Fig. 1.1: Schematic drawings of different anterior segment defects causing glaucoma. 5

Fig. 1.2: Semi diagrammatic figure of the anterior segment. 10

Fig. 1.3: Ion and water transfer and active transport across ciliary epithelium cells, leading to aqueous production. 13

Fig. 1.4: Aqueous outflow via trabecular meshwork and canal of schlemm. 14

Fig. 1.5: Uveoscleral outflow pathway. 17

Fig. 1.6: MMP domain structure 24

Fig. 2.1: Human scleral fibroblasts growth from explants cultured. 35

Fig. 2.2: Human ciliary muscle cell growth from explants cultured. 36

Fig. 2.3: Spectrofluorescence reading from the uveal side of 24 hours prostaglandin incubated tissue, after 4 hours in the ussing chamber. 46

Fig 2.4: Standard curve of 40kDa dextran bead concentration in relation to fluorescence reading (580nm). 47

Fig. 2.5: Example of x-ray diffraction. 50

Fig. 2.6: The arrangement of different layers within the transfer tank. 53

Fig. 3.1: Schematic diagram of the aqueous humor cycle. 56

Fig. 3.2: Haematoxylin and eosin staining of the anterior segment. 62

Fig. 3.3: Toluidine blue staining of human anterior segment. 63

Fig 3.4: Immunostaining of human ciliary muscle cells 64

Fig. 3.5: Immunolocalisation of PGF2α receptor and MMP 2 in human scleral fibroblasts (HSF) and ciliary muscle cells (HCM) cultures. 65

Fig 3.6: MMPs and TIMPs profile in conditioned medium. 66

Fig. 3.7 Correlation of the band intensity of serially diluted MMP-EM. 68

Fig. 3.8: MMP profile of HCM-CM, HSF-CM and MMP-EM. 69

Fig. 3.9: MMP-1 detection in medium via ELISA. 70

Fig. 3.10: The Effect of growth factor administration on MMP 2 secretion by human scleral fibroblast. 72

Fig. 3.11: The Effect of growth factor administration on MMP 3 secretion by human scleral fibroblast. 73

Fig. 3.12: The Effect of growth factor administration on MMP 7 secretion by human scleral fibroblast. 74

Fig. 3.13: The Effect of growth factor administration on MMP 9

secretion by human scleral fibroblast. 75

Fig. 3.14: The Effect of growth factor administration on MMP 2 secretion by human ciliary muscle cells. 78

Fig. 3.15: The Effect of growth factor administration on MMP 3 secretion by human ciliary muscle cells. 79

Fig. 3.16: The Effect of growth factor administration on MMP 7 secretion by human ciliary muscle cells. 80

Fig. 3.17: The Effect of growth factor administration on MMP 9 secretion by human ciliary muscle cells. 81

Fig. 3.18: Effect of growth factors on MMP-1 secretion by human scleral fibroblasts. 82

Fig. 3.19: Effect of growth factors on MMP-1 secretion by HCM cells. 83

Fig. 3.20: PGF2α effect on human scleral fibroblasts conditioned medium MMP 2 secretion and activation. 85

Fig. 3.21: PGF2α effect on human scleral fibroblasts conditioned medium MMP 3 secretion and activation. 86

Fig. 3.22: PGF2α effect on human scleral fibroblasts conditioned medium MMP 7 secretion and activation. 87

Fig. 3.23: PGF2α effect on human scleral fibroblasts conditioned medium MMP 9 secretion and activation. 88

Fig. 3.24: PGF2α effect on human ciliary muscle conditioned medium MMP 2 secretion and activation. 90

Fig. 3.25: PGF2α effect on human ciliary muscle conditioned medium MMP 3 secretion and activation. 91

Fig.3.26: PGF2α effect on human ciliary muscle conditioned medium MMP 7 secretion and activation. 92

Fig. 3.27: PGF2α effect on human ciliary muscle conditioned medium MMP 9 secretion and activation. 93

Fig. 3.28: The effect of PGF2α on MMP-1 secretion by human scleral fibroblast. 94

Fig. 3.29: The effect of PGF2α on MMP-1 secretion by human ciliary muscle cells. 94

Fig. 4.1: Drawing of Ussing system. 106

Fig. 4.2: Permeability coefficient of different sized dextran beads (10, 40 and 70kDa). 108

Fig. 4.3: Time dependent permeability of sclera to 40kDa dextran beads 110

Fig. 4.4: Time dependent permeability of sclera to 70kDa dextran beads. 111

Fig. 5.1: A schematic diagram of Collagen hierarchy. 119

Fig. 5.2 Sample holder for wide angle x-ray diffraction. 123

Fig. 5.3 Sample holder for small angle x-ray diffraction. 124

Fig. 5.4: Wide angle x-ray diffraction of human sclera. 126

Fig 5.5: Scaled 1D linear plots of intensity verses scattering angle of wide angle x-ray diffraction images. 127

Fig. 5.6: Small angle x-ray diffraction of human sclera. 129

Fig 5.7: Scaled 1D linear plot of intensity verses scattering angle of small angle x-ray diffraction images. 130

Fig 5.8: 1D linear plots of small angle x-ray diffraction images of scleral tissue incubated in Control, HCM-CM and HSF-CM for 12, 24 and 72 hours. 131

Fig 5.9: 1D linear plots of small angle x-ray diffraction images of scleral tissue treated in MMP1, 2 and 7 for 12, 24 and 72 hours. 132

Fig. 6.1: Schemmatic drawing of proteoglycan and glycosaminoglycan disaccharide. 138

Fig. 6.2: Percentage of GAG released in media and the percentage of GAG extracted from scleral tissue. 144

Fig. 6.3: Effect of PGF2α and MMP-EM on scleral aggrecan. 146

Fig. 6.4: Effect of PGF2α and MMP-EM on scleral biglycan. 147

Fig. 6.5: Effect of PGF2α and MMP-EM on scleral decorin. 148

Fig. 6.6: Effect of PGF2α and MMP-EM on scleral lumican. 149

TABLES

Table 1.1: Different types of glaucoma with their abnormalities and causes. 4

Table 1.2: Different medicinal treatments available currently. 6

Table 1.3: Laser and surgical treatments available. 7

Table1.4: Different types of MMPs and their function 23

Table 5.1: Collagen intermolecular packing distance and axial rise per residue values for human sclera samples. 128

Table 5.2: D-spacing values for human sclera. 131

Table 5.3: D-spacing values for human sclera treated with medium from HCM-CM and HSF-CM. 132

Table 5.4: D-spacing values for human sclera treated with MMPs. 133

Abbreviations

ADAM-TS	A disintegrin and metalloproteinase with thrombospondin motifs
Ala	Alanine
ALT	Argon laser trabeculoplasty
AMD	Age related macular degeneration
ANOVA	Analysis of variance
AP1	Activator protein 1
Asn	Asparagine
ATPase	Adenosine triphosphatase
BAB	Blood aqueous barrier
BCA	Bicinchoninic acid
BCIP	Bromo-chloro-indolyl phosphate
BOVS-1	Bovine scleral fibroblasts
BSA	Bovine serum albumin
$CaCl_2$	Calcium Chloride
cAMP	Cyclic adenosine monophosphate
CO_2	Carbon dioxide
ddH_2O	Double distilled water
DMEM	Dulbecco's modified eagle's medium
DMMB	1,9-dimethylmethylene blue
DMSO	Dimethyl Sulfoxide
ECM	Extracellular matrix
EDTA	Ethylenediamine tetraacetic acid
ELISA	Enzyme linked immunosorbent assay
FCS	Foetal calf serum
FGF	Fibroblast growth factor
GAG	Glycosaminoglycan
Glu	Glutamine
H & E	Haematoxylin & eosin
HCl	Hydrogen chloride
HCM	Human ciliary muscle
HSF	Human scleral fibroblast
IOP	Intraocular pressure
IL	Interleukin
ILP	Intermolecular lateral packing
IMS	Industrial methylated spirit
ITS	Insulin-transferrin-sodium selenite
K	Potassium
$MgCl_2$	Magnesium chloride
MMP	Matrix metalloproteinase
MMP-EM	MMP enriched media
MT-MMP	Membrane type-MMP
Na	Sodium

NaCl	Sodium chloride
NBF	Neutral buffered formalin
NBT	Nitroblue tetrazolium
NDRI	National disease research interchange
NPE	Non pigmented epithelium
NTG	Normal tension glaucoma
O_2	Oxygen
PBS	Phosphate buffered saline
Pc	Permeability coefficient
PDF	Pigmentory glaucoma
PFA	Paraformaldehyde
PGF2α	Prostaglandin F2alpha
PGs	Prostaglandins
Phe	Phenylalanine
POAG	Primary open angle glaucoma
PXF	Pseudoexfoliation
RPE	Retinal pigment epithilum
SAXD	Small angle x-ray diffraction
SAXS	Small angle x-ray scattering
SDS	Sodium dodecyl sulphate
SLRP	Small leucine rich proteoglycan
TGF	Transforming growth factor
TIMP	Tissue inhibitor of MMP
TM	Trabecular meshwork
TNF	Tumour necrosis factor
TSA	Tris saline
UKTS	United Kingdon transplant service
WAXD	Wide angle x-ray diffraction
WAXS	Wide angle x-ray scattering

CHAPTER 1

INTRODUCTION

CHAPTER 1

INTRODUCTION

1.0 General Introduction

Glaucoma is a disease leading to loss of vision (Olendoff, Jeryan *et al.* 1999; Quigley 1996). One cause of glaucoma is the malfunction of the aqueous humour drainage system resulting in the build up of intraocular pressure (IOP) (Forrester, Dick *et al.* 1999; Krohn 2004). Uveoscleral outflow is one of the drainage pathways. The uveoscleral pathway involves the flow of aqueous humour through the ciliary meshwork in the anterior chamber into the systemic blood supply via the scleral vasculature (Nilsson 1997). This study is focused on investigating whether metalloproteinases (MMPs) can affect the drainage system. Previously prostaglandins have been used as therapeutics for glaucoma (Drake 1996). Prostaglandins appear to increase MMP secretion and activation (Weinreb, Toris *et al.* 2002). MMPs are involved in extracellular matrix (ECM) degradation. It is, therefore, hypothesised that modulation of MMPs in the uveoscleral outflow pathway may facilitate aqueous outflow and hence lower intraocular pressure (IOP), without causing adverse effects. The use of MMPs to enhance tissue conductivity to improve drainage may also be the solution to allow drug delivery into the eye.

1.1 Glaucoma

Glaucoma is a condition characterised by the loss of retinal ganglion cells associated with vision field loss. In the commonest form of the disease, an elevated IOP is observed. If untreated, the optic nerve damage results in progressive, permanent vision loss, commencing with a reduction in peripheral sensitivity at the edge of the field of vision, progressing to tunnel vision and then to blindness (Moorthy, Mermoud *et al.* 1997).

Glaucoma disease has many classifications due to the nature of the abnormalities. The different classifications can be grouped into four types:

1. ***Open/ Closed Angle Glaucoma***

This relates to the anterior chamber angle being closed or open. In the case where the angle is closed, aqueous drainage is prevented/ diminished and IOP rises. In the case where the angle is open, the IOP rises due to other factors such as interference of normal trabecular drainage e.g. large proteins blocking drainage pathway.

2. ***Primary / Secondary***

Primary glaucoma states that the disease has no association with any other disease. Secondary glaucoma states that the disease was the result of another disease.

3. ***Congenital/ Infantile/ Juvenile/ Adult***

This relates to the age of onset of glaucoma.

4. ***Acute/ Subacute/ Chronic***

This relates to speed of onset. Acute glaucoma means a sudden occurrence with short duration. Chronic glaucoma persists for months or longer, and is less severe.

1.1.1 Abnormalities leading to Glaucoma

There are various abnormalities leading to various types of glaucoma. It is important for a clinician to identify the abnormality associated with glaucoma in order to give suitable treatment. Table 1.1 is a list of different types of glaucoma and their abnormalities/ causes, and Fig. 1.1 shows the changes in the anterior segment structure associated with different types of glaucoma.

Type of Glaucoma	Type of Disorder	Abnormality	Risk factors/ causes
Primary open angle Glaucoma (POAG)	Normal Tension Glaucoma (NTG)	Glaucomatous optic disc damage and visual field loss in presence of an IOP within normal range.	Age, race, gender, family history, myopia, systemic hypertension, damage in the eye.
	High Tension Glaucoma	Progressive optic nerve damage, with IOP higher than the nerve fibres can tolerate.	Age, race, gender, family history, myopia, systemic hypertension, damage in the eye.
Secondary open angle Glaucoma	Pseudoexfoliation (PXF) Syndrome	PXF block anterior segment structure	Diffuse deposition of whit-dandruff like flecks on the anterior segment structures of the eye.
	Pigmentory Glaucoma (PDS)	PDS particles block trabecular spaces.	Build up of pigment particles that are dispersed from the posterior iris and carried through anterior segment by aqueous convection currents.
	Uveitic Glaucoma	Elevation of IOP leading to glaucomatous damage to the optic nerve	Chronic, recurrent or severe acute inflammation
	Corticosteroid Induced Glaucoma	Permanent ocular tissue changes, such as posterior sub capsular cataracts.	Long term steroid therapy.
	Glaucoma associated with Hyphema	Obstruction of trabecular meshwork.	Blood and blood particles obstruct drainage pathway.
	Ghost cell Glaucoma	Ghost cells stay within vitreous cavity and obstruct trabecular meshwork.	Ghost cell formed during vitreous haemorrhage.
Primary Angle Closure Glaucoma	Pupillary Block	Appositional or synechial closure of the anterior chamber angle.	Hypermetropic, narrow angled eye. Restriction of aqueous outflow causes iris to be pushed forward to close angle.
	Plateau Iris	Closure of angle.	Angle closed in association with a flat iris plane and a deep central anterior chamber.
Secondary Angle Closure Glaucoma	Anterior Secondary Angle Closure Glaucoma	Iris pulled forward by a factor, and obstruct aqueous outflow.	Abnormal tissue bridging with the anterior chamber. Tissue could be fibrovascular membrane, descemet like membrane with endothelial layer, inflammatory precipitates and congenital fibrous.
	Posterior Secondary Angle Closure Glaucoma	Pressure builds up behind the iris or lens cause the iris to be pushed into the anterior chamber angle, leading to obstruction of outflow.	Increased pressure in posterior chamber.

Table 1.1: Different types of glaucoma with their abnormalities and causes. Information gathered from (Eid and Spaeth 2000; Harvey 1997; Kanski, McAllister *et al.* 1996; Litwak 2001).

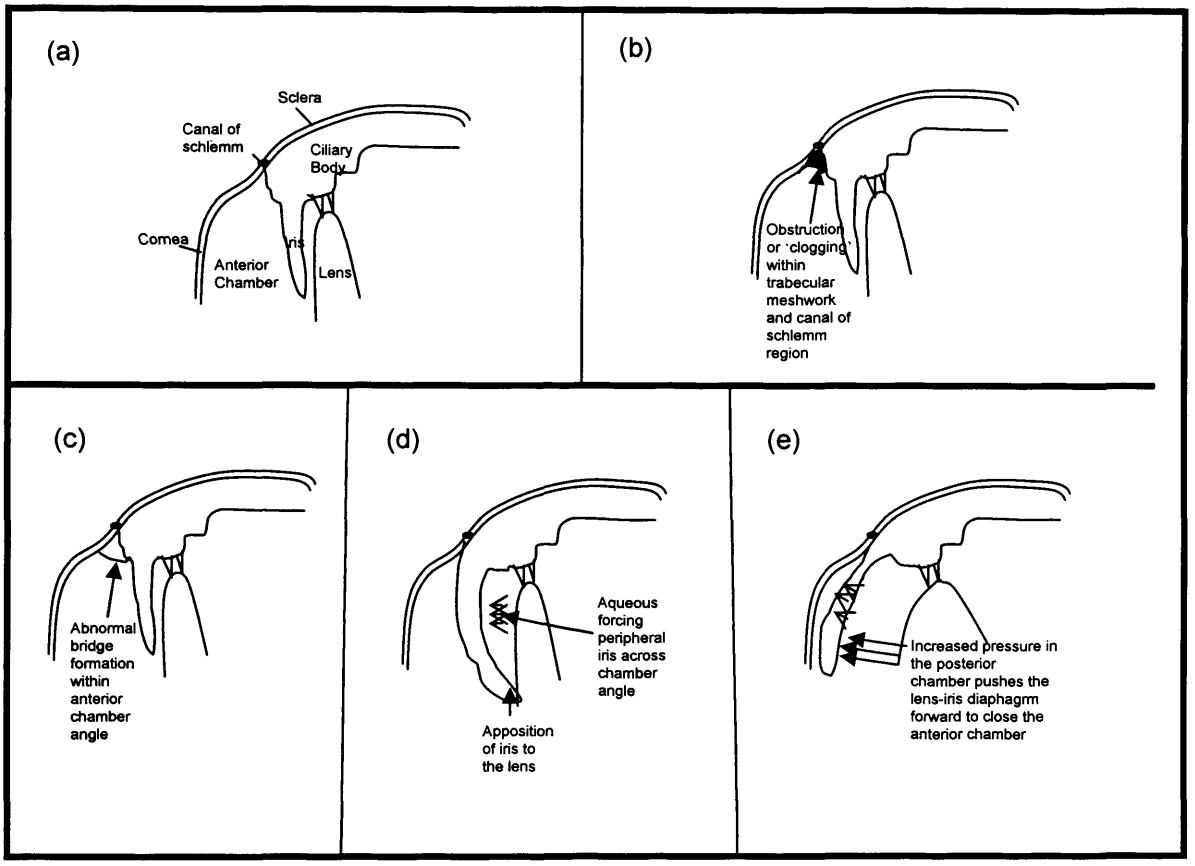

Fig. 1.1: Schematic drawings of different anterior segment defects causing glaucoma. (a) Anterior orbital structure under normal condition, (b) Trabecular meshwork clogged up in open angle glaucoma, (c) Abnormal tissue bridge formed in closed angle glaucoma, (d) Iris tilted down on the lens, creating pupillary block, in closed angle glaucoma, (e) Posterior form of secondary angle closure glaucoma without pupillary block adapted from (Eid and Spaeth 2000).

1.1.2 Methods Used to Treat Glaucoma

There are various methods used to treat glaucoma depending on the nature of the disease. The treatments may involve medicinal drug therapy or surgical intervention.

1.1.2.1 Medical Treatment

Drugs can be given either singly or in combination to reduce IOP. For example Atrophine when given with pilocarpine had a great additive effect in enhancing uveoscleral outflow (Bill 1967). Recent studies have also shown that miotics thought to have lowered uveoscleral outflow, do actually have an additive effect in lowering IOP when given alongside Latanoprost (Toris, Alm *et al.* 2002).

AGENT	MECHANISM OF ACTION	COMPLICATION
Drugs		
Beta Blockers Timolol, Betaxolol, Carteolol, Levobunolol, Metipranolol	Reduction of aqueous production via B-receptor blockage on ciliary body.	Exacerbation of pulmonary disease, heart failure, badycardia
Cholinergics (miotics) Pilocarpine, Carbachol, Echothiophate iodide, eserine	Increases trabecular meshwork outflow via stimulation of muscaronic receptors on ciliary muscle, which contracts and pulls the trabecular meshwork posteriorly, decrease uveoscleral outflow due blockage of space between ciliary muscle bundles.	Ocular stinging, dimming vision, spasm, gastrointentestinal upset, high concentration may narrow angle
Carbonic Anhydrase Inhibitors Dorzolamide (topical), Acetazolamide (oral)	Reduce aqueous production via inhibiting carbonic anhydrase	Hyperaemia, sulfa sensitivity, metabolic acidosis, potassium depletion aplastic anaemia
Adregenic Agonists Epinephrine, Dipivefrin (pro-drug), Apraclonodine	Decrease aqueous production via a-receptor stimulation on ciliary body, increase outflow through the trabecular meshwork via stimulation of b_2 receptors	Pupil dilation, hypertension, systemic tachycardia
Prostaglandins Latanoprost	Increase uveoscleral outflow	Hyperaemia, darkening iris, anterior uveitis
Osmotic Agents Glycerol, Mannitol, Isosorbide	Increase osmotic gradient of extracellular fluid, causes water from the eye to drain out	Nausea, vomiting, hyperglycaemia, chest pains.
Alternative Treatment		
Vitamin C, Vitamin B1 (thiamine), chromium, Zinc, rutin	Reduce IOP	Side effects could be seen if taken in excess
Marijuana	Lower IOP	carcinogenic agent
Solnum melonga (garden egg)	Lower IOP	Still new, long term effects have not been seen
Xylopia aethiopica (African guinea pepper)	Lower IOP	Still new, long term effects have not been seen

Table 1.2: Different medicinal treatments available currently. Information gathered from (Drake 1996; Igwe, Afonne *et al.* 2003; Igwe, Akunyili *et al.* 2003; Litwak 2001; Olendoff, Jeryan *et al.* 1999).

1.1.2.2 Laser/ Surgery Treatment

Laser or surgical intervention involves opening up the drainage canals or making an opening in the iris to increase the outflow of aqueous humor (Wilkins, Shah *et al.* 1997). This type of treatment can become a first priority if medical treatment is unsuccessful due to the patient developing side effects or the medicine is contra-indicated in the patient (e.g. heart disease or asthma patients). Table 1.3 below outlines the laser and surgery treatments available to patients.

TYPE OF SURGERY	METHOD	USE
Argon Laser Trabeculoplasty (ALT)	Stimulation of trabecular meshwork cells to divide and alter meshwork protein. Clear meshwork pathway and hence increase outflow	Open angle glaucoma
Trabeculectomy	Channel made through sclera from anterior chamber to sub-conjunctival space. From conjunctiva the aqueous is absorbed by capillaries or lymphatic in the cornea.	Open angle glaucoma
Laser Iridotomy	Open up anterior chamber channel, allows normal flow of aqueous into anterior chamber	Acute closed angle glaucoma
Surgical Iridectomy	Iris is pulled out, a small hole is created via cutting the iris, and then the iris is pushed back in, enhances outflow pathway.	Closed angle glaucoma
Cycloablative	Ciliary processes are destroyed and hence aqueous humour production is reduced.	Only given when surgery is not working or is unsuitable

Table 1.3: Laser and surgical treatments available. Information gathered from (Moorthy, Mermoud *et al.* 1997; Wilkins, Shah *et al.* 1997).

However, these types of treatments do not always have a long lasting effect and may cause optical inflammatory (Wilkins, Shah *et al.* 1997).

1.1.2.3 Current Research, Prostaglandin analogues

Many studies have been conducted in order to identify how IOP can be reduced within the eye. Many factors have been determined in various model studies, such as, myosin light chain kinase Inhibitor (ML-9) which can lower IOP in rabbit eye by increasing outflow facility (Honjo, Inatani *et al.* 2002), nitric oxide synthase inhibitor (L-NAME) found to cause ciliary vasoconstriction and thereby reduces aqueous production (Do, Kong *et al.* 2006; Kiel, Reitsamer *et al.* 2001) and the renin angiotensin system (RAS) which allows angiotensin II production which activates the calcium-signalling system that can enhance potassium ion channel activity leading to loss of cell volume (Cullinane, Leung *et al.* 2002). These are a few out of many factors being investigated to find a more applicable and lasting treatment of glaucoma.

The main interest of this study was based upon the effect of prostaglandin and its derivatives on the uveoscleral outflow pathway, which leads to reduced IOP. Prostaglandins (PGs) belong to a group of local hormones, eicosanoids, derived from fatty acid (Alm 1998). They consist of a 20 carbon skeleton with a 5-carbon ring. Different prostaglandin synthase are involved in synthesising different forms of PGs, i.e. prostaglandin F synthase is involved in the formation of prostaglandin F2α (PGF2α) (Komoto, Yamada *et al.* 2006). Several cell surface G-protein coupled receptors have been identified, with different affinity to the various forms of PGs (Coleman, Smith *et al.* 1994).

Prostaglandin analogues like latanoprost (Xalatan), bimatoprost (Lumigen) and travoprost (Travatan) have been shown to lower intraocular pressure by 30-35% (Wagner, Edwards *et al.* 2004). Latanoprost being the first prostaglandin based ocular hypotensive drug to be commercially available since 1996 (Linden and Alm 1999). These agents have been shown to be the most effective topical medication for reducing IOP. The ability of PGs in lowering IOP has been observed across various species (Lee, Podos *et al.* 1984), via increasing aqueous outflow. The most thoroughly studied analogue is PGF2α. The esterification of PGF2α remarkably increases its lipid solubility

(Villumsen, Alm *et al.* 1989). Thus an isopropylester form of PGF2α (PGF2α-IE) can penetrate cornea easily and become de-esterified during its passage. PGF2α has high affinity for FP receptor (Anthony, Lindsey *et al.* 2001; Crowston, Lindsey *et al.* 2004b). The binding of PGF2α to FP receptor causes an increase in uveoscleral outflow and thereby lowers IOP (Crawford and Kaufman 1987; Schachtschabel, Lindsey *et al.* 2000). PGs do not affect the trabecular meshwork drainage pathway (Kaufman 1986).

However, the hypotensive effect of topically applied prostaglandin analogues has various side effects (Hejkal and Camras 1999). Side effect such as anterior inflammation, irritation, darkening of the iris pigmentation, blurred vision and dry eyes (Cantor 2002; Linden and Alm 1999). This suggests the need to determine a more effective glaucoma treatment without any adverse effect.

1.1.3 Intraocular Pressure

The normal average IOP is approximately 15mmHg (Alimuddin 1956). IOP can vary dependent upon time of day, blood pressure level and respiration. Intraocular pressure (IOP) builds up due to aqueous humour production and the resistance to its outflow. This pressure helps maintain the shape of the eye and its optical transparency. There are three factors involved in determining IOP:

1 Rate of aqueous secretion.
2 Resistance encountered in the outflow channels.
3 Level of episcleral venous pressure.

Rate of outflow is proportional to the IOP minus the episcleral venous pressure:

$Po = (F/C) + Pe$ OR $F = C (Po-Pe)$

Po = IOP in mmHg

F = Rate of aqueous outflow (normal 2µl/min)

C = Facility of aqueous outflow (normal 0.2µl/min)

Pe = Episcleral venous pressure (normal 10 mmHg) (Aihara, Lindsey *et al.* 2003).

IOP increases due to build up of surfactant like material in aqueous humour, reduction of space between muscle bundles or malformation of the trabeculae and excess extracellular matrix in the outer meshwork (Moorthy, Mermoud *et al.* 1997). Glaucoma is most commonly related to IOP above 25mm Hg (Blackmore and Jennett 2001).

1.2 Aqueous Humour & the Drainage Pathways in the Eye

Fig. 1.2 below shows the general structure of the anterior segment of the eye, where aqueous humour is produced and drained.

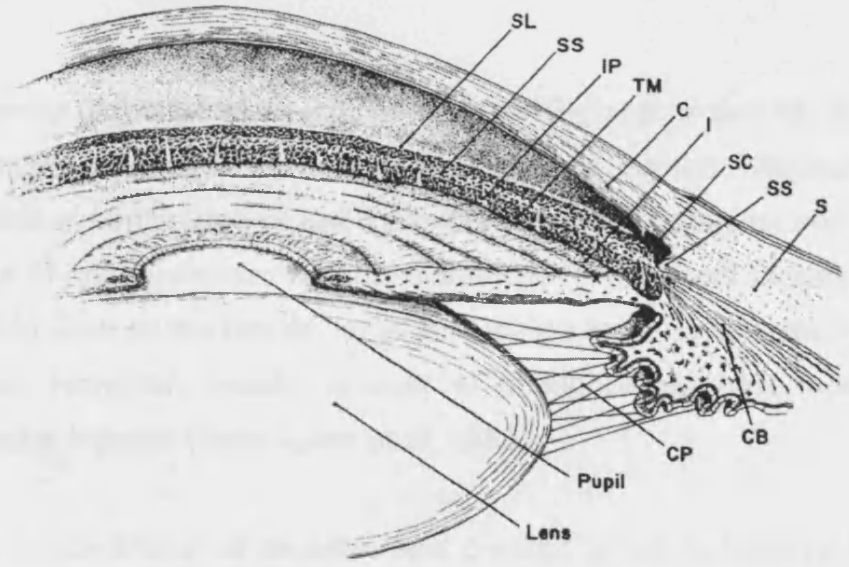

Fig. 1.2: Semi diagrammatic figure of the anterior segment. SL = Schwalbe's line SS= scleral spur, IP= iris process, TM= trabecular meshwork, C= cornea, I= iris, SC= Schlemm's canal, S= sclera, CB= ciliary body & CP= lens zonule (Bron, Tripathi *et al.* 2001).

1.2.1 Aqueous Humour

Aqueous humour has two important functions. Firstly, it is the medium by which the necessary metabolites are transported to the avascular lens and cornea. It also removes toxic metabolic waste products of the cornea and iris. Secondly, it has a hydromechanical function in controlling the intraocular pressure.

1.2.2 Aqueous Humour Composition

99% of aqueous humour is water. Aqueous humour composition undergoes continuous exchange of ionic and soluble substances across the vitreous, lens, cornea and iris. Aqueous contains ions which preserves its electric neutrality and also buffers metabolic acids that it contains (Kong, Chan *et al.* 2002).

Due to the existence of the blood aqueous barrier (BAB), large molecular and charged substances are unable to access the aqueous humour. Aqueous humour has a higher percentage of low molecular weight substances and a lower percentage of high molecular weight substances than plasma (Tripathi, Millard *et al.* 1989). Due to the barrier, large lipid molecules cannot enter the aqueous humour. However, minute amount of phospholipids have been detected in aqueous humour (Jahn, Leiss *et al.* 1983).

There is a large concentration of ascorbic acid present, which is believed to protect the eye from the harmful effects of sunlight (Koskela, Reiss *et al.* 1989). Some amino acids are present in higher concentration than in plasma, such as, arginine, leucine, isoleucine, methionine, phenylalanine and valine, which are transported into the aqueous via ciliary epithelium (Durham, Dickinson *et al.* 1971; Hayasaka, Yamada *et al.* 1997)). Trace components present in the aqueous include sex hormones, plasminogen activator, cytokines such as fibroblast growth factor (FGF) and transforming growth factor β (TGF-β) (Tripathi, Millard *et al.* 1989).The existence of such factors and other chemokines, suggest the aqueous also plays a role in the immune response (El-Asrar, Struyf *et al.* 2004).

Numerous enzymes are also present in the aqueous, such as antioxidants and lysosomal enzymes (Ferreira, Lerner *et al.* 2004). Studies have been carried out to test the presence of MMPs and their inhibitors in aqueous. The presence of MMP 1, 2, 3, 7 and 9 were detected (Huang, Adamis *et al.* 1996). Alongside this the presence of TIMP 1 and TIMP 2 was also established (Schlotzer-Schrehardt, Lommatzch *et al.* 2003).

1.2.3 Aqueous Production

The rate of aqueous humour production is 2μl/min (Brubaker 1982). However, this rate does fluctuate. The rate tends to be higher in daytime than at night time (Brubaker 1991). Normally the entire fluid is replaced every 100 minutes (Lawrence 1997).

Aqueous humour is formed in the epithelial cells in the ciliary body. The ciliary body is formed from ciliary muscles and ciliary processes surrounded by a microvasculature system. Ciliary processes project into the posterior chamber and the ciliary muscle is composed of bundles of smooth muscle cells embedded in connective tissue (Ockland 1998). Each ciliary process consists of a pigment layer which is continuous with the retinal pigment epithelium (RPE) and non pigment layer (NPE) which continues with the neuroretina. The BAB is formed by tight junctions between adjacent cells of the non pigment layer.

There are three main transport pathways used in order to produce aqueous:

1. **Diffusion** - The passive movement of solutes across the cell membrane in response to the concentration gradient. For example bicarbonate moves across BAB by diffusion (Eid and Spaeth 2000).
2. **Ultrafiltration** - This involves the passive movement of water and water soluble substance in response to the differential hydrostatic pressure in blood and the osmotic pressure in the ciliary body (Green and Pederson 1972; Roepke and Hetherington 1940).

3. **Active transport** – This accounts for 80% of aqueous production (Kanski, McAllister *et al.* 1996) and is due to energy-dependent movement of solutes across the cell membrane. NPE ciliary cells undergo an active metabolic process that depends on several enzyme systems. The most important enzyme involved is Na+/ K+ ATPase. This secretes Na+ ions into the posterior chamber and at the same time K+ into NPE cells (Fig. 1.3). The high concentration of Na+ causes an osmotic pressure difference across the ciliary epithelium, due to which water and negative ions (e.g. bicarbonate and chloride ions) move out (Jacob and Civan 1996). Ascorbic acid and amino acids are also actively transported across the BAB (Kong, Chan *et al.* 2002).

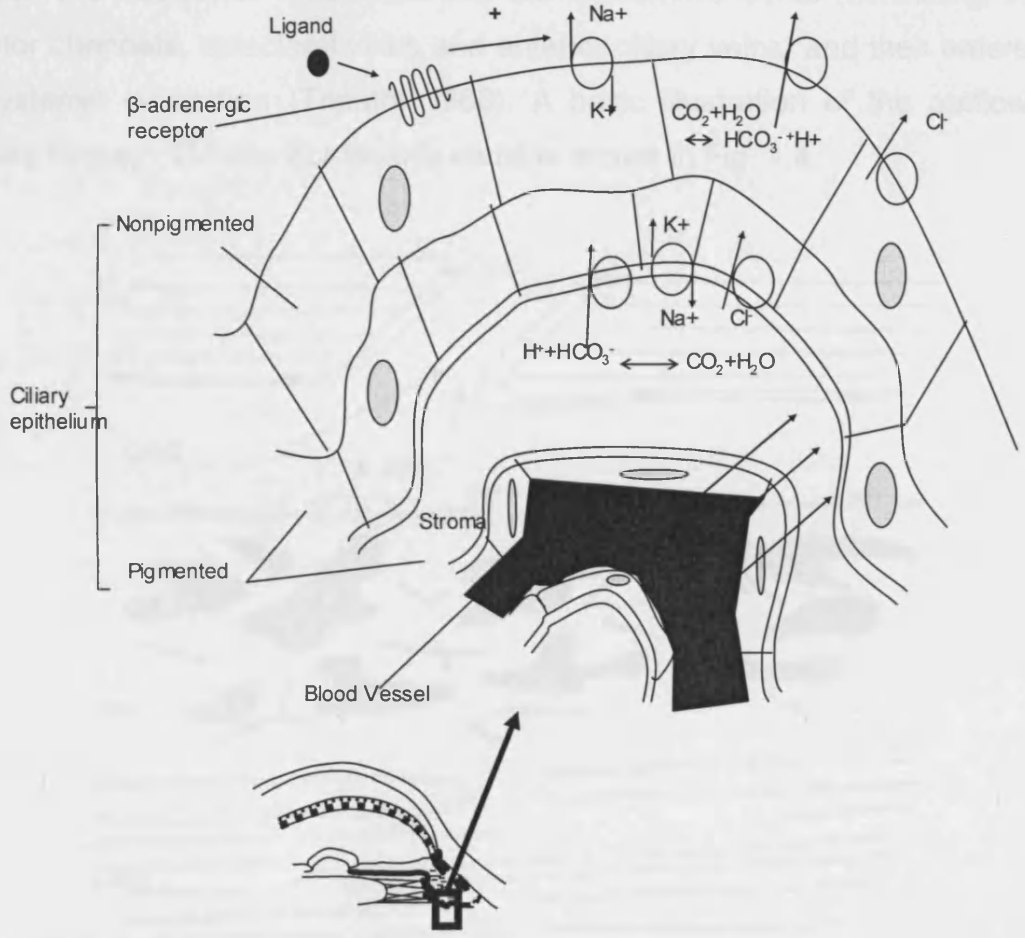

Fig. 1.3: Ion and water transfer and active transport across ciliary epithelium cells, leading to aqueous production (Forrester, Dick *et al.* 1999).

1.2.4 Aqueous Drainage

Primary aqueous is produced by the ciliary epithelium which enters the posterior chamber, where its concentration is altered to produce secondary aqueous, by either reabsorption or by addition of metabolites and other components from surrounding tissues. The secondary aqueous passes through the pupil into the anterior chamber and leaves the eye by two main routes: the Canal of Schlemm or the uveoscleral outflow pathway.

1.2.4.1 Canal of Schlemm

The route via the Canal of Schlemm is the conventional outflow pathway. It involves the movement of aqueous humour through the extracellular spaces between the trabecular meshwork into the Schlemm's canal (consisting of collector channels, episcleral veins and anterior ciliary veins) and then enters the systemic circulation (Tripathi 1968). A basic illustration of the outflow pathway through TM into Schlemm's canal is shown in Fig. 1.4.

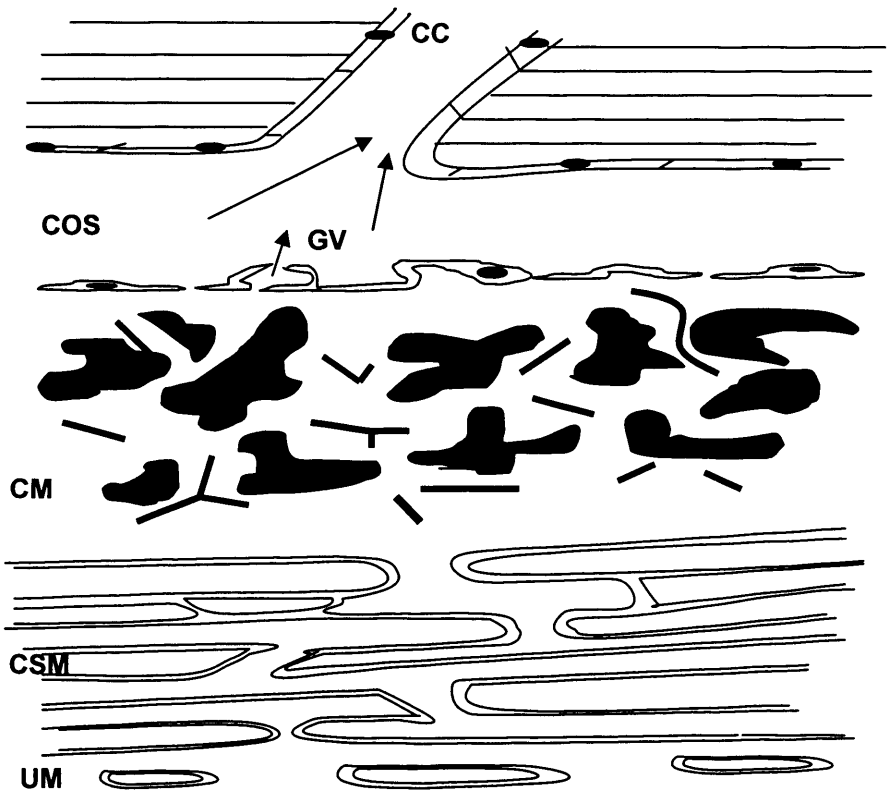

Fig. 1.4: Aqueous outflow via trabecular meshwork and canal of schlemm. CC = Collector channel, COS = canal of schlemm, GV = giant vacuole, CM = Cribriform meshwork, CSM = Cornescleral meshwork, UM = Uveal meshwork (reproduced from (Lawrence 1997).

The trabecular meshwork (TM) via which the aqueous humour travels consists of three layers:

1. Uveal Meshwork

This is the innermost layer of the TM. It forms an irregular net-like structure compromising 1-3 layers of cord-like trabecular beams. Aqueous passes freely through the pores between the uveal trabecular (Bill and Svedbergh 1972).

2. Corneoscleral Meshwork

This is formed from several layers of flattened trabecular sheets extending from scleral spur to the cornea. Perforations between successive sheets allows aqueous passage (Tripathi 1974a; Tripathi 1974b).

3. Cribriform Meshwork

This is the outermost layer beneath the Canal of Schlemm and it forms a sieve-like structure containing a network of elastic-fibres (Rohen, Futa *et al.* 1981). Unlike the rest of the meshwork, this layer is not arranged in lamellae, but consists of trabecular cells meshed in a loose extracellular matrix (ECM). The space between the cells has a high concentration of elastin and type VI collagen, alongside which fibrilin-1, fibronectin, decorin, vitronectin, tenascin, veriscan and hyaluronic acid can also be found (Ueda, Wentz-Hunter *et al.* 2002).

Aqueous humour passes from the anterior chamber through the intertrabecular and intratrabacular spaces, which are lined by the trabecular cells. These spaces get narrow closer towards the Canal of Schlemm. The trabecular cells are also phagocytic; they trap and remove debris from the aqueous humor as it percolates towards the Canal of Schlemm. They remove endogenous particulate matter e.g. melanin granules and cellular debris.

The Canal of Schlemm is an endothelial-lined channel filled with aqueous humor. It has a length of about 200-400μm and depth of 50- 60μm (Forrester,

Dick *et al.* 1999). The wall of the Canal of Schlemm consists of elongated cells; 75μm long and 4μm wide. Between these cells and on the surface of these cells, there are pores. Aqueous humor passes through these pores (Sampaolesi and Argento 1977). The bulk aqueous humor outflow resistance occurs at this inner wall of the Schlemm's canal (Johnson 2006; Johnson and Kamm 1983). The collapse of the Canal of Schlemm at high IOP, has been linked to primary open angle glaucoma (Nesterov 1970). A reduction in the number of these cells and giant vacuoles with age have been denoted in previous research (Grierson, Howes *et al.* 1984).

The canal has 25 to 30 collector channels and between 2 and 8 aqueous veins (Dvorak-Theobald 1934). The collector channels join intrascleral and episcleral venous plexi, which drain into conjunctival veins (Batmanov 1968).

The trabecular outflow pathway is largely a pressure-dependent route of aqueous humour drainage. This can be explained by the description of aqueous humor movement though the Canal of Schlemm. There are giant vacuoles at the inner wall of the Canal of Schlemm (0.5- 4.0 um in diameter) within endothelial cells (Lawrence 1997). Many of these vacuoles have openings towards the TM side, and some have openings on both sides. Aqueous humor passes through the Canal of Schlemm via these vacuoles. The number and size of vacuole openings increases with IOP increase.

1.2.4.2 Uveoscleral outflow pathway

This pathway was first discovered in 1965 when labelled ^{131}I-albumin was injected into the anterior chamber of cynomologus monkey and then recovered within the uveal tract and sclera (Weinreb 2000). A more recent publication involved the characterisation of this pathway using a dextran fluorescent label within the mouse (Lindsey and Weinreb 2002). As there is no epithelial barrier between the anterior chamber and the ciliary muscle, aqueous humor can move through the anterior surface of the ciliary body opposite the root of the iris and the scleral spur (Nilsson 1997). It then passes through the intracellular spaces between ciliary muscle fibres. These spaces

have communication with supraciliary and suprachorodial spaces, which ultimately connect to episcleral vasculature (Bill 1965). They connect either via tortuous pathways between collagen fibrils of the sclera or more directly, through loose connective tissue around blood vessels and nerves which penetrate the sclera (Lawrence 1997). Fig. 1.5 is an illustration of this pathway.

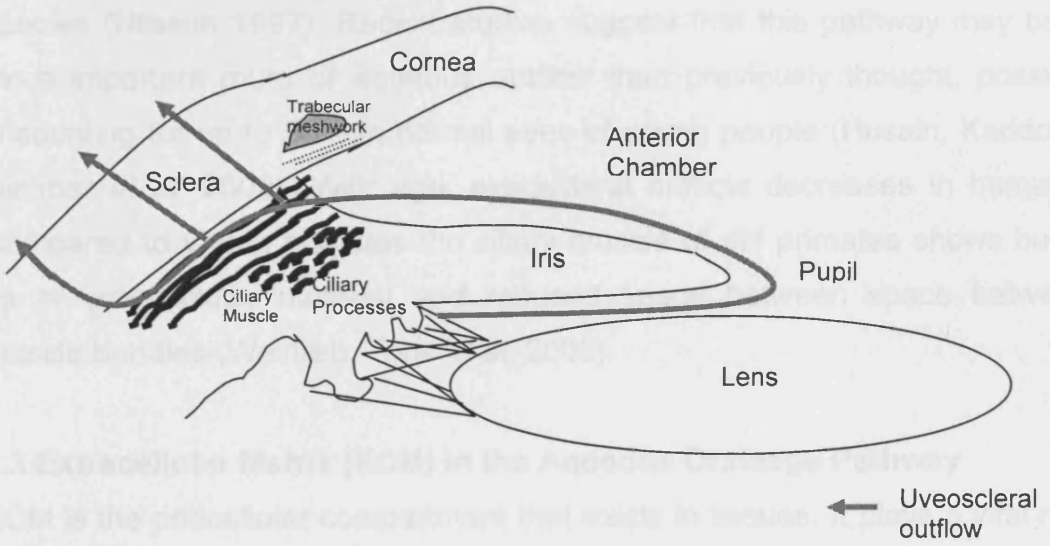

Fig. 1.5: Uveoscleral outflow pathway.

The uveoscleral outflow pathway is the non-conventional pathway which is not a pressure sensitive pathway (Alm 2000). The explanation for the uveoscleral outflow not being pressure sensitive is best understood if the pathway is considered as two routes, coupled in series. The first is from the anterior chamber to the suprachoridal space, the second from the suprachoridal space into the orbit (Alm 2000). IOP increases the pressure gradient in the suprachoridal space. However, the pressure gradient for the first part of the pathway will not increase; consequently the flow in the suprachoridal space will not increase. The flow through the sclera will increase, but the fact that total uveoscleral flow does not increase with higher IOP indicates that the first step, movement into the suprachoridal space, is the rate limiting step (Alm 2000).

Uveoscleral pathway may serve as the functional equivalent of a lymphatic drainage pathway, providing an exit route from the uvea for larger proteins and other tissue constituents (Weinreb, Toris *et al.* 2002). Rerouting aqueous humour outflow from a compromised or obstructed trabecular meshwork may serve to prevent or dampen the IOP rise, and to rid the uvea of the excess protein and cellular debris.

The extent at which this pathway is used varies from 3% to 60%, in different species (Nilsson 1997). Recent studies suggest that this pathway may be a more important route of aqueous outflow than previously thought, possibly accounting for up to 50% in normal eyes of young people (Husain, Kaddour-Diebbar *et al.* 2002). With age, uveoscleral outflow decreases in humans. Compared to young primates the ciliary muscle of old primates shows build-up of extracellular material and reduced space between space between muscle bundles (Weinreb, Toris *et al.* 2002).

1.3 Extracellular Matrix (ECM) in the Aqueous Drainage Pathway

ECM is the pericellular compartment that exists in tissues. It plays a vital role in cell shape formation; cell migration; differentiation and control on cell growth hormones. ECM consists of three main structural features:

1. **Fibrous protein:**

- Collagen: These are a large family of proteins with a triple helical structure which confers rigidity. They provide mechanical support to the ECM and surrounding cells.
- Elastin: These are a group of proteins with rubber-like elastic properties, which allows them to provide elasticity and resilience within ECM.

2. **Glycoprotein:**

A group of proteins covalently associate with carbohydrates to form glycoprotein. Glycoproteins are involved in mediating cellular interactions with collagenous structure and ECM organisation e.g. fibronectin & laminin. Fibronectin not only interacts with other ECM molecules to form a complex

ECM structure but, it is also involved in cell adhesion and migration. Laminin acts as an adhesion protein in basement membrane.

3. Proteoglycans & Polysaccharides:

Proteoglycans have a complex structure consisting of a core protein linked to Glycosaminoglycans (GAGs) e.g. aggrecan. The large molecules of proteoglycans provide comprehensive force around the cell. GAGs are polysaccharides formed from linear heteropolysaccharide possessing a characteristic disaccharide repeat sequence. GAGs such as hyaluronic acid associate with water molecules in order to create osmotic pressure and form a gel-like layer within ECM.

1.3.1 ECM in Ciliary Muscle

The extracellular fibrils synthesised by ciliary muscle cells are characteristically deposited in the region of the elongated ends of the bipolar muscle cells (Tamm, Baur *et al.* 1992). The fibrils form an apparent close transmembrane association with the cytoplasmic myofilaments and may be regarded as miniature muscle cell-tendon junctions providing anchoring function. The interaction between ECM and muscle cells may play an important role in maintaining mechanical tension and supporting the shape changes of ciliary muscle during accommodation (Tamm, Baur *et al.* 1992). The major components of the ECM within ciliary muscle tissue are:

a) ***Collagen*** – Type IV, I, II and VI collagen have been characterised within ciliary muscle tissue (Ockland 1998; Rittig, Lutjen-Drecoll *et al.* 1990; Tamm, Baur *et al.* 1992). They are believed to allow interaction and anchoring support within ciliary muscle cells.

b) ***Glycoproteins*** - Laminins are found to form a pericellular network surrounding individual ciliary muscle cells. Alongside collagen IV, laminin is also essential for basal laminae function (Tamm, Baur *et al.* 1992). Fibronectin is a multi-functional glycoprotein which interacts directly with cells and ECM.

c) ***GAGs*** - Glycosaminoglycans in the connective tissue of ciliary muscle, involved in maintaining fluid homeostasis (Ockland 1998).

1.3.2 ECM of Sclera

Sclera is known to contain low cellularity within dense connective tissue. It plays a role in maintaining intraocular pressure and also in protecting intraocular structure and covers 80% of surface area of the globe (Svoboda, Gong *et al.* 1998). Scleral stability is vital for clear vision and is made possible by the organisation and viscoelastic properties of scleral connective tissue (Watson and Young 2004). The sclera is composed of three layers: the episclera (inner most layer), stroma and lamina fusca (adjacent to uvea). The episcleral layer consists of loosely arranged bundles of collagen, intermingled with fibroblasts, melanocytes, proteoglycans and glycoproteins and is rich in blood supply. The stromal layer has larger collagen bundles associated with few elastic fibres. The lamina fusca consists of smaller collagen bundles and more abundant elastic fibres and also of ciliary vessels and nerve passage routes (Foster 1994).

Collagen forms 75% of scleral dry weight consisting of collagen type I, III, V and VI. The most abundant collagen is type I collagen (Thale and Tillmann 1993). Elastin forms less than 2% of scleral dry weight (Moses, Grodzki *et al.* 1978). Proteoglycans form 0.7 to 0.9% of dry scleral dry weight (Rada, Shelton *et al.* 2006). The most abundant proteoglycans in sclera have been identified as chondroitin and keratan sulphates (Rada, Achen *et al.* 1997). Immunoassay and western blotting revealed the presence of aggrecan, biglycan and decorin as the major scleral proteoglycans (Rada, Achen *et al.* 1997).

Changes in scleral connective tissue extracellular matrix have been associated with diseases such as rheumatoid arthritis, scleritis and more the commonly observed myopia (Watson and Young 2004). These diseases involve scleral thinning, via reduction of extracellular matrix components (Lachmann, Hazleman *et al.* 1978; Rada, Shelton *et al.* 2006). Selective connective tissue remodelling occurs within the scleral tissue in these disease states.

1.3.3 Age Related changes in ECM of Uveoscleral outflow pathway

The anterior part of the ciliary muscle exhibits an age-related increase in "plaque material", which is even more pronounced in primary open angle glaucoma (Tamm, Baur *et al.* 1992). Type VI collagen is involved in forming a sheath which surrounds the anterior elastic tendon between the ciliary muscle and trabecular meshwork, these sheaths thicken with age and form part of this "plaque material".

Scleral tissue reaches its maximum elasticity at the age of 12-13 years, after which a reduction in compliance and an increase in rigidity is observed, as a result of progressive cross-linking of lysine residues of collagen (Watson and Young 2004). A reduction in Type I and III collagen mRNA with age in mice eye has been reported, however immunoassays revealed a widespread distribution of protein, suggesting a slow turnover of matrix components (Ihanamaki, Salminen *et al.* 2001). This stability of collagen molecules could be related to increased collagen glycosylation and its resistance to solubilisation observed with aging (Keeley, Morin *et al.* 1984). Collagen fibres become thicker and less uniform with age. A disruption in collagen causes calcium deposition which leads to hyaline plaques (Watson and Young 2004).

Uveoscleral outflow decreases with age. Compared to young primates ciliary muscle of old primates showed a build up of extracellular material and therefore there is a reduction in space between muscle bundles (Gabelt and Kaufman 2005). The plaque formation in the sclera can also reduce aqueous outflow. As there is a reduction in uveoscleral outflow, this would mean there

is a reduction in exit route of large proteins and other tissue constituents. The build up of debris and large proteins would effect the trabecular meshwork and hence the conventional pathway. The phagocytic property of trabecular meshwork cells would be exceeded (Lawrence 1997). The reduction in aqueous outflow via both routes can cause a build up of IOP.

This project investigates possible methods to find lower IOP in glaucoma, via clearing blocked drainage pathway via ECM degradation.

1.4 ECM Degradation

ECM metabolism involves complex pathways in controlling ECM biosynthesis and degradation. These pathways are very tightly controlled in order to prevent disease states. The pathways involve numerous enzymes. ECM degradation involves different enzymes that specifically degrade certain components of the ECM. The main group of enzymes involved in matrix degradation are metalloproteinases (MMPs).

1.4.1 Matrix Metalloproteinases (MMPs) in the Uveoscleral Outflow Pathway

MMPs compromise a large ever growing family, with more than 20 proteolytic enzymes (Nelson, Fingleton *et al.* 2000). There are four main groups of MMPs involved in the site-specific cleavage of different ECM components; these are shown in Table 1.4.

Enzyme	MMP Example	Function
Collagenases	MMP-1	Unwind helical collagen fibre which forms denatured gelatin, which is susceptible to enzymatic cleavage by other MMPs and other protease.
Gelatinases	MMP-2 & MMP-9	Gelatinases are involved in degrading basement membrane, and also have high enzymatic activity towards denatured collagen.
Stromelysins	MMP-3	Stromelysins have broader substrate specificity. Substrates include fibronectin, proteoglycan, laminin and type IV collagen.
Membrane-type MMPs	MMP-14	This group of MMPs are involved in cleaving collagen (I, II and III), fibronectin and laminin.

Table1.4: Different types of MMPs and their function (Wong, Sethi *et al.* 2002)

1.4.2 MMP Homology

The above groups are classified due to their substrate specificity and enzyme structure. All MMPs have a similar domain structure, with a "pre" region to target for secretion, a "propeptide" region to maintain latency, and an active catalytic region that contains the zinc-binding active site (Fig. 1.6) (Nelson, Fingleton *et al.* 2000). The majority of MMPs have additional domains, these additional domains are important in substrate recognition and in inhibitor binding. Substrate specificity by MMP is very selective as has been demonstrated in the case of the selective hydrolysis of the triple helical structure by MMP2 (Lauer-Fields, Sritharan *et al.* 2003).

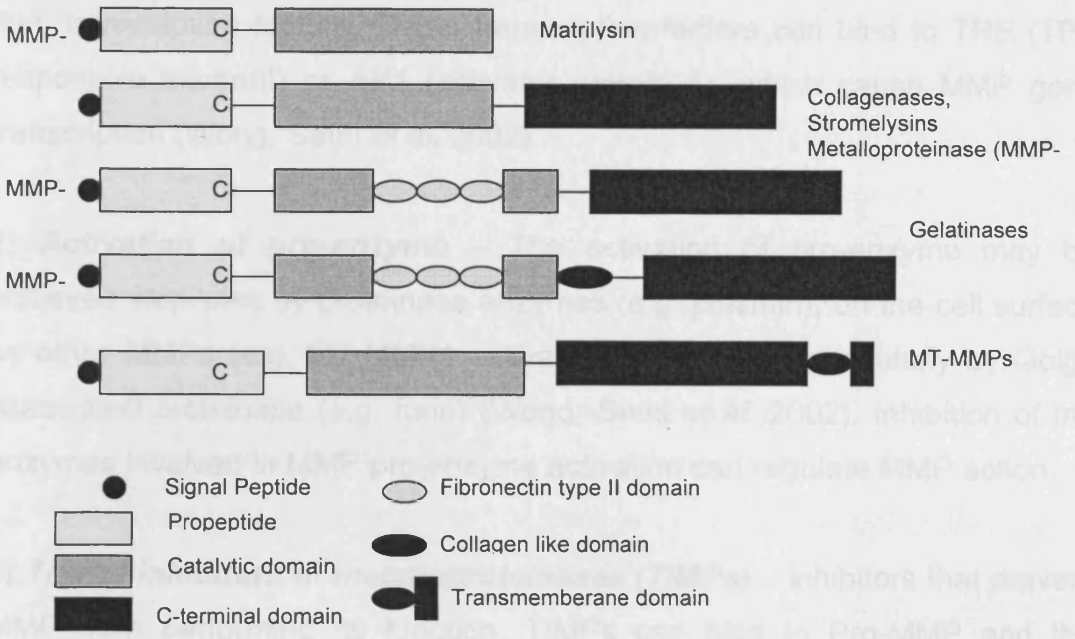

Fig. 1.6: MMP domain structure (Wong, Sethi *et al.* 2002).

1.4.3 MMP Synthesis and Activation

MMPs are synthesised by cells and secreted into the ECM or remain membrane-bound (membrane type MMP) as an inactive zymogen (Nelson, Fingleton *et al.* 2000). A 5' sequence of the proenzyme is critical in activating the enzyme (Gunja-smith, Nagase *et al.* 1989). The enzymes are activated by proteolytic processing, by other MMPs (e.g. stromelysin-1 can activate procollagenase) or by other proteases (e.g. plasmin activation of pro-stromelysins) (Nelson, Fingleton *et al.* 2000). MMPs are zinc-dependent enzymes and require calcium for full activity (Huang, Adamis *et al.* 1996).

1.4.4 Regulation of MMP action

Regulation of MMP action is very important in order to maintain tissue function. MMPs have been known to be involved in disease such as arthritis and cancer (Fossang, Last *et al.* 1996) (Nelson, Fingleton *et al.* 2000), where there is an imbalanced regulation of MMP action. MMP action can be regulated at three stages:

1) ***Transcription*** – The activation of transcription regulatory elements are controlled by hormones, growth factors and inflammatory cytokines. These factors effect MMP gene expression by activating or deactivating c-Fos and c-

Jun, transcription factors. These transcription factors can bind to TRE (TPA responsive element) or AP1 (activator protein 1), which cause MMP gene transcription (Wong, Sethi *et al.* 2002).

2) ***Activation of pro-enzyme*** – The activation of pro-enzyme may be achieved step-wise by proteinase enzymes (e.g. plasmin), on the cell surface by other MMPs (e.g. MT-MMP1 activate MMP2), or intracellularly by Golgi-associated proteinase (e.g. furin) (Wong, Sethi *et al.* 2002). Inhibition of the enzymes involved in MMP pro-enzyme activation can regulate MMP action.

3) ***Tissue inhibitors of metalloproteinases (TIMPs)*** – inhibitors that prevent MMP from performing its function. TIMPs can bind to Pro-MMP and the activated form of MMP. There are four different TIMPs (TIMP 1, 2, 3, 4) (Lan, Kumar *et al.* 2003). The concentration of MMP and TIMP in effect determines the rate of MMP activity (Lan, Kumar *et al.* 2003).

1.4.5 Distribution of MMPs and TIMPs in uveoscleral pathway

The distribution of MMPs and TIMPs in the iris and ciliary body has been established (Lan, Kumar *et al.* 2003). The presence of MMP1, 2, 3 & 9 and TIMP 1 – 4 were localised by immunoassay. The intensity of staining for MMP 1, 2, 3 & 9 and TIMP 1 – 4 was greater in the ciliary body compared to the iris. Patterns of intensity of the staining in the (a) ciliary body: non-pigmented epithelium>ciliary muscle>pigmented epithelium>stromal cells and (b) in the iris was: anterior border>anterior epithelium> stromal cells> posterior epithelium (Lan, Kumar *et al.* 2003).

1.5 The Role of MMPs & TIMPs in IOP reduction in Uveoscleral Outflow

All the treatments given to glaucoma patients have associated risks and/ or side effects. Due to this, research is continuously being carried out to find safer and more effective agents to treat glaucoma. Previous studies have suggested that remodelling of ECM of the ciliary body may help contribute to reduction in IOP (Weinreb, Toris *et al.* 2002). The reduction in IOP with prostaglandin derivatives is observed within 6 hours and upto 33.4%

reduction in IOP by three months (Hepsen and Ozkaya 2007). However, with a cyclodialysis cleft a greater reduction in IOP can be obtained within 2 days (Toris and Pederson 1985). Therefore, further study and understanding of ECM degradation within the aqueous drainage pathway is required to improve glaucoma treatment.

Latanoprost (a prostaglandin analogue), is a drug that brings about a significant increase in optical density in the iris root, ciliary muscle and adjacent sclera (Gaton, Sagara *et al.* 2001). Prostaglandins and their analogues show minimal effect on the BAB, and so limit adverse effects such as inflammation (Toris, Camras *et al.* 1997).

Prostaglandins bind to receptors. There are different receptor subtypes (EP, EP_2, FP) to bind to in human sclera (Anthony, Lindsey *et al.* 2001). However, to lower IOP it binds to $F_{2\alpha}$ receptor (Sagara, Gaton *et al.* 1999). Once bound to its receptor, it activates a G-protein activation cascade, which then enhances cyclic AMP production and increases intracellular calcium (Zhan, Camras *et al.* 1998) (Schachtschabel, Lindsey *et al.* 2000). The calcium released activates c-Fos (proto-oncogene) and c-Jun (associated transcription factor for apoptosis) (Lindsey, To *et al.* 1994) (Umihara, Lindsey *et al.* 2002). C-Fos and c-Jun form a hetrodimer, which bind to AP1. AP1 is a transcription regulatory element which then causes MMP gene transcription (Schachtschabel, Lindsey *et al.* 2000).

Prostaglandins induce the expression of MMP 1, MMP 2, MMP 3 and MMP 9 within ciliary muscle (Weinreb and Lindsey 2002). MMP1 is involved in cleaving collagen I and III and MMP3 cleaves collagens IV, IX, XI and fibronectin (Weinreb and Lindsey 2002). The reduction of ECM components, within spaces between ciliary muscle fibre bundles, adjacent to the cells, increases permeability within the uveoscleral pathway (Kim, Lindsey *et al.* 2001). Due to the increase in space within the ciliary muscle ECM and relaxation of the ciliary muscle, a reduction in hydraulic resistance in the uveoscleral outflow pathway is seen (Wong, Sethi *et al.* 2002). Prostaglandins

also increase the ability of cells to convert plasminogen to plasmin, an enzyme required to activate MMP (Ockland 1998).

AP1 also binds to the TIMP gene (Anthony, Lindsey *et al.* 2002). Previous experiments carried out showed that prostaglandins are also involved in enhancing TIMP 1 gene expression (Anthony, Lindsey *et al.* 2002). TIMP induction is similar to that of MMP induction with prostaglandin treatment. This shows how prostaglandin action prevents total degradation of ECM within the uveoscleral pathway. TIMP 1 is believed to have a major role to play in regulating MMP activity in human ciliary muscle tissue (Anthony, Lindsey *et al.* 2002).

1.6 Drug Delivery in the Eye

Drug delivery in the eye involves the development of a controlled and optimised delivery of the drug to its target tissue in the eye. It order to obtain this, many properties of the drug should be considered, such as lipophilicity, solubility, molecular size and shape, charge and its degree of ionisation (Bourlais, Acar *et al.* 1998). These factors influence the route and rate of delivery. There are many barriers to be considered in drug delivery in the eye:

(1) Drug loss at ocular surface with lacrimal fluid (Urtti and Salminen 1993).
(2) Corneal barrier: stroma being highly hydrophilic and corneal epithelium form tight junctions restricted drug permeability (Huang, Adamis *et al.* 1996).
(3) Blood-occular barrier. This includes blood-aqueous barrier and blood-retina barrier (Urtti 2006).

90% of drug delivery to the eye involves the use of topically administered drug. The advantages of topical drug administration include patient simplicity and ease of manufacturing. Topical drug administration is accomplished by eye drops, but they have short contact time with the eye surface. The contact and duration of drug action can be improved by the use of, suspensions, ointments or gels and mucosadhesive polmers systems (Ali and Lehmussaari

2006). However, peak concentration in the anterior chamber is reached after 20-30minutes, but this concentration is often 2 orders of magnitude lower than the instilled concentration even for lipophilic compounds (Urtti, Pipkin *et al.* 1990). This suggests the need to administer a high concentration of drug in order maintain drug action.

In order to gain direct drug entry into the eye subconjunctival injections could be used. This involves injecting drug into subconjuctival area, underneath the eyelid. The drug then penetrates across the sclera. The sclera is more permeable to macromolecules and is not dependent upon drug lipophilicity, unlike the cornea (Jiang, Geroski *et al.* 2006). However, in reaching the posterior eye, drug has to pass through choroids and retinal pigment epithelium (RPE). Its most likely that drug loss occurs via the blood stream of the choroids, and the RPE forms a tight barrier to hydrophilic compounds (Pitkanen, Ranta *et al.* 2005).The delivery of drug directly into the vitreous via intravitreal administration, allows direct access to the vitreous and retina. However, again the movement of molecules from the vitreous into the choroids is hindered by RPE barrier. The vitreous itself restricts the movement of large molecules, especially positively charged (Pitkanen, Ruponen *et al.* 2003).

1.6.1 Posterior Drug delivery

Choroidial neovascularisation in diseases such as glaucoma, age-related macular degeneration (AMD) and diabetic retinopathy require the delivery of drugs to the posterior pole. The treatments include monoclonal antibodies and aptamer oligonucleotides against the neovascular growth in AMD, antiviral for retinitis and neuroprotective agents for retinal degeneration for glaucoma. However, drug targeting and delivery to the posterior segment of the eye has proved difficult with many complications (Geroski and Edelhauser 2000; Kimura, Yasukawa *et al.* 2001). Topically administered drug does not reach posterior eye, systemic application causes adverse effect in non-targeted tissue and intravitreal application is an invasive method to deliver

drug (Ranta and Urtti 2006). This implies the need to develop a less invasive and longer acting drug delivery system.

1.6.2 Implication of study in drug delivery

The sclera and cornea form the main barrier in delivering an external factor to the back of eye. Due to the large scleral surface area, with variable thickness and its high permeability to macromolecules, sclera is a good target tissue via which factors could be delivered into posterior eye (Geroski and Edelhauser 2000). The manipulation of tissue involved in the uveoscleral outflow, i.e. sclera, to increase aqueous drainage via ECM degradation, could also play a role in improved drug delivery. An increase in scleral permeability could enhance drug delivery into the eye.

1.7 Aims of the Project

Previous studies have linked MMP expression to glaucoma as its level rises when prostaglandin treatment is applied (Gaton, Sagara *et al.* 2001). However, this may be a side effect of prostaglandin action. Based on the knowledge and understanding obtained my hypothesis is that direct action of MMP could improve uveoscleral outflow and drug delivery to the posterior pole. The aims of the project are:

- To identify methods suitable to analyse the effect of different inducers of MMPs (i.e. growth factors and prostaglandin) on MMP and TIMP levels within the human uveoscleral outflow pathway (ciliary muscle cells and scleral fibroblasts).
- To determine the impact of MMP upregulation on tissue permeability.
- To determine the effect of MMP upregulation on tissue structure.

CHAPTER 2

METHODS

CHAPTER 2

METHODS

2.1 Materials

Chemical reagents – chemicals used are listed in appendix (section 8.1) together with their source.

Solutions and media – solutions and media used are listed in appendix (section 8.2). All cell culture solutions and media were prepared using double distilled water and were either sterilised using filtration through a 0.2um filter or autoclaved.

Cell culture materials and equipment – materials used for culture, if not filter sterilised, were autoclaved prior to use apart from disposable items, which were purchased sterile. All culture manipulations were carried out aseptically, in a class II biological safety cabinet. Cell cultures were maintained at 37°C in a standard incubator within a humidified atmosphere containing 5% CO_2 and 95% O_2 air unless otherwise stated.

2.2 Characterisation of the Uveoscleral Outflow Pathway

Anterior chamber sections were viewed in order to locate the structures involved the uveoscleral outflow pathway. The immunolocalisation of PGF2α receptors and MMP 2 was conducted on cells cultured from the uveoscleral pathway.

2.2.1 Source of Tissue

All samples were obtained following consent for research purposes in accordance with the ethical guidelines of United Kingdom Transplant Service (UKTS) and the declaration of Helsinki. Initial human donors for immunolocalisation assays were obtained from National Disease Research Interchange (NDRI) Philadelphia, USA (see appendix for donor details). The globes were enucleated and fixed in 10% neutral buffered formalin (NBF) within 12 hours post-mortem. The remaining experiments involved the use of

human donor eye globes, aged 50-89 years (see appendix for donor details, section 8.3), and obtained within 48 hours post mortem from the Corneal Transplant Service Eye Bank (Bristol, UK) after corneal removal for transplant purposes. Globes were transported at 4°C in moist chambers. All donors were considered normal, without any previous ocular disease. Bovine skin was obtained from the abattoir within 6 hours of death, and transported on ice.

2.2.2 Wax Sections of Human Anterior Chamber

The cornea was removed and the anterior segment was detached from human donors and fixed in neutral buffered formalin (NBF). The anterior segment was sectioned into 4 quarters and wax embedded. Wax embedding involved immersing the tissue sections through a series of increasing alcohol concentrations: first 30 minutes in 50% alcohol in ddH_2O, followed by 1 hour in 70% alcohol, 1 hour in 90% and 1 hour in 100% alcohol. After a further 30 minutes in 100% alcohol the tissue sections were immersed in a solution contained 50% alcohol and 50% xylene for 30 minutes. The tissue then underwent two successive 30 minutes washes in 100% xylene. The tissue sections were then placed into hot vials containing wax and placed into an incubator 60°C for 1 hour followed by another 30 minutes in fresh wax. The tissue sections were then placed into moulds containing warm wax and placed on a cold plate for 30 minutes to set. Wax embedded tissue blocks were stored at 4°C before undergoing sectioning via a microtome (HM 325, Microm, Germany). Sections were cut at 7μm and transferred onto superfrost plus slides (Lamb Laboratories).

2.2.3 Morphological staining of anterior chamber

Two different morphological staining methodologies were applied to human anterior chamber wax sections (1) Toluidine Blue: quick and stained all general structures blue and (2) Haematoxylin and Eosin stain (H&E stain): haematoxylin stained nucleic acid blue and eosin stained cytoplasmic components, in cells, pink. The wax tissue sections were cleared in xylene and rinsed in industrial methylated spirit (IMS) before being stained. The

washes involved two 5 minutes xylene, two 1 minute washes in 100% IMS, followed by 1 minute in 90%, 70% and 50% IMS.

Toluidine blue involved staining sections very briefly (30 seconds) in toluidine blue stain and thereafter rinsed in tap water for 10 minutes. Whereas H&E stain involved 5 minutes in Haematoxylin, 10 minutes wash in running tap water, 2 minutes in Eosin and a further 10 minutes wash in running tap water. The sections were then dehydrated in graded alcohols (1 minute 50%, 70%, 90% IMS followed by two 1 minute washes in 100% IMS). The sections then underwent two 5 minutes washes in xylene. The sections were mounted using histomount and the slides were viewed by a Leica DMRA2 microscope. Images were captured using Q-Win Leica image analysis software.

2.2.4 Human Scleral Fibroblast (HSF) Cell Culture

Muscles and fat were removed from human donors in order to expose the sclera. The scleral tissue was then removed with the help of forceps and scissors. After scraping clean the internal and external surface of the sclera with a scalpel blade it was dipped in and out of 3% betadine followed by PBS. The sclera was then cut with a scalpel into small explants, 1mm^2 approximately. The explants were placed into six well plates. Foetal calf serum (FCS) was applied to each explant. The plates were left in the incubator overnight at 37°C under standard conditions (5% CO_2/ 95%O_2) to allow explants to adhere to the surface of the plate.

The following day, medium was added to each well and explants were cultured for a further week. Medium for scleral fibroblast culture consisted of 1:1 Ham's F-10 and DMEM containing 20% FCS, 1% antibiotics cocktail (containing 10mg/ml streptomycin sulphate, 10mg/ml kanamycin, 6mg/ml penicillin-G,), 2mM glutamine and 2.5mg/ml amphotericin B. Culture media was renewed every 3 to 4 days. Once the outgrowth of cells was detected the explants were removed. Cells were fed with fresh media every 3 or 4 days. Fig. 2.1 demonstrates the outgrowth of scleral fibroblasts from explants. When confluent (approximately 30-50 days) cells were sub-cultured and

placed into 25ml culture flasks (see section below). Following sub-culture the medium was changed twice weekly.

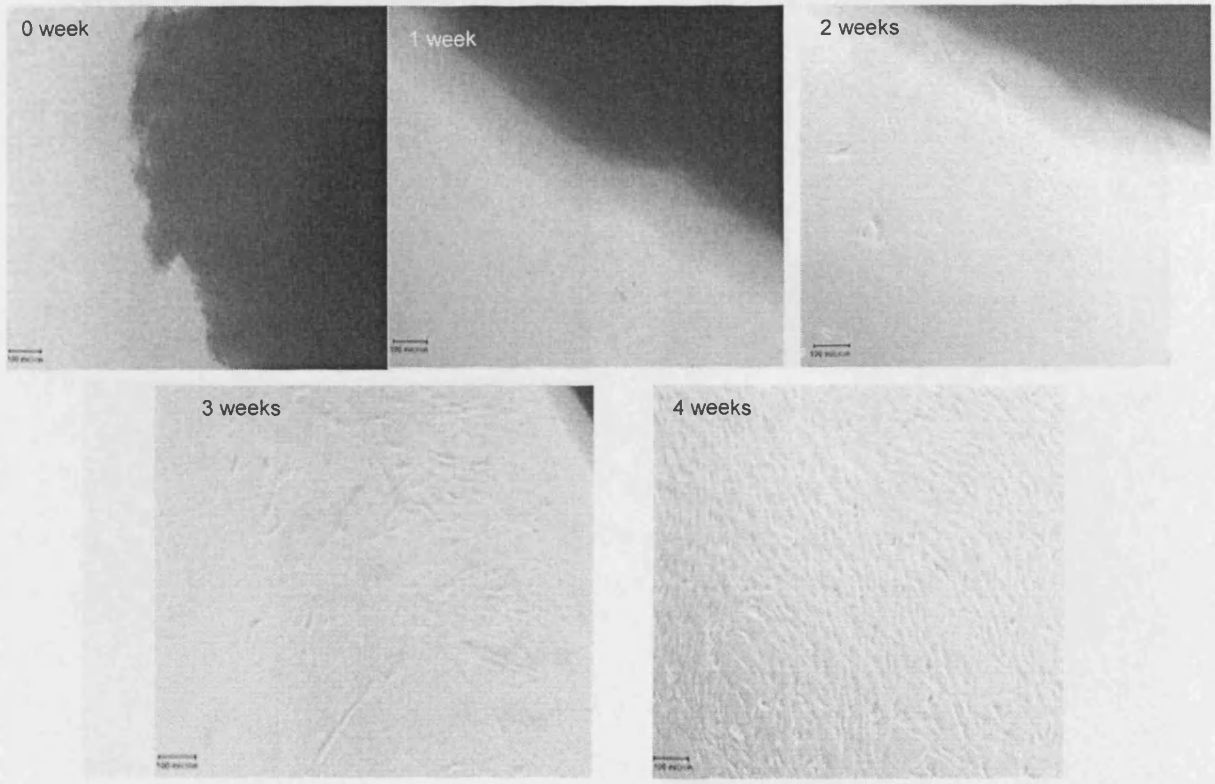

Fig. 2.1: Human scleral fibroblasts growth from explants cultured. The fibroblasts grew out of explants by 2 weeks, and achieved confluence by 4 weeks.

2.2.5 Human Ciliary Muscle Cell Culture

After removing the cornea, the iris, ciliary body (including the ciliary muscle) and lens were carefully dissected from the globe using of forceps and scissors. Ciliary muscle was then carefully dissected from the tissue. Small explants of ciliary muscle were cultured in six well plates in 250μl media: containing 1:1 DMEM and Ham's F12 with 10% FCS medium, 1% antibiotics cocktail (containing 10mg/ml streptomycin sulphate, 10mg/ml kanamycin, 6mg/ml penicillin-G,), 2mM glutamine and 2.5mg/ml amphotericin B. The cells were cultured at 37°C under standard incubator conditions (5% CO_2), overnight. The next day medium was added to cover the well. Following outgrowth of cells at approximately, 1 week, the explants were removed and the media was changed twice a week (Fig 2.2). When confluent (approximately 20-40 days) cells were sub-cultured and placed into 25ml

culture flasks (see section below). Following sub-culture the media was changed twice weekly.

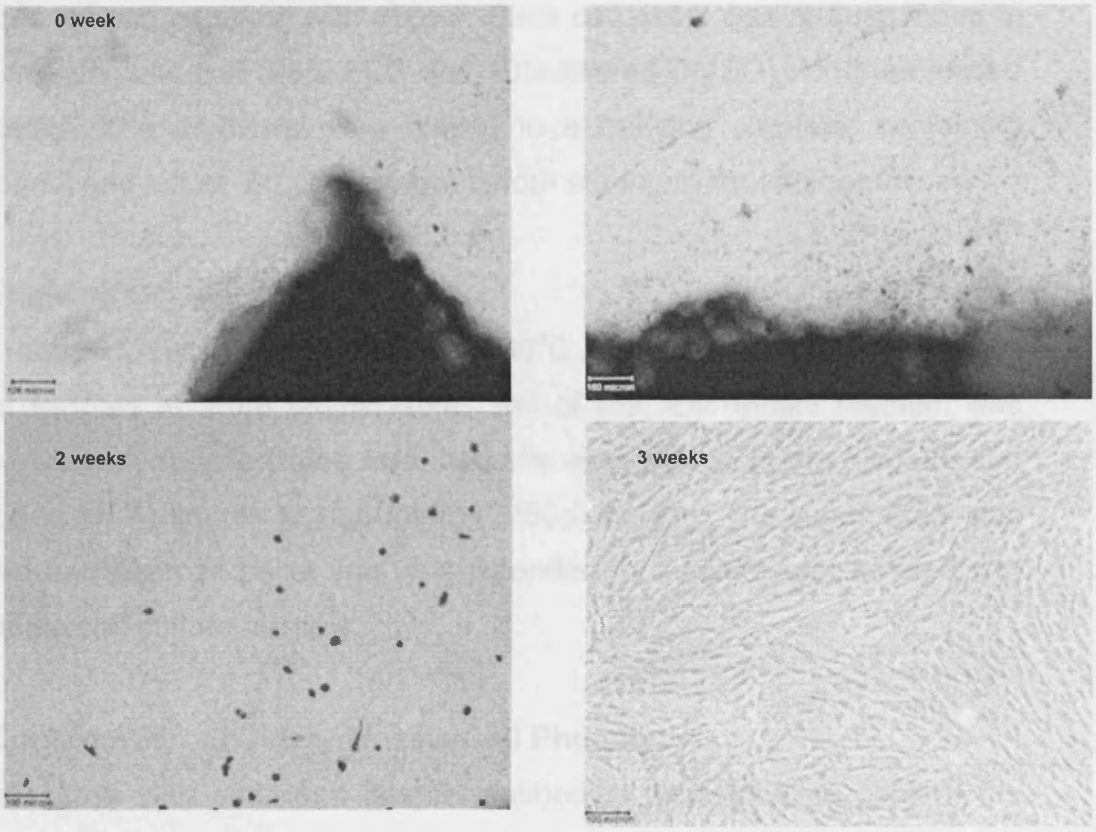

Fig. 2.2: Human ciliary muscle cell growth from explants cultured. The cells grew out by 1 week of culture, and achieved confluence by 3 weeks.

2.2.6 Sub-Culture of confluent cells

Once cells reached confluence, media was removed by an aspirator and the cells were washed briefly in 1X PBS. 2ml of 0.25% trypsin and 0.02% EDTA solution (see appendix, section 8.2) was added to cells and incubated at 37°C until the cells had detached from the culture dish (approximately 1 minute). 1ml of culture media containing FCS was added to inhibit trypsin activity. The cell suspension was centrifuged (600 series, Centurion Scientific Ltd, UK) for 7minutes at 15, 000 rpm (2268g) at 10°C. The supernatant was removed and the pellet of cells re-suspended in 5ml medium and then split into culture dishes in a ratio of 1:3 or 1:2, depending on the requirement of the following procedures.

2.2.7 Freezing cells

Following generation of primary cell lines, the cells were stored frozen in liquid nitrogen, at approximately -196°C, until required. Cells were detached as described for sub culturing with trypsin. Each cell pellet was re-suspended in 1ml of freezing solution (90% FCS and 10% filtered DMSO) and then placed in cryovials. The cryovials were placed in a freezing chamber containing isopropanol and left at -80°C overnight before storing in liquid nitrogen.

2.2.8 Thawing Cells

When required, cells were taken from –80°C or liquid nitrogen storage and allowed to thaw at room temperature. 3ml of the appropriate medium was placed in a centrifugation tube and the cells were added to the medium and centrifuged for 7 minutes at 15,000rpm (2268g) at 10°C. The supernatant was removed and the cell pellet was re-suspended in medium and seeded into appropriate cell culture vessels.

2.2.9 Confirmation of Ciliary Muscle Cell Phenotype

Immunoassays with actin and desmin antibodies were used to confirm the presence of ciliary muscle cells (Weinreb, Kashiwagi *et al.* 1997) in cells cultured from human donors. The cells were sub-cultured (see section 2.2.6) and $3x10^3$ cells were plated on in 4-well slides and cultured for 48 hours at 37°C under standard incubator condition (5% CO_2).

Cells were washed three times (10 minutes, each) with 1x PBS pH 7 (appendix, section 8.2) and then fixed in 1% paraformaldehyde (PFA) for three minutes. The cells were washed further (three times, 10 minutes each wash) before permeabilisation of cell membrane with 0.1% Triton-X-100 (15 minutes). After washing the cells in 1x PBS, the cells were incubated overnight in a primary antibody solution containing either mouse monoclonal anti-human α-smooth muscle actin (1A4 clone) or monoclonal antihuman desmin (D33 clone) at room temperature in a moist chamber. To determine which antibody concentrations were optimal for cell identification, cells were subjected to different dilutions of primary antibodies. Antibody concentrations

were tested by exposure to a range of primary antibody dilutions (1:100, 1:200 and 1:400 for α-smooth muscle actin and 1:100, 1:200 and 1:500 for desmin localisation).

Following incubation, the cells were washed three times in 1X PBS (10 minutes per wash). The cells were then incubated for 90 minutes in anti-mouse secondary antibody, Alexa Fluor 488 (Molecular Probes) at a dilution of 1:1000 in PBS). 2μg/ml bisbenzimide (Hoechst 33345) was added to the secondary antibody solution, in order to localise cell nuclei. The cells were washed again three times in 1x PBS. The cells were then mounted in gelvatol (see appendix, section 8.2) and viewed by a Leica DMRA2 microscope and images captured using Q-Fluoro and Q-win Leica image analysis software.

2.2.10 Detection of PGF2α receptor and MMP 2 in HSF and HCM cell cultures

Cultured HSFs and HCM cells (as described in sections 2.2.4 and 2.2.5) were placed on 4-wells slides as described in the previous section (2.2.9) and maintained for 48 hours at 37°C under standard incubator conditions (5% CO_2). The cells then underwent a few optimization steps before being stained with primary and secondary antibodies.

The optimization involved three 10 minutes washes in PBS followed by 3 minutes in 1% PFA. The cells were washed again three times (10 minutes, each) before permeabilisation of cell membrane with 0.1% Triton-X-100 for 15 minutes. After washing the cells three times with 1x PBS, the cells were placed in 2% donkey serum for 20 minutes.

Once the cells underwent a further 3 washes in PBS they were placed in primary antibodies overnight at 4°C. Cells were stained as described in section 2.2.4. The primary antibodies were rabbit polyclonal PGF2α receptor and mouse monoclonal MMP 2 antibodies. Both were optimised to be most effective at 1:100 dilutions in PBS. The negative controls involved sections being maintained in PBS overnight. Secondary antibody staining used Alexa

Fluor® 488 donkey anti-rabbit IgG (H+L) for slides with rabbit polyclonal PGF2α receptor primary and a negative control, and Alexa Fluor 488 donkey anti-mouse IgG (H+L) for slides with mouse monoclonal MMP 2 primary antibody and a negative control. The slides were incubated at room temperature for 2 hours with the secondary antibody. Thereafter, slides were washed three times in PBS for 10 minutes and mounted with gelavatol. The slides were viewed by a Leica DMRA2 microscope and images captured using Q-Fluoro Leica image analysis software.

2.2.11 Cell Counting

Cell counts were conducted in order to make sure sufficient and equal cell number was used for zymographical analysis. The cells were sub-cultured as above (see section 2.2.6) and the cell pellet re-suspended in appropriate (5ml) media. With a cover-slip in place, 16µl droplet of cell suspension was loaded into each of the two chambers of a Modified-Fuchs-Rosenthal Haemocytometer (Weber, UK) (Kouri, Gyory *et al.* 2003). Each chamber consisted of 9 large squares with triple line boundaries. The cells were counted in the central and four corner squares per chamber. The concentration of cells was calculated using the following:

$$\text{Cell concentration} = \frac{\text{Total number of cells counted}}{2\ (\text{dilution factor} \times 10^{-3})} = X10^{3} \text{ per ml}$$

2.2.12 Serum-Free Cell Culture

FCS is known to effect the level of MMPs and TIMPs in the medium (Kim, Lindsey *et al.* 2001). Cells were cultured in culture medium containing 1X ITS (1.0 mg/ml insulin from bovine pancreas, 0.55 mg/ml human transferrin (substantially iron-free), and 0.5µg/ml sodium selenite). This medium was enhanced by the addition of 0.2mmol/L ascorbic acid (Hadri, Moldes *et al.* 2002).

2.2.12.1 Preparation of MMP-enriched medium, HSF and HCM cell conditioned medium

MMP enriched medium (MMP-EM) was bovine skin fibroblast cell-conditioned medium. These cells were cultured in 10% FCS DMEM-glutamax medium containing 1% antibiotic cocktail (compromising 10mg/ml streptomycin sulphate, 10mg/ml kanamycin, 6mg/ml penicillin-G,), 2mM glutamine and 2.5mg/ml amphotericin B until confluency. The serum containing medium was then replaced by serum-free medium of DMEM-glutamex containing 1% antibiotic cocktail, 2mM glutamine, 2.5mg/ml amphotericin B and 1X ITS. The cells were grown in this medium for 5 days. The medium was collected, this medium was known as the MMP-enriched media (MMP-EM), and stored at –20°C. The cells were then re-cultured in serum containing medium, and allowed to settle for 24 hours before being sub-cultured (section 2.2.6). The process was repeated until sufficient conditioned media was collected.

Human scleral fibroblasts and ciliary muscles cells at passage 3 were cultured in serum-free medium (as described in section 2.2.12) and the medium was collected after 72 hours. The medium was analysed for MMP and TIMP activity via zymography and reverse zymography, respectively.

2.2.13 Zymography to detect Gelatinases, Stromelysins and TIMP activity in cell cultures

Zymography was performed similar to the method described by Kleiner and Stetler-Stevensen (Kleiner and Stetler-Stevensen 1994).

2.2.13.1 Preparation of Samples for zymography

50μl of sample was placed in 2X sample buffer (see appendix section 8.2) in a 1:1 ratio or 6x sample buffer in a ratio of 1:3 sample buffer: sample. The samples were denatured at 60°C for 30 minutes on a heat block.

2.2.13.2 Detection of MMPs by Zymography

Gelatin gels were set in order to detect gelatinase activity (i.e. MMP2 and 9). 7.5% gelatin resolving gel was prepared containing 1ml 7.25mg/ml gelatin (see appendix, section 8.2).

Casein gels were used to detect stromelysin activity (i.e. MMP 3 and 7). 12% casein resolving gel was prepared containing 1.5mg/ml casein (see appendix, section 8.2). The appropriate casein concentration for optimal results was determined by using resolving gel containing 1.5mg/ml (Ando, Twining *et al.* 1993) or 0.5mg/ml casein.

4% stacking gel was prepared (see appendix, section 8.2) and placed on the resolving gel. 10µl of sample was loaded into each well and the gel was run in 1X Lammeli buffer (appendix, section 8.2) at 100V for approximately 90 minutes. The gel was removed from the tank and washed in 2.5% Triton X-100 three times, 10 minutes per wash, in order to displace SDS and allow proteins to re-nature. The gel was then left in MMP proteolysis buffer in order to allow enzyme activation.

Gelatin gel proteolysis buffer

50mM Tris pH 7.8, 50mM $CaCl_2$, 0.5M NaCl, gel incubation at 37°C overnight (Kleiner and Stetler-Stevensen 1994).

Casein gel proteolysis buffer

To determine optimal enzyme activity in casein gel, different buffers containing different pH, $CaCl_2$ or NaCl concentrations were tested.

- 50mM Tris pH 7.8, 50mM $CaCl_2$, 0.5M NaCl, gel incubation at 37°C overnight (Kleiner and Stetler-Stevensen 1994).
- 50mM Tris pH 7.5, 10mM $CaCl_2$ as, gel incubation at 37°C overnight, as suggested by Ando et al (Ando, Twining *et al.* 1993).
- 50mM Tris pH 8.0, 5mM $CaCl_2$, 0.02% sodium azide, gel incubation at 37°C for 48 hours, as suggested by Ando et al (Ando, Twining *et al.* 1993).

Following activation, the gel was rinsed briefly with water and then placed in Coomassie brilliant blue R stain (see appendix, section 8.2) for 40 minutes, and then destained in methanol and acetic acid solution (see appendix, section 8.2). The destain solution was changed successively at 1, 15, 30 and 60 minutes, until lysis bands appear white on a dark blue background. Gel band intensities were analysed and quantified by laser scanning densitometry using Epson expression 1680 Pro scanner and Labworks 45 software.

2.2.13.3 Detection of TIMP by Reverse Zymography

Samples were prepared as described in section 2.2.9.4 for zymography.
To determine optimal conditions different percentage gels were tested according to previous studies; 12% resolving gel (Zhang, Moses *et al.* 2003), 15% resolving gel (Mandler, Dencoff *et al.* 2001) and 10% resolving gel (Singer, Marbaix *et al.* 1999).

The resolving gel contained 1ml MMP-EM (medium containing protease (see section 2.2.9.3)) along with gelatin (substrate). The optimal gelatin concentration within the resolving gel was determined following incorporation of either 350µl of 20mg/ml (Bris 2003) or 1ml of 2.2mg/ml gelatin (Oliver, Leferson *et al.* 1997) into a 12% resolving gel. A 4% stacking gel was prepared (see appendix, section 8.2) and placed on the resolving gel.

10µl of sample was loaded into each well and the gel was run in 1X Lammeli buffer (appendix, section 8.2) at 100V for approximately 90 minutes. The gel was removed from the eletrophoretic tank and washed in 2.5% Triton X-100 three times, 10 minutes per wash, in order to displace SDS and allow the proteins to re-nature.

The gel was then left in MMP proteolysis buffer for 24 hours at 37°C. Different pHs of proteolysis buffers were tested to determine optimal results: 50mM Tris, 0.2M NaCl, 5mM $CaCl_2$, pH8 (Zhang, Moses *et al.* 2003) and 50mM tris, 0.2mM NaCl and 5mM $CaCl_2$, pH7.6 (Mandler, Dencoff *et al.* 2001).

The gel was briefly rinsed in destain (Bris 2003) and then stained and destained in the same manor as described in section 2.2.1.3. Dark blue bands were observed where TIMPs had inhibited gelatin degradation activity by the protease incorporated within the gel matrix. Gel band intensities were analysed and quantified by laser scanning densitometry using Epson expression 1680 pro scanner and Labworks 45 software.

2.2.13.4 Sensitivity of band intensity to sample concentration

The effect of sample concentration on band intensity of zymograms and reverse zymograms was analysed. MMP-enriched media was serially diluted in DMEM. The diluted samples were placed in sample buffer and run on gelatin, casein and reverse zymogram. The results obtained were recorded by scanning densitometry of the zymograms by Epson Expression 1680 pro scanner. Gel band density was analysed with the use of Labworks45 analysis software.

2.2.14 Detection of MMP 1 using Enzyme-Linked ImmunoSorbent Assay (ELISA)

Media samples collected from cell cultures underwent ELISA assay in order to detect MMP 1 concentration. ELISA was conducted using a MMP-1 Biotrak ELISA kit according to manufacturer's instructions (Amersham, UK). In brief, a standard curve was created by serially diluting MMP-1 standard (200 ng/ml) to produce concentrations 0, 6.25, 12.5, 25, 100, 200 ng/ml. Duplicate 100µl aliquots of standards and samples were loaded into anti-MMP-1-coated wells in a microplate, and incubated at 20-25°C for 2 hours. After washing the wells with wash buffer three times, 100µl antiserum was applied to each well and the plate was left at 20-25°C for a further 2 hours. 100µl peroxidase conjugate was applied to each well after three washes and incubated at 20-25°C for an hour. After three further washes 100µl tetramethylbenzidine TMB substrate was applied to each well and the plate was placed on a shaker at room temperature for 30 minutes. 100µl of 1M sulphuric acid was applied to each well to stop the enzyme substrate reaction and plate was read at 450nm (Multiskan Ascent 354 model; Labsystems).

2.3 The effect of different MMP inducers on cells involved in uveoscleral outflow MMP secretion

HSFs and HCM cells were cultured and different growth factors were applied. The media collected was analysed using zymography and reverse zymography techniques. The effect of different test factors: transforming growth factor β1 (TGF- β1), tumor necrosis factor-α (TNF- α), interleukin-1α (IL-1α) and PGF2α on MMP activity was studied.

2.3.1 Cell Culture

HSFs and HCM cells were cultured as described previously in section 2.2.5 and 2.2.6, respectively. After undergoing 3rd passage the cells were plated on 24 well plates. 1ml of 3x10^3 cells was aliquoted into each well of a 24 well plate. Each cell-line occupied duplicate wells, for each test factor and control, and for each time time-point studied. The cells were maintained at 37°C under standard incubator conditions (5% CO_2) in serum containing medium for 48 hours in order to ensure the cells had attached, followed by 24 hours in serum-free medium.

After the 24 hours the serum-free medium was removed and replaced with serum-free medium containing the test factors. The concentration of test factors included 10ng/ml TGF- β1, 25ng/ml TNF-α, 25ng/ml IL1α and 100nM PGF2α, as reflected in previous literature (Hosseini, Rose *et al.* 2006; Kim, Shang *et al.* 2004). Negative controls involved cells cultured in serum-free medium without any test factors. 1ml media from cultured cells was collected after 24, 48 and 72 hours and stored at –20°C until used experimentally.

2.3.2 Zymography

MMP secretion into media collected was detected by Zymography as described in the above sections 2.2.13.-2.2.13.2. The results obtained were recorded by scanning densitometry of the zymograms by Epson Expression 1680 pro scanner. Gel band density was analysed with the use of Labworks 45 analysis software.

2.4 The effect of MMP and PGF2α on Scleral Permeability

An Ussing chamber was used in order to analyse scleral tissue permeability, via monitoring the flow of fluorescence dextran across the sclera.

2.4.1 Scleral tissue culture

Following removal of all ocular components, including optic nerve and extraocular muscles, the sclera was dissected into four equal sized ($1cm^2$) explants, which were scraped clean on both sides. Each scleral explant was immersed in 3% betadine for 30 seconds, and then thoroughly rinsed in sterile PBS (pH7.4).

The explants were cultured in MMP-EM, serum-free DMEM containing 100nM 17-phenyltrinor-PGF2α (Cayman Chemical Co, MI) or control medium (serum-free DMEM) for varying time periods from 0-72 hours at 37°C, under standard incubator conditions. Scleral explants were removed from media following appropriate incubation periods up to 72 hours.

2.4.2 Determination of scleral permeability using Ussing chamber

Each scleral tissue explant was clamped into an Ussing-system (WPI labs-model, UK). Phenol red-free HBSS medium (Gibco, UK) was loaded into both sides of the chamber via the reservoir. The orbital side of the chamber was supplemented with 0.25mg/ml rhodamine dextran beads (10, 40 or 70KDa) (Invitrogen, Molecular Probes, UK). 1ml media samples were extracted at 30 minutes and 4 hours from the uveal side and stored at -80°C prior to spectrophotometry.

2.4.2.1 Use of Spectrophotometer & Spectrofluorometer

Two blanks, cuvettes (1ml sample cuvette were used) with HBSS, were placed in the spectrophotometer (U-2800 Spectrophotometer, Digilab Hitachi, Jencons) to account for any background and produce a relevant blank at excitation and emission wavelengths of 550 and 580nm, at room temperature, respectively. One cuvette was loaded with sample and the absorption profile was produced blank to sample absorption. This was carried out to ensure that

the absorbance peaks attained were under 0.1, as this is the maximum range of absorbance for the spectrofluorometer at which relevant readings could be attained. Absorption profiles were produced with a UV solution 2.0 software.

In cases where absorption of a sample indicated more than 0.1nm peak, the sample was diluted and accounted for when conducting the calculations to determine fluorescence concentration. Samples were then placed in the spectrofluorometer (Digilad Hitachi F-4500, Jencons). Absorbance peak profiles were produced with excitation and emission wavelengths of 550 and 580nm at room temperature, respectively. Example figure has been shown in Fig 2.3.

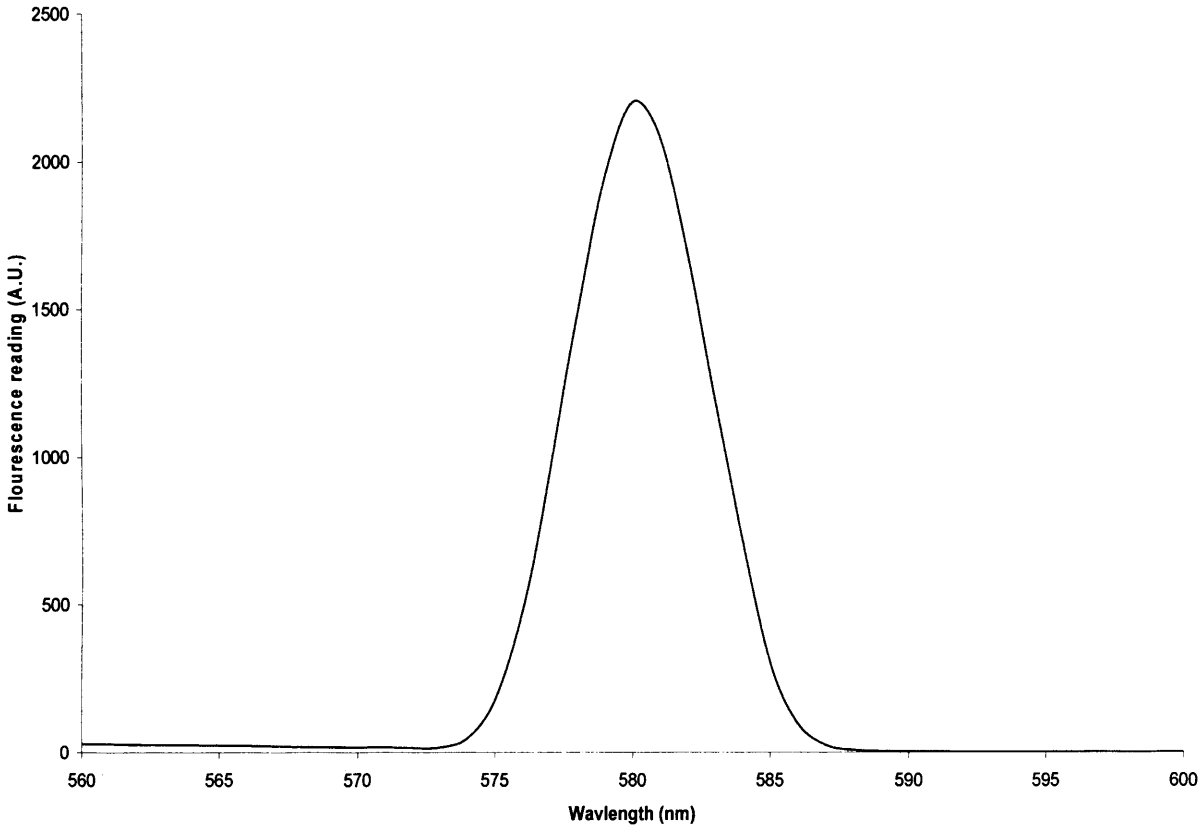

Fig. 2.3: Spectrofluorescence reading from the uveal side of 24 hours prostaglandin incubated tissue, after 4 hours in the Ussing chamber.

2.4.2.2 Standard Absorbance-Concentration for Spectrofluorometry

Standard absorbance-concentration curves were obtained by spectrofluorometry, using serial dilutions of rhodamine-dextran in phenol red-free HBSS medium. 0.25mg/ml rhodamine dextran bead suspensions (10, 40 or 70KDa) were diluted 1:1 in HBSS medium serially. Standard curves were produced using absorbance readings obtained from the different concentration of dextran beads. These curves were used to obtain sample concentrations from absorbance readings (standard curve obtained for 40kDa is included in Fig. 2.4).

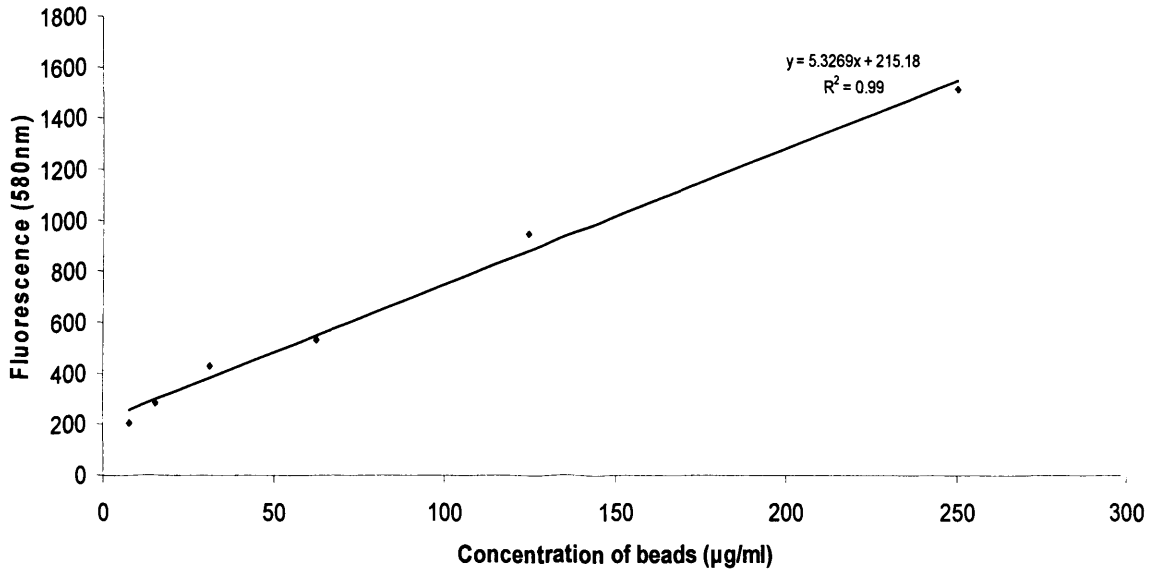

Fig. 2.4: Standard curve of 40kDa dextran bead concentration in relation to fluorescence reading (580nm).

2.4.2.3 Calculating Permeability coefficient (Pc)

The diffusion of dextran beads from orbital to uveal scleral side of the chamber was quantified as a measure of the permeability coefficient (Pc) using equation (Kim, Lindsey *et al.* 2001):

$$Pc\ (cm/sec) = ((C_{ut} - C_{u0.5})\ V^{-1})\ (AtC_0)^{-1}$$

Where:

$C_{u0.5}$ is the concentration of dextran beads at 30 minutes

C_{ut} is the concentration of dextran beads at t hours (4 hours).

C_0 is the initial rhodamine dextran concentration (25mg/ml).

A is the surface area of exposed sclera ($0.65cm^2$).

V is the volume of each chamber (0.75ml).

t is duration of steady state flux converted from hours to second

2.5 Effect of PGF2α and MMP on scleral collagen architecture

Human scleral tissue was incubated with MMP-EM or PGF2α. Separate experiments were conducted which involved scleral tissue being treated in human scleral fibroblasts conditioned medium (HSF-CM) or human ciliary muscle cells conditioned medium (HCM-CM). Specific MMP effect on the scleral tissue was also studied, by incubating sclera in MMP-1, MMP-2 or MMP-7. Scleral tissue incubated in serum-free medium without any factors acted as a negative control and positive control included medium containing collagenase. X-ray diffraction was conducted on the scleral tissue samples, in order to determine the effect of each incubation on scleral architecture.

2.5.1 Scleral tissue culture

Human scleral tissue was extracted in the same manner as described in section 2.4.1. However, all tissue explants were cut to an approximate size of $1cm^2$. The explants were cultured, in triplicate, in MMP-EM, HSF-CM, HCM-CM, serum-free DMEM containing 100nM 17-phenyltrinor-PGF2α, control medium (serum-free DMEM) , control medium containing 20nM MMP-1, MMP-2 or MMP-7 or control medium containing 2% collagenase for varying

time periods from 0-72 hours at 37°C, under standard incubator conditions. Sclera was removed from media following appropriate incubation periods (0, 3, 6, 12, 24, 48 or 72 hours) and stored at -80°C.

2.5.2 X-ray Diffraction

The treated scleral tissue was thawed and under moist condition placed into appropriate sample holders for x-ray diffraction beam passage. An example of X-ray diffraction is shown in Fig. 2.5. The incoming x-ray beam hits the sample, and is scattered from the interaction with electrons within the sample. The scattered beam is collected on the detector. X-ray diffraction images were viewed using FibreFix software (CCP13). The 2D x-ray diffraction image exhibited isotopic scattering and diffraction peaks which were visible as rings. It was therefore appropriate to convert the information into a linear intensity profile of intensity to reciprocal scattering vector. This allowed direct comparison of scattering (Goh, Hiller *et al.* 2005). PeakFit4 (AISL software) the one-dimensional peak fitting program was used to determine the peak size shapes and integrated intensity of linear profiles.

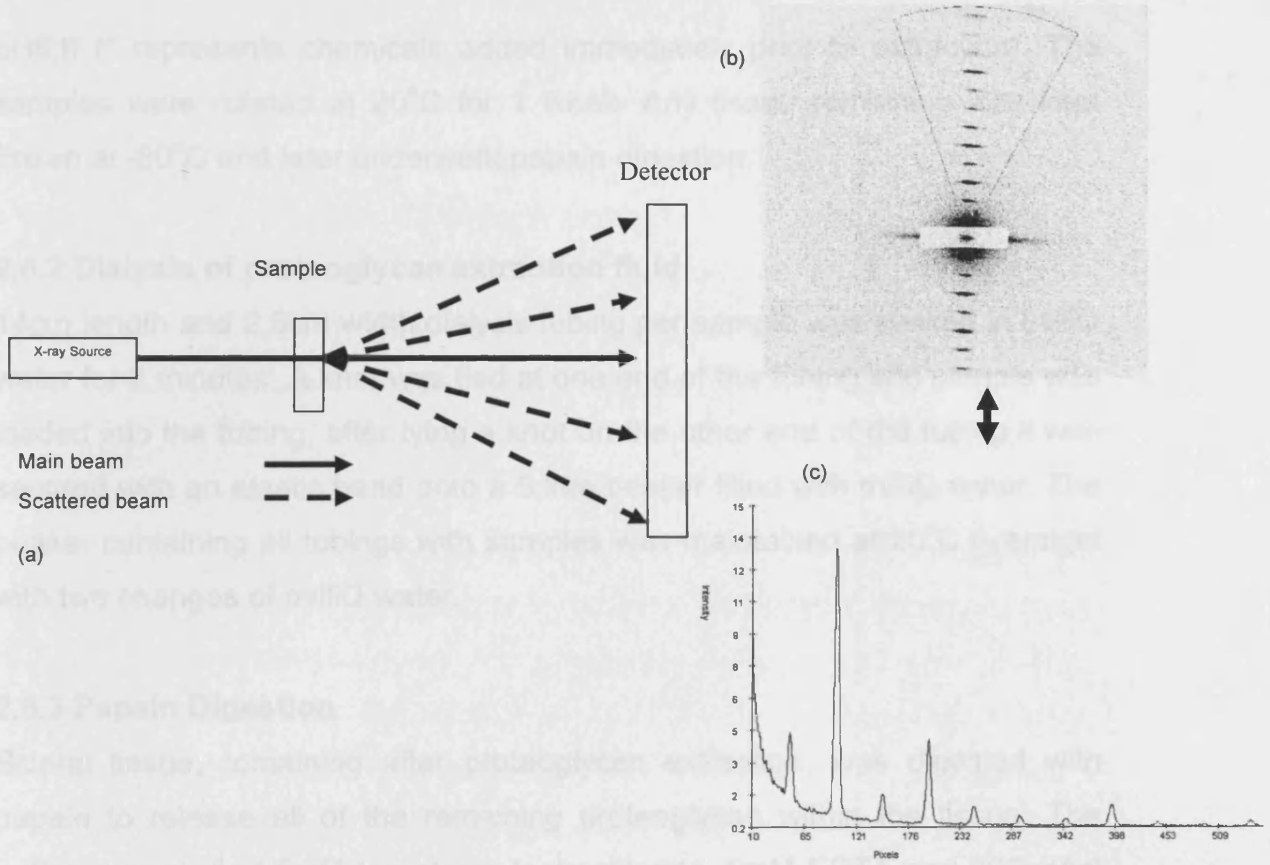

Fig. 2.5: Example of x-ray diffraction. a) Diagram showing x-ray diffraction and beam scatter b) A 2D X-ray diffraction image of Rat tail tendon (calibrant). c) A 1D linear trace of the 2D X-ray diffraction image of Rat tail tendon.

Wide angle diffraction was used to view collagen helical rise per residue and intermolecular lateral packing. Small angle x-ray diffraction images were taken to analyse D-periodicity. All image analysis was conducted by Clark Maxwell.

2.6 Effect of PGF2α and MMP on proteoglycans in human sclera

Western blotting was conducting in order to determine the proteoglycan composition in the sclera and any change in composition as a result of scleral incubation in MMP-EM or PGF2α.

2.6.1 Proteoglycan Extraction

Each tissue sample was freeze dried and weighed after incubation. The samples were placed in centrifuge tubes in 10ml extraction buffer containing 4M guanidine HCl, 0.05M sodium acetate, 0.01M EDTA, 0.1M 6-amino hexanoic acid, 0.005M benzamide HCl* and 0.5mM phenyl sulfonyl fluoride*

pH6.8 (* represents chemicals added immediately prior to extraction). The samples were rotated at 20°C for 1 week. Any tissue remaining was kept frozen at -80°C and later underwent papain digestion.

2.6.2 Dialysis of proteoglycan extraction fluid

14cm length and 2.5cm width dialysis tubing per sample was soaked in milliQ water for 2 minutes. A knot was tied at one end of the tubing and sample was loaded into the tubing, after tying a knot on the other end of the tubing it was secured with an elastic band onto a 5 litre beaker filled with milliQ water. The beaker containing all tubings with samples was maintained at 20°C overnight with two changes of milliQ water.

2.6.3 Papain Digestion

Scleral tissue, remaining after proteoglycan extraction, was digested with papain to release all of the remaining proteoglycan within the tissue. The buffer consisted of 5mM L-cysteine hydrochloride, 5mM EDTA and 600µg/ml papain for 48 hours. Once all scleral tissue was digested into solution, samples stored at -80°C until undergoing the dimethylene blue (DMMB) assay.

2.6.4 Dimethylene Blue (DMMB) Assay

40µl of each standard: 10, 20, 30 and 40µl/ml shark cartilage chondroitin sulphate C in water was loaded into a 96 well plate in triplicate. 40µl of each sample was loaded onto the 96 well plate, in duplicate. To each well 200µl of DMMB solution (1,9 dimethyl methylene blue, ethanol, 1M sodium hydroxide, 98% (v/v) formic acid and made up to 2 litres with double distilled water) was added. The plate was immediately read at 525 nm to provide GAG concentrations in µg/ml. In order for the antibodies to be detected it was necessary to have a minimum of 10µg of GAG per sample. The DMMB assay allowed the calculation of the appropriate volume to provide the appropriate GAG concentration using:

Concentration (µg/ml) = Weight (µg) / Volume (ml).

2.6.5 Protein Assay

Protein assay was conducted using a BCA Kit (Sigma), in which 10μl of serial diluted standard (8 times) in duplicate wells of a 96 well plate. 10μl samples were loaded into the remaining wells. A cocktail was prepared using buffers A and B. The ratio of buffer A: B was 1:50. To each well 200μl of A: B buffer cocktail was loaded. The plate was tap mixed and placed at 37°C incubator for 30 minutes. The plate was then read immediately at 555nm.

2.6.6 Deglycosylation

Deglycosylation was performed to reduce the size of the large proteoglycans e.g. aggrecan. This was a necessary step before performing western blotting, as large proteoglycans can not migrate through the gel matrix. Deglygosylation involved the addition of 10X Tris buffer (Appendix, section 8.2) to each calculated volume of sample. 1μl keratanase I, 2μl keratanase II (AMS biotechnology) and 1μl chondroitinase ABC (Sigma) was added to each sample for every 10μg GAG.

2.6.7 Western Blotting

5X Sample buffer (2X sample buffer: 0.125M Tris HCl pH 6.8 with 4% SDS, 20% glycerol and 0.01% bromophenol blue) was prepared and made to 1X sample by the addition of 3.5ml double distilled water then 0.5ml mercaptoethanol was added to 1 ml of 5X sample buffer. 200μl of 1X sample buffer was loaded into each sample bijoux; the samples were vortexed briefly, and then the samples were placed in boiling water for 10 minutes. The heat treatment completed the reduction reaction of β-mercaptoethanol. The samples were vortexed and then centrifuged briefly.

Tris-glycine (4-12% gradient gels; Invitrogen) were placed into clip-lock tanks and the tanks were loaded with running buffer (25mM Trizma, 192mM glycine and 0.1% SDS). 10μl molecular weight marker (Sigma) was loaded into the first well and 50μl of each sample into the remaining wells of each gel. The gels were run at 100V until the samples reached the bottom (approximately 1-1.5 hour).

Filter paper, nitrocellulose membranes with the blue cover and transfer blot sponges were cut to gel size (7.5cm by 8.5cm) and soaked in transfer buffer (25mM Trizma, 192mM glycine, 20% methanol). All the layers were arranged as shown in the figure below (Fig. 2.6). One layer of transfer sponge, 2 layers of filter paper was followed by gel (gel was removed from the plastic cover) and then the membrane (making sure to remove the blue cover without touching the membrane). Once the membrane was in place two more layers of filter paper, and one layer of transfer sponge was placed into the transfer tank and then the tank was clipped closed and placed into the wet tank.

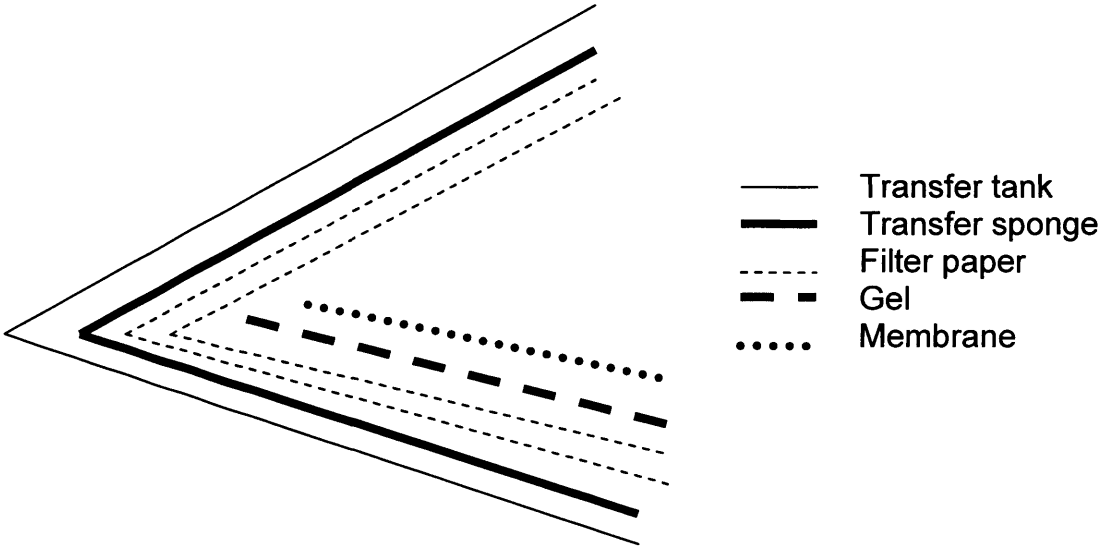

Fig. 2.6: The arrangement of different layers within the transfer tank.

The transfer tanks contained an ice block and were filled with transfer buffer. The transfer was set on a stirrer, at 100V for exactly an hour.

The membrane was removed and blocked for 30 minutes in 5% BSA in TSA (50mM Tris (pH 7.4), 200mM sodium chloride and 0.02% (w/v) sodium azide), on a rotator. The membranes were then left overnight at room temperature, on a rotator, in primary antibodies. The primary antibodies were diluted into 10ml 1% BSA in TSA per membrane.

Antibodies used included:

6B4*IGD- Aggrecan (Caterson, Flannery *et al.* 2000)

Pr8A4 – Biglycan (Roughley, White *et al.* 1993)

Lum-1 – Lumican (Bidanset, Guidry *et al.* 1992)

70.6 – Decorin (Carlson, Liu *et al.* 2005)

After overnight incubation in primary antibody, the membrane was washed three times in TSA, 10 minutes per wash. 1μl of secondary anti-mouse IgG (H+L), alkali phosphate (AP), and was prepared in 7.5ml of 1% BSA in TSA. 10ml of secondary mix was loaded onto each membrane and left on a rotator for an hour. After undergoing 3, 10minute washes in TSA, 10 ml of AP buffer (100mM trizma, 5mM MgCl2, 100mM NaCl pH 9.55) containing 33μl BCIP and 66μl NBT (Promega) was loaded onto each membrane. The membranes were left on the rotator until the band colour developed. To prevent intense band staining, the membranes were washed for 5 minutes in tap water. Membranes were left on filter paper to dry and then scanned using Epson Expression 1680 pro scanner. Band staining on blots were analysed using Labworks 45 analysis software.

CHAPTER 3

CHARACTERISATION OF THE UVEOSCLERAL OUTFLOW PATHWAY

CHAPTER 3
CHARACTERISATION OF THE UVEOSCLERAL OUTFLOW PATHWAY

3.1 Introduction

The anterior segment of the eye has two aqueous drainage pathways: via the trabecular meshwork and the uveoscleral outflow pathway (Fig. 3.1). The most common first line medication to treat glaucoma are prostaglandin derivatives, such as Latanoprost. This group of drugs act on the uveoscleral outflow pathway.

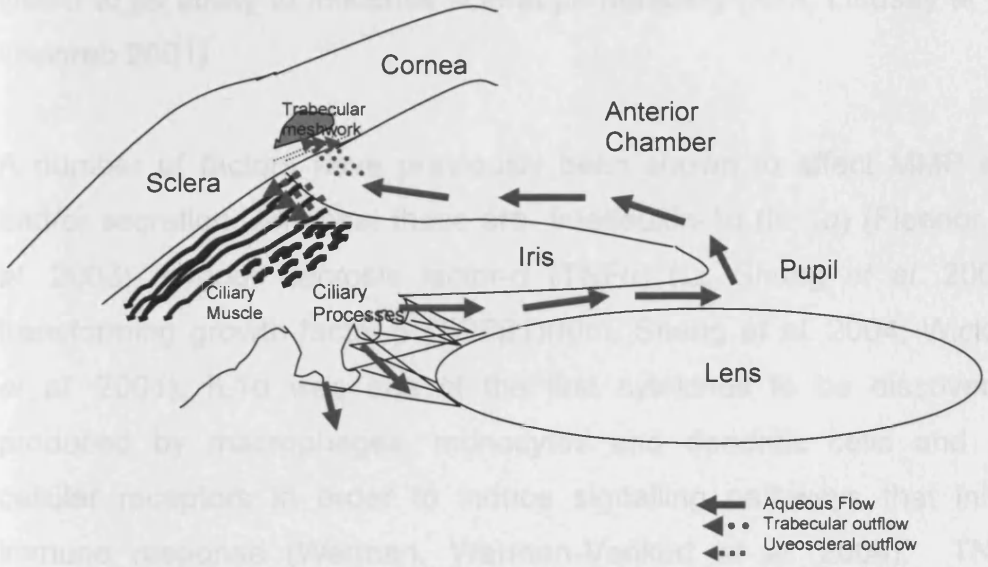

Fig. 3.1: Schematic diagram of the aqueous humor cycle.

Aqueous is formed by the ciliary process and secreted into the posterior chamber. It moves into the anterior chamber and exits the chamber via two pathways: trabecular and uveoscleral outflow.

Aqueous flow via the ciliary muscle and scleral tissue forms the main route of passage within the uveoscleral pathway which is influenced by prostaglandin. Previous studies have concluded that prostaglandin-based derivatives increase uveoscleral outflow, and reduce trabecular outflow (Gabelt and Kaufman 1989). Prostaglandins influence MMP secretion and activation

within the uveoscleral outflow pathway (Husain, Jafri *et al.* 2005; Schachtschabel, Lindsey *et al.* 2000).

The activation of FP receptors with Prostaglandin F2alpha (PGF2α) is postulated to upregulate MMP expression in the uveoscleral outflow pathway (Gaton, Sagara *et al.* 2001; Schachtschabel, Lindsey *et al.* 2000). A reduction in extracellular matrix with PGF2α treatment within the pathway has been demonstrated (Lutjen-Drecoll and Tamm 1988), which may consequently be linked to its ability to influence scleral permeability (Kim, Lindsey *et al.* 2001; Weinreb 2001)

A number of factors have previously been shown to affect MMP activation and/or secretion. Amongst these are interleukin-1α (IL-1α) (Fleenor, Pang *et al.* 2003), tumour necrosis factor-α (TNFα) (Li, Shang *et al.* 2003) and transforming growth factor-β (TGFβ1)(Kim, Shang *et al.* 2004; Wick, Platten *et al.* 2001). IL1α was one of the first cytokines to be discovered. It is produced by macrophages, monocytes and dendritic cells and binds to cellular receptors in order to induce signalling pathways that initiate the immune response (Werman, Werman-Venkert *et al.* 2004). TNF is an inducer which promotes apoptotic cell death, cellular proliferation, differentiation, inflammation, tumorigenesis, and viral replication. TNF's primary role is in the regulation of immune cells (Old 1985). TGFβ1 is a polypeptide growth factor, involved in cellular transformation, cell growth, differentiation and apoptosis (Lawrence 1996). All three factors are involved in cellular action and have been related to activation of MMPs in order to perform their functions.

The current chapter highlights the effect of known inducers of MMP activity on human scleral fibroblasts (HSFs) and human ciliary muscle (HCM) cells. This understanding is important in order to target factors which may influence MMP activity and thereby increase aqueous drainage via the uveoscleral outflow pathway.

3.2 Aims:

The aims of this chapter were to characterise:

- human anterior chamber morphology to distinguish different structures within the uveoscleral outflow pathway.
- the prescence of PGF2α receptor and MMP 2 in HSFs and HCM cells.
- the MMP and TIMP profile in MMP-Enriched Medium (MMP-EM).
- the MMP and TIMP profile produced by HSFs and HCM cells.
- the effect of MMP inducers on the MMP and TIMP profile secreted by HSFs and HCM cells

3.2 Experimental Design

3.2.1 Morphology of the anterior chamber

The morphology of structures in the anterior chamber were distinguished in histological sections (n=3), following either haematoxylin and eosin or toluidine blue staining (section 2.2.3).

3.2.2 Identification of the presence of PGF2α receptor and MMP 2 in HSFs and HCM cells

The phenotype of HCM cells was confirmed, as described in section 2.2.10, by positive immunolabelling for both α-actin and desmin, known markers of ciliary smooth muscle cells (Weinreb, Kashiwagi *et al.* 1997). The phenotype of human fibroblasts was confirmed by visualisation of their spindle-shaped morphology.

Third passage HSFs and HCM cells were cultured in triplicate wells on 4-well slides (Scientific Laboratory Supplies, U.K.) for 48 hours. The immunofluorescent localisation of PGF2α receptor and MMP2 was performed as described in section (section 2.2.11).

3.2.3 The MMP and TIMP profile in MMP-Enriched Medium (MMP-EM)

Media was collected from triplicate cultures of BOVS-1 cells (bovine skin fibroblasts, see section 2.2.12.2 for culture method). Since this media is known to contain a cocktail of MMPs and TIMPs, for the purpose of this thesis it is called MMP-enriched media (MMP-EM). MMP and TIMP profiles in MMP-EM were analysed by zymography (gelatin gels for gelatinase activity, casein gels for stromelysin activity) and reverse zymography respectively (see sections 2.2.13.3-2.2.13.5). In addition, MMP1 activity in the media was determined by ELISA (see section 2.2.13.8). Medium not exposed to cells acted as a negative control.

3.2.4 Sensitivity of Quantification

In order to detect the sensitivity of quantification methods MMP and TIMP levels were analysed in serially diluted MMP-EM in uncultured media. Following zymography and reverse zymography of samples (section 2.2.12.6), gel band intensities were analysed and quantified by laser scanning densitometry using Epson expression 1680 Pro scanner and Labworks 45 software.

3.2.5. MMP and TIMP profile of HSFs and HCM cells in culture.

Media were collected from third passage HSF and HCM cells from three different donors, cultured for 72 hours with and without FCS (see section 2.2.12.1). MMPs and TIMPs secreted into this media by HSF and HCM cells were analysed following zymography and reverse zymography respectively (see sections 2.2.12.3-2.2.12.5) . Medium not exposed to cells acted as a negative control. MMP-enriched medium (MMP-EM) acted as a positive control. MMP1 in the media was assessed by ELISA (section 2.2.12.8). MMPs and TIMPs in serum-free media were quantified as described above in 3.2.4.

3.2.6 The effect of known MMP inducers and PGF2α on MMP activation in HSF and HCM cell cultures

Fourth passage primary HSF and HCM cell cultures, from 4 different human donors, were seeded into 24 well plates at a cell density of 2×10^3 cells/ml (1 ml was seeded per well). The cells were cultured in serum-containing media for 48 hours. Once the monolayer of cells had reached 90% confluency, cells in triplicate wells were treated with known regulators of MMP activity, including 25ng/ml IL1α, 25ng/ml TNFα or 10ng/ml TGFβ1 in serum-free media. Concentrations were selected according to previous publications (Hosseini, Rose *et al.* 2006; Kim, Shang *et al.* 2004). 100nM PGF2α was also applied to cells in triplicate wells. Cells cultured in serum free media without any test factors were used as negative control.

500µl of medium was removed from each culture well after 24, 48 and 72 hours incubation and stored at -80°C until required. On the day of analysis, protein concentration were determined using the Bicinchoninic acid (BCA) protein assay (see section 2.6.5) and samples of equal protein concentration were loaded onto gelatin and casein gels. Following zymography (section 2.2.12), all gels were scanned using an Espon expression 1680 pro scanner and gel band max OD was measured using Labworks45 software. The data was entered into Excel 2003 to obtain charts and SPSS 14 in order to conduct statistical analysis of trends observed. ANOVA was conducted on parametric data and Kruskal Wallis test was contacted on non-parametric data.

3.3 Results

3.3.1 Morphology of the human anterior chamber

In order to understand orientation of structure within the anterior chamber haematoxylin and eosin staining and toluidine blue staining was conducted on wax sections of human anterior chambers(Fig. 3.2-3.3).

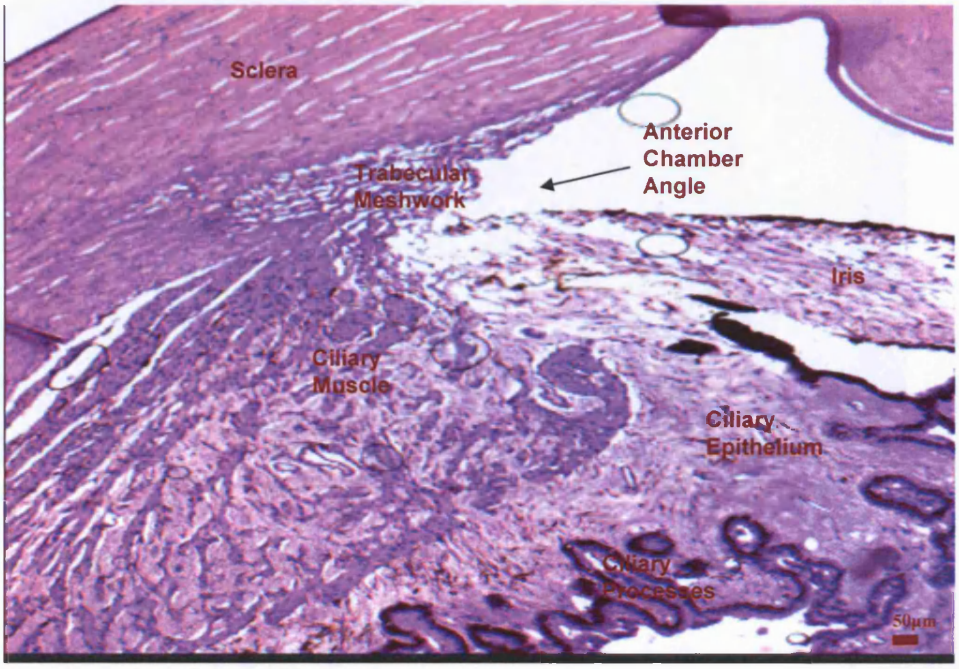

Fig. 3.2: Haematoxylin and eosin staining of the anterior segment.

Haematoxylin (blue) being is a dye which stains nucleic acids of the cell nucleus; and eosin (pink) is more acidic and therefore has greater affinity for cytoplasmic components of cells. Fig. 3.2 above illustrates the structures involved in forming the anterior segment of the eye. Of particular interest to this study are the sclera and ciliary muscle, both important structures in the uveoscleral outflow pathway.

Toludine blue is another basic dye and has affinity for nucleic acid in the nucleus of all cells. It is a quick stain to identify orientation of sections. Fig.3.3 demonstrates the staining of the anterior chamber with toluidine blue. Both of these histological stains identify that greater cellular activity, indicated by nuclear staining, exists within the cilliary body (including ciliary muscle and

ciliary processes) compared to the scleral layer. The sclera comprises scleral fibroblasts surrounded by dense connective tissue.

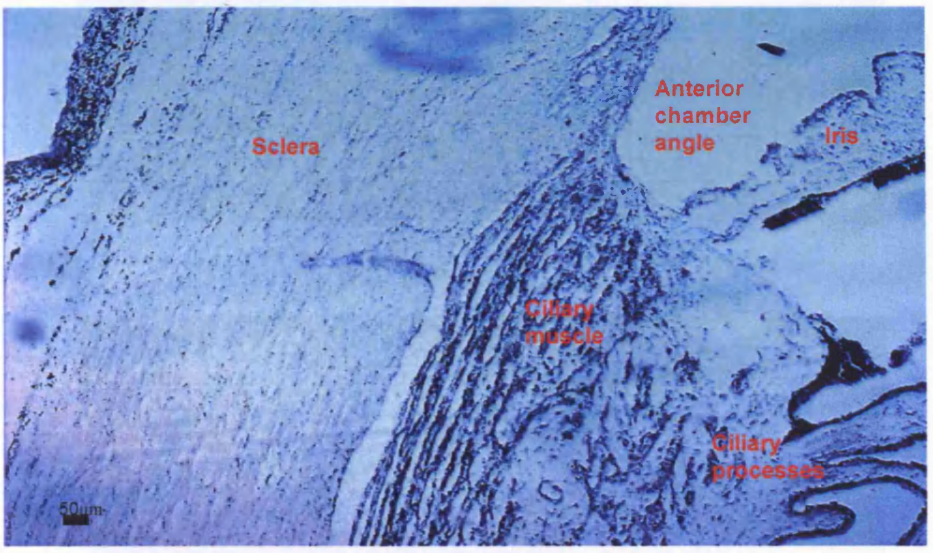

Fig. 3.3: Toluidine blue staining of human anterior segment.

3.3.2 Presence of PGF2α receptor and MMP 2 in HSFs and HCM cells

The HCM cell phenotype was confirmed by immunopositive localisation of actin and desmin (Figs. 3.4a and b) within the cells. 1:200 dilution of primary antibodies was found to be the optimal concentration for immunolocalisation of these markers. Fig. 3.5 demonstrates the presence of PGF2α receptor and MMP 2 within HSFs and HCM cells.

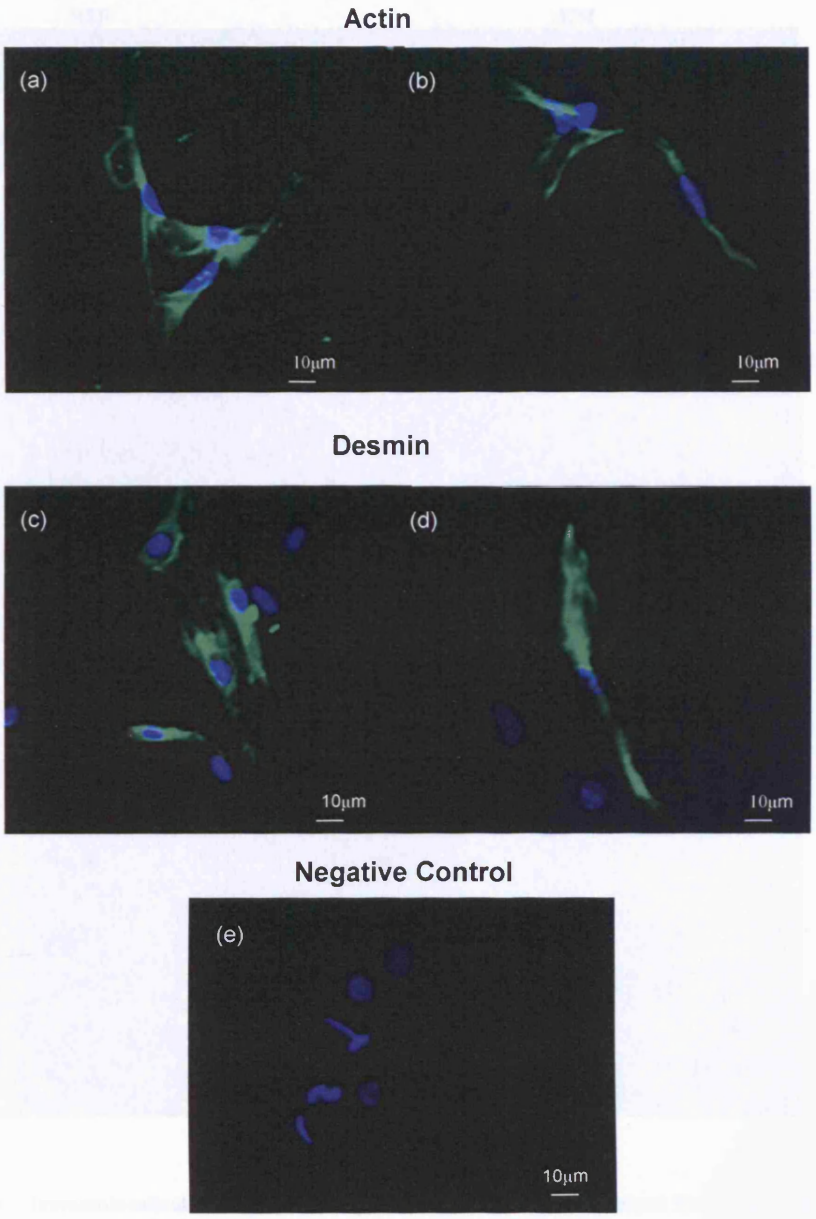

Fig 3.4: Immunostaining of human ciliary muscle cells. α-actin (green) (a) 1:200 and (b) 1:400 and desmin (green) (c) 1:200 and (d) 1:500 nuclei staining (blue) negative control (e)

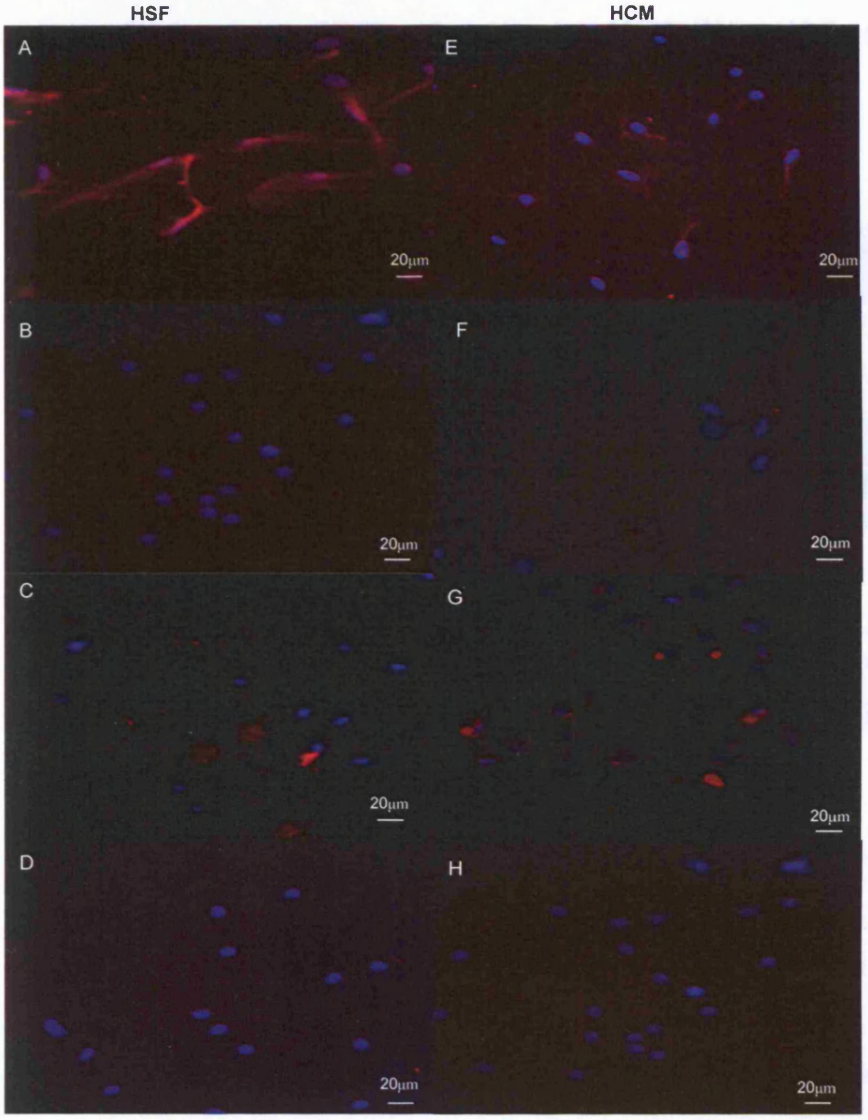

Fig. 3.5: Immunolocalisation of PGF2α receptor and MMP 2 in human scleral fibroblasts (HSF) and ciliary muscle cells (HCM) cultures. PGF2α receptor staining (A & E), negative control for anti-rabbit (B & F), MMP 2 staining (C & G) negative control for anti-mouse (D & H).

3.3.3 MMPs and TIMPs Profile in MMP-EM, HSF and HCM cells conditioned media

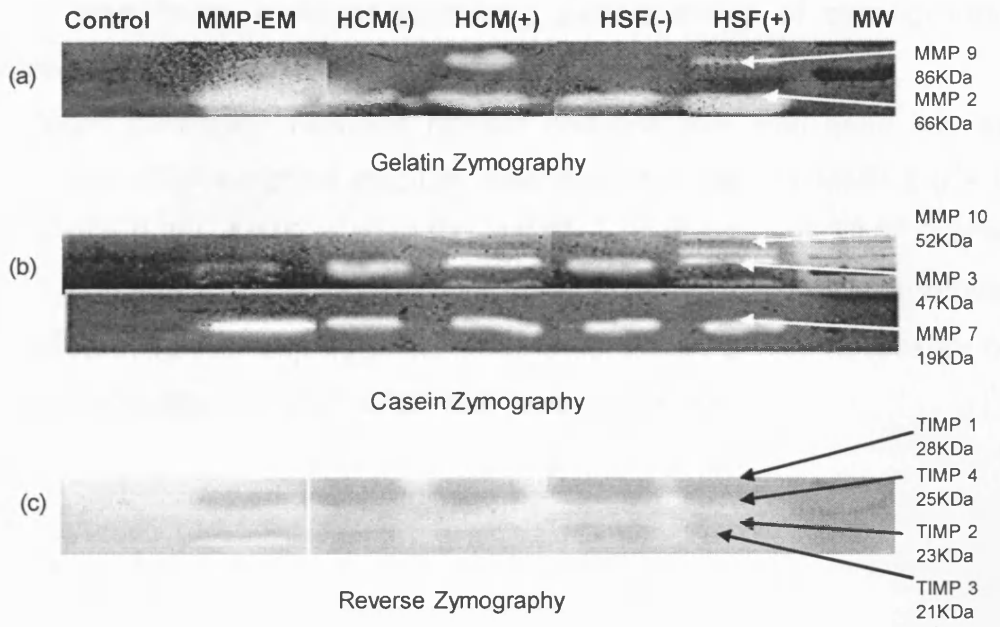

Fig 3.6: MMPs and TIMPs profile in conditioned medium. (a) gelatin zymogram, (b) casein zymogram and (c) reverse zymogram.Control: Uncultured media, MMP-EM, Conditioned HCM media (HCM), Conditioned HSF media (HSF) with (+) and without (-) serum and molecular weight marker

Gelatin zymography revealed the presence of gelatinase activity. MMP 2 in serum-free media of HSFs and HCM cells. However, MMP 2 and MMP 9 was detected in MMP-EM and HSF and HCM conditioned-medium with serum, as demonstrated in Fig. 3.6a.

Casein zymography confirmed the presence of stromelysins within samples. MMP 3 and MMP 7 in all samples of MMP-EM, HSF and HCM conditioned media. Other MMPs, such as MMP 10, were detected in conditioned media with serum (Fig. 3.6b).

Reverse zymogram revealed the presence of all four TIMPs in HSFs and HCM cells conditioned media with or without serum (Fig. 3.6c). However, in MMP-EM only TIMP 2 and 4 was detected.

The data demonstrated that the presence of serum influenced the TIMP and MMP expression profile of HSFs and HCM cells. This could influence

potential effect of treated cells. Further analysis of MMPs is therefore conducted in cells cultured in serum-free medium.

3.3.3.1 Sensitivity of laser scanning densitometry of zymograms and reverse zymograms.

Significant correlation between relative concentration and band intensity, in serum-free MMP-enriched medium, was demonstrated for MMP 2 (r^2= 0.91), MMP9 (r^2= 0.85), MMP 3 (r^2=0.91), MMP 7 (r^2=0.94) and TIMP 2 (r^2=0.91) (Fig. 3.7). TIMP 4 (r^2= 0.49) displayed poor correlation and therefore was not quantified in further experiments. This understanding was necessary before being able to quantify MMP and TIMP from zymograms.

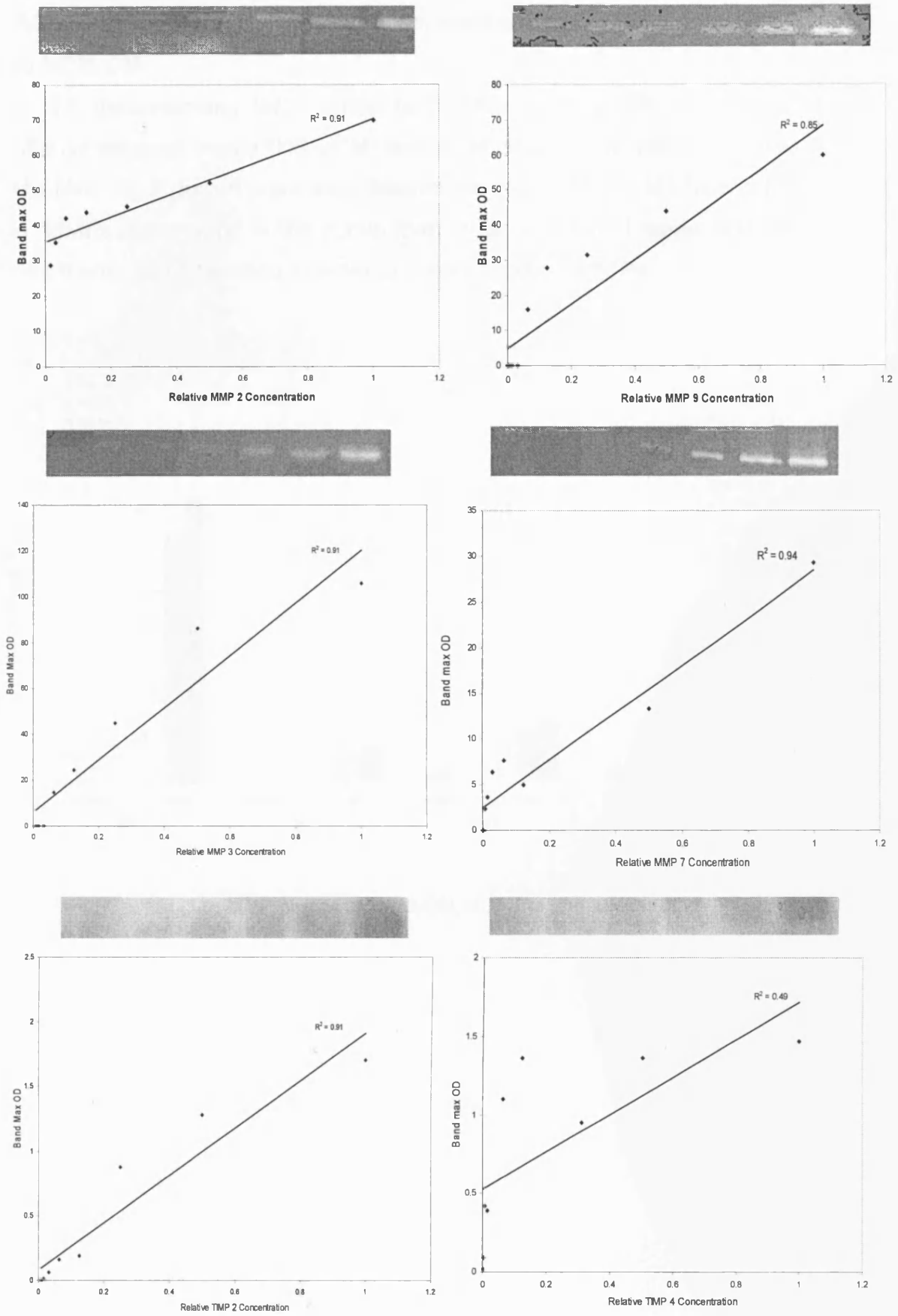

Fig. 3.7 Correlation of the band intensity of serially diluted MMP-EM.

3.3.3.2 Quantification of MMPs in serum free media MMP-EM, HSF-CM and HCM-CM

Fig. 3.8 demonstrates large amounts of MMP 2 in serum-free MMP-EM, HSFs conditioned media (HSF-CM) and HCM cells conditioned media (HCM-CM). MMP 3, 7, and 9 were also detected in HSF-CM, HCM-CM and MMP-EM. MMPs were found in the active form in all conditoned media and hence these media could be used in order to detect action of MMPs.

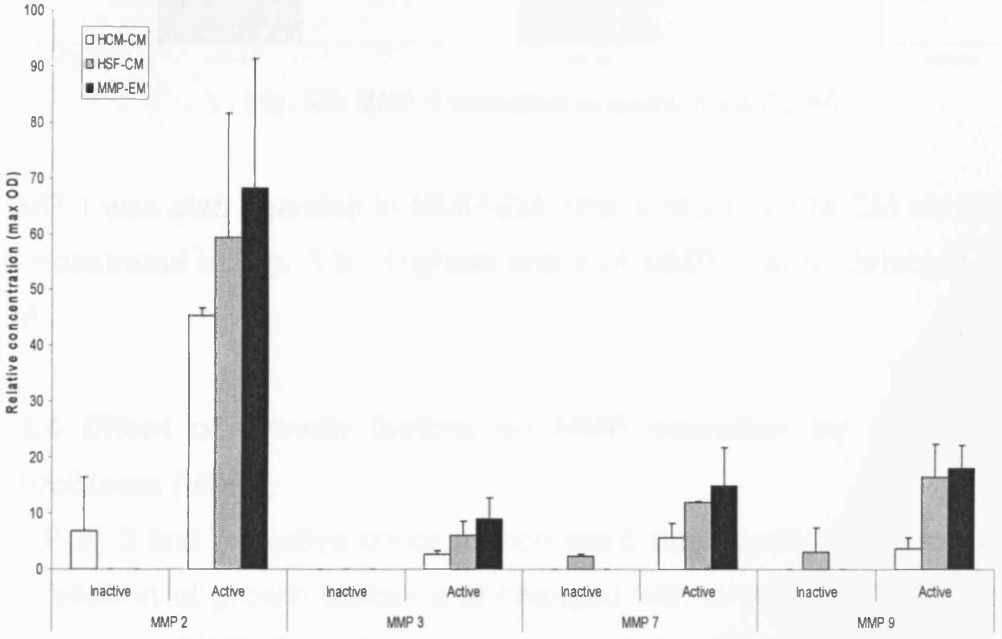

Fig. 3.8: MMP profile of HCM-CM, HSF-CM and MMP-EM.

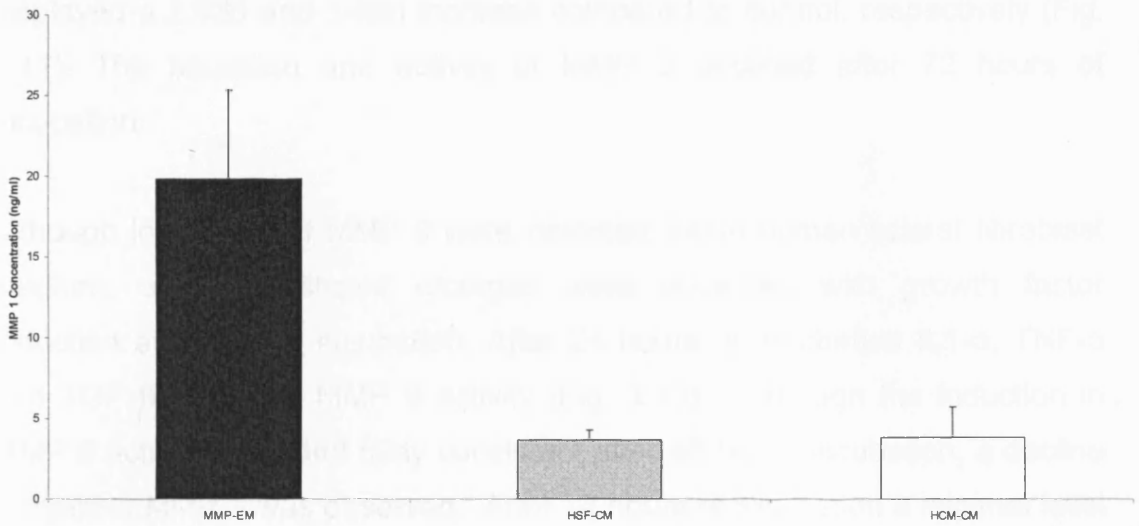

Fig. 3.9: MMP-1 detection in medium via ELISA.

MMP 1 was also detected in MMP-EM. HSF-CM and HCM-CM via ELISA as demonstrated in Fig. 3.9. Highest levels of MMP 1 were detected in MMP-EM.

3.3.4 Effect of growth factors on MMP secretion by Human Scleral Fibroblasts (HSFs)

MMP 2, 3 and 9 relative concentration were significantly increased following the addition of growth factors and changed with time in incubation ($p<0.05$). By contrast MMP 7, within human scleral fibroblast cell culture, did not increase (Fig. 3.12). No significant changes was observed in cell expression by different donors ($p<0.05$).

IL1-α and TGFβ1 induced MMP 2 secretion and activity strongly throughout the time-points, with a maximum level induction after 72 hours of incubation (Fig. 3.10). IL1-α was the strongest inducer of MMP 2 within human scleral fibroblasts. TNF-α caused an induction with the first 24 hours, however a very rapid decline was observed after 48 hours (lower than control) and an induction again after 72 hours.

MMP 3 secretion and activity was slightly induced within 24 hours, followed by a stronger induction after 48 hours of incubation. IL1-α demonstrated a 3-fold increase in MMP 3 activity compared to control, whereas TGF β1 and TNF-α

displayed a 2 fold and 1-fold increase compared to control, respectively (Fig. 3.11). The secretion and activity of MMP 3 declined after 72 hours of incubation.

Although low levels of MMP 9 were detected within human scleral fibroblast medium, some significant changes were observed with growth factor induction and time in incubation. After 24 hours of incubation IL1-α, TNF-α and TGF β1 induced MMP 9 activity (Fig. 3.13). Although the induction in MMP 9 activity remained fairly consistent after 48 hours incubation, a decline in inactive MMP 9 was observed. After 72 hours of incubation a minimal level of MMP 9 activity was observed.

(a)

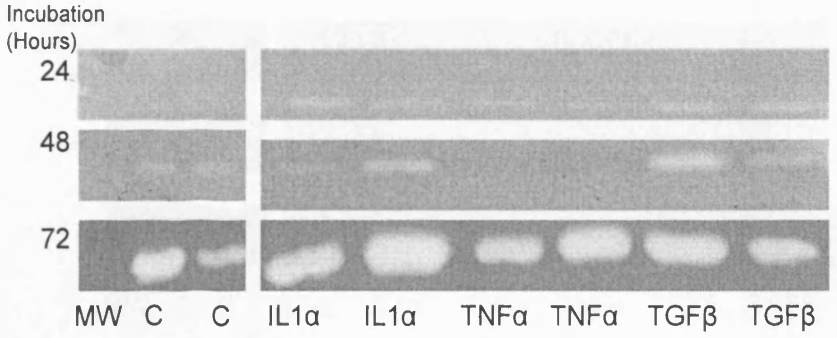

(b)

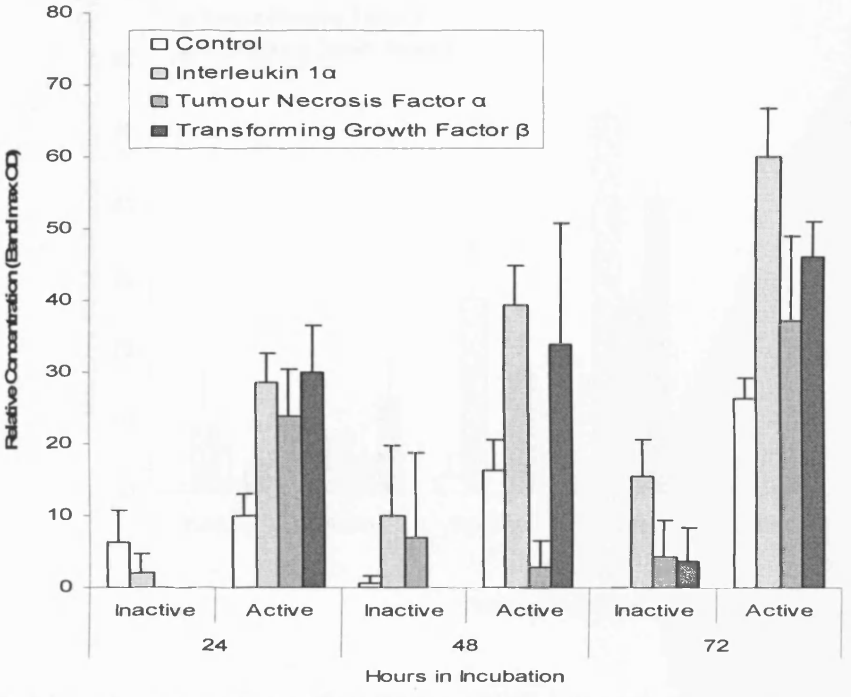

Fig. 3.10: The effect of growth factors on MMP 2 secretion by human scleral fibroblasts. Data includes both active and inactive forms of MMP 2. (a) Gelatin zymograghy: Molecular weight marker (MW), Control (C), IL1α, TNFα and TGFβ. (b) Chart of relative MMP 2 concentration with treatment.

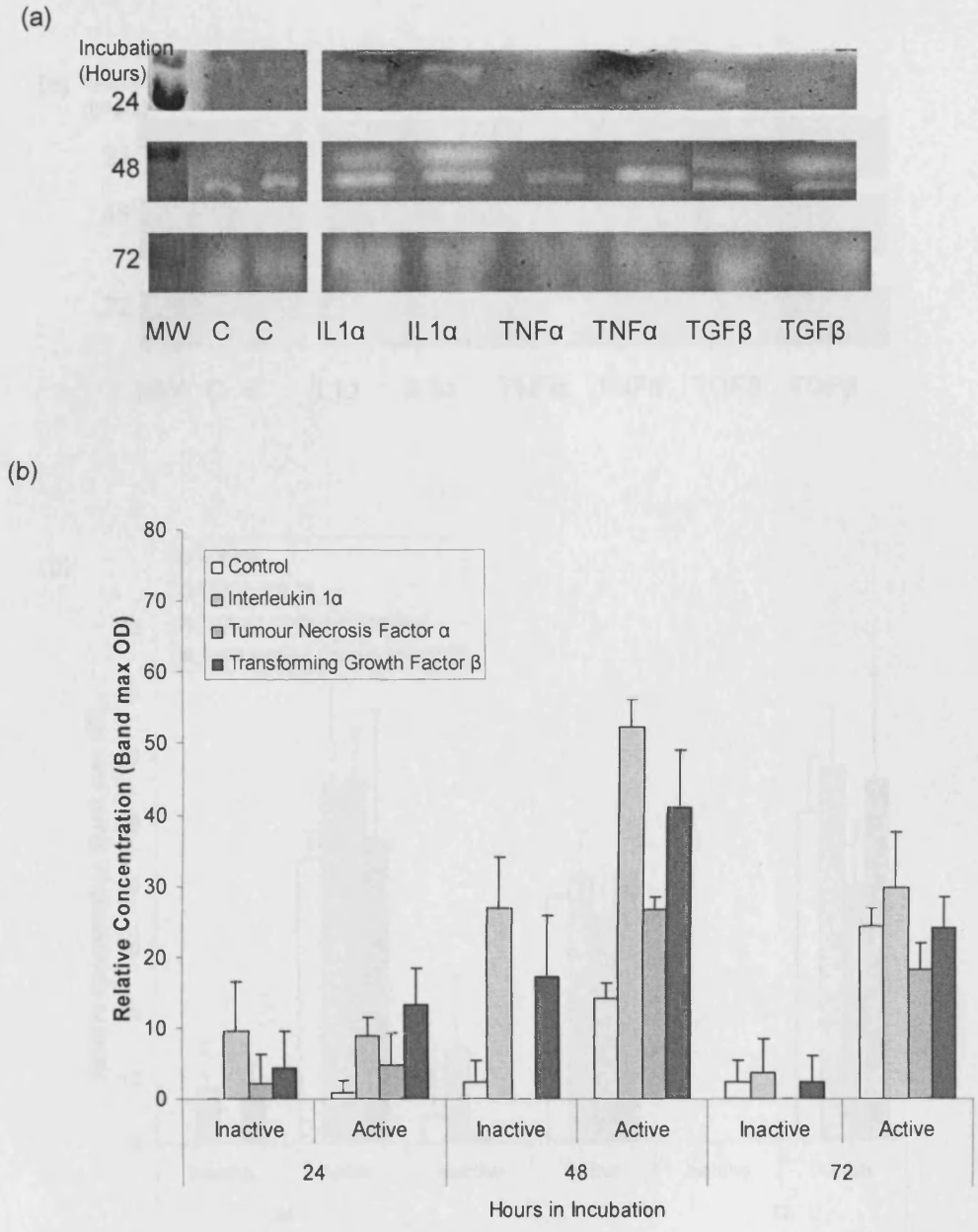

Fig. 3.11: The effect of growth factors on MMP 3 secretion by human scleral fibroblasts. Data includes both active and inactive forms of MMP 3. (a) casein zymography: Molecular weight marker (MW), Control (C), IL1α, TNFα and TGFβ. (b) Chart of relative MMP 3 concentration with treatment.

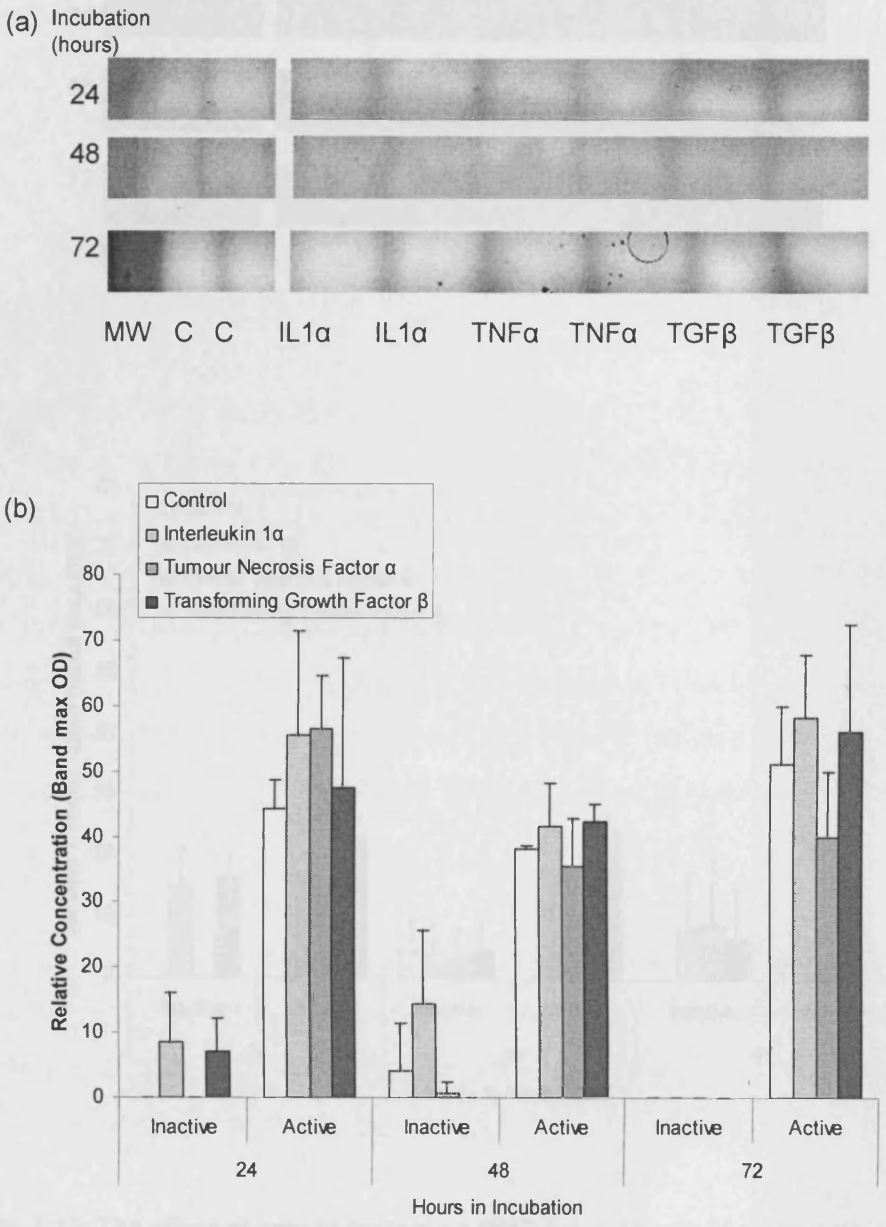

Fig. 3.12: The effect of growth factors on MMP 7 secretion by human scleral fibroblasts. Data includes both active and inactive forms of MMP 7. (a) Casein zymography: Molecular weight marker (MW), Control (C), IL1α, TNFα and TGFβ. (b) Chart of relative MMP 7 concentration with treatment.

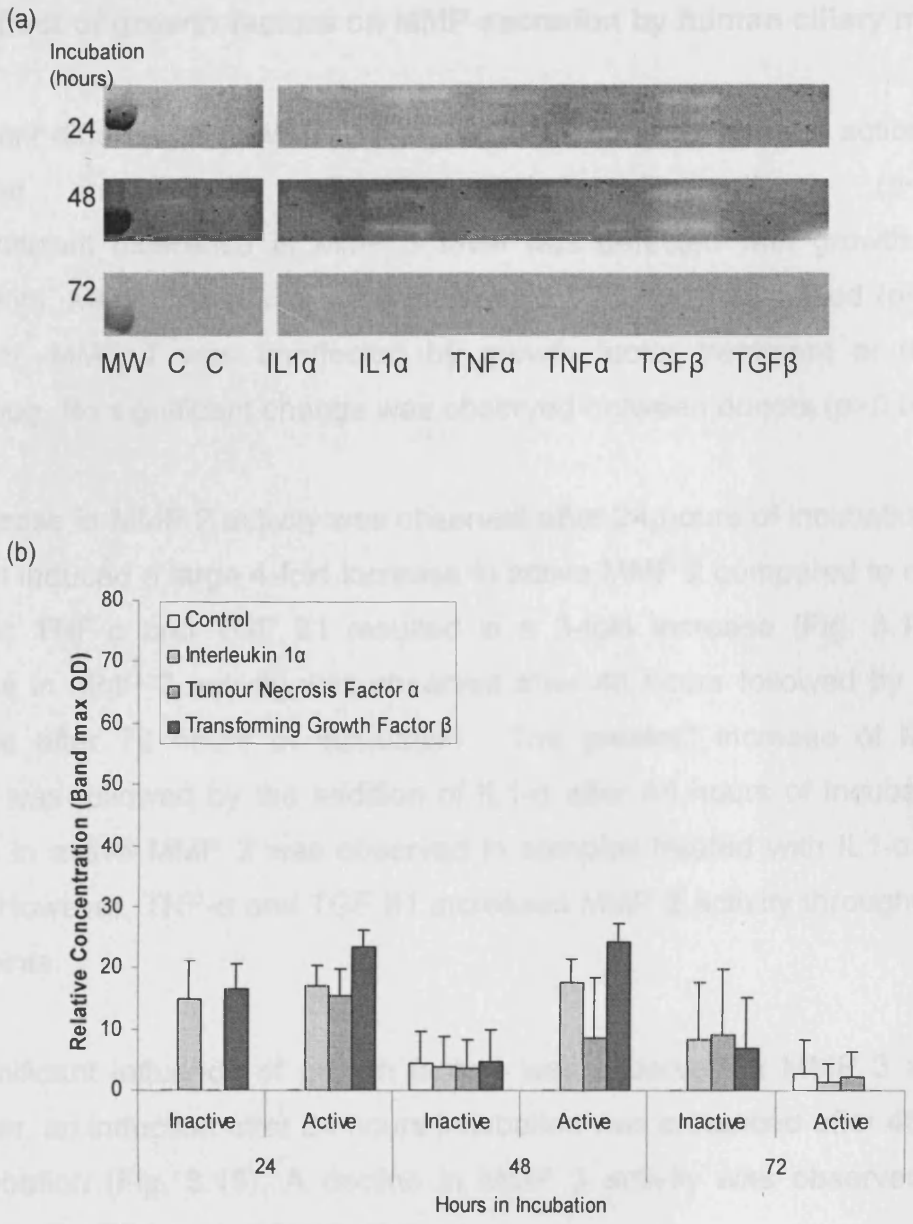

Fig. 3.13: The effect of growth factors on MMP 9 secretion by human scleral fibroblasts. Data includes both active and inactive forms of MMP 9. (a) Gelatin zymography: Molecular weight marker (MW), Control (C), IL1α, TNFα and TGFβ. (b) Chart of relative MMP 9 concentration with treatment.

3.3.5 Effect of growth factors on MMP secretion by human ciliary muscle cells

Significant differences in MMP 2 and 9 activity with growth factor action were observed in human ciliary muscle cell cultures ($p<0.05$). No significant difference in MMP 3 level was detected with growth factor treatments. MMP 2, 3 and 9 were influenced by incubation period ($p<0.03$). However, MMP 7 was unaffected by growth factor treatment or time of incubation. No significant change was observed between donors ($p>0.05$).

An increase in MMP 2 activity was observed after 24 hours of incubation. IL1-α action induced a large 4-fold increase in active MMP 2 compared to control, whereas TNF-α and TGF β1 resulted in a 3-fold increase (Fig. 3.14). An increase in MMP 2 activity was observed after 48 hours followed by further increase after 72 hours of incubation. The greatest increase of MMP 2 activity was followed by the addition of IL1-α after 48 hours of incubation, a decline in active MMP 2 was observed in samples treated with IL1-α for 72 hours. However, TNF-α and TGF β1 increased MMP 2 activity throughout the time points.

No significant influence of growth factors was observed in MMP 3 activity. However, an induction after 24 hours incubation was enhanced after 48 hours of incubation (Fig. 3.15). A decline in MMP 3 activity was observed in all samples after 72 hours of incubation.

MMP 7 activity was unaffected by the addition of growth factors or by the duration of incubation. However a consistent level of active and inactive MMP 7 was observed throughout all time points in all the samples (Fig. 3.16). The levels of active MMP 7 appeared to be about double that of inactive levels in all the samples. This was a significant observation in MMP 7 activity within ciliary muscle cell cultures ($p<0.05$).

Maximal induction of MMP 9 by all three growth factors was observed after 24 hours incubation (Fig. 3.17). Although a higher level of MMP 9 was observed

in growth factor treated samples than control after 48 hours incubation, both active and inactive MMP 9 levels declined after 48 hours. A further decline in MMP 9 levels was noted after 72 hours of incubation.

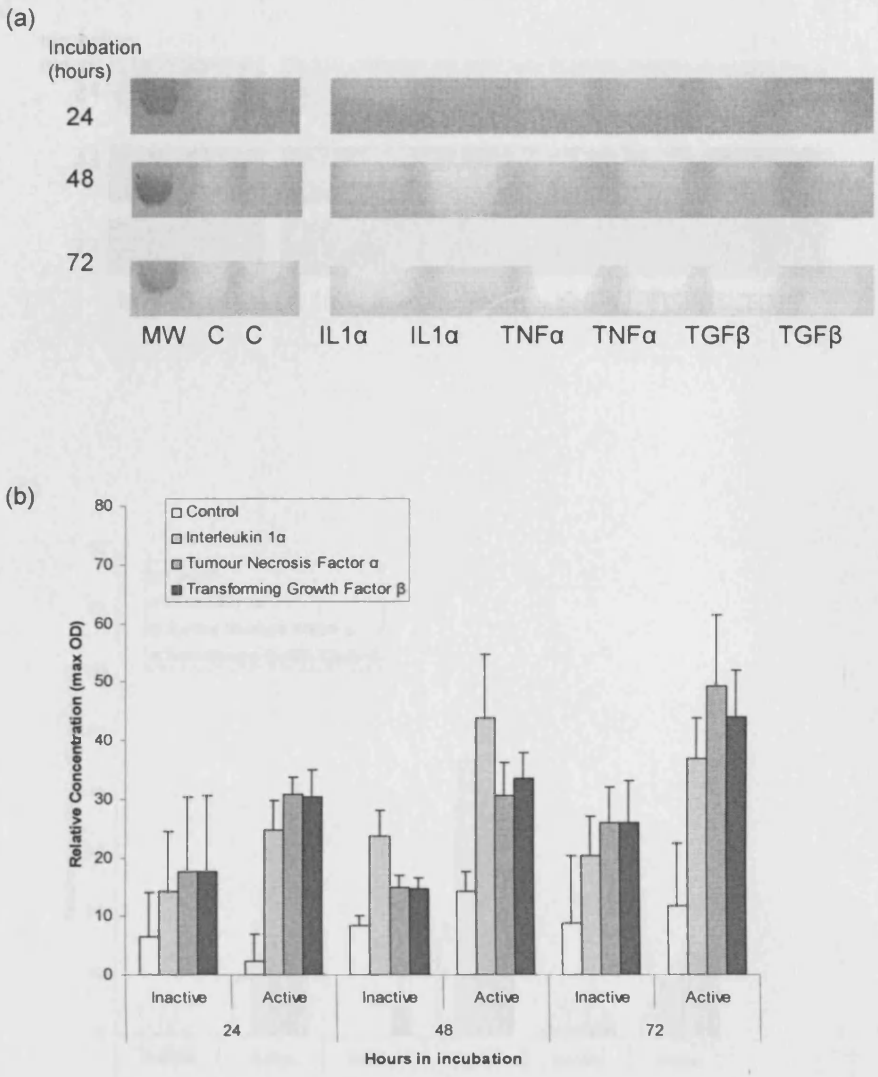

Fig. 3.14: The effect of growth factors on MMP 2 secretion by human ciliary muscle cells. Data includes both active and inactive forms of MMP 2. (a) Gelatin zymography: Molecular weight marker (MW), Control (C), IL1α, TNFα and TGFβ. (b) Chart of relative MMP 2 concentration with treatment.

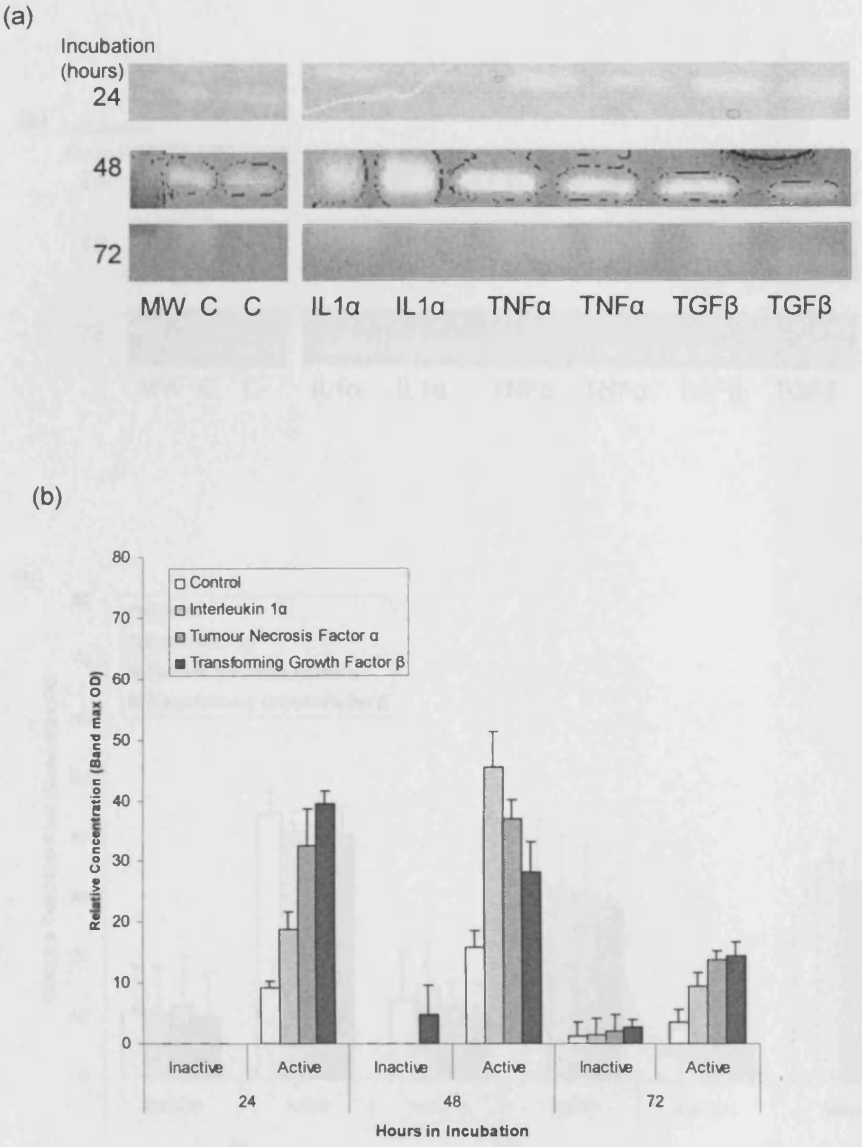

Fig. 3.15: The effect of growth factors on MMP 3 secretion by human ciliary muscle cells. Data includes both active and inactive forms of MMP 3. (a) Casein zymography: Molecular weight marker (MW), Control (C), IL1α, TNFα and TGFβ. (b) Chart of relative MMP 3 concentration with treatment.

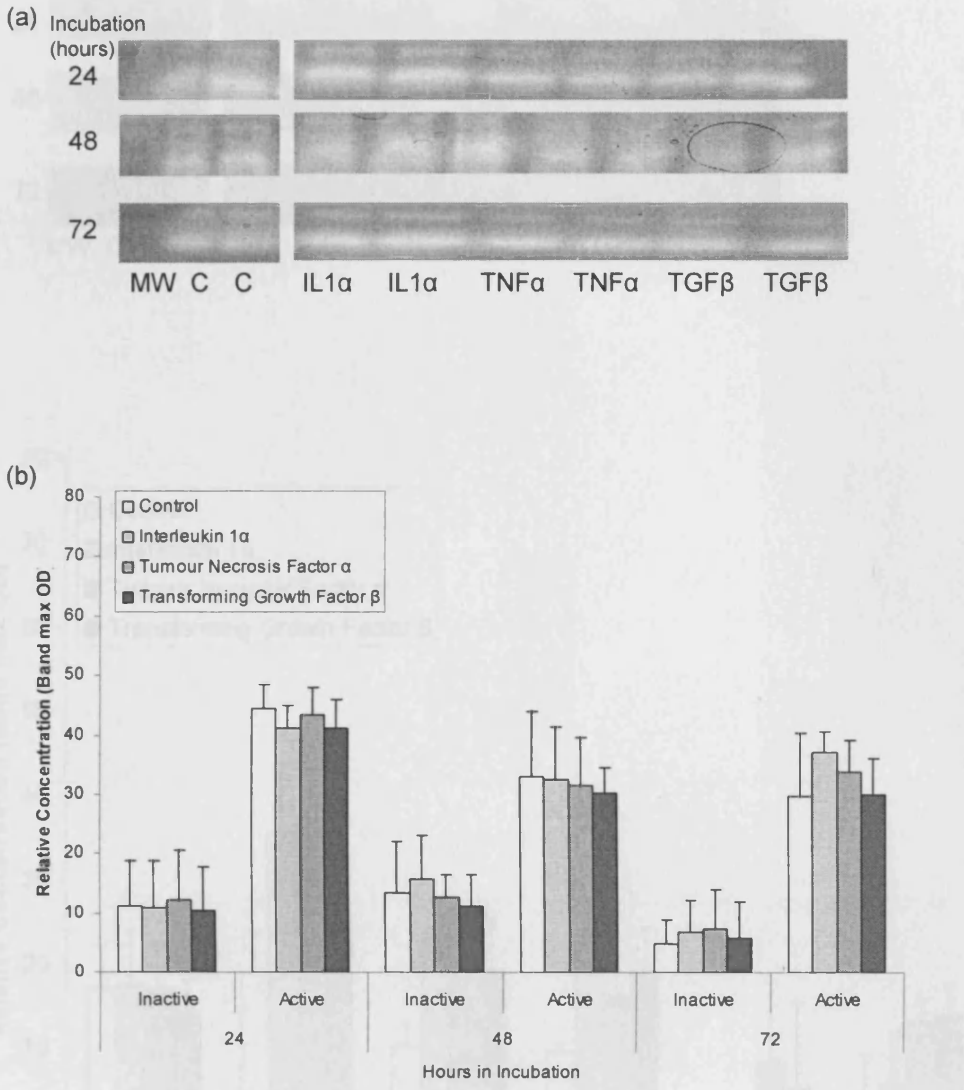

Fig. 3.16: The effect of growth factors on MMP 7 secretion by human ciliary muscle cells. Data includes both active and inactive forms of MMP 7. (a) Casein zymography: Molecular weight marker (MW), Control (C), IL1α, TNFα and TGFβ. (b) Chart of relative MMP 7 concentration with treatment.

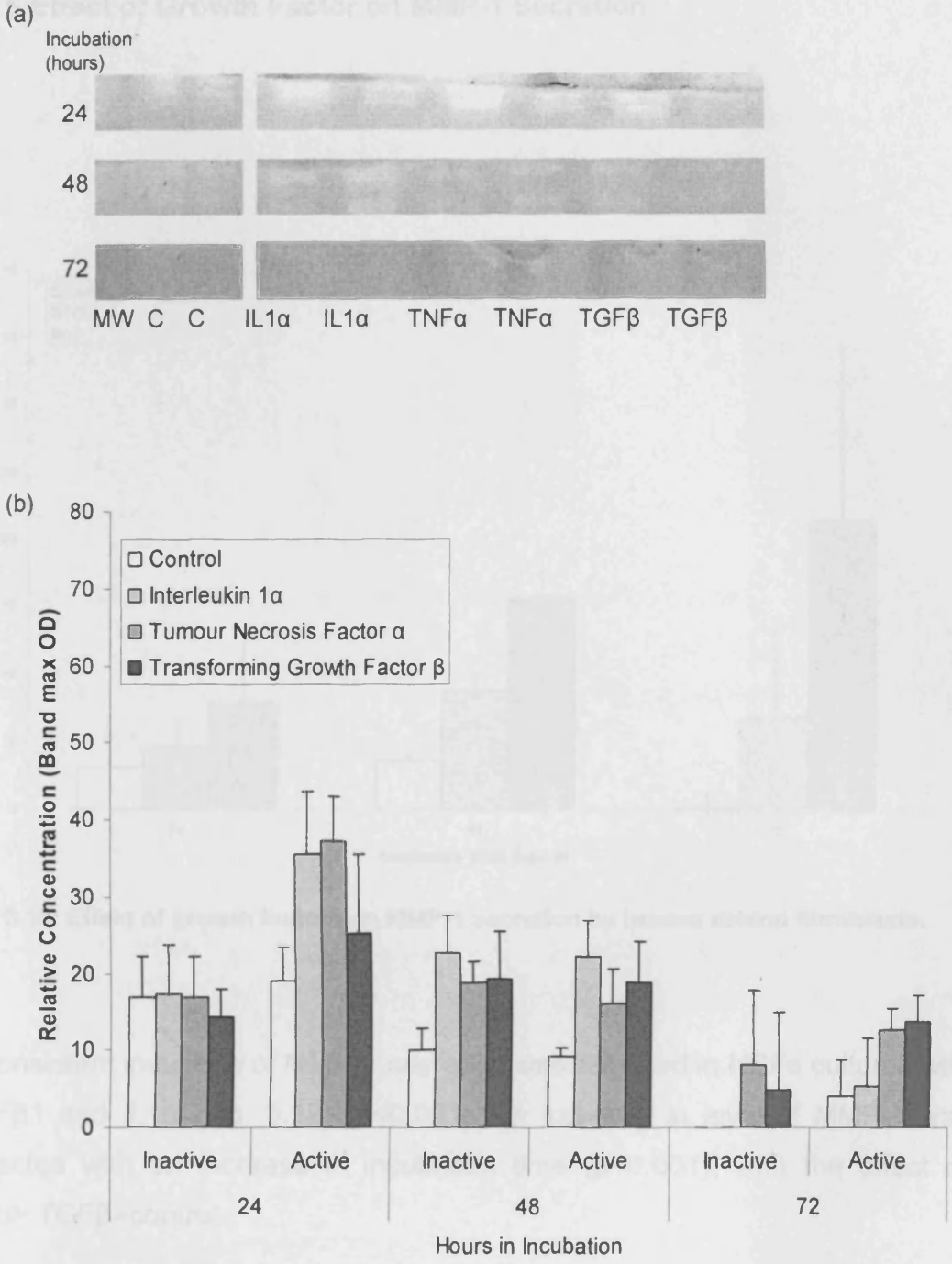

Fig. 3.17: The effect of growth factors on MMP 9 secretion by human ciliary muscle cells. Data includes both active and inactive forms of MMP 9. (a) Gelatin zymography: Molecular weight marker (MW), Control (C), IL1α, TNFα and TGFβ. (b) Chart of relative MMP 9 concentration with treatment.

3.3.6 Effect of Growth Factor on MMP-1 Secretion

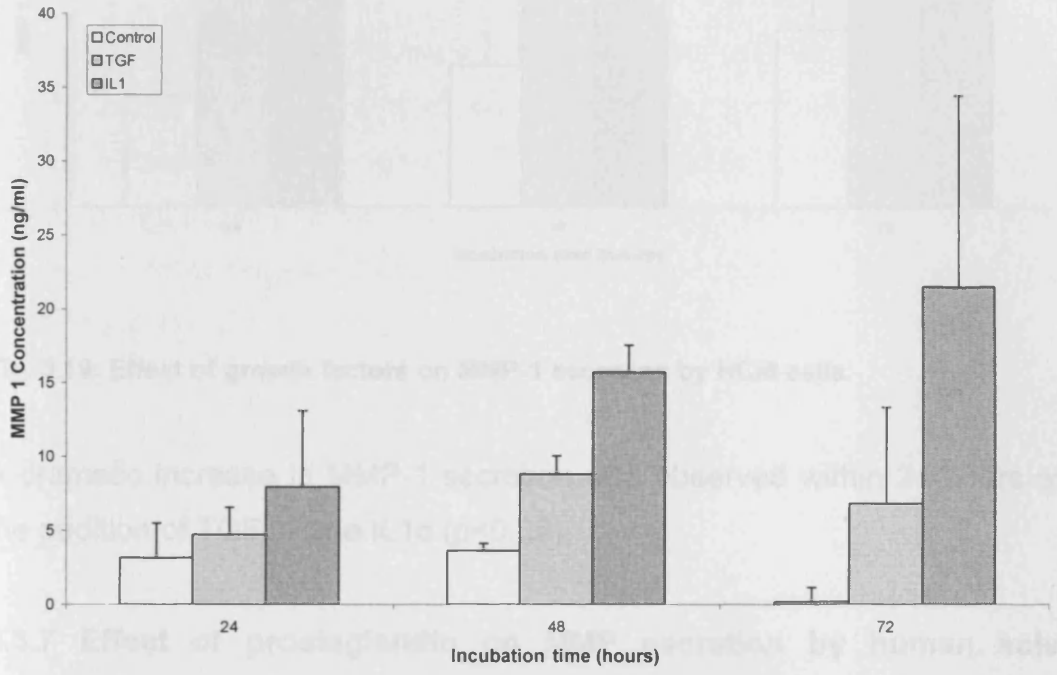

Fig. 3.18: Effect of growth factors on MMP-1 secretion by human scleral fibroblasts.

A consistent induction of MMP-1 secretion was detected in HSFs cultures with TGFβ1 and IL1α (Fig. 3.18) ($p<0.001$). An increase in level of MMP-1 was detected with an increase in incubation time ($p<0.001$), with the effect of IL1α> TGFβ>control.

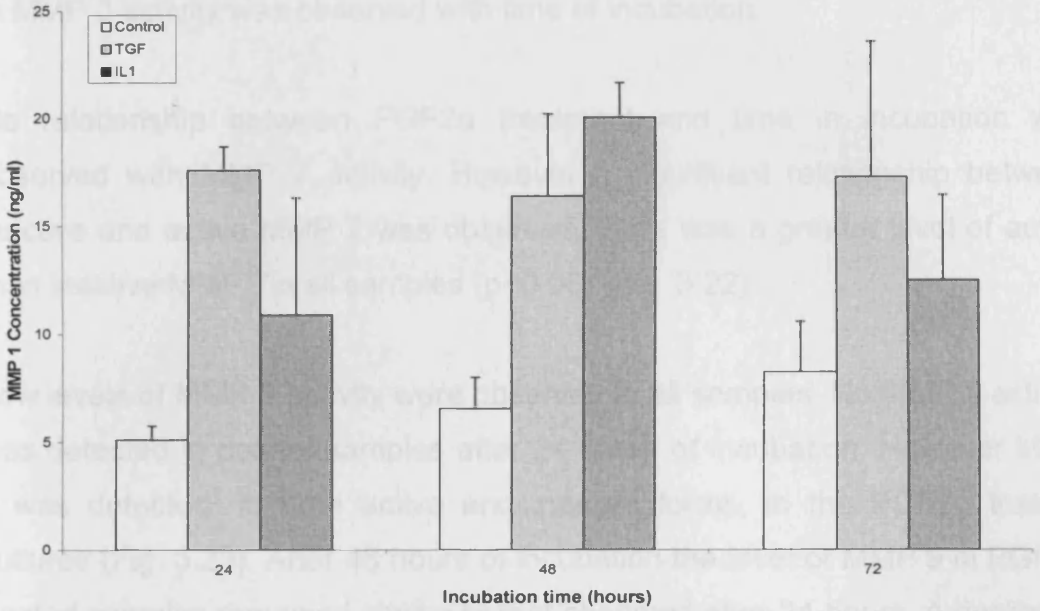

Fig. 3.19: Effect of growth factors on MMP-1 secretion by HCM cells.

A dramatic increase in MMP-1 secretion was observed within 24 hours after the addition of TGFβ1 and IL1α ($p<0.02$).

3.3.7 Effect of prostaglandin on MMP secretion by human scleral fibroblasts

Both PGF2α action and time of incubation influenced the levels of MMP 2, 3, and 9 ($p<0.05$). However, no significant impact on MMP 7 was observed ($p>0.05$).

An increased level of inactive and active MMP 2 was observed in scleral fibroblasts cultured in the presence of PGF2α for 24 hours (Fig. 3.20). Although a reduction in MMP 2 level was observed in both control and PGF2α treated samples after 48 hours, a further increase was observed after 72 hours. At all time-points PGF2α doubled the levels of inactive and active MMP 2 observed compared to control ($p<0.05$).

An induction of MMP 3 activity was observed after 24 hours of incubation with PGF2α treatment. However, after 48 hours the level of MMP 3 activity in both

control and PGF2α treated cultures were similar (Fig. 3.21). A slow increase in MMP 3 activity was observed with time of incubation.

No relationship between PGF2α treatment and time in incubation was observed with MMP 7 activity. However a significant relationship between inactive and active MMP 7 was observed, there was a greater level of active than inactive MMP 7in all samples ($p<0.05$) (Fig. 3.22).

Low levels of MMP 9 activity were observed in all samples. No MMP 9 activity was detected in control samples after 24 hours of incubation. However MMP 9 was detected, in both active and inactive forms, in the PGF2α treated cultures (Fig. 3.23). After 48 hours of incubation the level of MMP 9 in PGF2α treated samples remained similar to that observed after 24 hours. A decline in MMP 9 activity was observed after 72 hours of incubation.

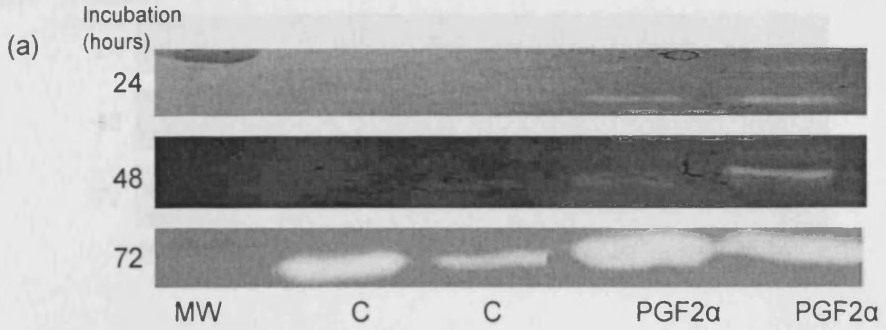

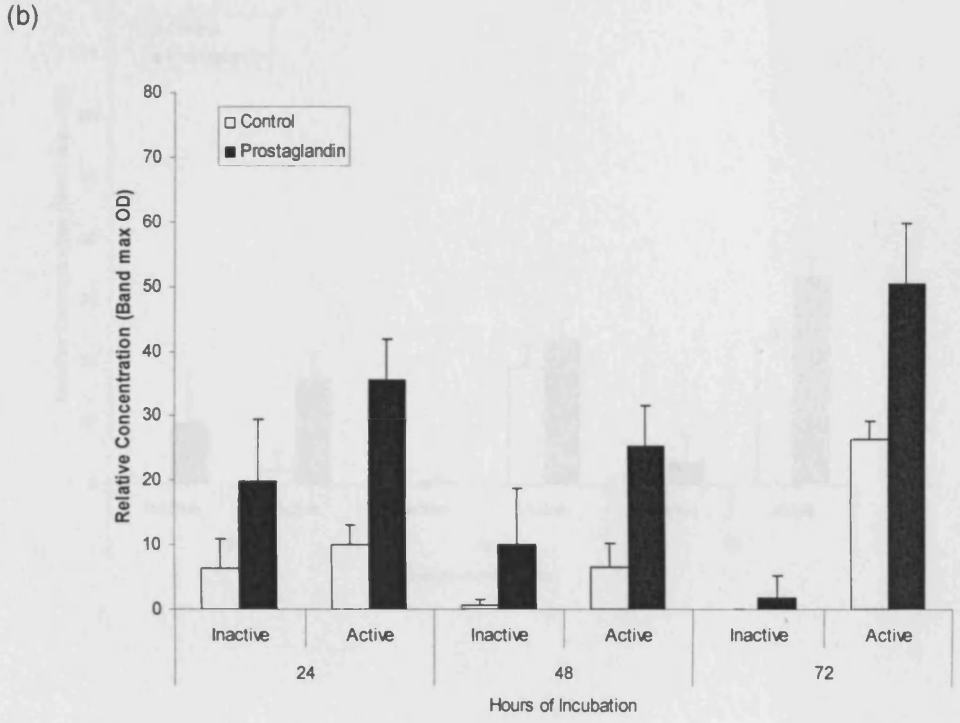

Fig. 3.20: PGF2α effect on human scleral fibroblasts conditioned medium MMP 2 secretion and activation. (a) Gelatin zymography: Control (C) and PGF2α. (b) Chart of relative MMP 2 concentration with treatment.

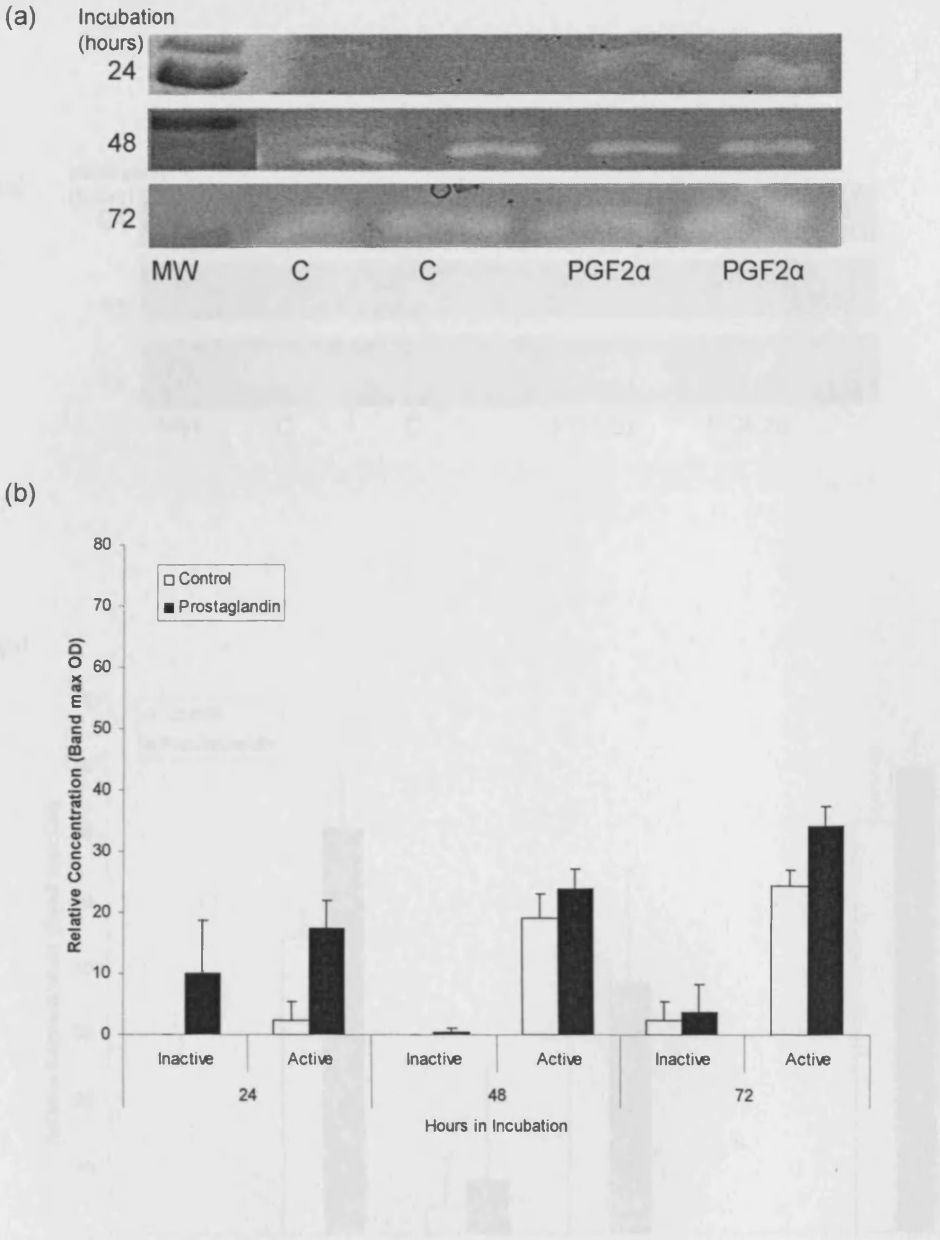

Fig. 3.21: PGF2α effect on human scleral fibroblasts conditioned medium MMP 3 secretion and activation. (a) Casein zymography: Control (C) and PGF2α. (b) Chart of relative MMP 3 concentration with treatment.

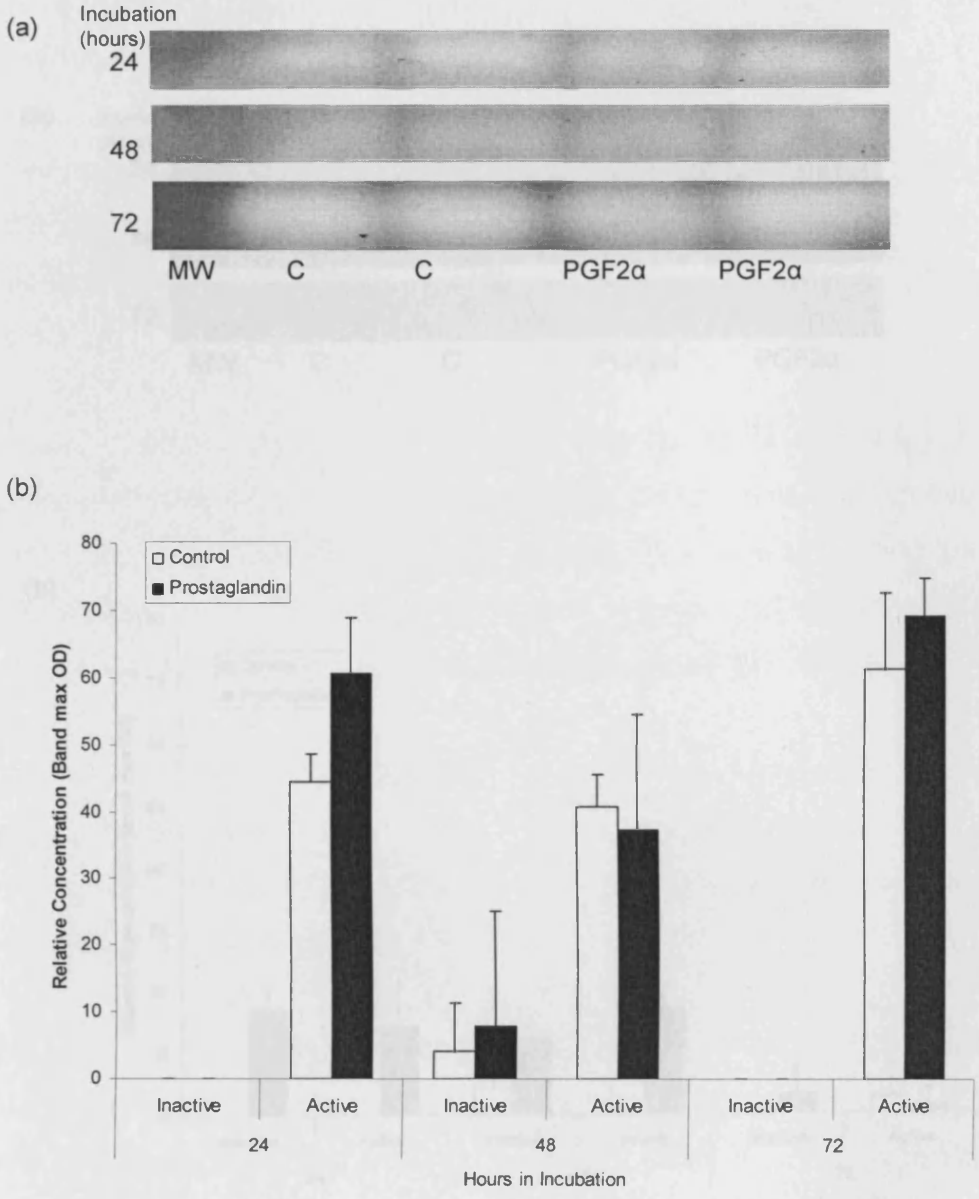

Fig. 3.22: PGF2α effect on human scleral fibroblasts conditioned medium MMP 7 secretion and activation. (a) Casein zymography: Control (C)and PGF2α. (b) Chart of relative MMP 7 concentration with treatment.

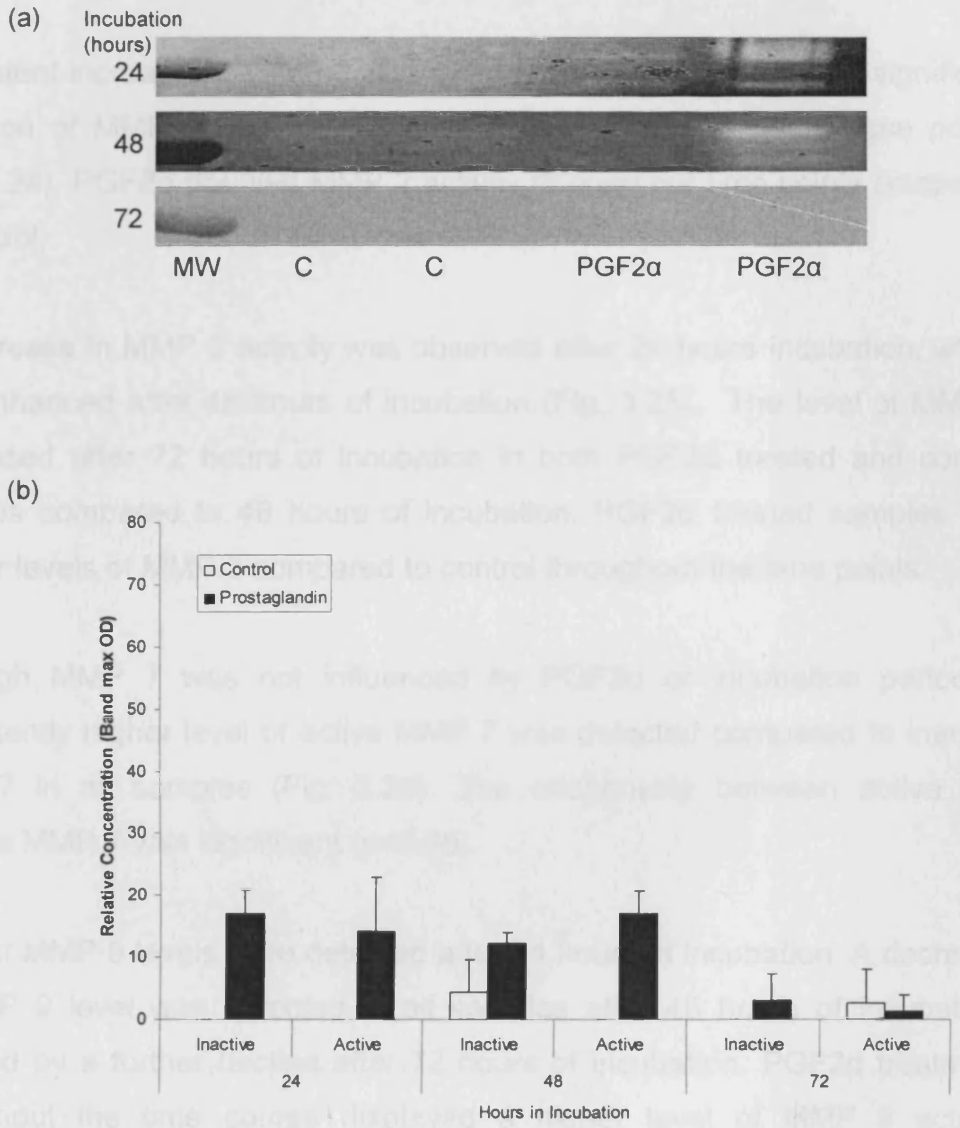

Fig. 3.23: PGF2α effect on human scleral fibroblasts conditioned medium MMP 9 secretion and activation. (a) Gelatin zymograpghy: Control (C) and PGF2α. (b) Chart of relative MMP 9 concentration with treatment.

3.3.8 Effect of Prostaglandin on MMP secretion by human ciliary muscle cells

PGF2α significantly increased the levels of active and inactive forms of MMP 2, 3 and 9 in ciliary muscle cell cultures ($p<0.05$). By contrast MMP 7 levels were unaffected by PGF2α treatment and incubation time ($p>0.05$).

Consistent increases in MMP 2 activity were observed with time. A significant induction of MMP 2 with PGF2α was observed throughout the time points (Fig. 3.24). PGF2α doubled MMP 2 activity through out time points compared to control.

An increase in MMP 3 activity was observed after 24 hours incubation, which was enhanced after 48 hours of incubation (Fig. 3.25). The level of MMP 3 decreased after 72 hours of incubation in both PGF2α treated and control samples compared to 48 hours of incubation. PGF2α treated samples had greater levels of MMP 3 compared to control throughout the time points.

Although MMP 7 was not influenced by PGF2α or incubation period, a consistently higher level of active MMP 7 was detected compared to inactive MMP 7 in all samples (Fig. 3.26). The relationship between active and inactive MMP 7 was significant ($p<0.05$).

Highest MMP 9 levels were detected after 24 hours of incubation. A decrease in MMP 9 level was detected in all samples after 48 hours of incubation, followed by a further decline after 72 hours of incubation. PGF2α treatment throughout the time course displayed a higher level of MMP 9 activity compared to control (Fig. 3.27).

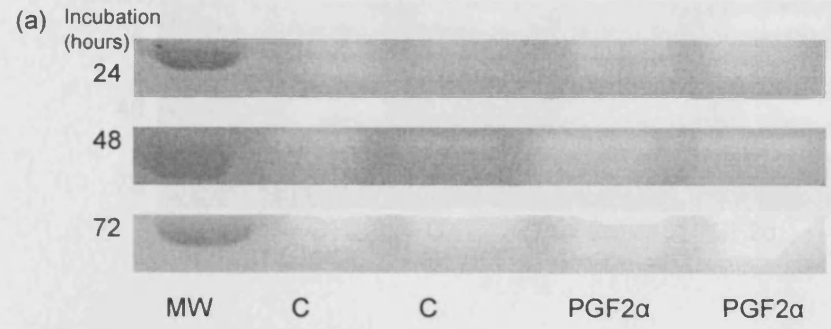

(b)

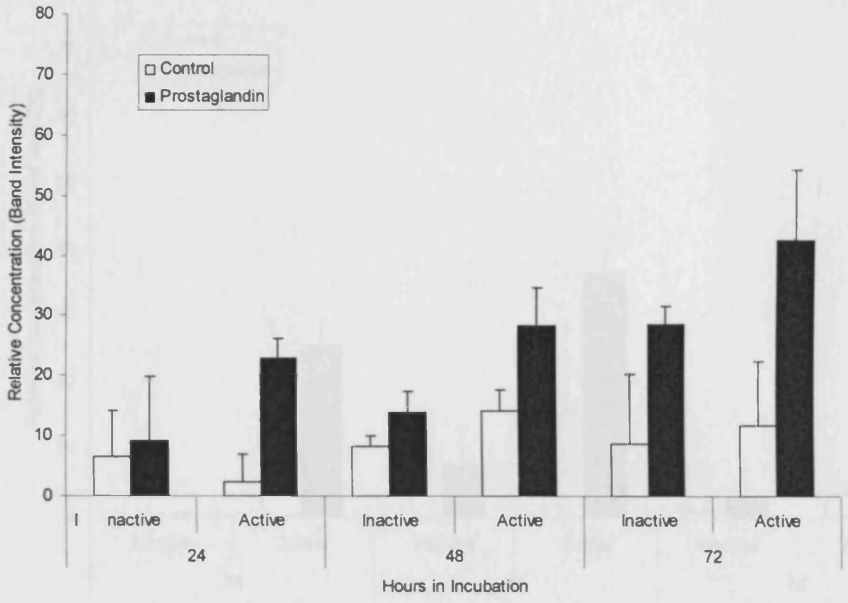

Fig. 3.24: PGF2α effect on human ciliary muscle conditioned medium MMP 2 secretion and activation. (a) Gelatin zymography: Control (C) and PGF2α. (b) Chart of relative MMP 2 concentration with treatment.

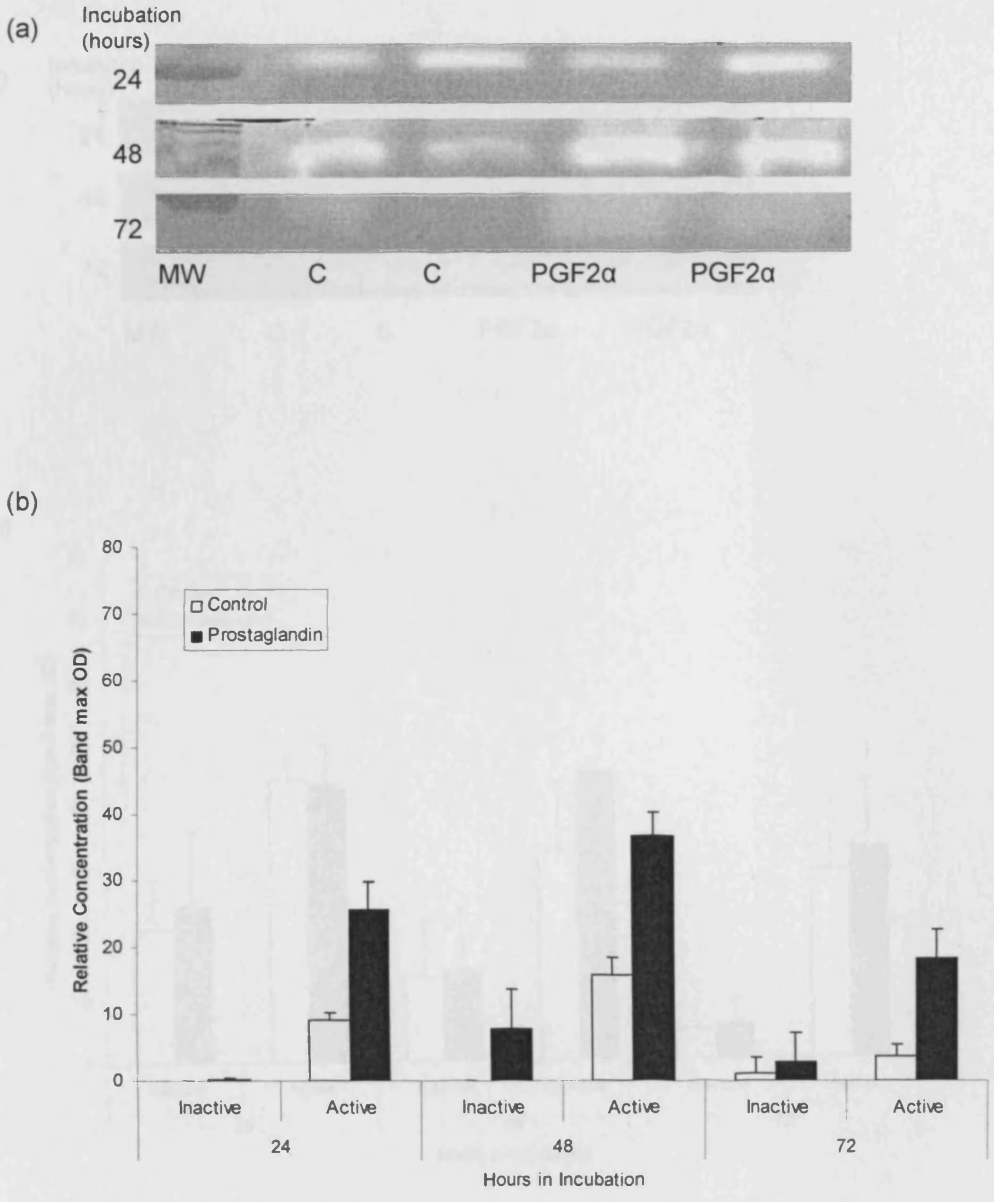

Fig. 3.25: PGF2α effect on human ciliary muscle conditioned medium MMP 3 secretion and activation. (a) Casein zymography: Control (C) and PGF2α. (b) Chart of relative MMP 3 concentration with treatment.

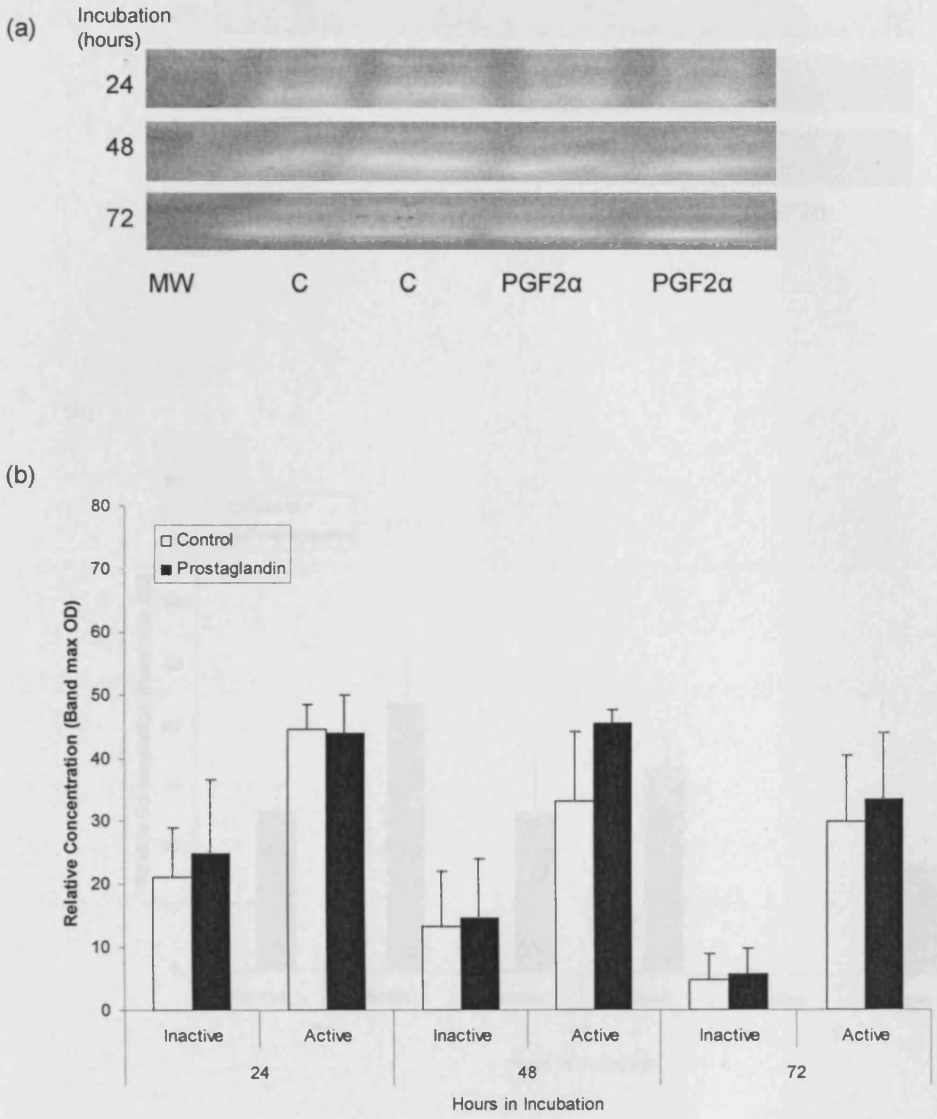

Fig.3.26: PGF2α effect on human ciliary muscle conditioned medium MMP 7 secretion and activation. (a) Casein zymography: Control (C) and PGF2α. (b) Chart of relative MMP 7 concentration with treatment.

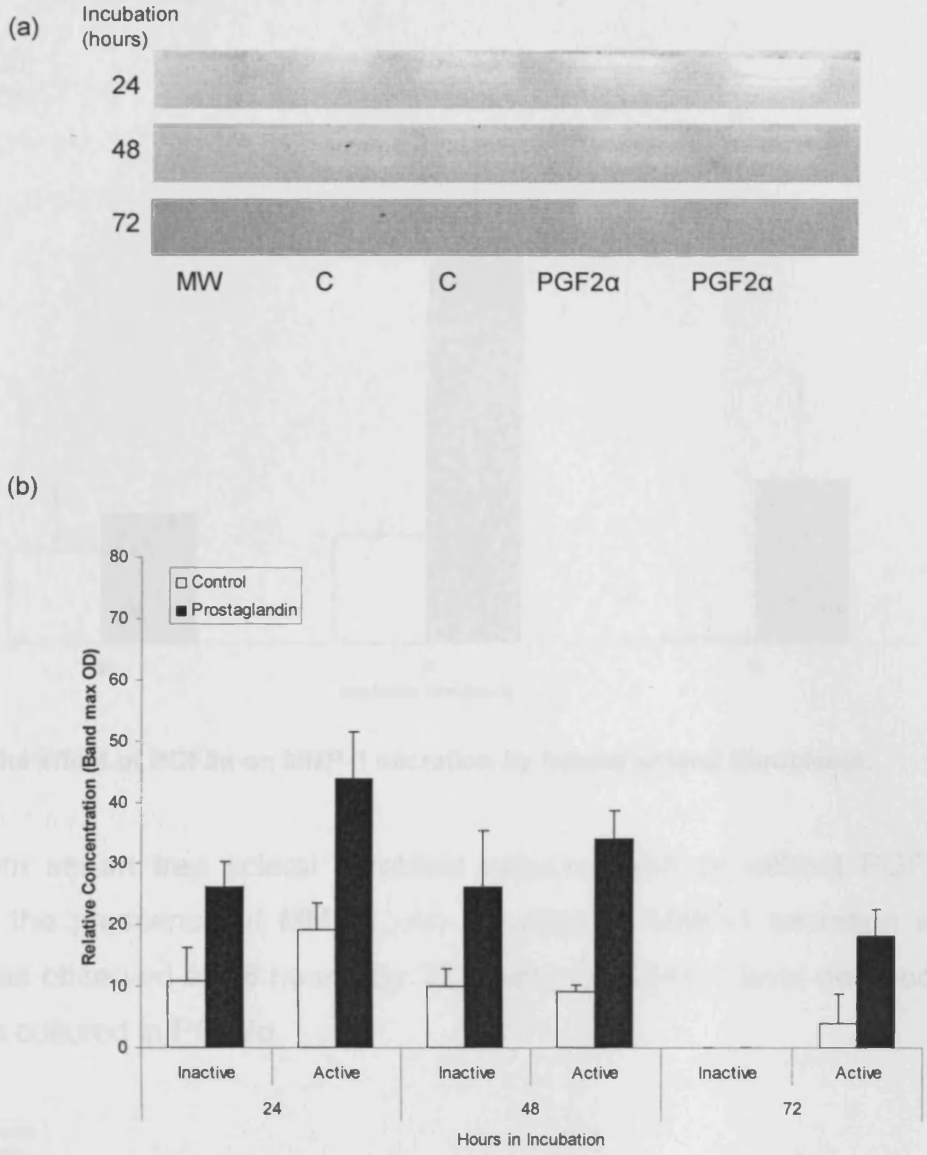

Fig. 3.27: PGF2α effect on human ciliary muscle conditioned medium MMP 9 secretion and activation. (a) Gelatin zymography: Control (C) and PGF2α. (b) Chart of relative MMP 9 concentration with treatment.

3.3.9 Effect of Prostaglandin on MMP-1 activity

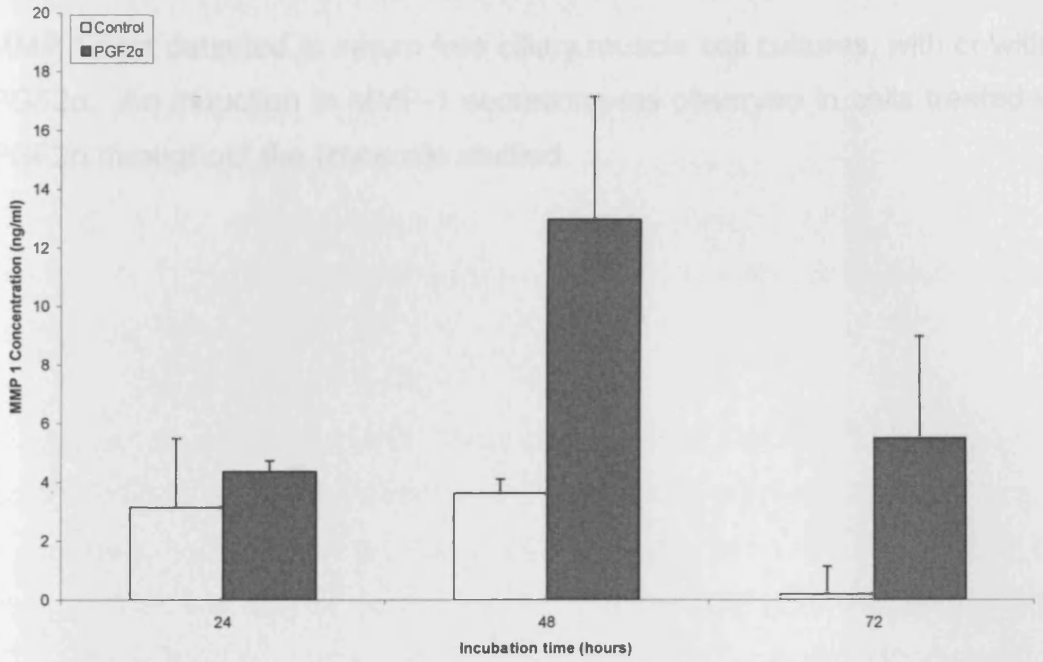

Fig. 3.28: The effect of PGF2α on MMP-1 secretion by human scleral fibroblasts.

Media from serum free scleral fibroblast cultures, with or without PGF2α, displayed the prescence of MMP-1. An induction of MMP-1 secretion with PGF2α was observed at 48 hours. By 72 hours, the MMP-1 level declined in fibroblasts cultured in PGF2α.

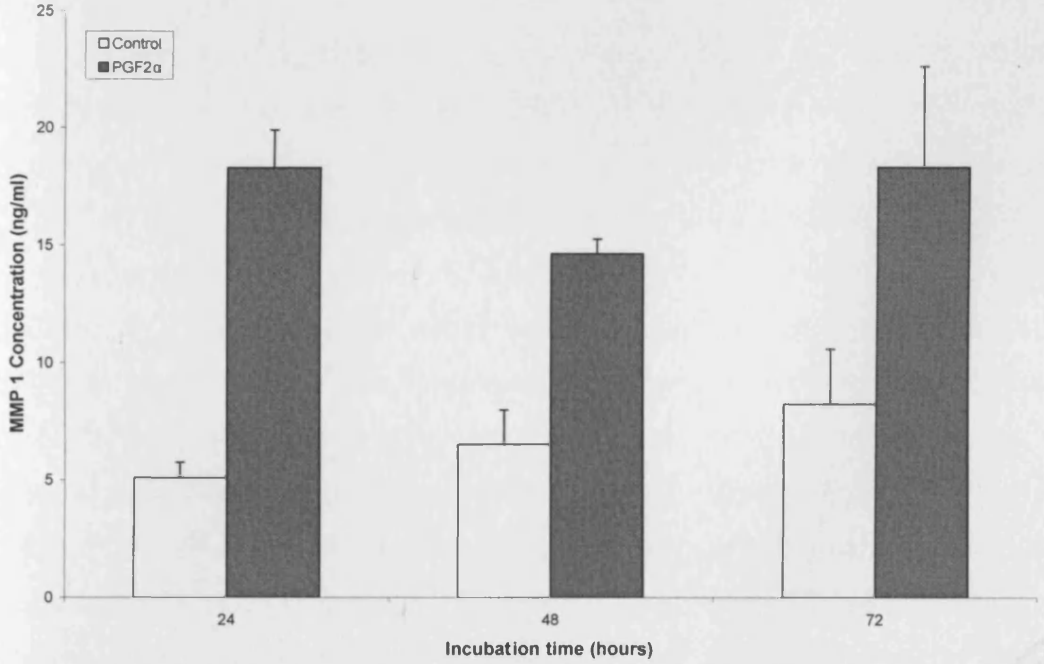

Fig. 3.29: The effect of PGF2α on MMP-1 secretion by human ciliary muscle cell.

MMP 1 was detected in serum free ciliary muscle cell cultures, with or without PGF2α. An induction in MMP-1 secretion was observed in cells treated with PGF2α throughout the timescale studied.

CARDIFF UNIVERSITY PRIFYSGOL CAERDYDD

3.4 Discussion

Morphological staining of anterior segment sections allowed the identification of structural features involved in the drainage of aqueous humor. Prostaglandin receptor agonists have been shown to cause morphological changes within anterior chamber, such as increased optical empty spaces between ciliary muscle the bundles (Richter, Krauss *et al.* 2003). These changes help in mediating an increase in uveoscleral outflow and thereby a lowering of IOP.

Ciliary muscle cells and scleral fibroblasts are both involved in the uveoscleral outflow pathway. Their involvement in the pathway made it necessary to study these cells further. Primary cells cultures were prepared of human ciliary muscle cells and scleral fibroblasts. In order to confirm cells cultured were ciliary muscle cells, after passage 1 cells were stained with α-actin and desmin (Weinreb, Kim *et al.* 1992). α-Actin is found in all smooth muscle cells and desmin is an intermediate filament found in different concentrations in smooth muscle cells. The presence of both of these factors confirmed that the cells cultured were smooth muscle cells extracted from the ciliary muscle section of the anterior chamber.

Previous studies have shown the importance of FP receptor in the IOP lowering effect of prostaglandin (Growston,· Lindsey *et al.* 2004). Although many prostaglandin receptor subtypes (i.e. EP1, EP2, EP3, EP4 and FP) have been identified in ocular tissues (Schlotzer-Schrehardt, Zenkel *et al.* 2002), FP receptor has been linked to effect prostaglandin on MMP gene expression (Weinreb, Lindsey *et al.* 2004). The current study confirmed the presence of PGF2α receptor within cells cultured from the uveoscleral outflow pathway. Previous research has shown a similar pattern of staining for MMPs and TIMPs (Lan, Kumar *et al.* 2003). Other research has identified the prescence of FP receptor in the sclera (Anthony, Lindsey *et al.* 2001) and the ciliary body (Mukhopadhyay, Geoghegan *et al.* 1997). However, the current study can link both FP receptor location to gelatinase localisation within cells cultured from the uveoscleral outflow pathway. This would mean that FP

receptor activation may have an impact on MMP action within ciliary muscle and sclera and thereby influence the uveoscleral outflow pathway.

Bovine skin fibroblasts (BOVS-1) were cultured in order to obtain MMP-enriched medium (Blain, Gilbert *et al.* 2001). Conditioned-medium from HCM and HSF were also collected from HCM and HSF cultured in serum-free medium. The zymograms obtained from the conditioned–media confirmed the prescence of MMP 1, 2, 3 & 7 in HCM culture and MMP 2 and 7 in the HSF cultures. However, all four TIMPs were also present in the conditioned medium. The MMP-enriched medium (MMP-EM) had significant levels of MMP 1, 2, 9, 3 and 7 and TIMP 3 and 4. These results suggested that BOVS-1 cells were capable of producing more active MMPs than HCM and HSF. These studies confirmed the potential of MMP-EM being used in evaluating the effects of MMPs on tissue and also the ability of HSFs and HCM cells to produce MMPs. Blastp searches were conducted and 85-93% sequence homology was determined between human and bovine MMPs. This meant that the influence of MMP-EM on human scleral tissue was not limited due to MMPs being taken to bovine cell cultures.

As zymograms were to be used in order to quantify MMPs and TIMPs in samples, it was important to determine the relationship between band intensity and MMP and TIMP concentrations. After having optimised gelatin, casein and reverse zymography, MMP-EM samples were run at different dilutions on all relevant zymograms. The bands observed correlated with the changes in sample concentration. This meant that quantification of MMPs from zymograms was an appropriate method to use in order to test the effect of different factors on MMP activity concentration. However, due to the low level of correlation between band intensity and TIMP 4 concentration, TIMP analysis was not possible using reverse zymograms. In the future perhaps with the use of other techniques, such as ELISA, TIMP could be quantified.

The current study detected the effect of growth factors and PGF2α on MMP secretion and activity within cultured HSFs and HCM cells, the cells involved

in the uveoscleral outflow pathway. The influence of growth factors and PGF2α on MMP secretion may relate to extracellular matrix modulation and hence lead to potential therapies to improve aqueous drainage via the uveoscleral outflow pathway.

MMP 2, 3 and 9 were affected by growth factors which appeared to influence MMPs to a different extent, depending on cell culture. Previous studies have suggested induction of MMP 3 and 9 by IL1α and TNFα at the protein level (Fleenor, Pang *et al.* 2003; Hosseini, Rose *et al.* 2006). The involvement of TGFβ1 in the induction of MMP 9 has also been demonstrated in other studies (Kim, Shang *et al.* 2004).

Although MMP 3 in scleral fibroblast culture was significantly affected by growth factors, this was not the case in the ciliary muscle cell culture. IL1α has demonstrated an induction of MMP 9 and stromelysin, with no influence on MMP 2 in trabecular meshwork cell cultures (Samples, Alexander *et al.* 1993), whereas it has been shown to be involved in both secretion of proMMP 2 and its activation in odentogenic keratocysts fibroblast (Kubata, Oka *et al.* 2001).

The influence of growth factors on MMP 2, 3 and 9 displayed a time dependent trend in induction and decline in both scleral fibroblast and ciliary muscle cultures. The action of the growth factor TNFα on MMP expression and secretion has been shown to occur in a time dependent manner in a previous study (Han, Tuan *et al.* 2000).

For all the MMPs studied, active forms were predominantly detected in both scleral fibroblasts and ciliary muscle cells cultures. This could be due to the time course selected, 24 hours being sufficient time in allowing MMP secretion and activation. In previous studies, 6 hours was sufficient in order for TGFβ1 to influence MMP secretion and activation (Kim, Shang *et al.* 2004). Some previous studies have also suggested the major MMP induction occurs within 0-24 hours incubation (Pang, Hellberg *et al.* 2003), while

another study suggested that peak MMP expression as a result of latanoprost treatment occurred after 6-12hours incubation period (Weinreb and Lindsey 2002). This may make it necessary to study earlier time points in order to understand the potency of the growth factor and prostaglandin effect, should it occur within the 0-24 hour time point.

A previous study measured the influence of antiglaucoma agents on the MMP and TIMP balance. The study suggested that a group of antiglaucoma drugs, β-blockers, decreased MMP levels and increased TIMP levels. An opposite effect was observed by prostaglandin-derived antiglaucoma drugs, which were shown to increase MMP and decrease TIMP (Ito, Ohguro *et al.* 2006). The study by Ito *et al.* supports the findings in the current study regarding the induction of MMPs with PGF2α treatment. Another supporting evidence in the induction of MMPs with PGF2α was published (Weinreb, Kashiwagi *et al.* 1997). This study demonstrated the induction of MMP 1, 2, 3 and 9 by PGF2α in human ciliary smooth muscle cells.

The effect of Latanoprost on mRNA expression of MMPs was detected within trabecular meshwork cultures in a previous study (Oh, Martin *et al.* 2006b). A similar study was conducted in order to understand the effect of Latanoprost on MMP expression in the ciliary body (Oh, Martin *et al.* 2006a). This study indicated there was an induction in mRNA for MMP 3 with latanoprost treatment, but a reduction in MMP 2 mRNA expression. However, in the current study MMP 2 activity was shown to increase with time in growth factor and PGF2α treated cultures of scleral fibroblasts and ciliary muscle cells. Similar results were obtained in a previous study, which suggested an induction of MMP-2 secretion and activity in a dose and time dependent manor (Husain, Jafri *et al.* 2005). As MMP 2 is expressed and secreted in a pro-active form, the detection of MMP 2 mRNA does not relate to its activity. This is why it is necessary to study MMP protein level expression rather than gene level expression.

Studies have also been conducted to understand the influence of Latanoprost treatment on TIMPs within human ciliary muscle cultures. A study suggested the induction of TIMP 2 gene expression within the first 6 hours, and was undetected during later time points. TIMP 1 gene expression was induced at later time points (Anthony, Lindsey *et al.* 2002). This study suggests that Latanoprost not only induces MMP, but also acts as a control mechanism in order to prevent MMPs from causing tissue damage.

CHAPTER 4

EFFECT OF PGF2α AND MMP ACTIVITY ON SCLERAL CONDUCTIVITY

CHAPTER 4

EFFECT OF PGF2α AND MMP ACTIVITY ON SCLERAL CONDUCTIVITY

4.1 Introduction

PGF2α is the treatment of choice for the non-surgical reduction of IOP in glaucoma. The reduction of IOP via PGF2α has been associated with the up-regulation of MMP activity (Ito, Ohguro *et al.* 2006), resulting in the elevation of MMP 1, 2, 3 and 9 activity (Ito, Ohguro *et al.* 2006; Tamm, Baur *et al.* 1992). Consistent with this, PGF2α treatment *in vivo* has lead to a reduction of extracellular matrix (ECM) (Crowston, Aihara *et al.* 2004; Gabelt and Kaufman 1989). Topical administration of prostanoid analogues in cynomologus monkey eyes has been associated with a reduction in Collagen type I, III and IV immunoreactivity in the ciliary muscle and adjacent sclera (Sagara, Gaton *et al.* 1999). This could explain the induction in uveoscleral outflow observed with PGF2α treatment. Taken together these findings suggest that direct MMP intervention within aqueous drainage pathway, could enhance IOP lowering effect in the eye.

In the previous chapter the effect of PGF2α on scleral fibroblast and ciliary muscle cells was demonstrated, resulting in the induction of MMP activity. Induced MMP 1, 2, 3 and 9 by human scleral fibroblasts and ciliary muscle cells, respectively, was observed.

Previously, enhanced scleral conductivity has been shown to occur as a result of the administration of prostaglandins and its analogues (PGF2α) (Kim, Lindsey *et al.* 2001), indicative of the effect of MMPs on scleral conductivity. In this study, the direct action of MMPs on scleral conductivity will be assessed and compared to that of PGF2α.

4.1.2 Aims

The aims of this chapter are:

1. to determine the effect of a cocktail of MMPs (MMP-EM) on scleral conductivity. In order to observe effect of MMP, it was necessary to use media with most abundant level of MMP, therefore MMP-EM was most appropriate compared to serum free media from scleral fibroblast or ciliary muscle cells (see section 3.3.3.2).
2. to compare the effect of PGF2α with that of MMP-EM on scleral conductivity

4.2 Experimental design

4.2.1 Source of sclera

Human donor eye globes (n=29), aged 50-89 years, were obtained with 48 hours post mortem from the Corneal Transplant Service Eye Bank (Bristol, UK) after corneal removal for transplant purposes. All human tissue samples were obtained following consent for research purposes in accordance with the ethical guidelines of United Kingdom Transplant Service (UKTS) and the Declaration of Helsinki. All human donor details and usage are included in appendix (section 8.3). All globes were transported at 4°C in moist chambers. For each time point and each size dextran bead 3, donors were used.

4.2.2 Effect of MMP-EM and PGF2α on scleral permeability

4.2.2.1 Scleral explant culture

Isolated sclera (see section 2.4.1), with approximate diameters of 14mm, were scraped clean on both sides. Each scleral explant was immersed in 3% betadine for 30 seconds, and then thoroughly rinsed in autoclaved PBS (pH7.4).

The explants, in triplicate, were cultured in serum-free DMEM containing 100nM 17-phenyltrinor-PGF2α (Cayman Chemical Co, MI), in MMP-EM (as a source of MMPs), or control media (serum-free DMEM) for time periods ranging from 0-72 hours at 37°C, under standard incubator conditions. Initially 24, 48 and 72 hours incubation was studied. However, as changes occurred at time points before 24 hours it became necessary to understand what was happening before the 24 hour time point, therefore 0, 3, 6, 12 hour time-points were also investigated.

4.2.2.2 Production of matrix metalloproteinase enriched medium (MMP-EM)

MMP-EM, known to contain MMPs 1, 2, 9, 3, and 7 and TIMPs 2 and 4 (section 3.3.3) was produced as described in chapter 2 (section 2.2.12.1).

4.2.2.3 Setting up the Ussing Chamber

Since increased permeability was observed from 0 to 24 hours incubation, 0, 12, 24 and 72 hour time-points were selected for later experiments. Scleral explants were removed from incubation media following appropriate incubation and clamped into the Ussing chamber. Experimental protocols for the Ussing chamber are as described in section 2.4.2.

The Ussing system (CHM2 model; WPI Labs, UK, (Fig. 4.1) included a reservoir for media and a chamber in which to clamp the tissue sample. Phenol red-free HBSS (Gibco, UK) was loaded into both sides of the chamber via the reservoir in order to completely fill the system. Rhodamine dextran beads (10, 40 or 70KDa) were added into HBSS media, at the orbital side, making a final concentration of 0.25mg/ml.

A heated water bath continuously supplied water at 42°C to the outer layer of the reservoir via a peristaltic pump (Millipore, UK), to maintain the reservoir medium at a constant temperature of 37°C. The distance between the water bath and the reservoir chamber was minimised to limit heat loss. The chamber medium was maintained at atmospheric air of 5% carbon dioxide via a gas cylinder connected to the reservoir.

Two Ussing systems were run in parallel so that control conditions (i.e. no test factor) could always be run alongside experimental tissue. In order to ensure that the flow of both water and gas supply to the reservoir was maintained at equal rates to both Ussing systems, adjustable clamps were applied to control the flow within tubing that was elevated using a clamp-stand. Black foil was used in order to cover the entire set of apparatus once the tissue was inserted and medium flow started. The black foil and lights were switched off to prevent light exposure and possible bleaching of the rhodamine dye. The gas bubbling within the reservoir caused the media to remain in constant motion from reservoir through to the chamber.

Scleral tissue remained in the Ussing chamber for 4 hours, as indicated in a previous study (Kim, Lindsey *et al.* 2001). Media samples were collected from the uveal side chamber at 30 minutes and 4 hours post-running of the experiment. Samples were frozen at -80°C spectrofluorimetric analysis.

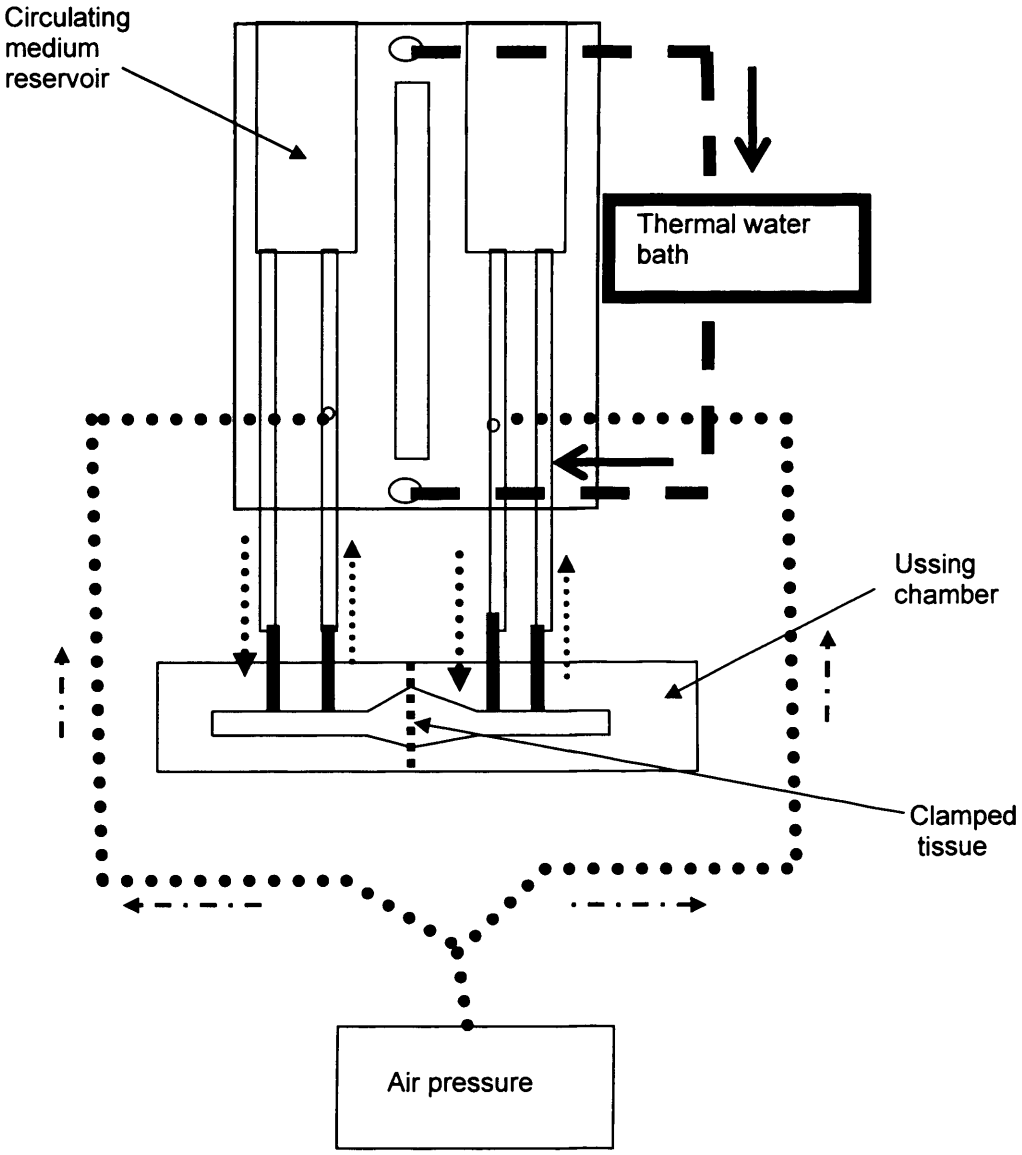

Fig. 4.1: Drawing of Ussing system. The tissue viability was maintained via flow of media, ...▶ flow of 5% oxygen and 95% carbon dioxide · · ➔ and the flow of water at 37°C ➔ .

4.2.2.4 Determination of permeability coefficient

Samples collected at 30 minutes and 4 hours were placed in the spectrofluorometer (Digilab Hitachi F-4500, Jencons). Rhodamine dextran bead fluorescence, at each time point, was measured by spectrofluorimetry (Digilab Hitachi F-4500, Jencons) at room temperature, at excitation and emission wavelengths of 550 and 580nm, respectively.

4.2.2.5 Calculation of Permeability Coefficient

Standard curves (fluorescence versus concentration) were determined for each dextran bead size. Using these standard curves, experimental spectrofluorimetric readings were converted to concentration values. Permeability coefficients were calculated for each experiment and plotted as a function of treatment and treatment duration (section 2.4.2.3).

4.2.2.6 Statistical analysis

All experiments were repeated at least three times. Since the data did not follow a normal distribution, statistical analysis was conducted using non-parametric methods (Kruskall-Wallis and Mann-Whitney tests). All statistical analysis was performed using SPSS 13.0 (SPSS Corp).

4.3 Results

4.3.1 Quantification of scleral permeability

The permeability coefficient (Pc) of different molecular weight dextran beads (10, 40, and 70kDa) (Fig 4.2) demonstrated that transcleral bead transit was inversely proportional to the molecular weight of the dextran bead, such that scleral permeability was least (0.02 +/- $6.0X10^{-3}$ cm/sec) for a 70kDa bead and highest (0.15 +/- $7X10^{-2}$ cm/sec) for 10kDa beads ($p<0.05$). In view of the comparatively low permeability for the 40-70KDa particles, these particle sizes were selected to determine whether significant increases in scleral permeability could be achieved through indirect or direct action of MMP activation.

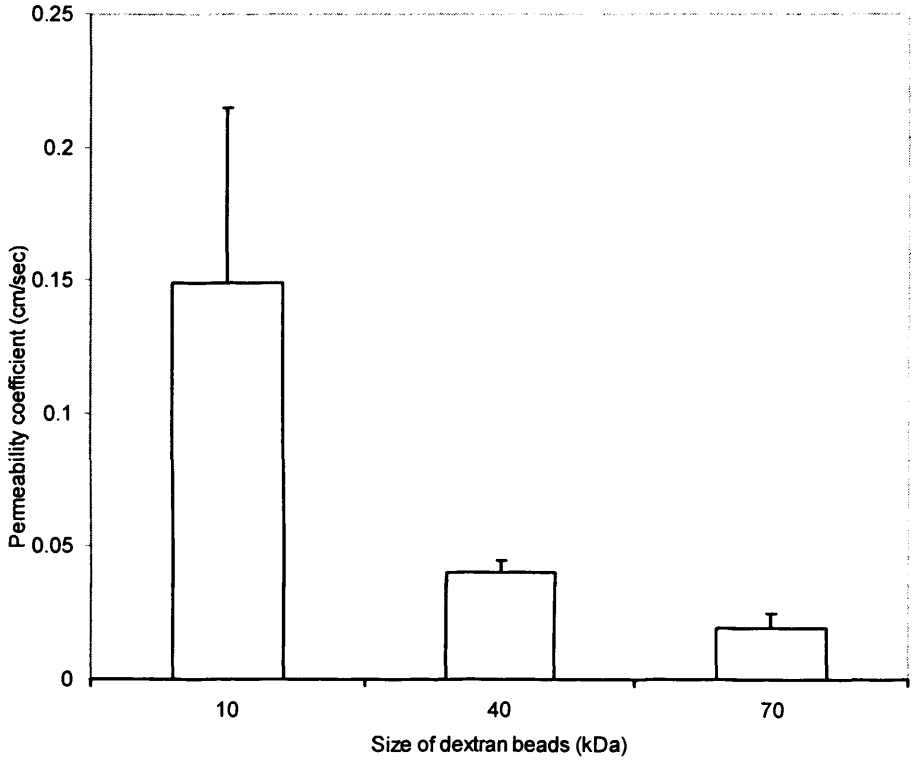

Fig. 4.2: Permeability coefficient of different sized dextran beads (10, 40 and 70kDa).

4.3.2 The effect of PGF2α and MMP-EM on transcleral permeability

Incubation in MMP-EM or PGF2α increased scleral permeability to 40kDa beads within 3 hours of treatment (Fig 4.3a and b). MMP-EM resulted in a greater increase scleral permeability compared to treatment with PGF2α. A significant increase in scleral permeability as a function of time, with the final measurements made at 72 hours was not observed. When expressed as

percent increases in permeability relative to control samples, the difference between the effect to PGF2a and MMP was readily apparent (Fig 4.3b), throughout the time course of incubation from 6 to 72 hours ($p<0.05$).

Both PGF2α and MMP-EM increased scleral permeability to the 70KDa particles with the greatest increase seen after 12 hours incubation relative to controls (Fig 4.4). (Fig 4.4a and b). Time-dependent changes in permeability were observed in sclera incubated in both PGF2α and MMP-EM (Fig 4.4a, $p<0.05$). In contrast, no significant differences were observed in transcleral conductivity in control samples at any time point (Fig 4.4)

Scleral permeability for both 40 and 70kDa beads increased up to 10-fold with MMP-EM and 3-fold following PGF2α compared with control samples ($p<0.01$, Figs 4.3b and 4.4b). The percent change in permeability, compared to control samples, increased as a function of time for both MMP and PGF2α treated sclera, reaching a peak at 24 hours for 40kDa beads (Fig 4.3b) and 12 hours for 70kDa beads (Fig 4.4b). Thereafter the percentage increase in scleral permeability declined for PGF2α and MMP-EM samples respectively although it continued to remain significantly above control levels ($p<0.05$).

(a)

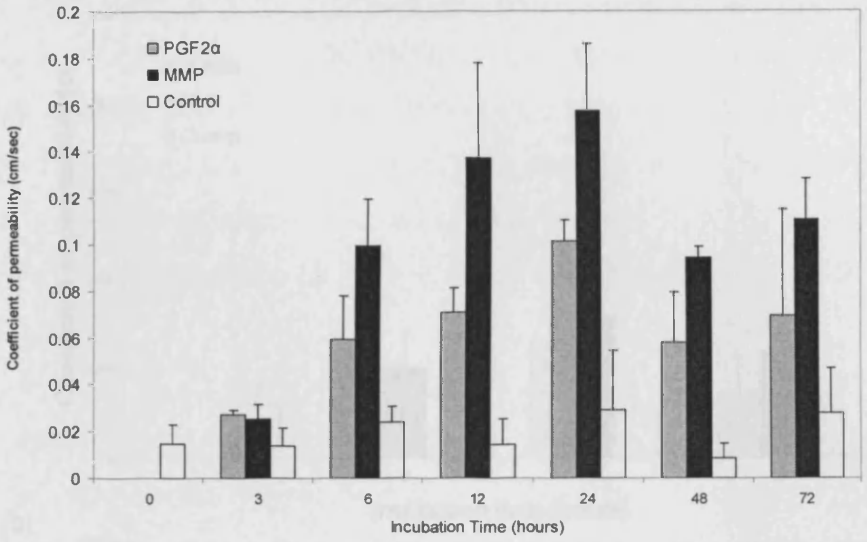

(b)

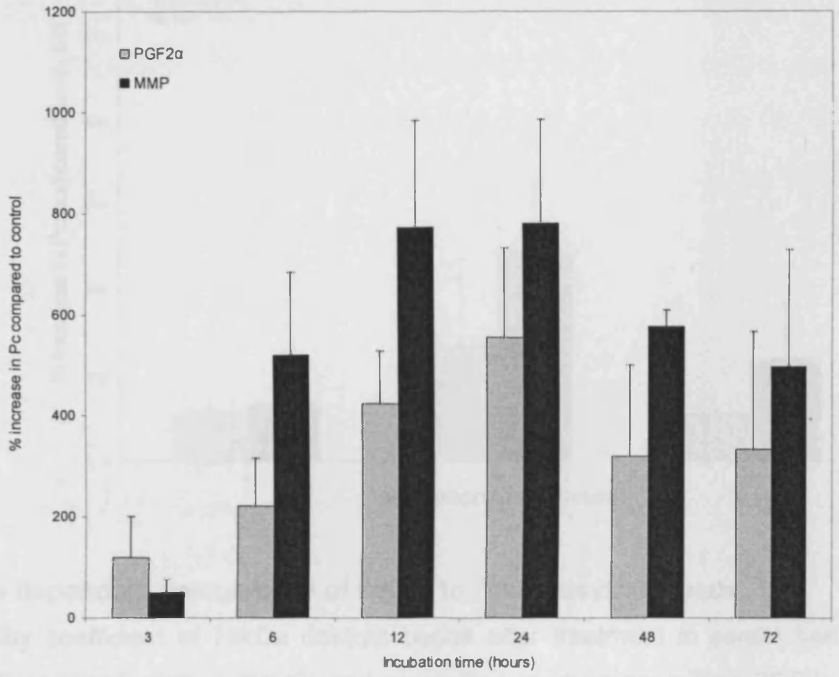

Fig. 4.3: Time dependent permeability of sclera to 40kDa dextran beads

a) Permeability coefficient of 40kDa dextran beads after incubation in serum free medium (control), MMP enriched medium (MMP) and serum free medium containing PGF2α (PGF2α) for 0-72 hours. b) Percentage increase in permeability compared to control.

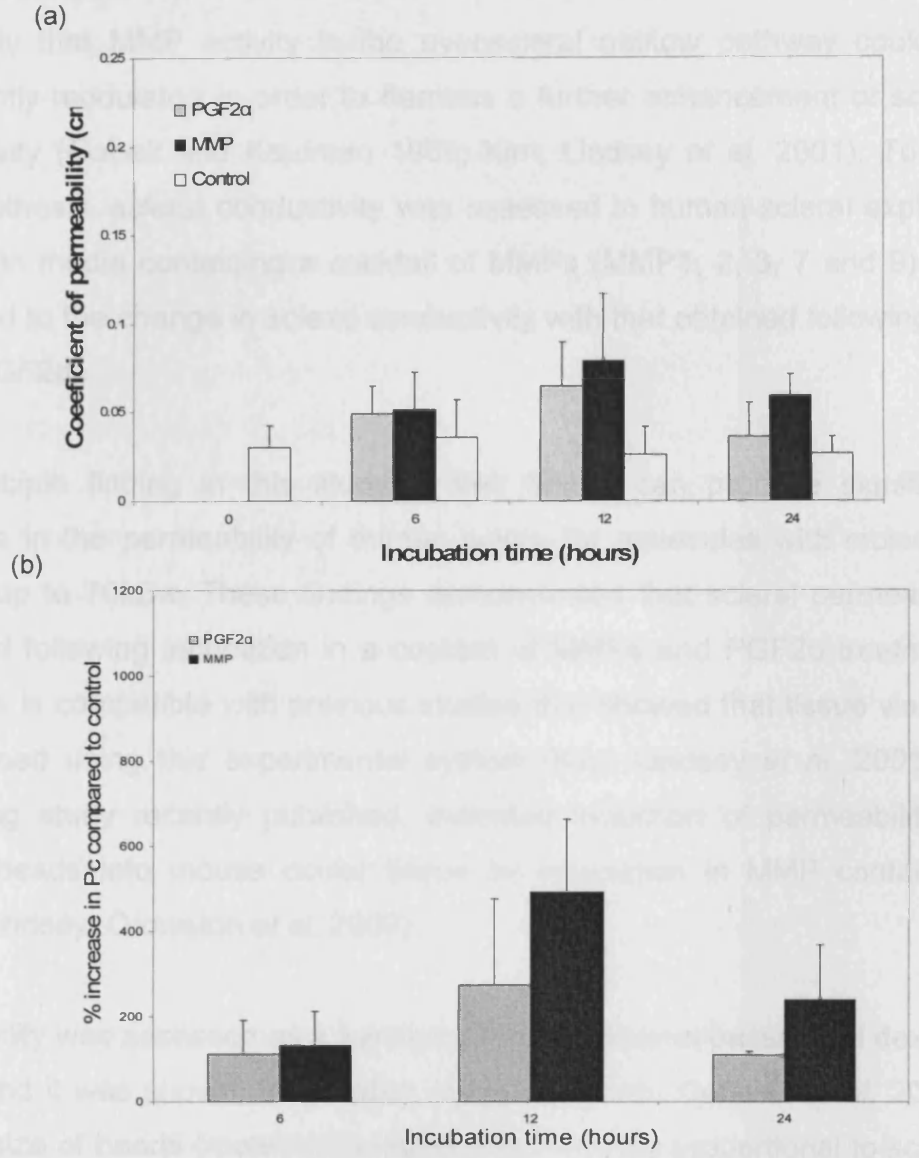

Fig. 4.4: Time dependent permeability of sclera to 70kDa dextran beads.

4a: Permeability coefficient of 70kDa dextran beads after treatment in serum free medium (control), MMP enriched medium (MMP) and serum free medium containing PGF2α (PGF2α) for 0, 6, 12 and 24 hours. 4b: percentage increase in permeability compared to control.

4.4 Discussion

It is likely that MMP activity in the uveoscleral outflow pathway could be significantly modulated in order to harness a further enhancement of scleral conductivity (Gabelt and Kaufman 1989; Kim, Lindsey *et al.* 2001). To test this hypothesis, scleral conductivity was assessed in human scleral explants cultured in media containing a cocktail of MMPs (MMP1, 2, 3, 7 and 9) and compared to the change in scleral conductivity with that obtained following the use of PGF2α.

The principle finding in this study is that MMPs can produce significant increases in the permeability of human sclera for molecules with molecular weights up to 70kDa. These findings demonstrated that scleral permeability increased following incubation in a cocktail of MMPs and PGF2α treatment. The latter is compatible with previous studies that showed that tissue viability is sustained using this experimental system (Kim, Lindsey *et al.* 2001). A supporting study recently published, indicated induction of permeability of dextran beads into mouse ocular tissue by incubation in MMP containing media (Lindsey, Crowston *et al.* 2007).

Permeability was assessed as a function of the transcleral passage of dextran beads, and it was shown, as in other studies (Ambati, Canakis *et al.* 2000), that the size of beads (molecular weight) was inversely proportional to scleral permeability. Both MMP-EM and PGF2α treatment increased scleral permeability to all dextran beads (10, 40 and 70KDa), demonstrating the efficacy of the transcleral passage of large molecules up to at least 70kDa. Previous studies have demonstrated that the movement of small molecules are not largely effected by the transcleral passage (Toris, Gregerson *et al.* 1987b). However, the movement of large molecules can be significantly improved by modification to the transcleral passage (Ambati, Canakis *et al.* 2000).

There are several possible causes of the change in sclera conductivity. The most likely explanation is that the scleral extracellular matrix (ECM) is

degraded as result of treatment by both PG and MMP-EM. The sclera is a microporous elastic tissue consisting of collagen fibrils and proteoglycans and approximately 70% water. The interfibrillar aqueous media created by the gel-like proteoglycans can act as an important media via which passive solute diffusion in conducted. Changes in ECM matrix within the sclera are likely to be important with respect to the control of intraocular pressure.

ECM is synthesised by human ciliary muscle cells (Tamm, Baur *et al.* 1992). In the uveoscleral pathway, aqueous is thought to pass through the ciliary muscle to enter the suprachoroidal space and then exit the eye via the sclera. Although the sclera is relatively inert metabolically, its structure has a large impact in maintaining visual acuity by regulating the passage of various factors from the extraocular to intraocular compartments (Watson and Young 2004). The importance of sclera in the uveoscleral outflow pathway was established in the 1980s, when Toris and Pederson (Suguro, Toris *et al.* 1985) demonstrated the flow of fluorescent tracers through the ciliary muscle and sclera. They subsequently established that the uveoscleral outflow involved bulk fluid flow rather than diffusion. They determined that different sized tracers (MW: 4000, 40,000 and 150,000) were permitted to flow via this pathway (Pederson and Toris 1987; Toris, Gregerson *et al.* 1987a).

An increase in ECM deposition with age could compromise drainage through this pathway, a mechanism that has been postulated in the development of elevated intraocular pressure (Weinreb 2000). Since increase in age is one of the most significant risk factors in the development of AMD and glaucoma, the increase in ECM deposition with age could limit the treatment of such disease further. Previous studies have supported a correlation between PGF2α treatment and the reduction in matrix components, such as collagen, within the uveoscleral outflow pathway (Sagara, Gaton *et al.* 1999; Schachtschabel, Lindsey *et al.* 2000). PGF2α treatment of sclera has also been shown to make the tissue more permeable to macromolecules such as basic fibroblast growth factor (FGF-2) (Weinreb 2001). Since MMPs are enzymes involved in the breakdown of ECM and PGF2α has been shown to

upregulate MMP expression in scleral fibroblasts (this study) and scleral explants (Weinreb and Lindsey 2002; Weinreb, Lindsey *et al.* 2004; Wong, Sethi *et al.* 2002), the increase in tissue permeability with PGF2α is not surprising. A key finding of the present study is that it reveals that the limited increase in scleral permeability that is induced by PGF2a. Greater increases in permeability can be achieved by the direct application of activated MMPs providing information on the potential increases in scleral permeability that can be achieved.

Previous studies have shown that the administration of the prostaglandin PGF2α significantly increased scleral permeability (Kim, Lindsey *et al.* 2001; Weinreb 2001). The findings of the present study extend these observations by establishing that with appropriate MMP activation scleral permeability can be significantly enhanced. Importantly, this study demonstrated that molecular weights exceeding 50kD can be transported across scleral tissue. This suggests that approaches directed at the manipulation of scleral architecture can be used to deliver further reductions in IOP and also be used as a technique for the enhanced delivery of novel therapeutic molecules for the treatment of retinal disease. This could potentially serve to lower IOP by augmenting aqueous drainage, but also shows that permeability can be enhanced to act as a conduit for the transcleral passage of large peptide drugs (Weinreb, Toris *et al.* 2002).

However, certain limitations in this model of study include scleral tissue permeability does not truly reflect the permeability of the anterior chamber. There are other tissues and other processes within the anterior chamber which may interfere with the drainage of aqueous humor within the anterior chamber. Future work needs to assess the effect of MMP-EM compared to PGF2α in perfusion chambers and animal models. MMP action generates a negative feedback process which leads to the activity of MMP inhibitors i.e. TIMP, which may in turn prevent further increase in scleral permeability. The decrease in permeability at the later time points could be due to tissue re-engineering itself after the generation of the negative feed-back loop. MMPs

are a group of enzymes with diverse functionality and mechanism of action. It would therefore be difficult to administer such enzymes in a cocktail version. A more workable model would involve identifying specific action of MMPs within the sclera which can be linked to upregulation of tissue permeability, which can be dealt with specifically.

CHAPTER 5

X RAY DIFFRACTION: ANALYSIS OF TISSUE ARCHITECTURE

CHAPTER 5

X RAY DIFFRACTION: ANALYSIS OF TISSUE ARCHITECTURE

5.1 Introduction

The application of prostaglandin derivatives to scleral fibroblasts resulted in increased levels of MMP1, 2, 3 and 9 (see chapter 3), implicated prostaglandins induce collagenase, gelatinase and stromelysin activity. The increased scleral conductivity identified in chapter 4, as a result of PGF2α and MMP application, is likely to be a consequence of either remodelling of the extracellular matrix or collagen destruction or a combination of the two.

Previous studies, using knockout mice, suggested that binding to the prostaglandin (FP) receptor is critical for the early effects of prostaglandins (Crowston, Lindsey *et al.* 2004a; Crowston, Lindsey *et al.* 2005). Studies using Ussing chambers to quantify the flow of large molecular weight molecules through the sclera have shown that significant increases in scleral permeability can be achieved by the administration of the prostaglandin PGF2α (Kim, Lindsey *et al.* 2001). Clinical experience with eyes, in which the suprachoroidal space is accessed directly (for example when a cyclodialysis cleft has been created), has shown that IOP can be reduced to a greater extent than is possible with treatment by topical prostaglandins. On the basis of these observations, it is likely that the dynamic range of the uveoscleral outflow pathway for the reduction of IOP is significantly greater than that achievable with existing medications. However, before applying novel therapeutic interventions targeted at the disruption of ocular connective tissue, in particular the sclera, it is important that the mode of scleral degradation is determined.

Collagen forms 75% of scleral dry weight, consisting of collagen types I, III, V and VI. The most abundant collagen is type I collagen, which is fibril forming collagen (Thale and Tillmann 1993). Collagen based tissue, such as sclera, is a hierarchically organised material where there is a close relationship between the molecular structure relating to the triple helical organisation

within individual collagen molecules. The well-defined nanoscopic axial molecule and lateral side by side organisation stagger giving rise to the D-spacing. Locally associated collagen molecules and thence the organisation of discrete fibrillar structures, as shown in Fig. 5.1 produce a functional tissue. Degradation of the collagen structure can be difficult to determine enzymatically, as collagen molecules exists in large fibrillar forms and would be difficult to run down gel matrix. However, collagen, because of its well ordered fibrillar structure can be analysed by biophysical techniques such as x-ray diffraction.

X-ray diffraction techniques have provided valuable insight to the structure of collagen. In this study, x-ray diffraction techniques were applied to scleral tissue subjected to a range of agents (including prostaglandins), which either contain MMP or are known to induce their production and activation. It allowed the examination of a large area of tissue sample in its native state without any additional treatment. Since analysis was applied on tissue in their hydrated state, it prevented the formation of any artefacts due to tissue dehydration (Meek, Fullwood *et al.* 1991; Price, Lees *et al.* 1997). The wide angle x-ray patterns studied are related to the atomic and molecular structure. Small angle patterns are obtained from diffraction from the axial structure of the collagen fibrils, and diffraction from the interfibrillar arrangement (Goodfellow, Elliott *et al.* 1978).

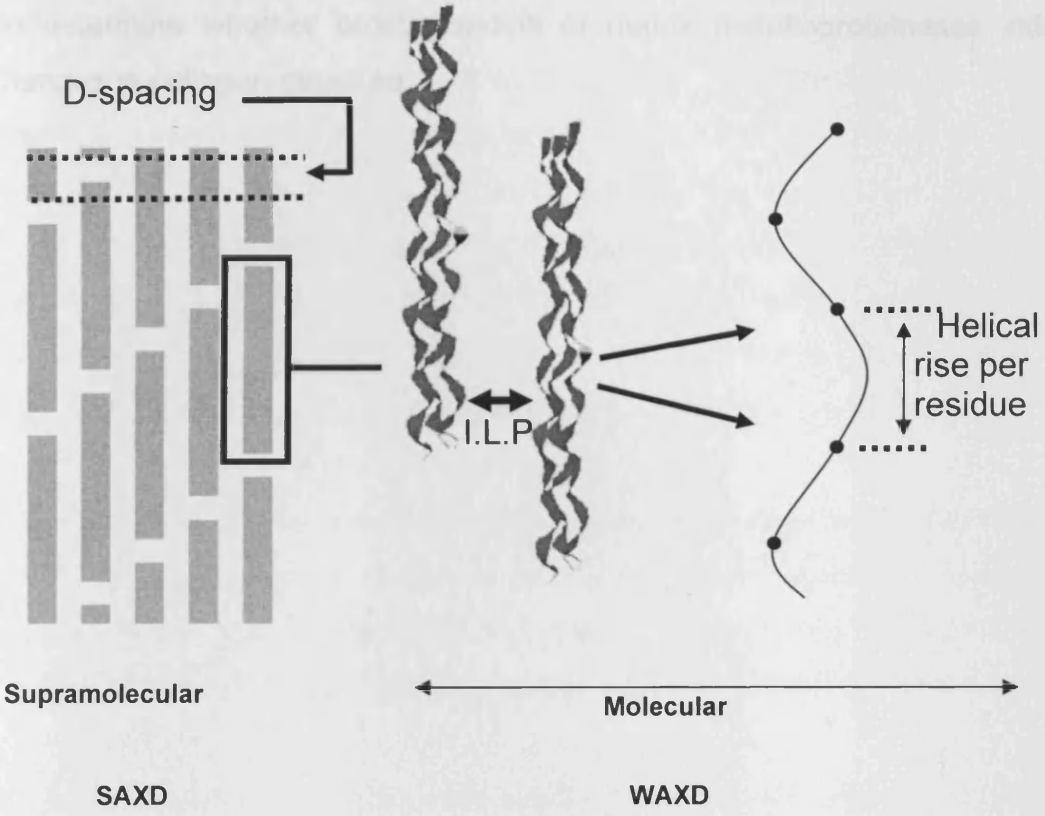

Fig. 5.1: A schematic diagram of collagen hierarchy. The supramolecular (observed by small angle x-ray diffraction (SAXD)) and the molecular level (observed by wide angle x-ray diffraction (WAXD)). A) Collagen microfibril with D-spacing; B) Collagen triple helix with intermolecular lateral packing (I.L.P); C) Collagen polypeptide chain with helical rise per residue labelled, not to scale.

5.1.2 Aim:

To determine whether prostaglandins or matrix metalloproteinases induce changes in collagen structure.

5.2 Experimental Design

5.2.1 Source of tissue

All samples were obtained following consent for research purposes in accordance with the ethical guidelines of United Kingdom Transplant Service (UKTS) and the declaration of Helsinki. Human donor eye globes, aged 55-83 years, were obtained with 48 hours post mortem from the Corneal Transplant Service Eye Bank (Bristol, UK) after corneal removal for transplant purposes. All globes were transported at 4°C in moist chambers. Bovine skin was obtained from the abattoir with 6 hours of death, and transported on ice.

5.2.2 Production of matrix metalloproteinase enriched media (MMP-EM)

MMP-EM was derived from bovine skin explants as described previously in chapter 2 (see section 2.2.12.3). As determined in Chapter 3, MMP-EM is a cocktail of MMPs consisting of MMPs 1, 2, 3, 7, 9 and TIMPs 2 and 4.

5.2.3 Production of conditioned media from human scleral fibroblasts (HSF-CM) and human ciliary muscle cells (HCM-CM)

The protocols used to produce conditioned media from human scleral fibroblasts and ciliary muscle cells (both cells within the uveoscleral pathway) have been described in full in Chapter 2 (see section 2.2.12.2). Briefly, human scleral fibroblasts or ciliary muscle cells were cultured in serum free medium in the presence or absence of PGF2α for a period of 72 hours. The media collected from these cells contains MMPs, which were previously determined and described in chapter 3 HSF-CM and HCM-CM contained MMPs 1, 2, 3, 7 and TIMPs 1-4.

5.2.4 Scleral tissue culture

Each human eye globe was immersed in 3% betadine for 30 seconds and then thoroughly rinsed in sterile PBS (pH7.4). The sclera was dissected into equal sized (1cm length,1cm width) with approximate thickness 0.5-0.6mm from uveal area.

The explants were then cultured in various serum free media containing 100nM PGF2α, 100nM MMP 2, 9 or 7. Explants were also cultured in MMP-EM, HSF-M and HCM-M medium. The negative control was serum free medium (without any MMP or its inducers), and the positive control was media containing collagenase. The explants were cultured for 3, 6, 12, 24, 48 and 72 hours. Each treatment was applied to triplicate scleral explants. Cultured explants were stored at -80°C until x-ray diffraction analysis.

5.2.5 X-ray Diffraction Analysis

The frozen scleral explants were transported to the synchrotron. The tissue sections were thawed and placed into a sample holder to obtain hydrated x-ray diffraction images with varying camera lengths (Wess and Orgel 2000). The different camera lengths provided information of the integrity of molecular and supramolecular hierarchies (Fig. 5.1).

5.2.5.1 Wide angle diffraction images obtained at station 14.1 technical details

Wide-angle x-ray diffraction (WAXD) images were taken on station 14.1 at SRS Daresbury (Daresbury, UK). Station 14.1, beamline was optimised for fibre diffraction. It has a focused x-ray beam at a wavelength of 1.488 , with a beam diameter of 200μm and a sample to detector distance of 25cm. This allowed features of collagen structure in the region of 0.22 and 3.0 nm to be observed. The sample holder (Fig. 5.2) has a computer controlled X-Y elevation stage for movement of the sample in specific and measurable directions (Maxwell, Wess *et al.* 2006). By moving the sample holder, it was possible to take 3 images, at 30 seconds exposure, at different positions of each sample piece. Blank sample cell images were taken in order to subtract background scatter from images. Calibration of sample to the Quantum 4 ADSC detector distance was calculated using the characteristic diffraction peaks of calcite. Calcite had been standerised previously, and produces well-defined peaks for collagen.

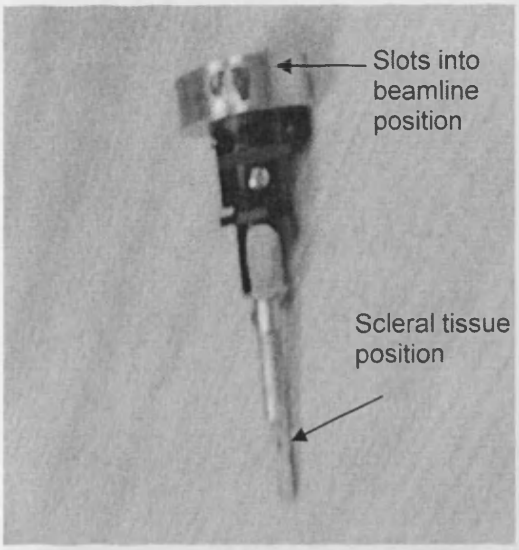

Fig. 5.2 Sample holder for wide angle x-ray diffraction.

5.2.5.2 Small angle diffraction at station 2.1 SRS Daresbury technical details

To observe the long-range interactions of collagen resulting from axial order (D-spacing), small angle X-ray scattering images were taken at SRS Daresbury, station 2.1. This station has a variable sample to camera (multiwire 2d area detector) length of 0.9 to 8.0 metres and is therefore capable of giving a spatial resolution from 1nm to 200nm. The sample to detector distance was set at 4.5 metres. A calibration factor (nm^{-1} per pixel) was obtained by analysis of rat tail tendon, meridional reflection in nm^{-1}, determined from the known $1/67nm^{-1}$ periodicity, by the corresponding distance in pixels (Quantock and Meek 1988). Again the elevation and movement of computer controlled sample holder (Fig. 5.3) enabled 3 images at 30 seconds exposure, at different locations of each sample. Blank sample cell images were taken in order to deduct background scatter from images. Complete technical details of this beam line have been previously reported by (Grossmann 2002).

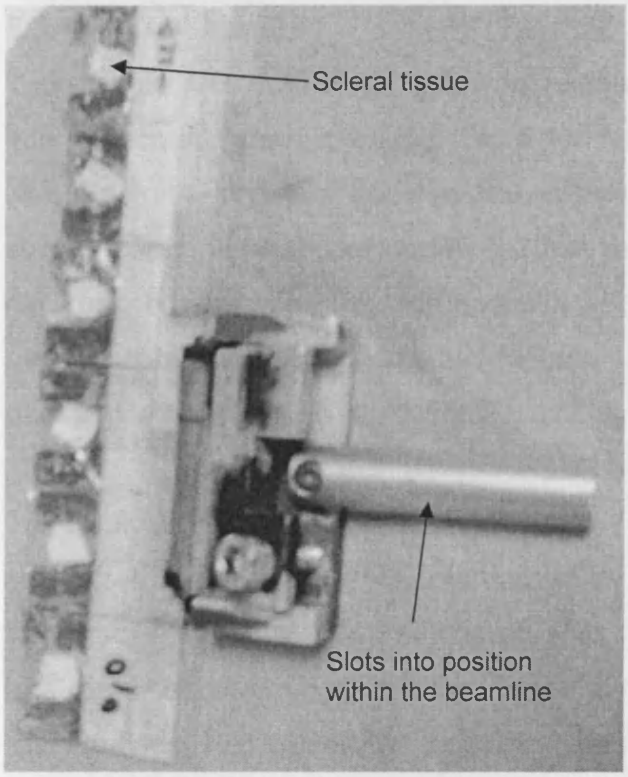

Fig. 5.3 Sample holder for small angle x-ray diffraction.

5.2.5.3 Analysis

X-ray diffraction involved placing treated scleral tissue in hydrated state and applying x-ray beam at the samples. Images were analysed according to techniques established by Maxwell *et al.* (2005). An example of x-ray diffraction is shown in section 2.5.2, chapter 2. The images displaying ring-formation due to beam scattering were viewed by FibreFix software (CCP13). Using PeakFit (AISL software) these images were converted into 1D linear profile.

5.3 Results

5.3.1 WAXD Results

Wide angle x-ray diffraction allowed analysis of helical rise per residue and intermolecular lateral packing (Fig.5.4). The analyses of the linear profiles with Peakfit4 software allowed the determination of data in Table 5.1. A strong reflection at approximately 0.29nm relates to axial rise distance (helical rise per residue) between the amino acid residues along the collagen molecular triple helices. Molecule-molecule interaction (intermolecular lateral packing) was observed at ~1.5nm (Maxwell, Bell *et al.* 2006).

The analysis of the images showed that the intermolecular lateral packing and axial rise per residue were unchanged by PGF2α and MMP-EM treatment throughout the time course studied (Fig. 5.5). However, with collagenase treatment the diffraction peak corresponding to the specific helical rise per residue was not observed and total destruction of intermolecular lateral packing was observed (Fig. 5.4).

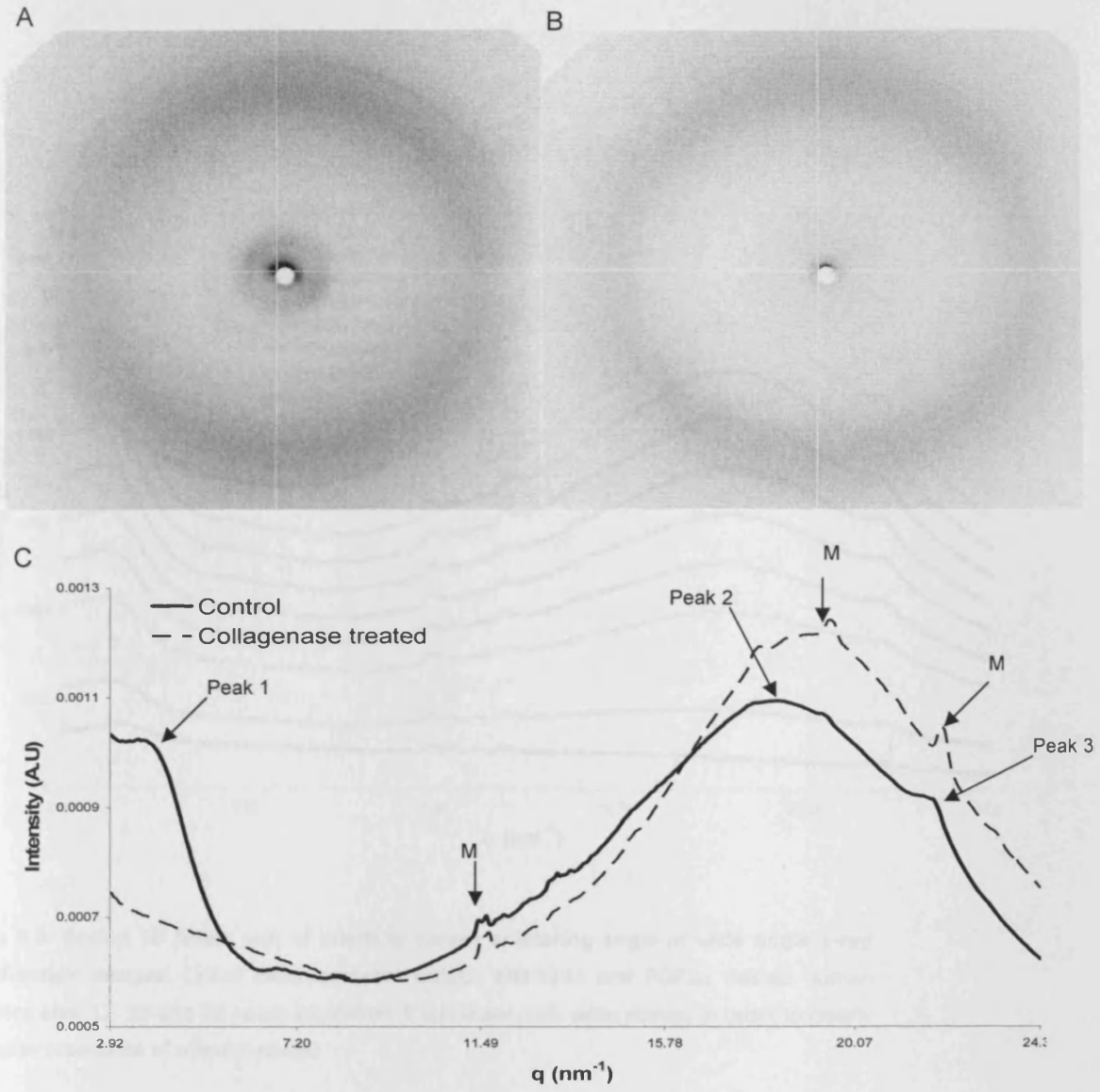

Fig. 5.4: Wide angle x-ray diffraction of human sclera. A) 2D X-ray diffraction image of human sclera (control) at 12hrs. B) 2D X-ray diffraction image of human sclera treated with collagenase for 72 hrs. C) 1D Linear plots of intensity verses scattering angle (q (nm^{-1}) of the X-ray diffraction images of human sclera. Peak 1 indicated intermolecular lateral packing at 1.2nm; Peak 2 illustrates the amorphous region and Peak 3 represents helical rise per residue at 0.29nm. Some unknown crystalline deposits were reflected as sharp peaks within the linear plots (M).

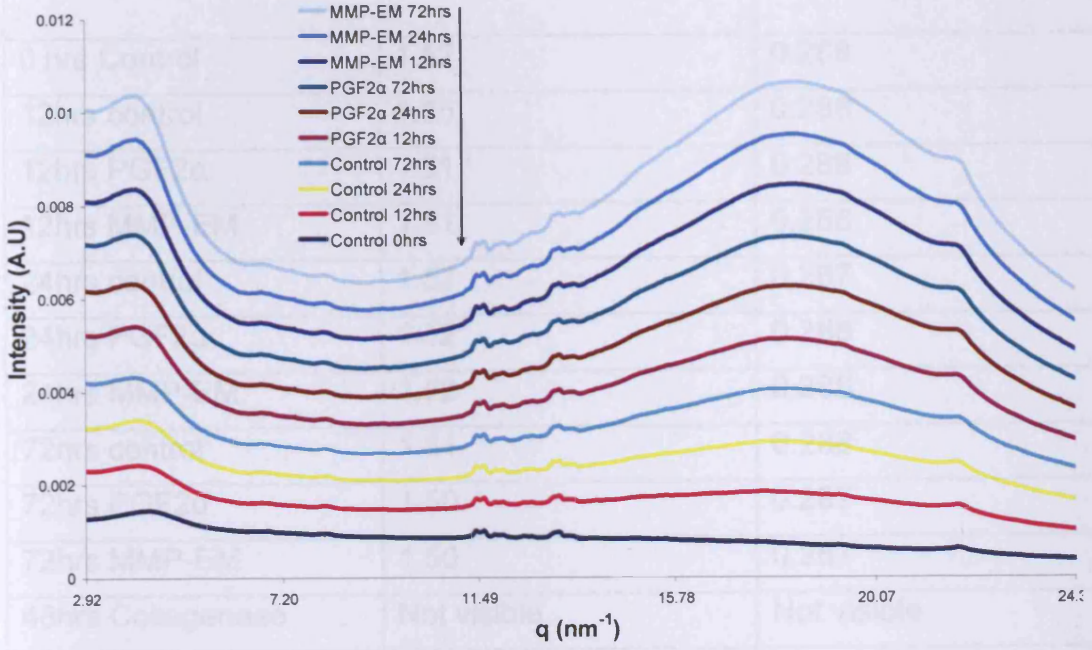

Fig 5.5: Scaled 1D linear plot of intensity verses scattering angle of wide angle x-ray diffraction images. Linear plots represent control, MMP-EM and PGF2α treated human sclera after 12, 24 and 72 hours incubation. Each linaer plots were scaled, in order to clearly display prescence of relevant peaks.

Hydrated Human Sclera	Intermolecular Lateral Packing (nm) (± 0.0080 nm)	Axial rise per residue (nm) (± 0.0003 nm)
0 hrs Control	1.52	0.288
12hrs control	1.55	0.288
12hrs PGF2α	1.51	0.288
12hrs MMP-EM	1.51	0.288
24hrs control	1.57	0.287
24hrs PGF2α	1.52	0.288
24hrs MMP-EM	1.52	0.288
72hrs control	1.51	0.288
72hrs PGF2α	1.50	0.287
72hrs MMP-EM	1.50	0.287
48hrs Collagenase	Not visible	Not visible

Table 5.1: Collagen intermolecular packing distance and axial rise per residue values for Human sclera samples. Standard deviation of error (I.L.P +/- 0.0080nm and axial rise per residue =/- 0.0003nm) represents maximal error observed between 3 images of each sample.

5.3.2 SAXD

Small angle 2D X ray diffraction images demonstrated a series of sharp Bragg reflections, caused by D-spacing diffraction (Fig. 5.6). These peaks reflect regular fluctuations in the electron density of collagen in the axial direction. Alterations in electron density along the fiber axis are reflected in changes to the intensity of these peaks (Maxwell, Bell *et al.* 2006). Peakfit4 software was used to fit the data and refine the localisation of the peaks, so that a D-spacing value could be determined (Table 5.2). Scleral tissue treated with collagenase displayed no rings in the 2D diffraction image. The collagenase treatment caused total destruction of supramolecular structure of collagen, as demonstrated by the lack of peaks (Fig.5.6).

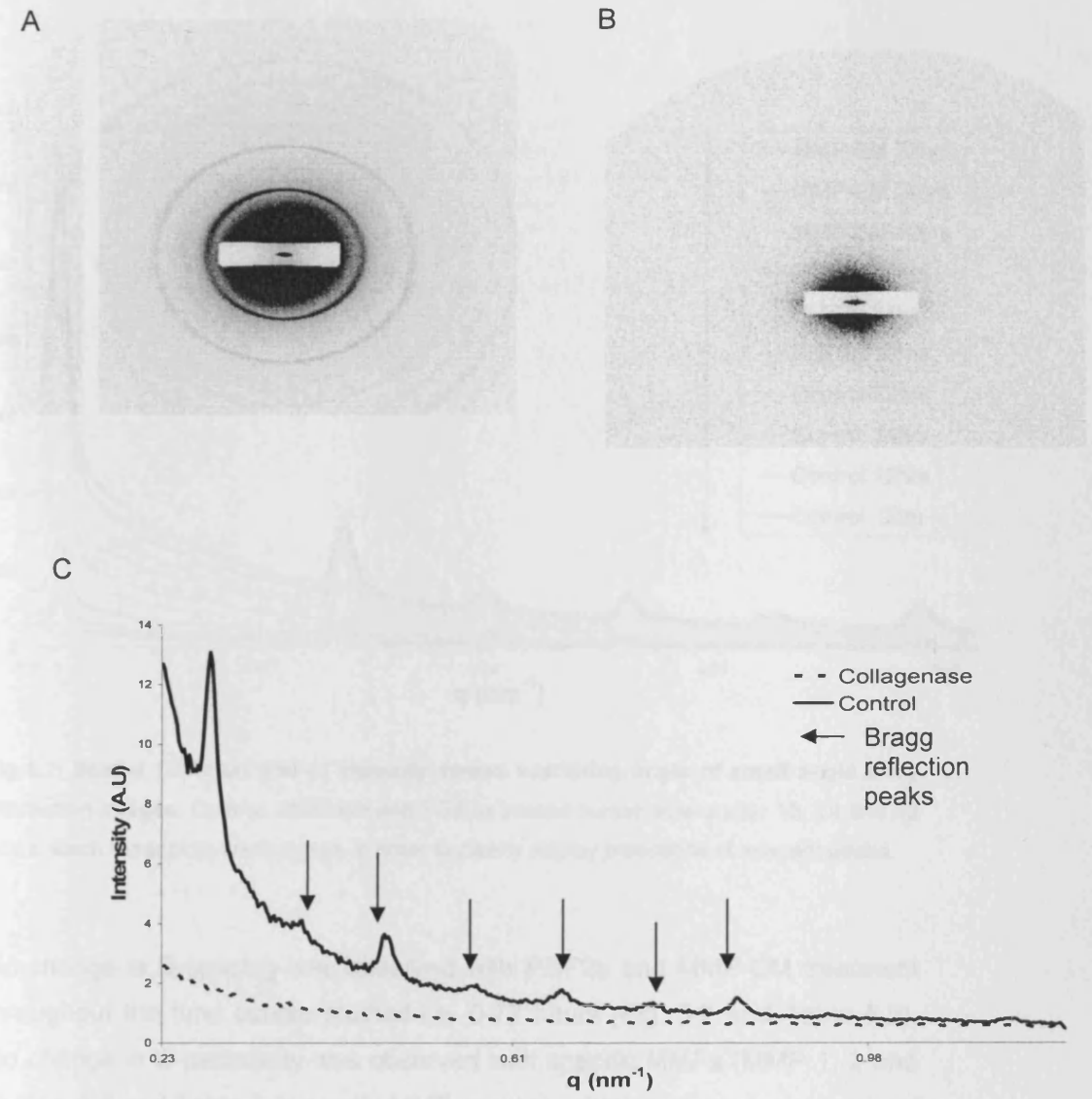

Fig. 5.6: Small angle x-ray diffraction of human sclera. 2D X-ray diffraction image of human sclera (control) at 0hrs. A) The diffraction rings are due to the electron density contrast between the gap and overlap of the collagen quarter staggered array (D-spacing). B) 2D X-ray diffraction image of human sclera treated with collagenase for 12 hrs. The absence of diffraction rings is due to the loss of collagen structural order. C) 1D Linear plots of intensity verses scattering angle of the X-ray diffraction images of human sclera.

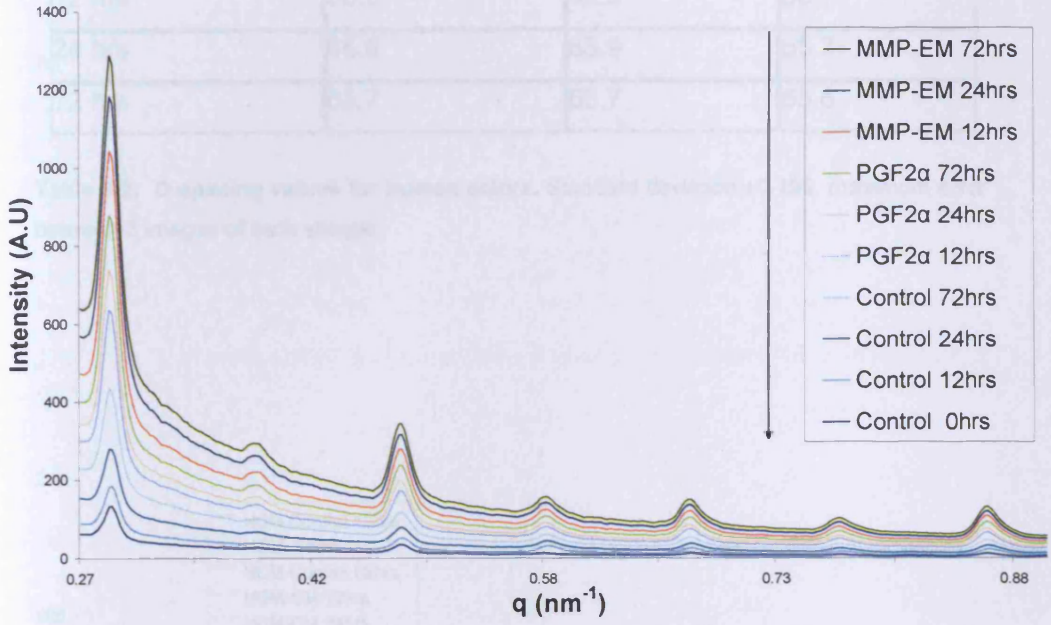

Fig 5.7: Scaled 1D linear plot of intensity verses scattering angle of small angle x-ray diffraction images. Control, MMP-EM and PGF2α treated human sclera after 12, 24 and 72 hours. Each linaer plots were scaled, in order to clearly display prescence of relevant peaks.

No change is D-spacing was observed with PGF2α and MMP-EM treatment throughout the time course studied i.e. 0-72 hours (Fig. 5.7 and Table 5.2). No change in D-periodicity was observed with specific MMPs (MMP 1, 2 and 7) (Fig. 5.8 and Table 5.3) or with MMP cocktails obtained from human scleral fibroblasts (HSF-CM) and ciliary muscle cell (HCM-CM) cultures (Fig. 5.9 and Table 5.4). The D-spacing value was approximately 66nm. A slightly higher D-spacing value, of approximately 67nm, was observed for scleral tissue treated in specific MMP and control.

	D-spacing (nm)		
Incubation Time	**Untreated**	**PGF2α**	**MMP-EM**
0 hrs	65.7	N/A	N/A
12 hrs	65.5	65.9	65.7
24 hrs	65.8	65.9	65.7
72 hrs	65.7	65.7	65.6

Table 5.2: D-spacing values for human sclera. Standard deviation ±0.199, maximum error between 3 images of each sample.

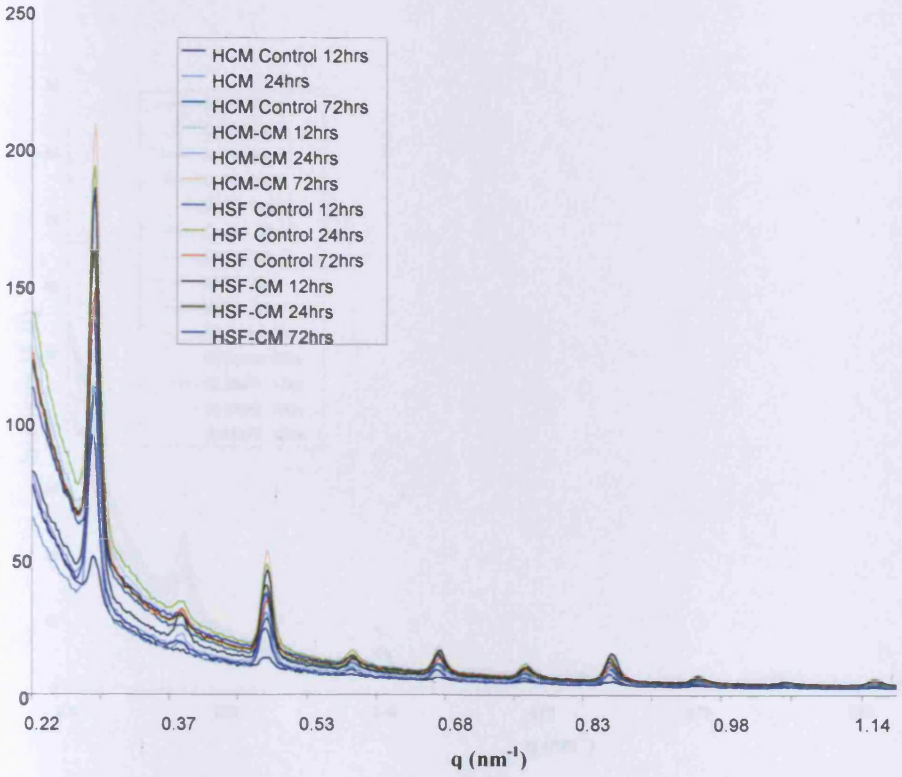

Fig 5.8: 1D linear plots of small angle x-ray diffraction images of scleral tissue incubated in Control, HCM-CM and HSF-CM for 12, 24 and 72 hours.

HCM-M Sample, Incubation time	D-spacing (nm) (± 0.135)	HSF-CM sample, Incubation time	D-spacing (nm) (± 0.058)
Control 12 hours	65.6	Control 12 hours	65.8
Control 24 hours	65.8	Control 24 hours	65.8
Control 72 hours	65.7	Control 72 hours	65.6
HCM-CM 12 hours	65.6	HSF-CM 12 hours	65.7
HCM-CM 24 hours	65.8	HSF-CM 24 hours	65.8
HCM-CM 72 hours	65.7	HSF-CM 72 hours	65.7

Table 5.3: D-spacing values for Human Sclera treated with medium from HCM-CM and HSF-CM.

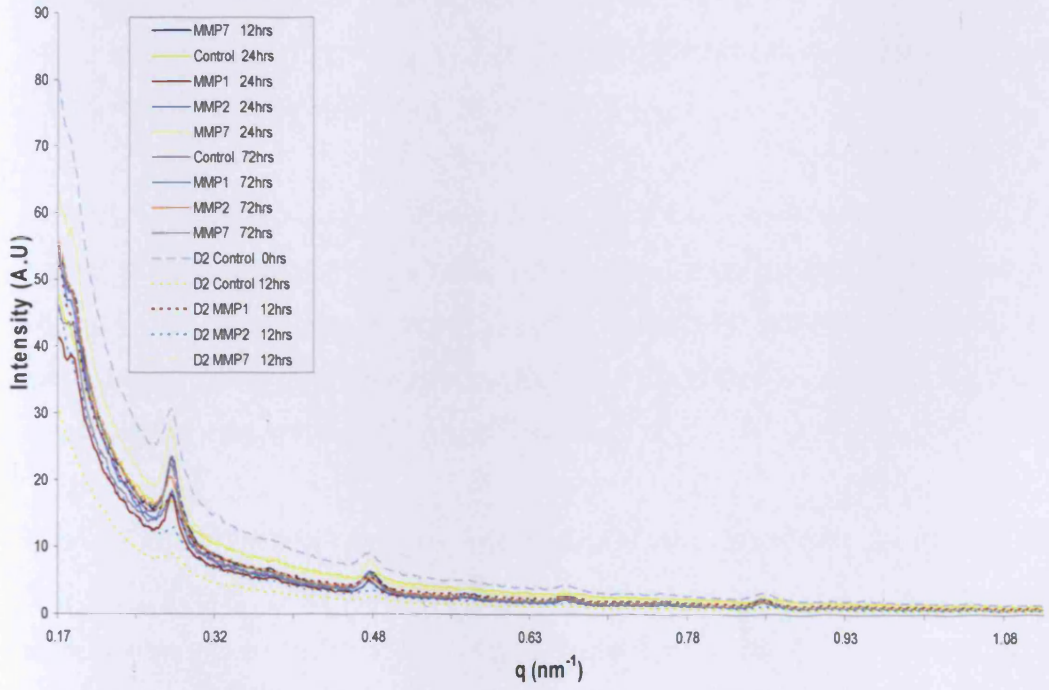

Fig 5.9: 1D linear plots of small angle x-ray diffraction images of scleral tissue treated in MMP1, 2 and 7 for 12, 24 and 72 hours.

Incubation Time	Control D-spacing (nm)	MMP1 D-spacing (nm)	MMP2 D-spacing (nm)	MMP7 D-spacing (nm)
0 hrs	66.6	n/a	n/a	n/a
12 hrs	66.7	66.6	66.5	66.7
24 hrs	66.3	66.7	66.9	66.5
72 hrs	66.8	66.7	66.8	66.9

Table 5.4: D-spacing values for human sclera treated with MMPs

6.4 Discussion

By dry weight 50-70% of the sclera is composed of collagen (Watson and Young 2004). The results obtained suggest that as collagen architecture is not disrupted by PGF2α or MMP-EM treatment, scleral collagen integrity over a number of length scales from atomic to mesoscopic are maintained after treatment. The previous chapter suggested an intensive increase in scleral permeability with MMP-EM treatment. The current suggests that although permeability is increased, the same treatment does not disrupt the collagen architecture within sclera at molecular and supramolecular levels.

Through the use of variable camera lengths it was possible to detect changes in the collagen structural hierarchy. PGF2α and MMP-EM treatment did not cause any changes in scleral collagen hierarchy. However, with collagenase treatment, total disruption of collagen architecture in terms of helical rise per residue, intermolecular lateral packing and D-spacing was observed. This demonstrated the feasibility of the analysis of structural changes in scleral collagen using x-ray diffraction methods.

Helical rise per residue is reflected by the diffraction pattern obtained due to amino acid sequence within the polypeptide chains that form the primary structure of the collagen molecule. The diffraction pattern observed due to molecule to molecule interaction within collagen fibrils reflected as the peak observed for intermolecular lateral packing.

The collagen molecules pack laterally and are staggered axially relative to their neighboring molecules by *D* _67 nm in tendon or _65.5 nm in skin. This arrangement is known as the Hodge-Petruska model (Goh, Hiller *et al.* 2005; Maxwell, Smiechowski *et al.* 2005; Obrink 1973). The *D* repeat is a characteristic feature of collagen. The stagger leaves a gap between linearly adjacent molecules as the molecular length (300 nm) is not an exact multiple of the *D* period, which results in a gap region and an overlap region within each D repeat. The gap region comprises 0.54 of D, and the overlap subsequently comprises 0.46 of D (Hodge 1989; Quantock, Meek *et al.*

2001). It has previously been shown that changes in hydration state leads to the movement of water within the gap regions, and therefore cause changes in tissue imaging (Price, Lees *et al.* 1997; White, Hulmes *et al.* 1977). For this reason if was important that scleral tissue was analysed in the hydrated state.

From the 29 known collagen types, type I, II, III, V, and XI are capable of forming fibrils. Scleral tissue is mainly composed of Type I collagen (Thale and Tillmann 1993) Sagara *et al.* (1999) suggested that a decrease in collagen type I and III, as determined by immunoassaying occurs following direct treatment of cynomolgus monkey eyes with PGF2α for a 5-day period. Although some intensity of staining changed for certain collagen types, the current study indicated that this does not cause denaturation of collagen architecture. This suggests scleral integrity was not affected by the application of either prostaglandins or MMPs. In scleral tissue, it has previously been demonstrated that there is a slow turnover of collagen molecules. Also an increase in glycosylation with aging is observed, which makes the molecules more stable and less soluble (Ihanamaki, Salminen *et al.* 2001; Keeley, Morin *et al.* 1984). As the tissues used in this study were from donors of an age range related to glaucoma i.e. high age range, it is possible that this explains the resistance of collagen to MMP action.

Unlike the corneal collagen regular lamellae structure, scleral collagen structure is composed of a loosely entangled matrix of collagen fibrils (Thale, Tillmann *et al.* 1996). This organisation suggests that some preferred orientation is detected in x-ray diffraction images and relates to the broadening of peak. The organization and the structural features of sclera allow it to remain an order of magnitude more permeable to macromolecules than the cornea. Scleral permeability and its surface area make it the most favourable target tissue for drug delivery.

The treatment of sclera with MMP-EM and PGF2α may cause the scleral collagen organisation to become more loosely entangled allowing the

increase in permeability, without causing major morphological changes which could cause adverse effects. It is important that any therapeutic measures applied to increase scleral permeability should not result in tissue destruction, which could possibly result in the development of staphylomata. These results suggest that that scleral collagen architecture is maintained although an increase in permeability is attained with MMP and PGF2α treatment.

Although collagen architecture does not change with treatment, a change in permeability has been observed in the previous chapter. It is important to understand how MMP-EM and PGF2α causes an increase in scleral permeability. It was suggested that although collagen fibrils may be intact, the spacing in between the fibrils may change. The main factors filling the space in between collagen fibrils are proteoglycans and water molecules. The next chapter focuses on understanding if changes in proteoglycan composition in sclera occur following the application of MMP-EM and PGF2α.

Scleral tissue treated with MMP and PGF2α did not show any change in helical rise per residue, lateral spacing and D-spacing. Whereas collagenase treatment distorted total collagen architecture, as was determined with the use of WAX and SAX analysis.

CHAPTER 6

THE EFFECT OF MMP & PGF2α ON PROTEOGLYCANS IN HUMAN SCLERA

CHAPTER 6

THE EFFECT OF MMP & PGF2α ON PROTEOGLYCANS IN HUMAN SCLERA

6.1 Introduction

The connective tissue of the sclera imparts strength enabling it to perform its role in protecting the internal ocular tissue, yet remaining fairly elastic to withstand changes in intraocular pressure (Watson and Young 2004). The scleral connective tissue includes a strong meshwork of collagen with proteoglycans (Young 1985). Proteoglycans interact with collagen at specific locations along the collagen fibrils (Scott 1988).

Proteoglycans are a large group of glycoproteins that are heavily glycosylated (Grzesik, Frazier *et al.* 2002). They consist of a core protein and one or more covalently attached glycosaminoglycans (GAGs) chain(s) (Fig. 6.1). These GAG chains are long, linear carbohydrate polymers that are negatively charged under physiological condition, due to the occurrence of sulphate and uronic acid groups.

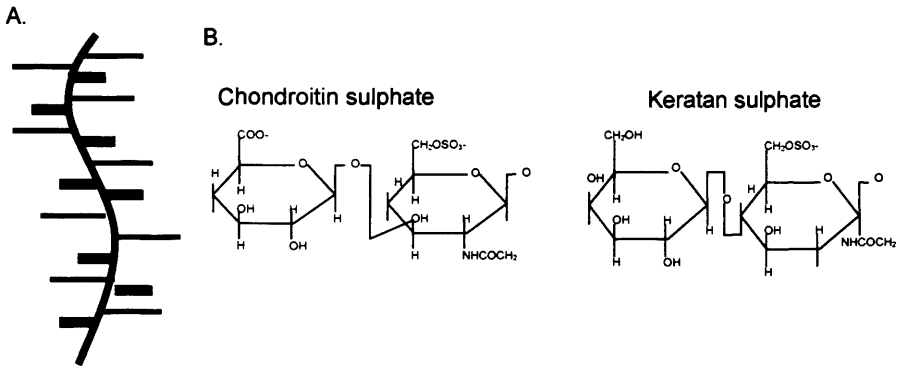

Fig. 6.1: Schematic drawing of proteoglycan and glycosaminoglycan disaccharide. A. Core protein (black) with attached glycosaminoglycan chains (red). B. Chondroitin and keratan sulphate disaccharide (Dudhia 2005).

A number of proteoglycans have been identified within sclera; these include biglycan, aggrecan, decorin and lumican. Aggrecan is the most abundant large proteoglycan in the sclera consisting of a protein core >350kDa size (Rada, Achen *et al.* 1997). Aggrecan contains more than 100 chondroitin sulphate chains and more than 30 keratan sulphate chains (Doege, Sasaki *et al.* 1991). Lumican is known to interact with aggrecan within the sclera, and has a core protein size of 70-80kDa (Dunlevy and Rada 2004). A large group of small leucine-rich repeat proteoglycans within human sclera include the small proteoglycans: biglycan and decorin (Johnson, Young *et al.* 2006). Both biglycan and decorin have a protein core of approximately 45kDa. Decorin contains one chondroitin or dermatan sulphate GAG side chains, whereas biglycan contains two such chains (Fisher, Termine *et al.* 1989).

In chapter 4, sclera subjected to organ culture in a cocktail of MMPs or PGF2α resulted in an increase in scleral permeability. Chapter 5 showed that neither PGF2α nor the MMP cocktail appeared to have an effect on collagen intermolecular or supramolecular structure, suggesting that factors other than collagen degradation or changes in collagen architecture had influenced changes in scleral permeability. In the present chapter, the proteoglycan component of sclera will be analysed to determine if any changes in composition result as a function of MMP action either indirectly by PGF2α or by direct action of the MMPs in the MMP cocktail.

6.1.2 Aims

The aims of the current chapter were to determine the effect of PGF2α and MMPs on:

1. The total sulphated GAG content in sclera.
2. Proteoglycans (aggrecan, lumican, decorin and biglycan) within sclera.

6.2 Experimental Design

Proteoglycans were extracted from scleral tissue following incubation of tissue in media containing PGF2α or MMP-EM. The GAG concentration was measured in the extract, incubation media and in the remaining scleral tissue. Proteoglycan content was semi-quantified following Western blotting.

6.2.1 Tissue Culture

Scleral tissue was isolated from human donors (n=3) and prepared as described in section 2.3.1. Since ageing causes variation in proteoglycan composition (Dudhia 2005; Rada, Achen *et al.* 2000) and interaction (Dunlevy and Rada 2004; Kimura, Kabayashi *et al.* 1995), donors within a similar age range, 60-80 were used. Variation in proteoglycan composition due to scleral location has also been demonstrated (Rada, Achen *et al.* 2000), therefore all tissue explants were isolated from the uveal area of the sclera.

The scleral tissue was dissected into $1cm^2$ explants which were then cultured in triplicate either in MMP-EM, 100nM PGF2α in serum free DMEM:Ham's F10 1:1 or control media (serum free DMEM:Ham's F10 1:1) for 0, 24, 48 or 72 hours (n=3 for each time point, see section 2.4.1).

6.2.2 Sulphated GAG content released into media, solubilised by Guanidine hydrochloride extraction and remaining in sclera.

6.2.2.1 GAG released into media

Media was collected following scleral culture and stored at -80°C. The GAG released into media during incubation was analysed using the DMMB assay (see section 2.6.4).

6.2.2.2 GAG Solubilised

Proteoglycans were extracted from scleral tissue explants in 4M guanidine hydrochloride (GuHCl) (see section 2.6.1). The solubilised extract was then dialysed (section 2.6.2) to remove any interfering ions. Total sulphated extracted GAGs was analysed using the DMMB assay (section 2.6.4).

6.2.2.3 Determination of Total GAG

Following incubation and guanidine extraction, the remaining scleral tissue was digested with papain (see section 2.6.3), in order to calculate the total amount of sulphated GAGs.

Total GAGs = GAGs media + GAGs solubilised + GAGs remaining in tissue.

This allowed percentage GAGs released in media and GAGs solubilised by extraction to be calculated.

%GAGs released = (GAGs media / Total GAGs) X 100

%GAGs solubilised = (GAGs solubilised / GAGs solubilised + GAGs remaining in tissue) X 100

6.2.3 Analysis of Proteoglycan in Sclera

6.2.3.1 Identification of Proteoglycans in Sclera

The presence of different proteoglycans, namely aggrecan, biglycan, decorin and lumican within the human sclera, were identified following electrophoresis of solubilised proteoglycans and immunoblotting (section 2.6.4-2.6.7).

6.2.3.2 Quantification of Proteoglycan

6.2.3.3 Deglycosylation

Solubilised samples were deglycosylated (section 2.6.6) and then dialysed (section 2.6.2) to remove any free single sugars generated by deglycosylation. Samples were then dried in a Speedvac (Thermo Savant, U.K.) for 4 hours.

6.2.3.4 Western Blotting

Dried samples were re-suspended in sample buffer with 10% mercaptoethanol and heat-treated for 10 minutes (section 2.6.7). For the quantification of proteoglycan levels, samples containing equal protein concentrations of 50μg (see section 2.6.5 for protein determination assay)

were loaded onto 4-12% gradient gels and electrophoresed at 100V. Proteins were then transferred onto nitrocellulose membrane by blotting at 100V for one hour (see section 2.6.7). The membranes were blocked in 5% BSA before being probed with primary antibodies for aggrecan, biglycan, decorin and lumican overnight at room temperature. Following washes in TSA, the membranes were placed in secondary anti-mouse IgG (H+L), alkaline phosphatase (AP) and specific proteoglycan bands were visualised following the development of colour in AP buffer containing bromo-chloro-indolyl phosphate (BCIP) and nitroblue tetrazolium (NBT). The reaction was stopped by immersion in water and after drying the membrane the developed bands were subjected to laser scanning densitometry to identify intact and degraded proteoglycans. Membranes were scanned using an Epson expression 1680 pro scanner and the gel band maximum OD was measured using Labworks 45 software.

6.2.4 Data analysis

Data was entered into Excel 2003 to obtain charts and SPSS 14 in order to conduct statistical analysis of data. As data displayed non-parametric trends tests such as Spearmans-Rank correlation, Kruskal Wallis and Wilcoxon rank tests were applied.

6.3 Results

6.3.1 Effect of PGF2α and MMPs on GAG composition

The percentage of GAGs released and the percentage of GAGs solubilised from tissue are shown in Figs. 6.2a-b.

(a)

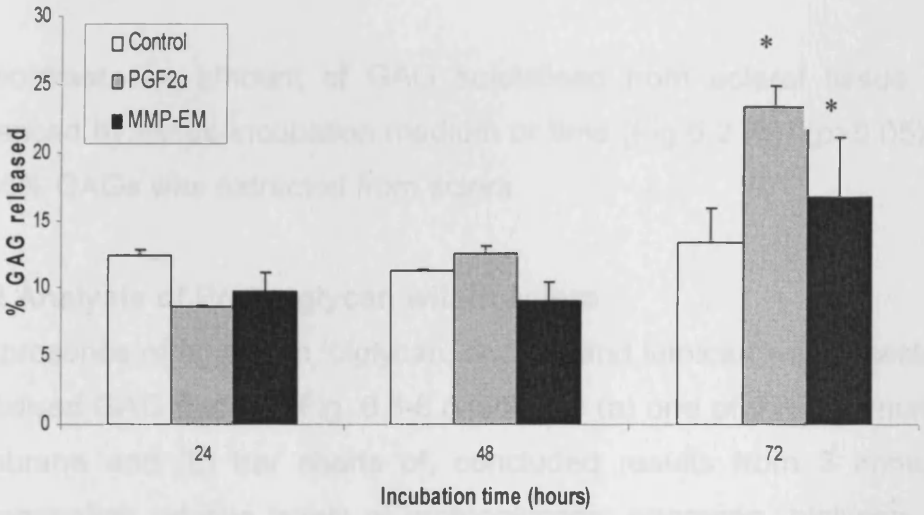

(b)

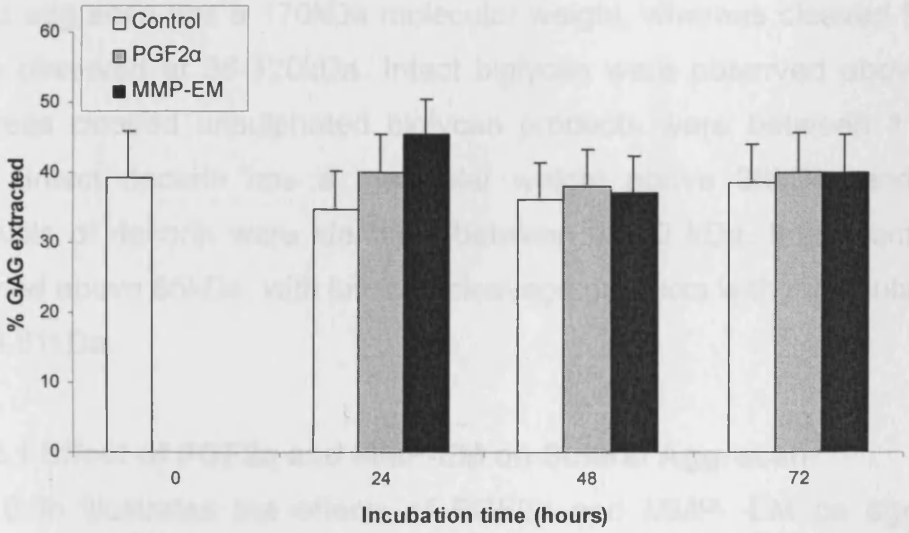

Fig. 6.2: Percentage of GAG released in media and the percentage of GAG extracted from scleral tissue. (a) percenta of GAG released in media compared to total GAG; (b) percentage of GAG extracted from tissue compared to total GAG in tissue.

Up-to 25% GAG was released into medium after 72 hours incubation (Fig. 6.2 (a)). GAG release increased with time in incubation ($p<0.001$). There was significant changes observed in terms of tissue treatment ($p<0.001$). A significant increase of 4-9% and 9-11% in percentage GAGs released was observed for sclera incubated in MMP-EM and PGF2α, respectably, compared to control after 72 hours incubation.

By contrast, the amount of GAG solubilised from scleral tissue was not influenced by tissue incubation medium or time (Fig 6.2 (b)) ($p>0.05$). Overall 35-46% GAGs was extracted from sclera.

6.3.2 Analysis of Proteoglycan within sclera

The presence of aggrecan, biglycan, decorin and lumican was detected in the solubilised GAG fraction. Fig. 6.3-6.6 includes (a) one of three immunoblotted membrane and (b) bar charts of, concluded results from 3 immunoblots, demonstrating relative levels of proteoglycans: aggrecan, biglycan, decorin, and lumican.

Intact aggrecan has a 170kDa molecular weight, whereas cleaved fragments were observed at 36-120kDa. Intact biglycan were observed above 36kDa, whereas cleaved unsulphated biglycan products were between 11 and 25 KDa. Intact decorin has a molecular weight above 36kDa, and cleaved products of decorin were identified between 21-30 kDa. Intact lumican was attained above 65kDa, with lumican cleavage products with molecular weights of 19-61kDa.

6.3.2.1 Effect of PGF2α and MMP-EM on Scleral Aggrecan

Fig. 6.3b illustrates the effects of PGF2α and MMP- EM on aggrecan in sclera. There were significant changes in aggrecan composition following culture with treatment of scleral tissue in PGF2α and MMP-EM ($p<0.05$). Upto 1.6+/-0.4, 0.6+/-0.3 and 0.4+/-0.1 relative levels of cleaved product observed for MMP-EM, PGF2α and control treated tissue respectably. A maximum aggrecan level in the extracted samples was observed after 48

hours of incubation. The percentage difference between intact and cleaved aggrecan was significantly different in all samples ($p<0.05$). Only cleaved aggrecan was observed in sclera incubated in MMP-EM. This suggests that the MMP cocktail cleaves aggrecan within 24 hours of incubation.

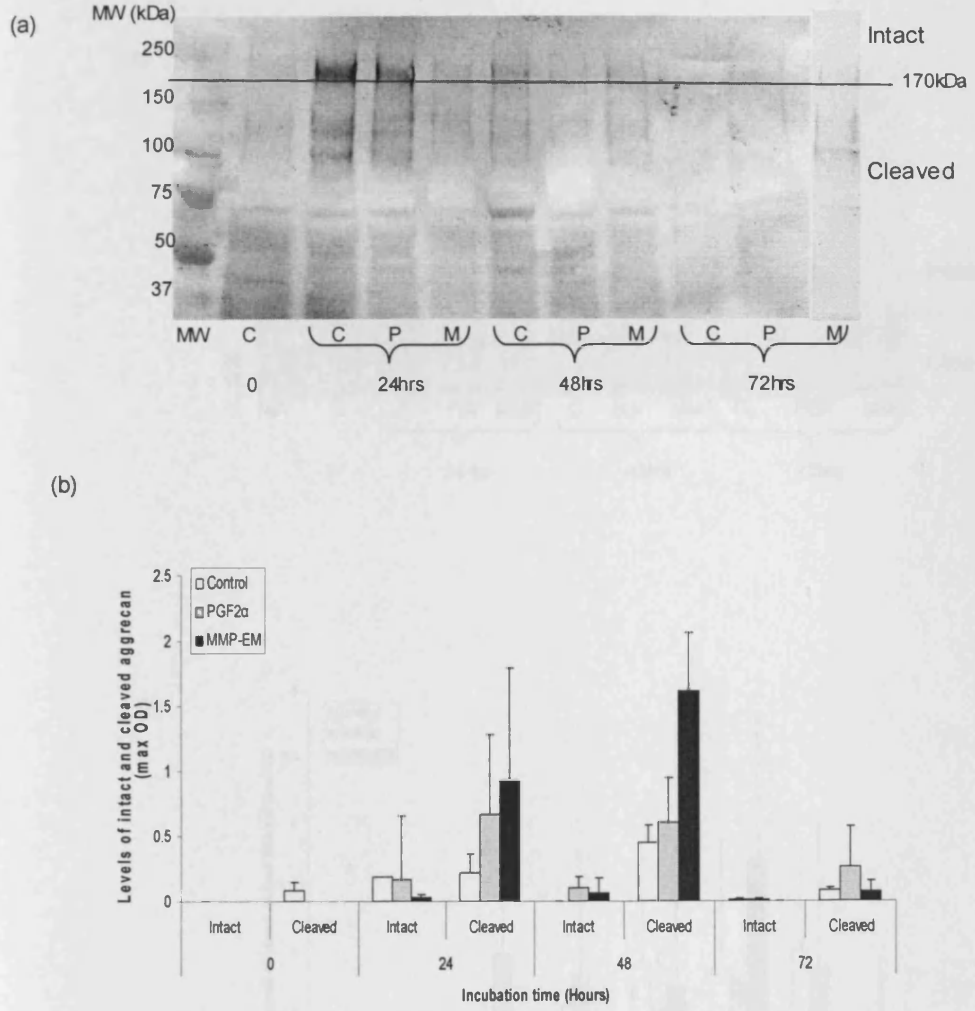

Fig. 6.3: Effect of PGF2α and MMP-EM on scleral aggrecan. (a) Immunoblot showing intact and cleaved aggrecans. Samples: Control (C), PGF2α (PGF) and MMP-EM (MMP). MW: Molecular weight marker. (b) Bar chart showing relative levels of intact and cleaved aggrecan.

6.3.2.2 Effect of PGF2α and MMP-EM on Scleral Biglycan

Fig. 6.4b illustrates the effects of PGF2α and MMP- EM on biglycan in sclera. MMP-EM or PGF2α treatment or incubation time had no significant influence on level of intact or cleaved biglycan ($p>0.05$).

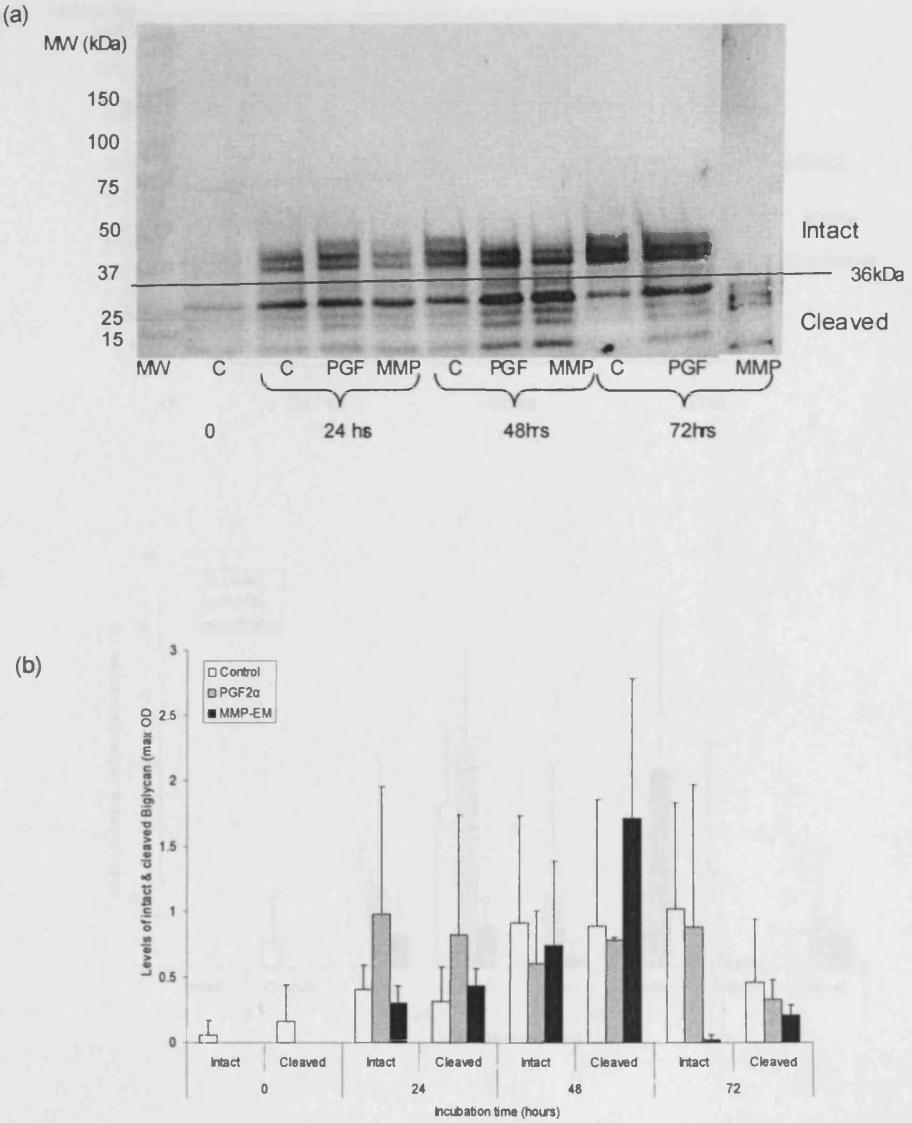

Fig. 6.4: Effect of PGF2α and MMP-EM on scleral biglycan. (a) Immunoblot showing intact and cleaved biglycans. Samples: Control (C), PGF2α (PGF) and MMP-EM (MMP). MW: Molecular weight marker. (b) Bar chart showing relative levels of intact and cleaved biglycan.

6.3.2.4 Effect of PGF and MMP-EM on Scleral Decorin

Fig. 6.5b illustrates the effects of PGF2α and MMP- EM on decorin in sclera. No significant changes in intact or cleaved decorin was observed with treatment or time-point ($p>0.05$).

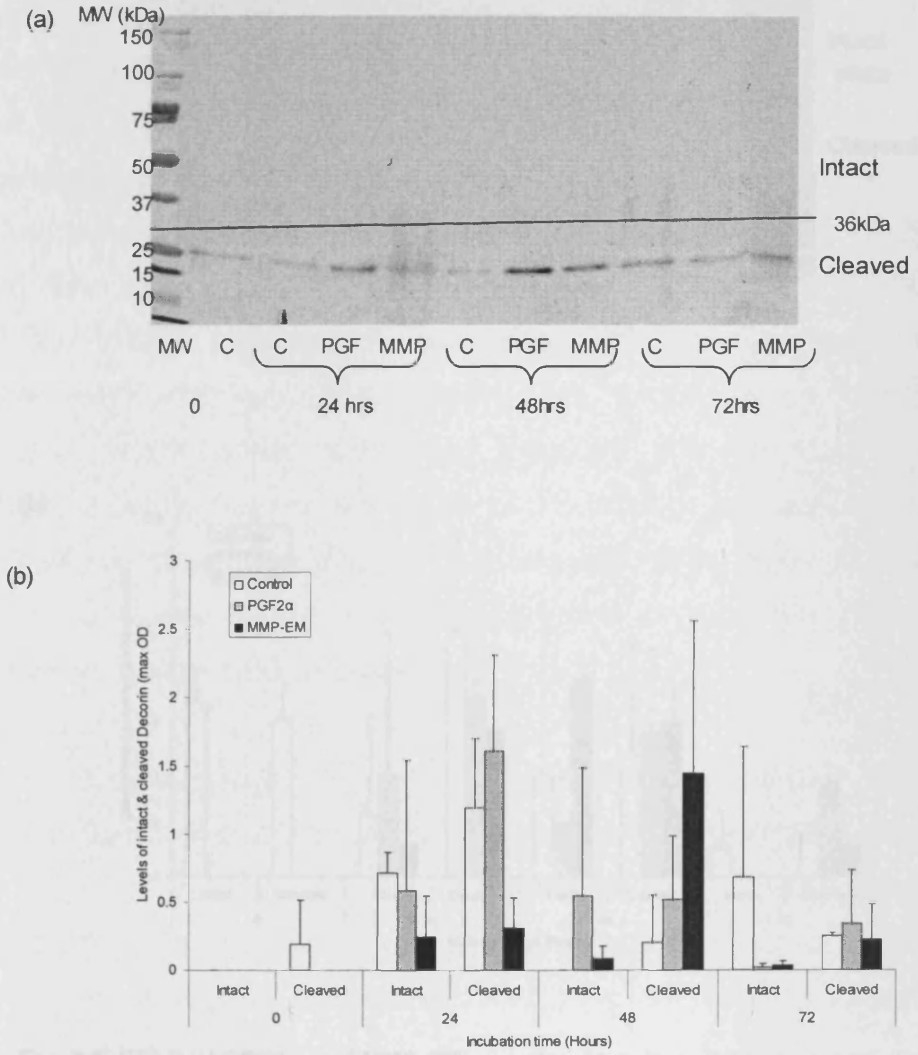

Fig. 6.5: Effect of PGF2α and MMP-EM on scleral decorin. (a) Immunoblot showing intact and cleaved decorins. Samples: Control (C), PGF2α (PGF) and MMP-EM (MMP). MW: Molecular weight marker. (b) Bar chart showing relative levels of intact and cleaved decorin.

6.3.3 Effect of PGF and MMP-EM on Scleral Lumican

Fig. 6.6b illustrates the effects of PGF2α and MMP- EM on lumican in sclera. No significant changes in lumican occurred due to treatment or time-point ($p>0.05$).

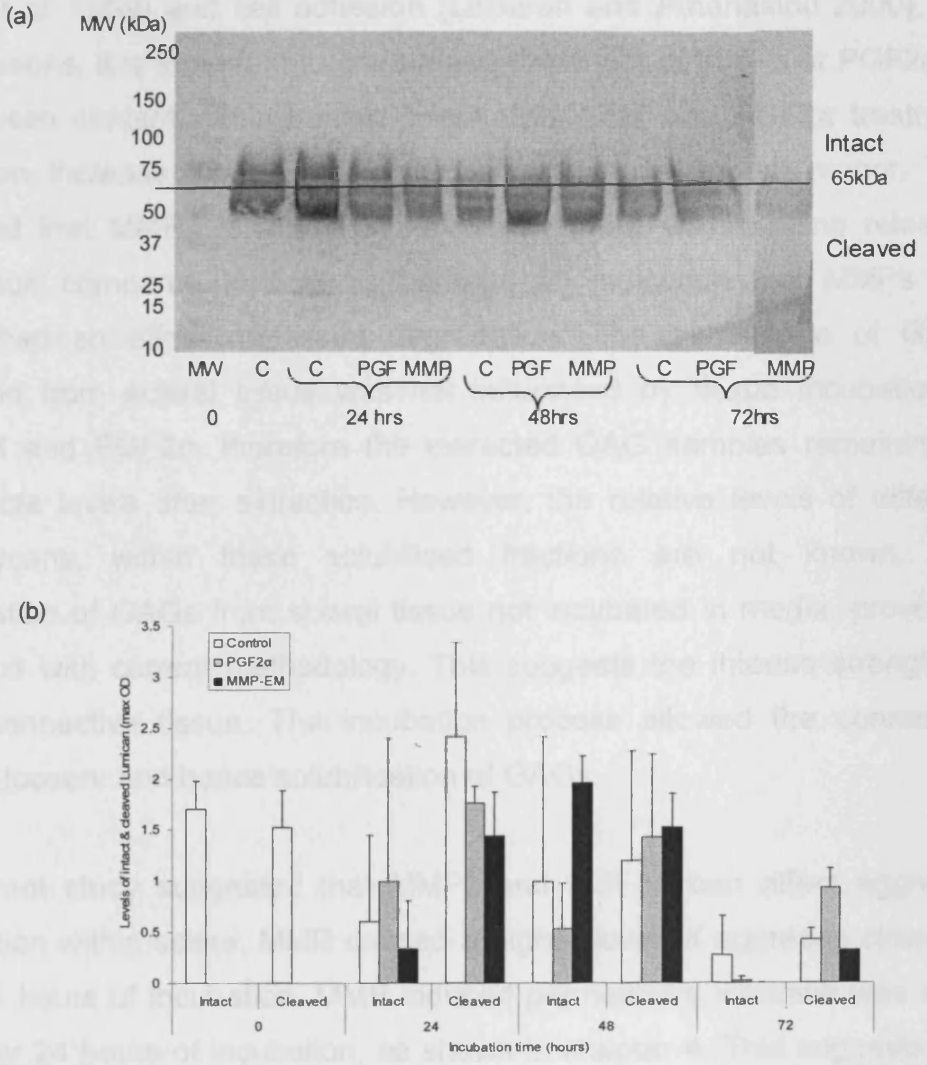

Fig. 6.6: Effect of PGF2α and MMP-EM on scleral lumican. (a) Immunoblot showing intact and cleaved lumicans. Samples: Control (C), PGF2α (PGF) and MMP-EM (MMP). MW: Molecular weight marker. (b) Bar chart showing relative levels of intact and cleaved lumican.

6.4 Discussion

Although proteoglycans represent a small proportion of scleral extracellular matrix (ECM), proteoglycans are essential in determining hydration (Naka, Morita *et al.* 2005), maintenance of structural integrity (Antoniou, Mwale *et al.* 2006), growth regulation (Su and Elam 2003), matrix organisation (Hamati, Britton *et al.* 1989) and cell adhesion (LeBaron and Athanasiou 2000). For these reasons, it is important to understand the effect of MMPs or PGF2α on proteoglycan content within human sclera. MMP-EM and PGF2α treatment caused an increase in GAGs released in a time dependent manor. This suggested that MMP-EM and PGF2α caused more GAGs being released from tissue compared to controls perhaps an indication that MMPs and PGF2α had an effect on tissue degradation. The percentage of GAGs solubilised from scleral tissue was not influenced by tissue incubation in MMP-EM and PGF2α, therefore the extracted GAG samples remaining at comparable levels after extraction. However, the relative levels of different proteoglycans, within these solubilised fractions are not known. The solubilisation of GAGs from scleral tissue not incubated in media, proved to be difficult with current methodology. This suggests the intense strength of scleral connective tissue. The incubation process allowed the connective tissue to loosen, and hence solubilisation of GAGs.

The current study suggested that MMPs and PGF2α can affect aggrecan composition within sclera. MMP caused a higher level of aggrecan cleavage within 24 hours of incubation. MMP induced permeability increase was at its peak after 24 hours of incubation, as shown in chapter 4. This suggests that the changes in aggrecan composition could be an influential factor in enhanced scleral conductivity.

Aggrecan is known to be involved in hydrating the collagen network, which provides compressibility and elasticity to the scleral tissue (Malfait, Liu *et al.* 2002). The MMP cleavage site within aggrecan monomers occurs in between the C-terminal G1-G2 double globe region in between Asn341-Phe342 (Lark, William *et al.* 1995). Aggrecanase (Lark, Bayne *et al.* 1997) and A Disintegrin

and Metalloproteinase with Thrombospondin (ADAM-TS) (Malfait, Liu *et al.* 2002) have many cleavage sites within aggrecan monomers, one of which is within G1-G2 region in between Glu373-Ala374. Further study into fragment sequencing would determine the proteinases that play key roles in degrading aggrecan within sclera.

Although small leucine-rich proteoglycans (SLRP) such as biglycan, decorin and lumican only form a small proportion of the total scleral proteoglycan mass, they are however distributed in similar proportions to large proteoglycans (Johnstone, Markopoulos *et al.* 1993). Previous studies have demonstrated that SLRP are resistant to proteolytic cleavage compared to aggrecan (Sztrolovics, White *et al.* 1999). The fact that SLRP are less susceptible to proteolytic cleavage could explain why the application of MMP-EM and PGF2α on scleral tissue did not influence the small proteoglycan composition.

SLRP are involved in protecting collagen fibrils from collagenase action (Geng, McQuillan *et al.* 2006). They cover the collagen fibrils and prevent access of proteolytic enzymes to the collagen fibrils. Investigations have demonstrated the interaction of proteoglycan within the D-period of collagen fibrillar architecture (Young 1985), no change in SLRP suggests why change D-period was not observed in the previous chapter. The previous chapter demonstrated that collagen architecture remained intact even after 72 hours incubation in MMPs or PGF2α. This could be due to the accumulation of SLRP, which are unaffected by MMPs or PGF2α application, sustain their role in protecting the collagen fibrous structure within the scleral tissue.

The degradation of large aggrecan molecules identified with MMP and PGF2α would be sufficient in order to increase permeability. As the large aggrecan molecules have the potential interact with large amounts of water molecules, the depletion of aggrecan should empty spaces within the extracellular matrix and reduce resistance to aqueous outflow and drug inflow.

As aggrecan degradation has been denoted as the appropriate method to increase tissue permeability, without causing tissue destruction, it would now be possible to use specific MMPs or aggrecanases which selectively cleave aggrecan within the tissue. Although MMP 3 is involved in aggrecan cleavage (Little, Flannery *et al.* 1999), it is also involved in the cleavage of other ECM components (Ashworth, Murphy *et al.* 1999). Aggrecanases, such as ADAMTS4 (Tortorella, Burn *et al.* 1999) and ADAMTS11 (Abbaszade, Liu *et al.* 1999) are enzymes which cleave aggrecan only. The use of such enzymes on scleral tissue could be tested in the future.

CHAPTER 7

DISCUSSION

CHAPTER 7

DISCUSSION

7.1 Introduction

The basis of the current research project was to understand the impact of matrix metalloproteinases (MMPs) on the uveoscleral outflow pathway, which may in future contribute to the enhanced treatment of glaucoma. Prostaglandins derivatives (such as PGF2α) are the most commonly used drug in the control of intraocular pressure (IOP) in glaucoma. The ocular hypotensive effects of prostaglandin has been linked to their ability to induce MMPs expression (Oh, Martin *et al.* 2006a), reduce extracellular matrix (ECM) products (Lindsey, Kashiwagi *et al.* 1997), and thereby enhance uveoscleral outflow (Schachtschabel, Lindsey *et al.* 2000). These observations made it necessary to understand whether the induction of MMP expression was a direct effect of prostaglandins and if the direct effect of MMPs to the eye could be harnessed to further reduce IOP.

This study initially analysed the impact of MMP inducers on MMP secretion and activation by cells involved in the uveoscleral outflow pathway. The use of PGF2α and other inducers resulted in an increased MMP secretion and activation by human ciliary muscle cells (HCM cells) and human scleral fibroblasts (HSFs). The effect of the direct action of MMPs on the uveoscleral pathway is not fully understood. This study therefore has focussed on looking at the effect of PGF2α and MMPs on scleral integrity, since sclera is a major component of the uveoscleral outflow pathway. It is critical that while MMPs can be added to increase scleral conductivity, this should not compromise scleral integrity.

7.2 Induction of MMP secretion and activity in the uveoscleral outflow pathway

Current glaucoma treatments are focussed on the reduction of IOP, either via downregulation of aqueous formation or the upregulation of aqueous drainage. The main aim of this study was to investigate the mechanism of

action of PGF2α and MMPs in augmenting aqueous outflow via the uveoscleral outflow pathway. MMPs are a group of biological enzymes which are involved in the degradation of ECM. There are many MMPs which have been grouped according to their structure and enzymatic activity (Murphy, Murphy *et al.* 1991). Collagenases (e.g. MMP 1) are known to cleave the triple helical structure of collagen at a specific location, thereby distorting the collagen structure and making it susceptible to further degradation. The gelatinases (e.g. MMP 2 and 9) act on basement membranes and have high specificity to denatured collagen. The stromelysins, such as MMP 3 and 7, have broader substrate specificity and have the ability to degrade a range of ECM products including collagen types IV, IX and X, laminin, proteoglycans and fibronectin (Girolamo, Lloyd *et al.* 1997). Membrane-associated MMPs (MT-MMPs) are so-called because they are membrane-bound and not secreted into the extracellular matrix (Takino, Sato *et al.* 1995).

This study firstly determined the MMP profile of cells within the uveoscleral outflow pathway. *In vitro* studies demonstrated the production of a collagenase (MMP 1), the gelatinases (MMP 2 and 9) and stromelysins (MMP 3 and 7) by scleral fibroblasts and ciliary muscle cells. Since these cells are present within the uveoscleral outflow pathway, it is likely that if they are stimulated to produce such MMPs, their action is likely to affect the surrounding ECM.

Interleukin-1α (IL-1α), tumour necrosis factor-α (TNFα) and transforming growth factor-β (TGF), have previously been shown to influence MMP activation. IL-1α has previously been shown to be involved in increasing aqueous outflow (Kee and Seo 1997). IL-1α, TNFα and TGFβ have all been linked to the induction of MMP secretion and activity in various cell cultures (Hosseini, Rose *et al.* 2006; Kim, Shang *et al.* 2004). The current study measured the production of collagenase, gelatinase and stromelysin activity following the application of these growth factors within *in vitro* cultures of scleral fibroblast and ciliary muscle cells, the cells present in the uveoscleral outflow pathway. The therapeutic use of these cytokines have been limited,

since they cause neurodestruction, (Yuan and Neufeld 2000), anterior subcapsular cataracts (Srinivasan, Lovicu *et al.* 1998), and lacrimal gland inflammation (Zoukhri, Macari *et al.* 2007). Such possible ocular complications and other as yet undetermined more problematic situations, need to be avoided in any ocular therapy.

Prostaglandin derivatives are well tolerated by glaucomatous eyes (Drake 1996; Sharif, Kelly *et al.* 2003). Many studies have been conducted into understanding how these drugs lower IOP, and the main findings involve the upregulation of MMPs (Gaton, Sagara *et al.* 2001; Weinreb, Kashiwagi *et al.* 1997) and degradation of ECM products (Lindsey, Gaton *et al.* 2001; Sagara, Gaton *et al.* 1999) within the uveoscleral outflow pathway (Gabelt and Kaufman 1989). The current study confirmed the induction of MMPs (MMP 1, 2, 3 and 9) with a prostaglandin analogue (PGF2α) within *in vitro* cultures of human scleral fibroblasts and ciliary muscle cells. Previous studies have implicated MMPs in the destruction of scleral tissue leading to scleritis (Girolamo, Lloyd *et al.* 1997). This is a sight threatening inflammatory disorder caused by scleral matrix degradation (Okhravi, Odufuwa *et al.* 2005; Watson and Young 2004). Again this is an ocular complication to be avoided if direct MMP action on ocular structures is to be harnessed.

MMP activity is controlled at three levels: (i) gene expression, (ii) post-translational modification required to activate MMPs and (iii) the presence of MMP inhibitors i.e. tissue inhibitors of matrix metalloproteinase (TIMPs). Prostaglandin up-regulation of MMP activity can be controlled by a negative feedback effect which enhances TIMPs (Ito, Ohguro *et al.* 2006; Oh, Martin *et al.* 2006b), thereby preventing inflammation and scleritis. If MMP action is to be used in ocular therapy, a critical balance between MMPs and TIMPs must be maintained.

7.3.1 The effect of PGF2α and MMPs on Scleral Integrity

Explant cultures of scleral tissues in the presence of PGF2α or MMPs resulted in increased scleral permeability after 3 to 24 hours of incubation. Interestingly, the MMP cocktail induced a greater increase in scleral permeability than the prostaglandin analogue (PGF2α).

Compatible with these findings previous studies have demonstrated that prostaglandins (PGF2α) were able to enhance scleral permeability (Kim, Lindsey *et al.* 2001; Weinreb 2001) and thereafter suggested that prostaglandins can induce MMPs expression and activity (Weinreb 2001). The current study is the first to show that the direct application of MMPs has greater effect on scleral conductivity than PGF2α.

The findings in chapter 4 suggest that scleral permeability can be increased in order to allow macromolecules with molecular mass up to 70kDa through and thereby drug delivery can be improvised. This suggests that tissue permeability can be enhanced for drug delivery, without making any chemical or physiological changes to the drug. A limitation to this study is that molecular weight of rhodamine dextran beads have been considered. The size, polarity and possible ionic charge of these molecules have not been considered. These factors will influence the transcleral passage of molecules.

The eye consists of two segments: the anterior segment (includes the cornea, anterior chamber, crystalline lens and ciliary body) and the posterior segment (includes the vitreous body, retina, and choroids). Age-related macular degeneration (AMD), diabetic retinopathy, posterior uveitis and retinitis due to glaucoma are leading posterior segment diseases which lead to vision loss (Olejnik and Hughes 2005). Drug delivery to the posterior segment of the eye has been limited via various factors. Currently four routes are used in drug delivery to the posterior segment including topical, systemic, intravitreal and transcleral (Geroski and Edelhauser 2000). There are limitations linked to all conventional drug delivery pathways including low drug delivery percentage, side effects such as retinal detachment and the requirement of periodical

surgeries (Kimura, Yasukawa *et al.* 2001). Many studies are being conducted in order to improve drug delivery such as the use of transcleral iontophoresis (Myles, Neumann *et al.* 2005) and nanoparticles (Patil, Reshetnikov *et al.* 2007). The safety and the efficacy of such delivery systems still require further investigation.

Scleral tissue, which is the main protective layer of the eye, is considered the main barrier to the application of substances into the eye. However, due to the large surface area covering approximately 95% of the globe, it is considered a more advantageous media for drug delivery than the cornea. Due to different tissue thicknesses throughout the scleral surface area (1.0mm thickness around optic nerve, 0.53mm in corneoscleral limbus and 0.39nm around the equator) (Watson and Young 2004), a safer and less invasive drug delivery route could be devised.

The data in chapter 4 has shown that an increase in scleral permeability can be harnessed, with MMP action, in order to allow high molecular weight molecules to gain intraocular access. Further work is required to determine the effect of increased scleral conductivity in the transport of novel therapeutic agents to the posterior pole for the treatment of diseases such as glaucoma and diabetes. If MMP actions are to be utilised, the integrity of the media through which drug delivery is to take place, first needs to be determined to avoid potential side effects.

7.3.2 Sclera retained its collagen architecture at molecular and supramolecular levels following MMP treatment

Collagenase, gelatinase and stromelysin activity (within MMP-EM) and induced by PGF2α did not influence collagen architecture at the molecular and supramolecular level, as determined by measurements of axial rise per residue, intermolecular lateral packing and D-periodicity. MMP collagenases (e.g. MMP 1) play a function in cleaving helical collagen structure, which dismantles the collagen molecular structure and leads to destruction of the collagen fibril. Specific MMPs (MMP 1, 2 and 7) and MMP directly secreted by

human scleral fibroblast and ciliary muscle cell cultures were also tested, and also showed no effect on collagen molecular and supramolecular structure.

Thus, the application of MMPs enhanced scleral tissue permeability but did not result in degradation of the collagen architecture at the molecular and supramolecular levels. This is an important finding as collagen is a major component of the sclera (Keeley, Morin *et al.* 1984), and the disruption of scleral collagen architecture could lead to adverse effects, such as scleritis (Watson and Young 2004). Collagen architecture is influenced by different MMPs at different levels (Minond, Lauer-Fields *et al.* 2004) and can develop stability via interacting with other extracellular matrix components, such as proteoglycans (Dunlevy and Rada 2004). These factors suggest how collagen stabilises itself against proteolytic cleavage by MMPs.

7.3.3 Changes in Scleral Proteoglycans following MMP action

Proteoglycans form a small percentage of scleral by dry weight. However, they play vital roles in cell and matrix interactions. The presence of proteoglycans such as aggrecan, biglycan, decorin and lumican within the sclera was determined within this study.

The findings of the current study suggest that greater levels of cleaved scleral aggrecan were present in sclera subjected to the direct action of MMPs, compared to control and PGF2α treated tissue. Aggrecan is a large proteoglycan which embeds itself in between collagen fibrils. Due to the large amount of negatively charged glycosaminoglycans (GAGs) chains interacting with the aggrecan core, it generates an electrostatic repulsive force, which acts as a space-filling molecule and binds to a large amount of water molecules (Muir 1982). An increase in aggrecan is observed with age within sclera (Rada, Achen *et al.* 2000). Since age is a major risk factor to the development of glaucoma, it could be suggested that the accumulation of scleral aggrecan increases outflow resistance in the uveoscleral pathway, and thereby increase IOP. The accumulation of aggrecan has also been linked to increased axial length leading to myopia (Rada, Johnson *et al.* 2002).The loss

of aggrecan may contribute to increased scleral permeability due to MMP activity.

However, it is important to keep the protease action under control, as the level of protease involvement will determine whether aggrecan degradation is destructive or non-destructive (Duirgova, Roughley *et al.* 2007; Maitre, Pockert *et al.* 2007; Muir 1982). Proteoglycans are the organisers of the intracellular matrix; excessive aggrecan degradation could cause tissue destruction. It is important to understand the mechanisms of aggrecan degradation within sclera via MMPs and PGF2α in order to ensure that scleral tissue function is maintained, especially if this was to be used as a method of ocular therapy. It is important to understand if MMP and PGF2α activity cleaves aggrecan at its side chains or within the core protein and if after the aggrecan degradation it disappears as debris or can re-build itself. Such knowledge will be required in order determine the best mode of ocular treatment via aggrecan degradation i.e. the efficiency of such treatment.

Small leucine rich proteoglycans (SLRPs), in the case of sclera biglycan, decorin and lumican, were unaffected by MMP or PGF2α throughout the incubation period, as determined in this study. These are small proteoglycans that perform various functions within tissue involving regulation of extracellular matrix and cell adhesion. They are known to have structural correlation, including a similar leucine rich internal repeat structure and cysteine- rich N and C-terminus (McEwan, Scott *et al.* 2006). SLRP interact with the surface of collagen and coat the fibril surface, thereby preventing collagenolytic proteolytic activities (Geng, McQuillan *et al.* 2006). Since the application of MMPs and PGF2α has no effect on collagen molecular and supramolecular structure, it is reasonable to suggest that the SLRP composition within sclera protect the collagen architecture against proteolytic cleavage.

The potential to increase scleral permeability without damaging the collagenous architecture, by the controlled removal of aggrecan could play a vital role in lowering eye pressure and improving ocular drug delivery.

7.4 Conclusion

The initial aim of the project was to determine the effect of MMP inducers on the uveoscleral outflow pathway. Zymographical analysis allowed an understanding of how growth factors and prostaglandins induced MMP secretion and activation from human scleral fibroblasts and ciliary muscle cells. The controlled reduction of extracellular matrix components with induction of MMP activity within the uveoscleral outflow pathway could improve aqueous drainage and tissue permeability to drug delivery. Secondly, the Ussing chamber made it possible to analyse the direct impact of MMPs, as well as prostaglandin, on scleral conductivity. An increase in scleral tissue permeability was determined following the application of MMPs, that was greater than that achieved by prostaglandins alone.

Thus MMPs can enhance tissue permeability, but an understanding of the effect on scleral architecture and composition remained to be determined. To analyse the effect of MMPs on extracellular matrix components within scleral tissue, x-ray diffraction and western blotting was used. X-ray diffraction analysis of sclera indicated that neither MMPs nor PGF2α had an effect on collagen architecture. However biochemical analysis, using western blotting techniques, showed that scleral aggrecan composition was altered, although no changes in SLRPs were identified. These findings provided an understanding of scleral tissue modulation by the action of MMPs and PGF2α.

It has been postulated previously that PGF2α acts to lower IOP by induction of MMP activation in the uveoscleral outflow pathway (Schachtschabel, Lindsey *et al.* 2000), thereby augmenting aqueous outflow as a result of ECM degradation (Ito, Ohguro *et al.* 2006). The current study does agree with this mechanism, as the direct action of MMPs on sclera caused ECM modulation, which could be the reason behind increased tissue conductivity. The increase in scleral conductivity could harness aqueous outflow via the uveoscleral outflow pathway and thereby lower IOP. The safe use of MMPs to modulate scleral permeability is likely to benefit many clinically important therapeutics.

This study indicates the potential for developing therapeutic drugs which involve matrix degradation without causing harm to the architectural arrangement of the tissue. This research could have a major impact on the pharmacological field, should it be possible to pre-treat sclera to improve permeability without adverse effect. It would become more manageable to administer drugs to treat posterior disease. The delivery of aptamer oligonucleotides against the neovascular growth in AMD, prolonged action anti-virals for treatment of CMV retinitis and neuroprotective agents to treat degenerations of the retina would become more applicable without any compromisation due to delivery difficulties. The delivery of such therapeutics via the transcleral pathway would prove to be less invasive and longer acting.

7.5 Future prospects

The findings of this study suggest that direct application of MMPs to scleral tissue could improve aqueous drainage and drug delivery. However, MMPs are matrix degrading enzymes which would be difficult to control. The use of TIMPs as treatment to various diseases such as congestive heart failure and arthritis has been investigated for many years, but such biological factors tend to fail (Peterson 2004). Further work is required in the use of such treatment and to obtain the treatment with maximum therapeutic impact in glaucoma patients and drug delivery.

Future work will involve:

1) **Quantification of changes in MMP, collagen and proteoglycan composition**

   As zymography, x-ray diffraction and Western blotting were semi-quantitative methods used to measure changes in protein levels; future work will use techniques such as ELISA and column chromatography to assess MMP, collagen and proteoglycan levels. ELISA involves the determination of antibody or antigen concentration in a sample. ELISA kits are available for biological proteins, such as MMPs. MMP-1 ELISA kit has been used in the current study. Column chromatography involves the passage of protein through a column that is designed to trap or slow up the passing of proteins based on size, charge or composition. With particular interest would be affinity chromatography, and gel filtration chromatography. Affinity chromatography involves a column of ligands, which sample proteins can bind to. A gel filtration column has a matrix of fine porous beads which allow the separation of proteins according to their size. Both ELISA and column chromatography would allow the determination of specific protein concentration in a protein sample.

2) **Understanding the effect of prostaglandins on the uveoscleral outflow pathway**

   Prostaglandins may be involved in up or downregulation of other factors besides MMPs within the uveoscleral outflow pathway which may be

involved in IOP reduction. Gene microarray analysis may help in determining such factors.

3) Determination of other inducers of MMPs

MMPs being a cocktail of biological factors with various influential affect it will be difficult to apply a cocktail of MMPs directly to tissue as a treatment, due to the diversity of its action. It would be important to determine the best suited method to induce MMP activity within the required location of the eye and with specific action within tissue, without causing adverse effects.

4) Determination of matrix degradation mechanism within scleral tissue

An understanding of the mechanism of matrix degradation is required to improve methods that could be used in order to improve treatment. This can be determined by further in depth study of the extracellular products produced as a result of MMP and PGF2α action on scleral tissue, using techniques such as polymerase chain reaction and western blotting.

5) Use of aggrecanase and chondroitinase to enhance tissue permeability

As aggrecan is a potential substrate for matrix degradation in order to clear uveoscleral outflow pathway for aqueous drainage an understanding of the use enzymes i.e. chondroitinase and aggrecanase on tissue permeability would be an important determination.

6) Determine if tissue treatment improves the delivery of drug molecules across scleral tissue.

The use of treatments such as an MMP cocktail as a pre-drug delivery mechanism could be tested. This would involve treating tissue with MMPs and then assessing its ability to allow the passage of drugs, such as Avastin and Lucentis, using the Ussing chamber.

7) Understand the impact of MMP and PGF2α treatment on perfusion chamber cultures, in aqueous drainage.

The MMP and PGF2α treatments have been applied to scleral tissue. However, other factors may influence the effect of tissue when applied to perfused anterior chambers. The purfused chamber could be used to monitor how the treatments affect aqueous outflow, at various IOP. Therefore, further investigations are required of the MMP treatment on such models.

REFRENCES

Abbaszade I, Liu RQ, *et al.* (1999) Cloning and characterization of ADAMTS11, an aggrecanase from the ADAMTS family. *Journal of Biological Chemistry* **274**, 23443-23450.

Aihara M, Lindsey JD, Weinreb RN (2003) Aqueous humor dynamics in mice. *Investigative Ophthalmology & Visual Science* **44**, 5168-5173.

Ali Y, Lehmussaari K (2006) Industrial perspective in ocular drug delivery. *Advanced Drug Delivery Reviews* **58**, 1258-1268.

Alimuddin M (1956) Normal intra-ocular pressure. *British Journal of Ophthalmology* **40**, 366-372.

Alm A (1998) Prostaglandin derivates as ocular hypotensive agents. *Progress in Retinal and Eye Research* **17**, 291-312.

Alm A (2000) Uveoscleral outflow. *Eye* **14**, 488 - 491.

Ambati J, Canakis CS, Miller JW, Gragoudas ES, Edwards A, Weissgold DJ, Kim I, Delori FC, Adamis AP (2000) Diffusion of high molecular weight compounds through sclera. *Investigative Ophthalmology & Visual Science* **41**, 1181-5.

Ando H, Twining SS, Yue BYJT, Zhou X, Fini ME, Kaiya T, Higginbotham EJ, Sugar J (1993) MMPs and proteinase inhitors in the human aqueous humor. *Investigative Ophthalmology & Visual Science* **34**, 3541 - 3548.

Anthony TL, Lindsey JD, Aihara M, Weinreb RN (2001) Detection of prostaglandin EP1, EP2 and FP receptor subtypes in human sclera. *Investigative Opthalmology & Visual Science* **42**, 3182 - 3186.

Anthony TL, Lindsey JD, Weinreb RN (2002) Latanoprost effects on TIMP-1 and TIMP-2 expression in human ciliary muscle cells. *Investigative Ophthalmology & Visual Science* **43**, 3705 - 3711.

Antoniou J, Mwale F, Demers CN, Beudoin G, Goswami T (2006) Quantitative magnetic resonance imaging of enzymatically induced degradation of the nucleus pulposus of intervertebral discs. *Spine* **31**, 1547-1554.

Ashworth JL, Murphy G, Rock MJ, Sherratt MJ, Shapiro SD, Shuttleworth CA, Kielty CM (1999) Fibrillin degradation by matrix metalloproteinases: implication for connective tissue remodelling. *Biochemical Journal* **340**, 171-81.

Batmanov YE (1968) Structure of the eye drainage system in man. *Vestn. Oftalmol.* **4**, 27-31.

Bidanset DH, Guidry C, Rosenberg LC, Choi HU, Timpl R, Hook M (1992) Binding of proteoglycan decorin to collagen type VI. *The Journal of Biological Chemistry* **267**, 5250-5256.

Bill A (1965) Movement of albumin and dextran through the sclera. *Archives of Ophthalmology* **74**, 248-252.

Bill A (1967) Effects of atrophine and pilcaprine on aqueous humor dynamics in cynamologus monkeys (macacarrus). *Optical Eye Research* **6**, 120 - 125.

Bill A, Svedbergh B (1972) Scanning electron microscopic studies of the trabecular meshwork and the canal of schlemm-an attempt to localize the main resistance to outflow of aqueous humor in man. *Acta Ophthalmology* **50**, 295-320.

Blackmore C, Jennett S (2001) 'The Oxford Companion to the Body.' (Oxford University Press)

Blain EJ, Gilbert SJ, Wardale RJ, Capper SJ, Mason DJ, Duance VC (2001) Up-regulation of matrix metalloproteinase expression and activation following cyclical compressive loading of articular cartilage in vitro. *Archives of Biochemistry and Biophysics* **396**, 49-55.

Bourlais C, Acar L, Zia H, P.A. S, Needham T, Leverge R (1998) Ophthalmic drug delivery systems - recent advances. *Progress in Retinal and Eye Research* **17**, 33-58.

Bris (2003) Reverse zymography. In.

Bron AJ, Tripathi RC, Tripathi BJ (2001) 'Wolff's anatomy of the eye and orbit.' (Arnold Publishers)

Brubaker RF (1982) The flow of aqueous humor in the human eye. *Trans American Ophthalmology Society* **LXXX**, 391-474.

Brubaker RF (1991) Flow of aqueous humor in humans. *Investigative Ophthalmology & Visual Science* **13**, 3145-3166.

Cantor LB (2002) An update on bimatoprost in glaucoma therapy. *Expert Opinion on Pharmacotherapy* **3**, 1753-1762.

Carlson EC, Liu CY, Chikama T, Hayashi Y, Kao CWC, Birk DE, Funderburgh JL, Jester JV, Kao WWY (2005) Keratocan, a cornea-specific karatan sulfate proteoglycan, is regulated by Lumican. *The Journal of Biological Chemistry* **280**, 25541-25547.

Caterson B, Flannery CR, Hughes CE, Little CB (2000) Mechanism involved in cartilage protoeglycan catabolism. *Matrix Biology* **19**, 333-344.

Coleman RA, Smith WL, Narumiya S (1994) VIII. International union of pharmacology classification of prostanoid receptors: properties, distribution, and structure of the receptors and their subtypes. *Pharmacological Reviews* **46**, 209-224.

Crawford K, Kaufman PL (1987) Pilocarpine antagonizes prostaglandin F2α-induced ocular hypotension in monkeys. Evidence for enhancement of uveoscleral by prostaglandin F2α. *Archives of Ophthalmology* **105** , 1112-1116.

Crowston JG, Aihara M, Lindsey JD, Weinreb RN (2004) Effect of latanoprost on outflow facility in the mouse. *Investigative Ophthalmology & Visual Science* **45**, 2240-2245.

Crowston JG, Lindsey JD, Aihara M, Weinreb RN (2004a) Effect of latanoprost on intraocular pressure in mice lacking the prostaglandin FP receptor. *Investigative Ophthalmology & Visual Science* **45**, 3555-9.

Crowston JG, Lindsey JD, Aihara M, Weinreb RN (2004b) Effect of latanoprost on intraocular pressure in mice lacking the prostaglandin FP receptor. *Investigative Ophthalmology & Visual Science* **45**, 3555-3559.

Crowston JG, Lindsey JD, Morris CA, Wheeler L, Medeiros FA, Weinreb RN (2005) Effect of bimatoprost on intraocular pressure in prostaglandin FP receptor knockout mice. *Investigative Ophthalmology & Visual Science* **46**, 4571-7.

Cullinane AB, Leung PS, Ortego J, Coca-Prados MS, Harvey BJ (2002) Renin angiotensin system expression and secretory function in cultured human ciliary body non-pigmented epithelium. *British Journal of Ophthalmology* **86**, 676 - 683.

Do CW, Kong CW, Chan CY, Lam C, To CH (2006) Aqueous humor formation and its regulation by nitic oxide: A Mini Review. *Neuroembryology and Aging* **07**, 8-12.

Doege KJ, Sasaki M, Kimura T, Yamada Y (1991) Complete coding sequence and deduced primary sequence of the human certilage large aggregating proteoglycan aggrecan. *Journal of Biological Chemistry* **266**, 894-902.

Drake MV (1996) New medical therapy for glaucoma. *New Drugs in Ophthalmology* **36**, 53 - 60.

Dudhia J (2005) Aggreca, ageing and assembly in articular cartilage. *Cellular and molecular life science* **62**, 2241-2256.

Duirgova M, Roughley PJ, Mort JS (2007) Mechanism of proteoglycanaggregate degradation in cartilage stimulated with oncostatin M. *Osteoarthritis and Cartilage* **Article in press**, 1-7.

Dunlevy JR, Rada JAS (2004) Interaction of lumican with aggrecan in the ageing human sclera. *Investigative Ophthalmology & Visual Science* **45**, 3849-3856.

Durham DG, Dickinson JC, Hamilton PB (1971) Ion exchange chromatography of free amino acids in human intraocular fluids. *Clinical Chemistry* **17**, 285-289.

Dvorak-Theobald G (1934) Schlemm's canal: its anastomoses and anatomic relations. *Trans American Ophthalmology Society* **32**, 574-585.

Eid TM, Spaeth GT (2000) 'The glaucomas concepts and fundamentals.' (Lippincott Williams and Wilkins)

El-Asrar AMA, Struyf S, Descamps FJ, Al-Obeidan SA, Proost P, Damme JV, Opdenakker G, Geboes K (2004) Chemokines and gelatinases in aqueous humor of patients with active uveitis. *American Journal of Ophthalmology* **138**, 401-411.

Ferreira SM, Lerner SF, Brunzini R, Evelson PA, Llesuy SF (2004) Oxidative stress markers in aqueous humor of glaucoma patients. *American Journal of Ophthalmology* **137**, 62-69.

Fisher LW, Termine JD, Young MF (1989) Deduced protein sequence of bone small proteoglycan I (biglycan) shows homology with proteoglycan II (decorin) and several nonconnective tissue proteins in a variety of species. *Journal of Biological Chemistry* **264**, 4571-4576.

Fleenor DL, Pang IH, Clark AF (2003) Involvement of AP-1 in interleukin-1a-stimulated MMP3 expression in human trabecular meshwork cells. *Investigative Ophthalmology & Visual Science* **44**, 3494 - 3501.

Forrester J, Dick A, McMenamin P, Lee W (1999) 'The eye: Basic science in practice.' (Harcourt Brace & Company Ltd.)

Fossang AJ, Last K, Maciewicz RA (1996) Aggrecan is degraded by matrix metalloproteinase in human artheritis. *Journal of Clinical Investigation* **98**, 2292 - 2299.

Foster CS (1994) 'The sclera.' (Springer-Verlag)

Gabelt BT, Kaufman PL (1989) Prostaglandin F2 alpha increases uveoscleral outflow in the cynomolgus monkey. *Experimental Eye Research* **49**, 389-402.

Gabelt BT, Kaufman PL (2005) Changes in aqueous humor dynamics with age and glaucoma. *Retinal and Eye Research* **24**, 612-637.

Gaton DD, Sagara T, Lindsey JD, Gabelt BT, Kaufman PL, Weinreb RN (2001) Increased MMP 1, 2, 3 in Monkey uveoscleral outflow pathway after

topical prostaglandin F(2 alpha) - isopropyl ester treatment. *Archives of Ophthalmology* **119**, 1165 - 1170.

Geng Y, McQuillan D, Roughley PJ (2006) SLRP interaction can protect collagen fibrils from cleavage by collagenase. *Matrix Biology* **25**, 484-491.

Geroski DH, Edelhauser HF (2000) Drug delivery for posterior segment eye disease. *Investigative Ophthalmology & Visual Science* **41**, 961.

Girolamo ND, Lloyd A, McCluskey P, Filipic M, Wakefield D (1997) Increased expression of matrix metalloproteinase in vivo in scleritis tissue and in vitro in cultured human scleral fibroblasts. *American Journal of Pathology* **150**, 653-666.

Goh KL, Hiller J, Haston JL, Holmes DF, Kadler KE, Murdoch A, Meakin JR, Wess TJ (2005) Analysis of collagen fibril diameter distribution in connective tissues using small-angle X-ray scattering. *Biochemica et Biophysica Acta* **1722**, 182-188.

Goodfellow JM, Elliott GF, Woolgar AE (1978) X-ray diffraction studies of the corneal stroma. *Journal of Molecular Biology* **119**, 237-252.

Green K, Pederson JE (1972) Contribution of secretion and filtration to aqueous humor formation. *American Journal of Physiology* **222**, 1218-1226.

Grierson I, Howes RC, Wang Q (1984) Age-related changes in the canal of schlemm. *Experimental Eye Research* **39**, 505-512.

Grossmann JG (2002) "Shape determination of biopmolecules in solution from synchatron X-ray scaterring." (Academic Press)

Growston JG, Lindsey JD, Aihara M, Weinreb RN (2004) Effect of latanoprost on intraocular pressure in mice lacking the prostaglandin FP receptor. *Investigative Ophthalmology & Visual Science* **45**, 3555-3559.

Grzesik WJ, Frazier CR, Shapiro JR, Sponseller PD, Robey PG, Fedarko NS (2002) Age-related changes in human bone proteoglycan structure *Journal of Biological Chemistry* **277**, 43638-43647.

Gunja-smith Z, Nagase H, Woessner F (1989) Purification of neutral proteoglycan degrading metalloproteinase from human articular cartilage tissue and its identification as stromelysin matrix metalloproteinase-3. *Biochemical Journal* **258**, 115 - 119.

Hadri KE, Moldes M, Mercier N, Andreani M, Pairault J, Feve B (2002) Semicarbazide-sensitive amine oxidase in vascular smooth muscle cells. *Arteriosclerosis, Thrombosis, and Vascular Biology* **22**, 89 - 94.

Hamati HF, Britton EL, Carey DJ (1989) Inhibition of proteoglycan synthesis alters extracellular matrix deposition, proliferation, and cytoskeletal

organization of rat aortic smooth muscle cells in culture. *Journal of Cell Biology* **108**, 2495-505.

Han YP, Tuan TL, Wu H, Hughes M, Garner WL (2000) TNF-α stimulates activation of pro-MMP2 in human skin through NF- KB mediated induction of MT1-MMP. *Journal of Cell Science.*

Harvey WJF (1997) 'Glaucoma: Glaucoma module parts 1-12: Continuing professional development.' (M Hunter)

Hayasaka S, Yamada T, Nitta K, Kaji Y, Hiraki S, Tachinami K, Matsumoto M, Yamamoto S, Yamamoto S (1997) Ascorbic acid and amino acid values in the aqueous humor of a patient with Lowe's syndrome. *Graefes Archive for Clinical Experimental Ophthalmology* **235**, 217-221.

Hejkal TW, Camras CB (1999) Prostaglandin analogs in the treatment of glaucoma. *Semin Ophthalmology* **14**, 114-123.

Hepsen IF, Ozkaya E (2007) 24-h IOP control with latanoprost, travoprost and bimatoprost in subjects with exfoliation syndrome and ocular hypertension. *Eye* **21**, 453-458.

Hodge AJ (1989) Molecular models illustrating the possible distributions of 'holes' in simple systematically staggered arrays of type I collagen molecules in native-type fibrils. *Connective Tissue Research* **21**, 137-47.

Honjo M, Inatani M, Kido N, Sawamura T, Yue BJT, Honda Y, Tanihara H (2002) A myosin light chain kinase inhibitor, ML-9, lowers the IOP in rabbit eyes. *Experimental Eye Research* **75**, 135 - 142.

Hosseini M, Rose AY, Song K, Bohan C, Alexander JP, Kelley MJ, Acott TS (2006) IL-1 and TNF induction of matrix metalloproteinase-3 by c-Jun N-terminal kinase in trabecular meshwork. *Investigative Ophthalmology & Visual Science* **47**, 1469-76.

Huang SN, Adamis AP, Weiderschain DG, Shima DT, Shing Y, Mooses MA (1996) MMP and their inhibitors in aqueous humor. *Experimental Eye Research* **62**, 481 - 490.

Husain S, Jafri F, Crosson CE (2005) Acute effects of PGF2α on MMP-2 secretion from human ciliary muscle cells: A PKC- and ERK-Dependent process. *Investigative Ophthalmology & Visual Science* **46**, 1706-1713.

Husain S, Kaddour-Diebbar I, Abdel-Latif AA (2002) Alterations in arachidonic acid release and phospholipase C-B1 expression in glaucomatous human ciliary muscle cells. *Investigative Ophthalmology & Visual Science* **43**, 1127 - 1134.

Igwe SA, Afonne JC, Ghasi SI (2003) Ocular dynamics of systemic aqueous extracts of Xylopia Aethiopica (African guinea pepper) Seeds on Visually Active Volunteers. *Journal of Ethnopharmacology* **86**, 139 - 142.

Igwe SA, Akunyili DN, Ogbogu C (2003) Effects of Solanum Melongena (garden egg) on some visual functions of visually active Igbos of Nigeria. *Journal of Ethnopharmacology* **86**, 135 - 138.

Ihanamaki T, Salminen H, Saamanen AM, Pelliniemi LJ, Hartmann DJ, Sandberg-lall M, Vuorio E (2001) Age-dependent changes in the expression of matrix components in the mouse eye. *Experimental Eye Research* **72**, 423-431.

Ito T, Ohguro H, Mamiya K, Ohguro I, Nakazawa M (2006) Effects of antiglaucoma drops on MMP and TIMP balance in conjunctival and subconjunctival tissue. *Investigative Ophthalmology & Visual Science* **47**, 823-30.

Jacob TJC, Civan MM (1996) Role of ion channels in aqueous humor formation. *American Journal of Physiology* **40**, C703-C720.

Jahn CE, Leiss O, Von-Bergmann K (1983) Lipid composition of human aqueous humor. *Opthalmic Research* **15**, 220-224.

Jiang J, Geroski DH, Edelhauser HF, Prausnitz MR (2006) Measurement and prediction of lateral diffusion within human sclera. *Investigative Ophthalmology & Visual Science* **47**, 3011-3016.

Johnson JM, Young TL, Rada JAS (2006) Small leucine rich repeat proteoglycans (SLRPs) in the human sclera: Identification of abundant levels of PRELP. *Molecular Vision* **12**, 1057-66.

Johnson M (2006) What controls aqueous humour outflow resistance? *Experimental Eye Research* **82**, 545-557.

Johnson MC, Kamm RD (1983) The role of Schlemm's canal in aqueous outflow from the human eye. *Investigative Ophthalmology & Visual Science* **24**, 320-325.

Johnstone B, Markopoulos M, Neame P, Caterson B (1993) Identification and characterization of glycanated and non-glycanated forms of biglycan and decorin in the human invertebral disc. *Biochemical Journal* **292**, 661-666.

Kanski JJ, McAllister JA, Salmon JF (1996) 'Glaucoma a colour manual of diagnosis and treatment.' (Butterworth-Heinemann)

Kaufman PL (1986) Effects of intracamerally infused prostaglandins on outflow facility in cynomolgus monkey eyes with intact or retrodisplaced ciliary muscle. *Experimental Eye Research* **43**, 819-827.

Kee FW, Seo K (1997) The effect of interleukin-1alpha on the outflow facility in rat eye. *Journal of Glaucoma* **6**, 246-249.

Keeley FW, Morin JD, Vesely S (1984) Characterization of collagen from normal human sclera. *Experimental Eye Research* **39**, 533-542.

Kiel JW, Reitsamer HA, Walker IS (2001) Effects of nitric oxide synthase inhibition on ciliary blood flow, aqueous production & IOP. *Experimental Eye Research* **73**, 355 - 364.

Kim HS, Shang T, Chen Z, Pflugfelder SC, Li DQ (2004) TGFβ1 stimulates production of gelatinase (MMP-9), collagenases (MMP-1, -13) and stromelysins (MMP-3, -10, -11) by human corneal epithelial cells. *Experimental Eye Research* **79**, 263-274.

Kim JW, Lindsey JD, Wang N, Weinreb RN (2001) Increased human scleral permeability with prostaglandin exposure. *Investigative Ophthalmology & Visual Science* **42**, 1514 - 1521.

Kimura H, Yasukawa T, Tabata Y, Ogura Y (2001) Drug targetting to chorodial neovascularization. *Advanced Drug Delivery Reviews* **52**, 79-91.

Kimura S, Kabayashi M, Nakamura M, Hirano K, Awaya S, Hoshino T (1995) Immunoelectron microsopic localization of decorin in aged human corneal and scleral stroma. *Journal of Electron Microscopy* **44**, 445-449.

Kleiner DE, Stetler-Stevensen WG (1994) Quantitative zymography: Detection of Picogram quantities of gelatinases. *Analytical Biochemistry* **218**, 325 - 329.

Komoto J, Yamada T, Watanabe K, Woodward DF, Takusagawa F (2006) Prostaglandin F2alpha formation from prostaglandin H2 by prostaglandin F synthase (PGFS): crystal structure of PGFS containing bimatoprost. *Biochemistry* **45**, 1987-1996.

Kong TCH, Chan CW, Shahidullah M, Do CW (2002) The mechanism of aqueous humour formation. *Clinical Experimental Optometry* **85**, 335-349.

Koskela TK, Reiss GR, Brubaker RF, Ellefson RD (1989) Is the high concentration of ascorbic acid in the eye an adaptation to intense solar irradiation? *Investigative Ophthalmology & Visual Science* **30**, 2265-2267.

Kouri T, Gyory A, Rowan RM (2003) ISLH recommended reference procedure for the enumeration of particles in urine. *Laboratory Hematology* **9**, 58-63.

Krohn J (2004) Morphology and clinical aspects of the aqueous humour drainage routes with special emphasis on uveoscleral outflow. *Acta Opthalmologica Scandinavica*, 483-484.

Kubata Y, Oka S, Nakagawa S, Shirasuna K (2001) Interleukin-1α enhances Type I collagen-induced activation of Matrix Metalloproteinase-2 in odentogenic keratocyst fibroblats. *Journal of Dental Research* **81**, 23-27.

Lachmann SM, Hazleman BL, Watson PG (1978) Scleritis and associated disease. *British Medical Journal* **1**, 88-90.

Lan J, Kumar RK, Girolamo ND, Mcklusskey P, Wakefield D (2003) Expression and distribution of MMP and their inhibitors in the iris and ciliary body. *British Journal of Ophthalmology* **87**, 208 - 211.

Lark MV, Bayne EK, *et al.* (1997) Aggrecan degradation in human cartilage. *Journal of Clincal Investigation* **100**, 93-106.

Lark MV, William H, *et al.* (1995) Quantification of a matrix metalloproteinase-generated aggrecan G1 fragment using momospecific anti-peptide serum. *Biochemical Journal* **307**, 245-252.

Lauer-Fields JL, Sritharan T, Stack MS, Nagase H, Fields GB (2003) Selective hydrolysis of triple helical substrates by MMP 2 & 9. *Journal of Biological Chemistry* **278**, 18140 - 18145.

Lawrence DA (1996) Transforming growth factor-beta: a general review. *European Cytokine Network* **7**, 363-374.

Lawrence JG (1997) 'Glaucoma: Glaucoma module parts 1-12: continuing professional development.' (M Hunter)

LeBaron RG, Athanasiou KA (2000) Extracellular matrix cell adhesion peptides: Functional applications in orthopedic materials. *Tissue Engineering* **6**, 85-103.

Lee PY, Podos SM, Severin C (1984) Effect of prostaglandin F2α on aqueous humor dynamics of rabbit, cat and monkey. *Investigative Ophthalmology & Visual Science* **25**, 1087-1093.

Li QD, Shang TY, Kim HS, Solomon A, Lokeshwar BL, Pflugfelder SC (2003) Regulated expression of collagenases MMP-1, -8, and -13 and stromelysins MMP-3, -10, -11 by human corneal epithelial cells. *Investigative Ophthalmology & Visual Science* **44**, 2928-2936.

Linden C, Alm A (1999) Prostaglandin analogues in the treatment of glaucoma. *Drugs Aging* **14**, 387-398.

Lindsey JD, Crowston JG, Tran A, Morris C, Weinreb RN (2007) Direct matrix metalloproteinase enhancement of transscleral permeability. *Investigative Ophthalmology & Visual Science* **48**, 752-755.

Lindsey JD, Gaton DD, Sagara T, Polansky JR, Kaufman PL, Weinreb RN (2001) Reduced TIGR/ Myocilin protein in the monkey ciliary muscle after

topical prostaglandin F2α treatment. *Investigative Ophthalmology & Visual Science* **42**, 1781-1786.

Lindsey JD, Kashiwagi K, Kashiwagi F, Weinreb RN (1997) Prostaglandins action on ciliary smooth muscle extracellular matrix metabolism: Implications for uveoscleral outflow. *Survey of Ophthalmology* **47**, S53 - S59.

Lindsey JD, To HD, Weinreb RN (1994) Induction of c-Fos by prostaglandins F2alpha in the human ciliary smooth muscle cells. *Investigative Ophthalmology & Visual Science* **35**, 242 - 250.

Lindsey JD, Weinreb RN (2002) Identification of mouse uveoscleral outflow pathway using flourscent dextran. *Investigative Ophthalmology & Visual Science* **43**, 2201 - 2205.

Little CB, Flannery CR, Hughes CE, Mort JS, Roughley PJ, Dent C, Caterson B (1999) Aggrecanase versus matrix metalliproteinases in the catabolism of the interglobular domain of aggrecan in vitro. *Biochemical Journal* **344**, 61-68.

Litwak AB (2001) 'Glaucoma Handbook.' (Butterworth-Heinemann)

Lutjen-Drecoll E, Tamm E (1988) Morphological study of the anterior segment of cynomolgus monkey eyes following treatment with Prostaglandin F2 alpha. *Experimental Eye Research* **47**, 761-769.

Maitre CLL, Pockert A, Buttle DJ, Freemont AJ, Hoyland JA (2007) Matrix synthesis and degradation in human intervertebral disc degeneration. *Biochemical Society Transactions* **35**, 652-655.

Malfait AM, Liu RQ, Ijiri K, Komiya S, Tortorella D (2002) Inhibition of ADAM-TS4 and ADAM-TS5 prevents aggrecan degradation in Osteoarthritic cartilage. *The Journal of Biological Chemistry* **277**, 22201-22208.

Mandler RN, Dencoff JD, Midani F, Ford CC, Ahmed W, Rosenberg GA (2001) Matrix metalloproteinases and tissue inhibitors of metalloproteinases in cerebrospinal fluid differ in multiple sclerosis and Devic's neuromyelitis optica. *Brain* **124**, 493-498.

Maxwell CA, Bell N, Kennedy CJ, Wess TJ (2006) X-ray diffraction and FT-IR study of Caprine and Ovine hide. *The Paper Conservatory* **29**, 55-62.

Maxwell CA, Smiechowski K, Zarlok J, Sionkowska A, Wess TJ (2005) X-ray studies of a collagen material for leather production treated with chromium salt. *Journal of American Leather Chemist' Association* **100**, 9-17.

Maxwell CA, Wess TJ, Kennedy CJ (2006) X-ray study into the effects of liming on the structure of collagen. *Biomacromolecules* **7**, 2321-2326.

McEwan PA, Scott PG, Bishop PN, Bella J (2006) Structural correlations in the family of small leucine-rich repeat proteins and proteoglycans. *Journal of Structural Biology* **155**, 294-305.

Meek KM, Fullwood NJ, Cooke PH, Elliott GF, Maurice DM, Quantock AJ, Wall RS, Worthington CR (1991) Synchroton x-ray diffraction studies of the cornea, with implications for stromal hydration. *Biophysics Journal* **60**, 467-474.

Minond D, Lauer=Fields JL, Nagase H, Fields GB (2004) Matrix metalloproteinase triple-helical peptidase activities are differentially regulated by substrate stability. *Biochemistry* **43**, 11474-11481.

Moorthy RS, Mermoud A, Baerveldt G, Minckler DS, Lee PP, Roa NA (1997) Glaucoma associated with uveitis. *Survey of Ophthalmology* **41**, 361 - 385.

Moses RA, Grodzki WJ, Starcher BC, Galione MJ (1978) Elastin content of scleral spur, trabecular mesh, and sclera. *Investigative Ophthalmology & Visual Science* **17**, 817-818.

Muir H (1982) Proteoglycans as organizers of the intrecellular matrix. *Biochemical Society Transactions Seventeenth CIBA Medical Lectures* **11**, 613-622.

Mukhopadhyay P, Geoghegan TE, Patil RV, Bhattacherjee P, Peterson CA (1997) Detection of EP2, EP4, and FP receptors in human ciliary epithelial and ciliary muscle cells. *Biochemical Pharmacology* **53**, 1249-1255.

Murphy GJP, Murphy G, Reynolds JJ (1991) The origins of matrix metalloproteinases and their familial relationships. *FEBS* **289**, 4-7.

Myles ME, Neumann DM, Hill JM (2005) Recent progress in ocular drug delivery for posterior segment disease: emphasis on transcleral iontophoresis *Advanced Drug Delivery Reviews* **52**, 2063-2079.

Naka MH, Morita Y, Ikeuchi K (2005) Influence of proteoglycan contents and of tissue hydration on the frictional characteristics of articular cartilage. *Journal of Engineering in Medicine* **H3**, 175-182.

Nelson AR, Fingleton B, Rothenberg ML, Matrisian LM (2000) Matrix metalloproteinase: Biological activity and clinical implications. *Journal of Clinical Oncology* **18**, 1135 - 1163.

Nesterov AP (1970) Role of bloackade of Schlemm's canal in pathogenesis of primary open angle glaucoma. *American Journal of Ophthalmology* **70**, 691-6965.

Nilsson SF (1997) The uveoscleral outflow routes. *Eye* **11**, 149 - 154.

Obrink B (1973) A study of the interactions between monomeric tropocollagen and glycosaminoglycan. *European Journal of biochemistry* **33**, 387-400.

Ockland A (1998) Effect of latanoprost on extracellular matrix of the ciliary muscle - A study on cultured cells and tissue sections. *Experimental Eye Research* **67**, 179 - 191.

Oh DJ, Martin JL, Williams AJ, Peck RE, Pokorny C, Russell P, Birk DE, Rhee DJ (2006a) Analysis of expression of matrix metalloproteinases and tissue inhibitors of metalloproteinases in human ciliary body after latanoprost. *Investigative Ophthalmology & Visual Science* **47**, 953-63.

Oh DJ, Martin JL, Williams AJ, Russell P, Birk DE, Rhee DJ (2006b) Effect of latanoprost on the expression of matrix metalloproteinase and their inhibitors in human trabecular meshwork cells. *Investigative Ophthalmology & Visual Science* **47**, 3887-3895.

Okhravi N, Odufuwa B, McCluskey P, Lightman S (2005) Scleritis. *Survey of Ophthalmology* **50**, 351-363.

Old LJ (1985) Tumor necrosis factor (TNF). *Science* **230**, 630-632.

Olejnik O, Hughes P (2005) Drug delivery strategies to treat age-related macular degeneration. *Advanced Drug Delivery Reviews* **57**, 1991-1993.

Olendoff D, Jeryan C, Boyden K (1999) 'The Gale Encylopedia of Medicine.' (Gale Research)

Oliver GW, Leferson JD, Stetler-Stevensen WG, Kleiner DE (1997) Quantitative reverse zymography: Analysis of Picogram amounts of metalloproteinase inhibitors using gelatinase A and B reverse zymograms. *Analytical Biochemistry* **244**, 161 - 166.

Pang IH, Hellberg PE, Fleenor DL, Jacobson N, Clark AF (2003) Expression of matrix metalloproteinase and their inhibitors in human trabecular meshwork cells. *Investigative Ophthalmology & Visual Science* **44**, 348503493.

Patil S, Reshetnikov S, Halder MK, Seal S, Mallik S (2007) Surface-derivatized manoceria with human carbonic anhydrase II inhibitors and fluorophores: A potential durg delivery device. *Journal of Physical Chemistry* **111**, 8437-8442.

Pederson JE, Toris CB (1987) Uveoscleral outflow: diffusion or flow? *Investigative Ophthalmology & Visual Science* **28**, 1022-4.

Peterson JT (2004) Matrix metalloproteinase inhibitors development and the remodelling of drug discovery. *Heart Failure Reviews* **9**, 63-79.

Pitkanen L, Ranta VP, Moilanen A, Urtti A (2005) Permeability of retinal pigment epithelium: effect of permeant molecular weight and lipophilicity. *Investigative Ophthalmology & Visual Science* **46**, 641-646.

Pitkanen L, Ruponen M, Nieminen J, Urtti A (2003) Vitreous is a barrier in non-viral gene transfer by cationic lipids and polymers. *Pharmacological Research* **20**, 576-583.

Price RI, Lees S, Kirschner DA (1997) X-ray diffraction analysis of tendon collagen at ambient and cryogenic temperatures: role of hydration. *International Journal of Biological Macromolecules* **20**, 23-33.

Quantock AJ, Meek KM (1988) Axial electron density of human scleral collagen. *Biophysics Journal* **54**, 159-164.

Quantock AJ, Meek KM, Chakravarti S (2001) An x-ray diffraction investigation of corneal strcuture in Lumican-deficient mice. *Investigative Ophthalmology & Visual Science* **42**, 1750-1756.

Quigley HA (1996) Number of people with glaucoma worlwide. *British Journal of Ophthalmology* **80**, 389-93.

Rada JA, Achen VR, Penugonda S, Schmidt RW, Mount BA (2000) Proteoglycan composition in the human sclera during growth and aging. *Investigative Ophthalmology & Visual Science* **41**, 1639-1648.

Rada JA, Johnson JM, Achen VR, Rada KG (2002) Inhibition of scleral proteoglycan synthesis blocks deprivation-induced axial elongation in chicks. *Experimental Eye Research* **74**, 205-215.

Rada JAS, Achen VR, Perry CA, Fox PW (1997) Proteoglycans in the human sclera: Evidence for the prescence of aggrecan. *Investigative Ophthalmology & Visual Science* **38**, 1740-1751

Rada JAS, Shelton S, Norton TT (2006) The sclera and myopia. *Experimental Eye Research* **82**, 185-200.

Ranta VP, Urtti A (2006) Transcleral drug delivery to the posterior eye: prospects of pharmacokinetic modeling. *Advanced Drug Delivery Reviews* **58**, 1164-1181.

Richter M, Krauss AHP, Woodward DF, Lutjen-Drecoll E (2003) Morphological changes in the anterior eye segment after long-term treatment with different receptor selective prostaglandin agomists and a prostamide. *Investigative Ophthalmology & Visual Science* **44**, 4419-4426.

Rittig W, Lutjen-Drecoll E, Rauterberg J, Jander R, Mollenhauer J (1990) Type VI collagen in human iris and ciliary body. *Cell & Tissue Research* **259**, 305 - 312.

Roepke RR, Hetherington WA (1940) Osmotic relation between aqueous humor and blood plasma. 340-345.

Rohen JW, Futa R, Lutjen-Drecoll E (1981) The fine structure of the cribriform meshwork in normal and glaucomatous eyes as seen in tangentail sections. *Investigative Ophthalmology & Visual Science* **21**, 574-585.

Roughley PJ, White RJ, Magny MC, Liu J, Pearce H, Mort JS (1993) Non-proteoglycan forms of biglycan increase with age in human articular cartilage. *Biochemical Journal* **295**, 421-426.

Sagara T, Gaton DD, Lindsey JD, Gabelt BT, Kaufman PL, Weinreb RN (1999) Topical prostaglandin F2alpha treatment reduces collagen type I, III and IV in the monkey uveoscleral outflow pathway. *Archives of Ophthalmology* **117**, 794 - 801.

Sampaolesi R, Argento C (1977) Scanning electron microscopy of the trabecular meshwork in normal and glaucomatous eyes. *Investigative Ophthalmology & Visual Science* **16**, 302-314.

Samples JR, Alexander JP, Acott TS (1993) Regulation of the levels of human trabecular matrix metalloproteinases and inhibitor by interleukin-1 and dexamethasone. *Investigative Ophthalmology & Visual Science* **34** , 3386-3395.

Schachtschabel U, Lindsey JD, Weinreb RN (2000) The mechanism of action of prostaglandins on uveoscleral outflow. *Current Opinion Ophthalmology* **11**, 112-115.

Schlotzer-Schrehardt U, Lommatzch J, Kuche M, Konstas AGP, Naumann GOH (2003) Matrix metalloproteinases and their inhibtors in aqueous humor of patients with pseudoexfoliation syndrome/ glaucoma and primary open angle glaucoma. *Investigative Ophthalmology & Visual Science* **44**, 1117-1125.

Schlotzer-Schrehardt U, Zenkel M, Nusing RM (2002) Expression and Localization of FP and EP Prostanoid Receptor subtypes in human ocular tissues. *Investigative Ophthalmology & Visual Science* **43**, 1475-1487.

Scott JE (1988) Proteoglycan-fibrillar collagen interactions. *Biochemical Journal* **252**, 313-323.

Sharif NA, Kelly JY, Crider GW, Williams GW, Xu SX (2003) Ocular hypotensive FP Prostaglandin (PG) analogs: PG receptor subtype binding affinities and selectivities, and agonist potencies at FP and other PG receptor in cultured cells. *Journal of Ocular Pharmacology and Therapeutics* **19**, 501-512.

Singer CF, Marbaix E, Lemoine P, Courtoy PJ, Eeckhout Y (1999) Local cytokines induce differential expression of matrix metalloproteinases but not

their tissue inhibitors in human endometrial fibroblats. *European Journal of Biochemistry* **259**, 40-45.

Srinivasan Y, Lovicu FJ, Overbeek PA (1998) Lens-specific expression and transforming growth factor β1 in transgenic mice causes anterior subcapsular cataracts. *The American Society of Clinical Investigation* **101**, 625-634.

Su YK, Elam JS (2003) Proteoglycan regulation of goldfish retinal explant growth on optic tectal membranes. *Developmental Brain Research* **142**, 169-175.

Suguro K, Toris CB, Pederson JE (1985) Uveoscleral outflow following cyclodialysis in the monkey eye using a fluorescent tracer. *Investigative Ophthalmology & Visual Science* **26**, 810-3.

Svoboda KKH, Gong H, Trinkaus-Randall V (1998) Collagen expression and orientation in ocular tissue. *Prog. Polym. Sci.* **23**, 329-374.

Sztrolovics R, White RJ, Poole AR, Mort JS, Roughley PJ (1999) Resistance of small leucine-rich repeat proteoglycan to proteolytic degradation during interleukin-1 stimulated cartilage catabolism. *Biochemical Journal* **339**, 571-577.

Takino T, Sato H, Shinagawa A, Seiki M (1995) Identification of the second membrane-type matrix metalloproteinase (MT-MMP2) gene from human placenta cDNA library. *The Journal of Biological Chemistry* **270**, 23013-23020.

Tamm E, Baur A, Lutjen-Drecoll E (1992) Synthesis of extracellular matrix components by human ciliary muscle cells in culture. *Current Eye Research* **11**, 333 - 341.

Thale A, Tillmann B (1993) The collagen architecture of the sclera - SEM and immunohistochenical studies. *Annals of Anatomy* **175**, 215-220.

Thale A, Tillmann B, Rochels R (1996) Scanning electron-microscopic studies of collagen architecture of the human sclera - normal and pathological findings. *Ophthalmologica* **210**, 137-141.

Toris CB, Alm A, Camras CB (2002) Latanoprost and cholinergic agonists in combination. *Survey of Ophthalmology* **47**, S141 - S147.

Toris CB, Camras CB, Yablonski ME, Brubaker RF (1997) Effects of exogenous prostaglandins on aqueous humor dynamics and blood aqueous barrier functions. *Survey of Ophthalmology* **41**, S69 - S75.

Toris CB, Gregerson DS, Pederson JE (1987a) Uveoscleral outflow using different-sized fluorescent tracers in normal and inflamed eyes. *Experimental Eye Research* **45**, 525-32.

Toris CB, Gregerson DS, Pederson JE (1987b) Uveoscleral outflow using different-sized fluorescent tracers in normal and inflamed eyes. *Experimental Eye Research* **45**, 525-32.

Toris CB, Pederson JE (1985) Effect of intraocular pressure on uveoscleral outflow following cyclodialysis in the monkey eye. *Investigative Ophthalmology & Visual Science* **26**, 1745-1749.

Tortorella MD, Burn TC, *et al.* (1999) Purification and cloning pf aggrcanase-1: A member of the ADAMTS family of proteins. *Science* **284**, 1664-1666.

Tripathi RC (1968) Ultrastructure of schlemm's canal in relation to aqueous outflow. *Experimental Eye Research* **7**, 335-341.

Tripathi RC (1974a) 'Comparative physiology and anatomy of the aqueous outflow pathway.' (Academic Press: New York)

Tripathi RC (1974b) Tracing the bulk outflow route of cerebrospinal fluid by transmission and electron microscopy. *Brain Research* **80**, 503-506.

Tripathi RC, Millard CB, Tripathi BJ (1989) Protein composition of human aqueous humor: SDS-PAGE analysis of surgical and post-mortem samples. *Experimental Eye Research* **48**, 117-130.

Ueda J, Wentz-Hunter K, Yue BJT (2002) Distribution of myocilin and extracellular matrix components in the juxta-canalicular tissue of human eyes. *Investigative Ophthalmology & Visual Science* **43**, 1068 - 1076.

Umihara J, Lindsey JD, Weinreb RN (2002) Simultaneous expression of c-Jun and p53 in retinal ganglion cells of adult rat retinal slice cultures. *Current Eye Research* **24**, 147 - 159.

Urtti A (2006) Challenges and obstacles of ocular pharmacokinetics and drug delivery. *Advanced Drug Delivery Reviews* **58**, 1131-1135.

Urtti A, Pipkin JD, Rork GS, Sendo T, Finne U, Repta AJ (1990) Controlled drug delivery devices for experimental ocular studies with timolol. *International Journal of Pharmacology* **61**, 241-249.

Urtti A, Salminen L (1993) Minimizing systemic absorption of topically administered ophthalmic drugs. *Survey of Ophthalmology* **37**, 435-457.

Villumsen J, Alm A, Soderstrom M (1989) Prostaglandin F2α-isopropylester eye drop: effect on intraocular pressure in the open angle glaucoma. *British Journal of Ophthalmology* **73**, 975-979.

Wagner JA, Edwards A, Schuman JS (2004) Characterization of uveoscleral outflow in enucleated porcine eyes perfused under constant pressure. *Investigative Ophthalmology & Visual Science* **45**, 3203-3206.

Watson PG, Young RD (2004) Scleral structure, organisation and disease. A review. *Experimental Eye Research* **78**, 609-23.

Weinreb RN (2000) Uveoscleral outflow: The other outflow pathway. *Journal of Glaucoma* **9**, 343 - 345.

Weinreb RN (2001) Enhancement of scleral macromolecular permeability with prostaglandin. *Trans American Ophthalmology Society* **99**, 319-343.

Weinreb RN, Kashiwagi K, Kashiwagi F, Tsukahara S, Lindsey JD (1997) Prostaglandins increase matrix metalloproteinase release from human ciliary smooth muscle cells. *Investigative Ophthalmology & Visual Science* **38**, 2772 - 2780.

Weinreb RN, Kim DM, Lindsey JD (1992) Propagation of ciliary smooth muscle cells in vitro and effects of prostaglandins F2a on calcium efflux. *Investigative Ophthalmology & Visual Science* **33**, 26790-2686.

Weinreb RN, Lindsey JD (2002) Metalloproteinase gene transcription in human ciliary muscle cells with latanoprost. *Investigative Ophthalmology & Visual Science* **43**, 716 - 722.

Weinreb RN, Lindsey JD, Marchenko G, Marchenko N, Angert M, Strongin A (2004) Prostaglandin FP agonists alter metalloproteinase gene expression in sclera. *Investigative Ophthalmology & Visual Science* **45**, 4368-4377.

Weinreb RN, Toris CB, Gabelt BT, Lindsey JD, Kaufman PL (2002) Effects of Prostaglandins on the aqueous humor outflow pathway. *Survey of Ophthalmology* **47**, S53 - S64.

Werman A, Werman-Venkert R, R. W, Lee JK, Werman B, Krelin Y, E. V, Dinarello CA, Apte RN (2004) The precursor form of IL-1alpha is an intracrine proinflammatory activator of transcription. *Proceedings of the National Academy of Sciences U S A.* **101**, 2434-2439.

Wess TJ, Orgel JP (2000) Changes in collagen structure: drying, dehydrothermal treatment and relation to long term deterioration. *Thermochimica Acta* **365**, 119-128.

White SW, Hulmes DJS, Miller A (1977) Collagen-mineral axial relationship in calcified turkey leg tendon by X-ray and neutron diffraction. *Nature* **266**, 421-425.

Wick W, Platten M, Weller M (2001) Glioma cell invasion:regulation of metalloproteinase activity by TGF-beta. *Journal of Neurooncology* **53**, 177-185.

Wilkins M, Shah P, Khaw PT (1997) 'Glaucoma: Glaucoma module parts 1-12: Continuing professional development.' (M Hunter)

Wong TTL, Sethi C, Daniels JT, Limb GA, Murphy G, Khaw PT (2002) Matrix metalloproteinase in disease and repair process in the anterior chamber. *Survey of Ophthalmology* **47**, 239 - 251.

Young RD (1985) The ultrastructral organization of proteoglycan and collagen in human and rabbit scleral matrix. *Journal of Cell Science* **74**, 95-104.

Yuan L, Neufeld AH (2000) Tumor necrosis factor-α: A potentially neurodestructive cytokine produced by glia in the human glaucomatous optic nerve head. *GLIA* **32**, 42-50.

Zhan GL, Camras CB, Tang L, Ohia SE (1998) Effect of prostaglandins on cyclic AMP production in cultured human ciliary muscle cells. *Journal of Ocular Pharmacology and Therapeutics* **14**, 45 - 55.

Zhang B, Moses MA, Tsang PCW (2003) Temporal and spatial expression of tissue inhibitors of metalloproteinases 1 and 2 (TIMP-1 and -2) in the bovine corpus luteum. *Reproductive biology and endrocrinology* **1**, 1-11.

Zoukhri D, Macari E, Kublin CL (2007) A single injection of interleukin-1 induces reversible aqueous-tear deficiency, lacrimal gland inflammation, and aciner and ductal cell proliferation. *Experimental Eye Research* **84**, 894-904.

APPENDIX

8.0 APPENDIX

8.1 Chemicals & Manufacturers

Chemical	*Manufacturer*
α-actin (mouse monoclonal antihuman α-smooth muscle actin 1A4)	Sigma
Acetone	Sigma
Alexa Fluoro 488 donkey anti-mouse	Molecular Probes
Alexa Fluoro 488 donkey anti-rabbit	Molecular Probes
6-amino hexanoic acid	Sigma
Ammonium Persulphate	Sigma
Amphotericin B	Gibco
Anti-mouse IgG (H+L), AP antibody	Promega
Ascrobic acid	Sigma
BCA kit	Sigma
BCIP	Promega
Betadine	Setan Healthcare group
40% Bisacrylamide/ acrylamide	Sigma
Benzamide hydrochloride	Sigma
Bisbenzamide	Sigma
Bovine serum albumin (BSA)	Sigma
Bromphenol Blue	Sigma
Calcium chloride ($CaCl_2$)	Sigma
Casein	Sigma
Chloroform	BDH
Chodroitinase ABC	Sigma
Collagenase	Gibco
Coomassie brilliant blue	Sigma
Desmin (mouse monoclonal antihuman desmin D33)	Dako
DABCO	Sigma
Dimethyl methylene blue (DMMB)	Sigma
DMEM	Gibco
DMSO (Dimethyl sulfoxide)	Sigma

Donkey serum	Gibco-invitrogen
EDTA	BDH
Eosin	BDH
Ethanol	Sigma
Feotal calf serum	Bio-Sera
40% Formaldehyde	Sigma
98% Formic Acid	BDH
Gelatin	Sigma
Gelvacol	Fisher
Glacial Acetic Acid	Fisher
Glycerol	Sigma
Glycine	Sigma
Guanidine Hydrochloride	Sigma
Haematoxylin	BDH
Ham's F10	Gibco
Ham's F12	Gibco
HBSS	Gibco
Hydrochloric Acid (HCl)	Fisher
IMS	BDH
Interleukin-1α	R & D Systems
ITS (Insulin/ Transferrin/ selenium)	Sigma
Kanamycin	Sigma
L-cysteine hydrochloride	Sigma
L-Glutamine	Sigma
Liquid Nitrogen	BOC
Keratanase I & II	AMS Biotechnology
Magnesium Chloride	BDH
Mercaphoethanol	Sigma
Methanol	BDH
MMP-1	Sigma
MMP-2	Sigma
MMP-7	Sigma
MMP-2 (mouse monoclonal) antibody	Serotec

MMP-1 ELISA kit	Amersham
Molecular weight marker	Sigma
NBT	Promega
Papain	Sigma
Paraformaldehyde	Sigma
Penicilin-G	Sigma
PGF2α	Cayman chemicals
PGF2α receptor (rabbit polyclonal) antibody	Serotec
Phenyl Sulfonyl Flouride	Sigma
Protein marker	Sigma
Protein Assay BCA kit	Sigma
Proteinase K	Dako
Potassium Chloride (KCl)	BDH
Potassium dihydro orthophophate (KH_2PO_4)	BDH
Recombinant human basic fibroblast growth factor	R&D systems
Rhodamine dextran beads	Invitrogen
Shark cartilage chondoritin sulphate	Promega
Sodium azide	BDH
Sodium Chloride (NaCl)	BDH
Sodium dodecyl sulphate	Sigma
Sodium hydroxide	Sigma
Sodium Phosphate, monobasic, monohydrate	Sigma
Sodium Phosphate, dibasic, anhydrase	Acros Organic
Streptomycins sulphate	Sigma
TEMED	Sigma
Toluidine Blue	BDH
Transforming growth factor-β1	R & D Systems
Triton-X-100	Sigma
Tris Base	Sigma

Tris-glycine 4-12% gradient gel	Invitrogen
Trypsin	Sigma
Tumor necrosis factor-α	R & D Systems
Vinyl alcohol	BDH
Xylene	BDH

8.2 Solutions

Alkali Phosphate (AP) buffer: 100mM trizma, 5mM Magnesium chloride ($MgCl_2$), 100mM sodium chloride (NaCl), pH 9.55.

Antibiotics and Glutamine stock: Contained 1g Streptomycins sulphate, 1g Kanamycin, 600g Penicilin-G, 1.46g L-Glutamine in 100ml ddH_2O.

DMMB Solution: 16mg 1,9 Dimethyl methylene blue (DMMB), 25ml ethanol, 1M sodium hydroxide and 4ml of 98% formic acid to a total volumne of 2L with ddH_2O.

Cell freezing solution: 9ml FCS and 1ml DMSO.

Fungisone stock: Contained 250ug/ml Amphotericin B.

Gelvatol

0.08g $NaHPO_4$ and 0.03g KH_2PO_4 was placed in 40ml ddH_2O and the pH was adjusted to pH 7.2. 0.0327g of NaCl, 0.024g sodium azide and 0.6g DABCO were added. 10g of gelvacol was added and the solution was stirred to allow complete desolution. 20ml glycerol was added and stirred and the pH was adjusted to pH 6.7. The solution was centrifuged at 12000 rpm for 15minutes and then at 18000rpm for 25minutes. This solution was stored at 4°C.

10X Lammeli buffer: Prepared containing 100g SDS, 300g tris, 1.44Kg glycine in 10L of dH_20.

10% Neutral Buffered Formuline (NBF): 40% Formaldehyde 100ml, 4g $NaH_2PO_4H_2O$ (sodium phosphate, monobasic, monohydrate), 6.5g $NaHPO_4$ (Sodium phosphate, dibasic, anhydrous) and 900ml ddH_2O.

4% Paraformaldehyde

8ug solid PFA was added to 100ml 1x PBS in a conical flask and placed on stirrer in fume hood for one 1hour at 65°C. Sodium hydroxide was added to

the solution dropwise to make solution clear. The solution was filtered and aliquoted appropriately and acid/ alkali was added to make pH 7.4. The aliquots were kept at -20°C until required.

10% Phosphate Buffered Saline (PBS): 80g Sodium chloride (NaCl), 2.0g Patassium Chloride (KCl), 14.4g Sodium phosphate (Na_2HPO_4), 2.4g Patassium phosphate (KH_2PO_4) was dissolved in 800ml ddH_2O. The pH was adjusted to pH 7.4 and the volumn was adjusted to 1L with the addition of ddH_2O.

Running buffer: 25mM Trizma, 192mM glycine and 0.1% SDS.

2X Sample Buffer: 0.125M Tris HCl pH 6.8, 4% SDS, 20% glycerol and 0.01% bromophenol blue.

Transfer buffer: 25mM Trizma, 192mM glycine, 20% methanol.

Tris Saline (TSA): 50mM Tris pH 7.4, 200mM sodium chloride and 0.02% (w/v) sodium azide.

Trypsin-EDTA Solution (0.25% w/v stock): Contained 0.25g Trypsin (Sigma) and 0.02g EDTA (BDH) in 100ml 1x PBS.

Zymography destain: 7.5% glacial acetic acid and 10% methanol.

Zymography stain: Prepared containing 0.25% (w/v) coomassie brilliant blue, 10% glacial acetic acid and 45% methanol.

REAGENTS	RESOLVING		GEL	STACKING GEL
	7.5% Gelatin	12% Casein	12% Reverse zymography gel	4%
40% Bis/ acrylamide	2.72ml	3.3ml	3.3 ml	575ul
1M tris/HCl pH 8.8	3.63ml	2.5ml	2.5ml	n/a
1M tris/HCl pH6.8	n/a	n/a	n/a	1.3ml
10% (w/v) SDS	100ul	100ul	100ul	50ul
10% (w/v) APS	75ul	100ul	100ul	37ul
dH2O	6.16ml	3.85ml	2.85ml	4.075ml
Gelatin (7.25mg/ml)	1ml	n/a	n/a	n/a
Gelatin (20mg/ml)	n/a	n/a	350ul	n/a
Casein (1.5mg/ml)	n/a	1ml	n/a	n/a
Conditioned medium (see section 5.3.1)	n/a	n/a	1ml	n/a
TEMED	15ul	15ul	15ul	7.5ul

Table 8.1: Zymography gel preparation.

8.3 Human Tissue

8.3.1 NDRI

Donor	Sex/ Age	Date of death	Cause of death
D1	Male, 90	20/10/2002	Coronary artery disease
D2	Male, 82	6/7/2001	Renal Failure
D3	Female, 81	11/4/2001	Intracranial haemorrhage
D4	Male, 66	25/7/1997	Cardio Respiratory arrest

Table 8.2: Tissue from NDRI detail.

8.3.2 Bristol Eye Bank

Date	Donor (Ref, Age, Sex, Death)	Used for
07/06/05	D1, 71, female, SEPSIS	HCM & HSF culture
14/06/05	D2, 60, male, Cancer	HCM & HSF culture
	D3, 78, male, cancer	HCM & HSF culture
20/06/05	D4, 77, male, cardiac arrest	HCM & HSF culture
	D5, 69, female, cancer	HCM & HSF culture
11/07/05	D6, 80, male, Stroke	HCM & HSF culture
15/07/05	D7, 87, female, myocardial event	HCM & HSF culture
20/07/05	D8, 63, male, cancer	HCM & HSF culture
	D9, 79, male, haemorrhage	HCM & HSF culture
21/07/05	D10, 53, female, cancer	HCM & HSF culture
28/07/05	D11, 77, male, cancer liver	HCM & HSF culture
	D12, 63, female, colon cancer	HCM culture Ussing Chamber
	D13, 57, male, celebrial infection	Western Blotting
	D14, 77, male, renal failure	Western Blotting
	D15, 85 female, cardiac arrest	Western Blotting
29/07/05	D16, 66, female, CVA	HCM & HSF culture 1 globe sclera used for ussing chamber
01/08/05	D17, 79, male, stroke	HCM cultured
	D18, 56, male, cadio respiratory failure	HCM cultured
	D19, 79, female, cancer	HCM & HSF culture

	D20, 86, female, cancer	HCM & HSF culture
	D21, 57, male, brain damage	HCM & HSF culture
23/08/05	D22, 79, female, CVA	X ray diffraction
29/08/05	D23, F, 80, Hypoxia	Ussing chamber
30/08/05	D24,M, 83, Pneumonia	Ussing chamber
19/09/05	D25, 56, male, cardiac arrest	X ray diffraction
	D26, 60, male, cancer	HCM & HSF culture Ussing Chamber
23/09/05	D27, 84, Female, multi organ failure	HCM & HSF culture
	D28, 77, female, cancer	HCM & HSF culture
27/09/05	D29, 80, female, cancer	HCM culture Ussing chamber Western blotting
05/10/05	D30, 57, male, cancer	Western blotting
	D31, 64, female, haemorrhage	Ussing chamber Western blotting
12/10/05	D32, 83, male, malignant melanoma	Ussing Chamber
1/11/05	D33, 74, male, cancer rectum d/t: 31/10 9.44 encun:31/10 10.30	X diffraction
14/11/05	D34, 72, male, lung cancer	HCM culture Ussing Chamber
	D35, 72 male, cardiac arrest	HSF & HCM
	D36, 66, male, cancer	HCM culture Ussing chamber
05/12/05	D37, 59, male, stroke	HCM & HSF culture
	D38, 85, female, cancer	HCM culture Ussing chamber
09/02/06	D39, Male, 88, SEPSIS	Cultured HCM & HSF X ray diffraction
21/02/06	D40, Female, 80, cancer	Ussing chamber
21/02/06	D41, Female, 75, CA oesophagus	Western blotting
22/2/06	D42, Female, 61, cardiac arrest	Ussing chamber
28/2/6	D43, Male, 75, cardiac& renal failure	Ussing chamber

2/3/6	D44, Female, 62, CVA	Ussing chamber
2'/3/6	D45, Male, 79, stroke	Western blotting, HCM and HSF culture
10/3/6	D46, Female, 60, renal failure	X ray diffraction HCM & HSF culture
	D47, Female, 72, Cancer stomach	X ray diffraction HCM & HSF culture
15/3/6	D48, Male, 40, ICB	Ussing chamber
	D49, Female , 84 Cancer bowel	Ussing chamber
	D50, Male, 59, heart disease	Culture HCM & MSF
28/3/6	D51, Male, 84, Pneumonia	Ussing chamber
30/3/6	D52, Male, 66, Cancer prostate	Ussing chamber
17/5/5	D53, Male, 78, haemorrhage	Cultured HCM HSF
25/5/6	D54, Female, 62, breast cancer	Western blotting
1/6/6	D55, male, 43, ICH	Western blotting
	D56, male, 61, cardiac arrest	Western blotting Cultures: HCM & HSF
	D57, Female, 94, SEPSIS	Western blotting Cultures: HCM & HSF
12/6/6	D58, Male, 50, lung cancer	Using blotting
14/6/6	D59, Male, 68, Myocardial infarction	Using chamber
15/6/6	D60, Male, 75, artery disease	Ussing chamber
26/6/6	D61, Male, 78, cardiac arrest	Ussing chamber
	D62, Male, 72, cardiac arrest	Ussing chamber
28/6/6	D63, Female, 86, cancer	Ussing chamber
4/7/6	D64, Male, 70, renal failure	Using chamber
5/7/6	D65, Female, 66, breast cancer	Ussing chamber
10/7/6	D66, Male, 81, giloma	Using chamber HCM & HSF culture
12/7/6	D67, Female, 27, liver failure	Culture HCM & HSF
	D68, Female, 84, cardiac arrest	Ussing chamber
27/7/6	D69, Male, 83, CA prostate	HCM and HSF cell culture
3/8/6	D70, Male, 63, Heart Disease	HCM and HSF cell culture

	D72, Male, 75, Pneumonia	HCM and HSF cell culture
15/8/6	D73, Male , 75 Oesophagus cancer	X ray diffraction
	D74, Male, 65, respiratory failure	X ray diffraction

Table 8.3: Tissue from the Bristol Eye Bank details.

8.4 Raw data

8.4.1 Blastp Search for Bovine MMP protein sequence compared to human.

```
tr  A6QPN5          Matrix metallopeptidase 2 (Gelatinase A, 72kDa     661
    A6QPN5_BOVIN    gelatinase, 72kDa                                  AA
                    type IV collagenase) [MMP2] [Bos taurus            align
                    (Bovine)]
```

Score = 1290 bits (3338), Expect = 0.0
Identities = 601/659 (91%), Positives = 616/659 (93%)

```
CLUSTAL FORMAT for T-COFFEE Version_1.37, CPU=0.00 sec, SCORE=35100,
Nseq=2, Len=661

P08253|MMP2_HUMAN     -
MEALMARGALTGPLRALCLLGCLLSHAAAAPSPIIKFPGDVAPKTDKELAVQYLNTFYG
A6QPN5|A6QPN5_BOVIN
MTEARVSRGALAALLRALCVLGCLLGRAAAAPSPIIKFPGDVAPKTDKELAVQYLNTFYG
                         ** ::****:.
*****:*****.:**********************************

P08253|MMP2_HUMAN
CPKESCNLFVLKDTLKKMQKFFGLPQTGDLDQNTIETMRKPRCGNPDVANYNFFPRKPKW
A6QPN5|A6QPN5_BOVIN
CPKESCNLFVLKDTLKKMQKFFGLPQTGELDQSTIETMRKPRCGNPDVANYNFFPRKPKW

****************************:***.**************************

P08253|MMP2_HUMAN
DKNQITYRIIGYTPDLDPETVDDAFARAFQVWSDVTPLRFSRIHDGEADIMINFGRWEHG
A6QPN5|A6QPN5_BOVIN
DKNQITYRIIGYTPDLDPQTVDDAFARAFQVWSDVTPLRFSRIHDGEADIMINFGRWEHG

******************:*******************************************

P08253|MMP2_HUMAN
DGYPFDGKDGLLAHAFAPGTGVGGDSHFDDDELWTLGEGQVVRVKYGNADGEYCKFPFLF
A6QPN5|A6QPN5_BOVIN
DGYPFDGKDGLLAHAFAPGPGVGGDSHFDDDELWTLGEGQVVRVKYGNADGEYCKFPFRF

******************.*************************************** *
```

```
P08253|MMP2_HUMAN
NGKEYNSCTDTGRSDGFLWCSTTYNFEKDGKYGFCPHEALFTMGGNAEGQPCKFPFRFQG
A6QPN5|A6QPN5_BOVIN
NGKEYTSCTDTGRSDGFLWCSTTYNFDKDGKYGFCPHEALFTMGGNADGQPCKFPFRFQG

*****.*******************:*******************:************

P08253|MMP2_HUMAN
TSYDSCTTEGRTDGYRWCGTTEDYDRDKKYGFCPETAMSTVGGNSEGAPCVFPFTFLGNK
A6QPN5|A6QPN5_BOVIN
TSYDSCTTEGRTDGYRWCGTTEDYDRDKKYGFCPETAMSTVGGNSEGAPCVLPFTFLGNK

**************************************************:********

P08253|MMP2_HUMAN
YESCTSAGRSDGKMWCATTANYDDDRKWGFCPDQGYSLFLVAAHEFGHAMGLEHSQDPGA
A6QPN5|A6QPN5_BOVIN
HESCTSAGRSDGKLWCATTSNYDDDRKWGFCPDQGYSLFLVAAHEFGHAMGLEHSQDPGA

:************:*****:****************************************

P08253|MMP2_HUMAN
LMAPIYTYTKNFRLSQDDIKGIQELYGASPDIDLGTGPTPTLGPVTPEICKQDIVFDGIA
A6QPN5|A6QPN5_BOVIN
LMAPIYTYTKNFRLSHDDIQGIQELYGASPDIDTGTGPTPTLGPVTPELCKQDIVFDGIS
                     ***************:***:*************
**************:**********:

P08253|MMP2_HUMAN
QIRGEIFFFKDRFIWRTVTPRDKPMGPLLVATFWPELPEKIDAVYEAPQEEKAVFFAGNE
A6QPN5|A6QPN5_BOVIN
QIRGEIFFFKDRFIWRTVTPRDKPTGPLLVATFWPELPEKIDAVYEDPQEEKAVFFAGNE
                     ********************** **********************
*************

P08253|MMP2_HUMAN
YWIYSASTLERGYPKPLTSLGLPPDVQRVDAAFNWSKNKKTYIFAGDKFWRYNEVKKKMD
A6QPN5|A6QPN5_BOVIN
YWVYSASTLERGYPKPLTSLGLPPGVQKVDAAFNWSKNKKTYIFAGDKFWRYNEVKKKMD

**:*********************.**:*********************************

P08253|MMP2_HUMAN
PGFPKLIADAWNAIPDNLDAVVDLQGGGHSYFFKGAYYLKLENQSLKSVKFGSIKSDWLG
A6QPN5|A6QPN5_BOVIN
PGFPKLIADAWNAIPDNLDAVVDLQGGGHSYFFKGAYYLKLENQSLKSVKFGSIKSDWLG

************************************************************

P08253|MMP2_HUMAN    C
A6QPN5|A6QPN5_BOVIN  C
                     *
```

sp P28053 MMP1_BOVIN **Interstitial collagenase precursor (EC 3.4.24.7) (Matrix metalloproteinase-1) (MMP-1) (Fibroblast collagenase) [MMP1] [Bos taurus (Bovine)]** 469 AA align

Score = 51.3 bits (110), Expect = 2e-04
Identities = 17/21 (80%), Positives = 19/21 (90%)

Query: 263 SQNPVQPIGPQTPKACDSKLT 283

Sbjct: 263 SQNPTQPVGPQTPEVCDSKLT 283

```
CLUSTAL FORMAT for T-COFFEE Version_1.37, CPU=0.00 sec, SCORE=21440,
Nseq=2, Len=470

VIRT9940|Blast_submission  MHSFPPLLLLLFWGVVSHSFPA-
TLETQEQDVDLVQKYLEKYYNLKNDGRQVEKRRNSGP
P28053|MMP1_BOVIN          -
MPRLPLLLLLLWGTGSHGFPAATSETQEQDVETVKKYLENYYNLNSNGKKVERQRNGGL
                             .  ******:**. **.*** * *******:
*:****:****:.:*::**::**.*

VIRT9940|Blast_submission
VVEKLKQMQEFFGLKVTGKPDAETLKVMKQPRCGVPDVAQFVLTEGNPRWEQTHLTYRIE
P28053|MMP1_BOVIN
ITEKLKQMQKFFGLRVTGKPDAETLNVMKQPRCGVPDVAPFVLTPGKSCWENTNLTYRIE
                           :.*******:****:**********:**************
**** *:. **:*:******

VIRT9940|Blast_submission
NYTPDLPRADVDHAIEKAFQLWSNVTPLTFTKVSEGQADIMISFVRGDHRDNSPFDGPGG
P28053|MMP1_BOVIN
NYTPDLSRADVDQAIEKAFQLWSNVTPLTFTKVSEGQADIMISFVRGDHRDNSPFDGPGG

******.*****:**************************************************

VIRT9940|Blast_submission
NLAHAFQPGPGIGGDAHFDEDERWTNNFREYNLHRVAAHELGHSLGLSHSTDIGALMYPS
P28053|MMP1_BOVIN
NLAHAFQPGAGIGGDAHFDDDEWWTSNFQDYNLYRVAAHEFGHSLGLAHSTDIGALMYPS
                           *********.*********:**
**.**::***:******:******:************

VIRT9940|Blast_submission
YTFSGDVQLAQDDIDGIQAIYGRSQNPVQPIGPQTPKACDSKLTFDAITTIRGEVMFFKD
P28053|MMP1_BOVIN
YTFSGDVQLSQDDIDGIQAIYGPSQNPTQPVGPQTPEVCDSKLTFDAITTIRGEVMFFKD
                           *********:************
****.**:*****:.**********************

VIRT9940|Blast_submission
RFYMRTNPFYPEVELNFISVFWPQLPNGLEAAYEFADRDEVRFFKGNKYWAVQGQNVLHG
P28053|MMP1_BOVIN
RFYMRTNPLYPEVELNFISVFWPQLPNGLQAAYEVADRDEVRFFKGNKYWAVKGQDVLRG

********:********************:****.****************:**:**:*

VIRT9940|Blast_submission
YPKDIYSSFGFPRTVKHIDAALSEENTGKTYFFVANKYWRYDEYKRSMDPGYPKMIAHDF
```

```
P28053|MMP1_BOVIN
YPRDIYRSFGFPRTVKSIDAAVSEEDTGKTYFFVANKCWRYDEYKQSMDAGYPKMIAEDF
                              **:*** ********* ****:***:***********
*******:***.*******.**

VIRT9940|Blast_submission
PGIGHKVDAVFMKDGFFYFFHGTRQYKFDPKTKRILTLQKANSWFNCRKN
P28053|MMP1_BOVIN
PGIGNKVDAVFQKGGFFYFFHGRRQYKFDPQTKRILTLLKANSWFNCRKN
                              ****:****** *.******** *******:*******
***********
```

sp P52176 MMP9_BOVIN **Matrix metalloproteinase-9 precursor (EC 3.4.24.35) (MMP-9) (92 kDa type IV collagenase) (92 kDa gelatinase) (Gelatinase B) (GELB) [MMP9] [Bos taurus (Bovine)]** 712 AA align

Score = 766 bits (1979), Expect = 0.0
Identities = 354/444 (79%), Positives = 381/444 (85%)

```
CLUSTAL FORMAT for T-COFFEE Version_1.37, CPU=0.00 sec, SCORE=31870,
Nseq=2, Len=712

P14780|MMP9_HUMAN
MSLWQPLVLVLLVLGCCFAAPRQRQSTLVLFPGDLRTNLTDRQLAEEYLYRYGYTRVAEM
P52176|MMP9_BOVIN
MSPLQPLVLALLVLACCSAVPRRRQPTVVVFPGEPRTNLTNRQLAEEYLYRYGYTPGAEL
                      **  *****.****.** *.**:**.*:*:***:
*****:**************  **:

P14780|MMP9_HUMAN
RGESKSLGPALLLLQKQLSLPETGELDSATLKAMRTPRCGVPDLGRFQTFEGDLKWHHHN
P52176|MMP9_BOVIN
SEDGQSLQRALLRFQRRLSLPETGELDSTTLNAMRAPRCGVPDVGRFQTFEGELKWHHHN
                       :.:**  ***
:*::***********:**:***:*******:********:*******

P14780|MMP9_HUMAN
ITYWIQNYSEDLPRAVIDDAFARAFALWSAVTPLTFTRVYSRDADIVIQFGVAEHGDGYP
P52176|MMP9_BOVIN
ITYWIQNYSEDLPRAVIDDAFARAFALWSAVTPLTFTRVYGPEADIVIQFGVREHGDGYP
                     ****************************************.
:********* *******

P14780|MMP9_HUMAN
FDGKDGLLAHAFPPGPGIQGDAHFDDDELWSLGKGVVVPTRFGNADGAACHFPFIFEGRS
P52176|MMP9_BOVIN
FDGKNGLLAHAFPPGKGIQGDAHFDDEELWSLGKGVVIPTYFGNAKGAACHFPFTFEGRS
                     ****:********** **********:**********:**
****.******** *****

P14780|MMP9_HUMAN
YSACTTDGRSDGLPWCSTTANYDTDDRFGFCPSERLYTRDGNADGKPCQFPFIFQGQSYS
P52176|MMP9_BOVIN
YSACTTDGRSDDMLWCSTTADYDADRQFGFCPSERLYTQDGNADGKPCVFPFTFQGRTYS
                     ***********.: ******:**:* :***********:*********
*** ***::**

P14780|MMP9_HUMAN
ACTTDGRSDGYRWCATTANYDRDKLFGFCPTRADSTVMGGNSAGELCVFPFTFLGKEYST
P52176|MMP9_BOVIN
ACTSDGRSDGYRWCATTANYDQDKLYGFCPTRVDATVTGGNAAGELCVFPFTFLGKEYSA
```

```
                    ***:******************:***:******.*:**
***:******************:

P14780|MMP9_HUMAN
CTSEGRGDGRLWCATTSNFDSDKKWGFCPDQGYSLFLVAAHEFGHALGLDHSSVPEALMY
P52176|MMP9_BOVIN
CTREGRNDGHLWCATTSNFDKDKKWGFCPDQGYSLFLVAAHEFGHALGLDHTSVPEALMY
                    **
***.**:**********.*******************************:********

P14780|MMP9_HUMAN  PMYRFTEGPPLHKDDVNGIRHLYGPRPEPEPRPPTTTT-----
PQPTAPPTVCPTGPPTV
P52176|MMP9_BOVIN
PMYRFTEEHPLHRDDVQGIQHLYGPRPEPEPRPPTTTTTTTTEPQPTAPPTVCVTGPPTA
                    *******  ***:***:**:******************
********** *****.

P14780|MMP9_HUMAN
HPSERPTAGPTGPPSAGPTGPPTAGPSTATTVPLSPVDDACNVNIFDAIAEIGNQLYLFK
P52176|MMP9_BOVIN
RPSEGPTTGPTGPPAAGPTGPPTAGPSAAPTESPDPAEDVCNVDIFDAIAEIRNRLHFFK
                    :*** **:******:************:*.* .
.*.:*.***:******** *:*::**

P14780|MMP9_HUMAN
DGKYWRFSEGRGSRPQGPFLIADKWPALPRKLDSVFEEPLSKKLFFFSGRQVWVYTGASV
P52176|MMP9_BOVIN
AGKYWRLSEGGGRRVQGPFLVKSKWPALPRKLDSAFEDPLTKKIFFFSGRQVWVYTGASL
                     *****:*** * * *****:
.***********.**:**:**:***************:

P14780|MMP9_HUMAN
LGPRRLDKLGLGADVAQVTGALRSGRGKMLLFSGRRLWRFDVKAQMVDPRSASEVDRMFP
P52176|MMP9_BOVIN
LGPRRLDKLGLGPEVAQVTGALPRPEGKVLLFSGQSFWRFDVKTQKVDPQSVTPVDQMFP
                    ***********.:********   .**:*****: :******:*
***:*.: **:***

P14780|MMP9_HUMAN
GVPLDTHDVFQYREKAYFCQDRFYWRVSSRSELNQVDQVGYVTYDILQCPED
P52176|MMP9_BOVIN
GVPISTHDIFQYQEKAYFCQDHFYWRVSSQNEVNQVDYVGYVTFDLLKCPED
                    ***:.***:***:********:*******:.*:****
*****:*:*:****
```

tr	Q148N3	**Matrix metallopeptidase 7 (Matrilysin, uterine)**	267
	Q148N3_BOVIN	**[MMP7] [Bos taurus**	AA
		(Bovine)]	align

Score = 419 bits (1076), Expect = e-115
Identities = 198/267 (74%), Positives = 225/267 (84%)

```
CLUSTAL FORMAT for T-COFFEE Version_1.37, CPU=0.00 sec, SCORE=10760,
Nseq=2, Len=267

P09237|MMP7_HUMAN
MRLTVLCAVCLLPGSLALPLPQEAGGMSELQWEQAQDYLKRFYLYDSETKNANSLEAKLK
Q148N3|Q148N3_BOVIN
MRLVLLCAACLLPGSPALPLGPGPGGEGDPRWQLAQDYLKRFYSSDSKIKNANSLEVRLK
                     ***.:***.****** ****   .** .: :*: *********  **:
*******.:**
```

```
P09237|MMP7_HUMAN
EMQKFFGLPITGMLNSRVIEIMQKPRCGVPDVAEYSLFPNSPKWTSKVVTYRIVSYTRDL
Q148N3|Q148N3_BOVIN
RMEGFFHLPITGILSPRIIEIMEKPRSGVPDVAEFSLFPNHPKWTSKVVTYRIMSYTSDL
                         .*: ** *****:*..*:****:***.*******:*****
************:*** **

P09237|MMP7_HUMAN
PHITVDRLVSKALNMWGKEIPLHFRKVVWGTADIMIGFARGAHGDSYPFDGPGNTLAHAF
Q148N3|Q148N3_BOVIN
PHITVNQLVAKAFKIWSEAIPLTFKRLRWGTADIMIGFARRAHGDPYPFDGPGATLAHAF
                         *****::**:**:::*.: *** *::: ************
****.******* ******

P09237|MMP7_HUMAN
APGTGLGGDAHFDEDERWTDGSSLGINFLYAATHELGHSLGMGHSSDPNAVMYPTYGNGD
Q148N3|Q148N3_BOVIN
APGPGLGGDAHFDEDERWTDGIGIGVNFLYVATHELGHSLGLSHSSDPNAVMYPTYSKED
                         ***.*****************
.:*:****.**********:.*************.: *

P09237|MMP7_HUMAN     PQNFKLSQDDIKGIQKLYGKRSNSRKK
Q148N3|Q148N3_BOVIN   SKNFKLSQDDINGIQLLYGKRNDSRKK
                      .:*********:*** *****.:****
```

8.5 Published Abstract

Molik B, Albon J, Maxwell C, Wess T, Boulton ME & Morgan JE (2006). The role of PGF2α in extracellular matrix degradation and alteration of scleral architecture. ARVO, Florida.

Molik. B, Albon. J, Boulton, M, Morgan, JE (2005). Matrix metalloproteinase (mmp) expression the uveoscleral outflow pathway: novel approaches to the control of intraocular pressure. CITER, Carmathen.